



---

## PhD thesis

Valdemar Lykke Andersen

# Development of PET-tracers for the 5-HT<sub>7</sub> receptor

Academic advisor: Gitte Moos Knudsen

Submitted: 02/10/14

Title: Development of PET-tracers for the 5-HT<sub>7</sub> receptor

Author: Valdemar Lykke Andersen

Institution: Faculty of Health and Medical Sciences, University of Copenhagen, Denmark

Department: Neurobiology Redsearch Unit, Neuroscience Center, Copenhagen University Hospital Rigshospitalet, Denmark

Principal supervisor: Professor Gitte Moos Knudsen, Neurobiology Research Unit and Center for Integrated Molecular Brain Imaging

Co-supervisors: Associate professor Jesper Langgaard Kristensen, Department of Drug Design and Pharmacology, University of Copenhagen, Denmark  
Matthias Manfred Herth, Neurobiology Research Unit, Copenhagen University Hospital, Denmark

Date of Submission: October 2<sup>nd</sup>, 2014

Date of Defense: December 1<sup>st</sup>, 2014

Review committee:

- Associate Professor Paul Robert Hansen (Chairperson), Department of Drug Design and Pharmacology, University of Copenhagen, Denmark
- Dr. Kjell Någren. Department of nuclear medicine, Odense University Hospital, Denmark
- Jan Passchier. Imanova limited, United Kingdom

## Preface

This thesis represents a 3 year Ph.D programme funded by the SHARE cross faculty Ph.D initiative. The work was carried out in the period Oct. 2011 to June 2014. Organic syntheses were carried out at the department of drug design and pharmacology, University of Copenhagen and radiolabeling was carried out at the PET and cyclotron unit, Copenhagen University Hospital.

Compounds **3**, **18** and **19** were synthesized by Matthias M Herth.

Binding assays of compounds **1**, **2**, **3** and **11** were performed by the NIMH Psychoactive Drug Screening Programme at the Department of Biochemistry, Case Western Reserve University, Cleveland, Ohio, USA.

## Abstract

Serotonin (5-HT) is an important neurotransmitter responsible for the regulation of multiple processes such as mood, appetite, aggression, memory and sleep. Dysfunction in the serotonergic system has been linked to various disorders such as Parkinson's disease, anxiety, migraine and depression. Amongst other receptors the 5-HT<sub>7</sub> receptor has been investigated in relation to various disorders. The use of positron emission tomography (PET) can be a way of gaining knowledge about 5-HTs as well as the 5-HT<sub>7</sub> receptor's role in these as well as physiological processes.

PET depends on the use of radiolabeled compounds. A widely used isotope for this purpose is Carbon-11. The most common way of introducing Carbon-11 into a molecule is through nucleophilic substitution involving a hydroxy group, thiol or amine on the target molecule and either [<sup>11</sup>C]MeI or [<sup>11</sup>C]MeOTf. This restricts the library of compounds viable for labeling. The use of cross-coupling is a way of expanding the library of viable compounds. The two most applied cross-couplings are the Stille reaction and the Suzuki reaction. Both of these have been applied to a wide array of substrates yet still have to have their full scope of substrates investigated.

In this thesis the aim has been two-fold: Firstly, to synthesize and label compounds with potential as PET-ligands for the 5-HT<sub>7</sub> receptor. Secondly, to investigate the labeling of amine containing compounds using the Suzuki reaction and if possible devise a general method for the labeling of these and apply this to the labeling of biologically active compounds and potential 5-HT<sub>7</sub> receptor PET-ligands

During the Ph.D a method for the labeling of amine containing compounds was devised. It was used to label a range of model compounds containing different amine motifs. Furthermore it was used to label the biologically active compounds [<sup>11</sup>C]Vortioxetine, [<sup>11</sup>C]Cimbi-712 and [<sup>11</sup>C]Cimbi-772.

[<sup>11</sup>C]Vortioxetine was successfully labeled. In this context the state of the pd-catalyst was found to be crucial when competing N-methylation is to be avoided. When injected into Danish landrace pigs, [<sup>11</sup>C]Vortioxetine was found to bind in cortex, hippocampus, thalamus, striatum and cerebellum. As such it is not a suitable 5-HT<sub>7</sub> receptor PET-ligand but could none the less be a valuable tool in other applications such as investigating the drugs mode of action and as tool for the investigation of depression in general.

[<sup>11</sup>C]Cimbi-712, [<sup>11</sup>C]Cimbi-772, [<sup>11</sup>C]Cimbi-775 belong to a group of compounds that has shown potential as PET-ligands on account of their affinity for the 5-HT<sub>7</sub> receptor, the (phenylpiperazinyl-butyl)oxindoles. [<sup>11</sup>C]Cimbi-712 and [<sup>11</sup>C]Cimbi-772 was labeled using the previously devised method. [<sup>11</sup>C]Cimbi-775 was labeled using O-methylation. The three PET-ligands were found not to be viable 5-HT<sub>7</sub> receptor PET-ligands on account of either slow kinetics or lack of *in vivo* specificity.

Finally, [<sup>11</sup>C]E-55888 an agonist with high selectivity towards the 5-HT<sub>7</sub> receptor was synthesized and labeled. Labeling was achieved as an N-methylation although a labeling using the Suzuki reaction could be envisaged as well. When injected into Danish landrace pigs it enters the brain, shows reversible kinetics but showed very little specific binding.

To summarize, the Suzuki reaction was found to tolerate amine motifs and a method to utilize this was devised. This method was applied to the labeling of [<sup>11</sup>C]Vortioxetine, [<sup>11</sup>C]Cimbi-712 and [<sup>11</sup>C]Cimbi-772. Furthermore [<sup>11</sup>C]Cimbi-775 and [<sup>11</sup>C]E-55888 were labeled via an O and N-methylation respectively. The compounds were evaluated in Danish landrace pigs yet none were found to be viable as a 5-HT<sub>7</sub> receptor PET-ligand.

## Dansk resumé

Serotonin (5-HT) er en vigtig neurotransmitter der er ansvarlig for reguleringen af adskillige processer så som humør, appetit, aggression, hukommelse og søvn. Dysfunktion i det serotonerge system er blevet forbundet med forskellige sygdomme så som Parkinsons sygdom, angst, migræne og depression. Iblant andre receptorer har 5-HT<sub>7</sub> receptoren blevet undersøgt i forbindelse med forskellige sygdomme. Brugen af positron emission tomografi (PET) kan være en måde at erhverve viden om 5-HT og 5-HT<sub>7</sub> receptorens rolle i disse såvel som fysiologiske processer.

PET afhænger af brugen af radiomærkede forbindelser. En meget anvendt isotop til dette formål er kulstof-11. Den mest almindelige måde at introducere kulstof-11, i et molekyle, er gennem nukleofil substitution involverende en hydroxy gruppe, thiol eller amin, på molekylet der skal mærkes, og [<sup>11</sup>C]MeI eller [<sup>11</sup>C]MeOTf. Dette indsnævrer mængden af stoffer der kan mærkes. En måde at udvide denne mængde er via anvendelsen af krydskoblinger. De to mest anvendte krydskoblinger er Suzuki reaktionen og Stille reaktionen. Disse reaktioner er begge blev brugt til at mærke et bredt spektrum of substrater. Hvilke substrater der kan mærkes via disse metoder og dog stadig ikke fuldt udforsket.

Formålet i denne afhandling har været: 1) At syntetisere og mærke stoffer med potentiale som 5-HT<sub>7</sub> receptor PET-ligander. 2) At undersøge mærkningen af amin indeholdende forbindelser ved brug af Suzuki reaktionen og hvis muligt udvikle en generel metode hvorved disse kan mærkes. Denne metode skulle dernæst anvendes til mærkningen af biologisk aktive stoffer og potentielle 5-HT<sub>7</sub> receptor PET-ligander.

I løbet af Ph.D arbejdet blev en metode for mærkningen af amin indeholdende forbindelser udviklet. Denne metode blev anvendt til at mærke en række modelstoffer indeholdende forskellige amin motiver. Denne metode blev derudover anvendt til at mærke de biologisk aktive stoffer [<sup>11</sup>C]Vortioxetine, [<sup>11</sup>C]Cimbi-712 og [<sup>11</sup>C]Cimbi-772.

[<sup>11</sup>C]Vortioxetine blev succesfuldt mærket. I denne sammenhæng blev tilstanden af den anvendte Pd-katalysator fundet til at være altafgørende hvis konkurrerende N-methylering skal undgås. Ved injektion i Dansk landrace grise blev der observeret binding i cortex, hippocampus, thalamus, striatum og cerebellum. [<sup>11</sup>C]Vortioxetine er derfor ikke en passende 5-HT<sub>7</sub> receptor PET-ligand

men kunne dog være et værdifuldt som et værktøj til undersøgelse af hvordan vortioxetine virker og som et værktøj til at udvide forståelsen af depression.

[<sup>11</sup>C]Cimbi-712, [<sup>11</sup>C]Cimbi-772, [<sup>11</sup>C]Cimbi-775 tilhører en gruppe af stoffer der har vist potentiale som PET-ligander i form af deres affinitet og selektivitet for 5-HT<sub>7</sub> receptoren, (phenylpiperazinyl-butyl)oxindoler. [<sup>11</sup>C]Cimbi-712 og [<sup>11</sup>C]Cimbi-772 blev mærket via den forud udviklede metode. [<sup>11</sup>C]Cimbi-775 blev mærket via O-methylering. De tre stoffer blev ikke dømt brugbare som PET-ligander pga en blanding af langsom kinetik og manglende effekt af blokade med SB-269970.

Til sidst blev [<sup>11</sup>C]E-55888, en agonist med høj selektivitet for 5-HT<sub>7</sub> receptoren syntetiseret og mærket. Mærkningen blev udført via N-methylering men mærkning via Suzuki reaktionen er også en mulighed. Ved injektion i Dansk landrace grise observeredes der reversibel kinetik men stoffet kunne ikke blokeres.

Afhandlingen beskriver således udviklingen af en metode hvorved stoffer indeholdende aminer kan mærkes. Denne metode blev anvendt til at mærke stofferne [<sup>11</sup>C]vortioxetine, [<sup>11</sup>C]Cimbi-712 samt [<sup>11</sup>C]Cimbi-772. [<sup>11</sup>C]Cimbi-775 og [<sup>11</sup>C]E-55888 blev mærket via henholdsvis O- og N-methylering. Kandidaterne blev evalueret i Dansk landrace grise men ingen blev fundet anvendelige som en 5-HT<sub>7</sub> PET-ligand.

## Acknowledgements

The last three years have been a thrilling experience fraught with ups and downs. Without numerous people the conclusion of this Ph.D would not have been a reality. First of all I would like to thank my day-to-day supervisor Matthias M. Herth for introducing me to the exiting world of radiochemistry. He was responsible for showing me the ropes in radiochemistry and has provided invaluable guidance, encouragement and know-how. Thank you.

I would likewise like to thank my co-supervisor Jesper L. Kristensen. Your optimistic view on things, encouragement and guidance has helped me out of many tight spots when the research was not going as planned.

My gratitude to my principal supervisor Gitte M. Knudsen could not be overstated. If she had not chosen me amongst the various Ph.D candidates I would not have had the opportunity to undertake this exiting endeavor. Throught the Ph.D her support has never faltered. Her extensive knowledge and guidance has been a source of great inspiration.

A big thank you goes out to all my colleagues on the 3<sup>rd</sup> floor at the department of drug design and pharmacology for creating a fantastic work environment. It has been three years rich in helpful input, discussions, laughter and shawamas. The people at the PET and cyclotron unit should also be thanked for creating a friendly and supportive work environment. A special thank you should be said to Szabolcs Lehel who has always been willing to lend a helping hand when problems occurred. Without him many a synthesis would have failed. The CIMBI platform one group at NRU has my sincere gratitude for many a fruitful discussion about results. Hanne D. Hansen performed the *in vivo* experiments in Danish landrace pigs and has always been open for discussion and further explanations about the results thereof. For this I could not thank her enough.

Lastly I would like to thank my family, girlfriend and friends. Their support and encouragement has been dauntless.



## List of publications:

The following publications are included in the thesis:

**V. L. Andersen**, M. M. Herth, S. Lehel, G. M. Knudsen, and J. L. Kristensen, 'Palladium-Mediated Conversion of Para-Aminoarylboronic Esters into Para-Aminoaryl-C-11-Methanes', *Tetrahedron Letters*, 54 (2013), 213-16.

H. D. Hansen, M. M. Herth, A. Ettrup, **V. L. Andersen**, S. Lehel, A. Dyssegaard, J. L. Kristensen, and G. M. Knudsen, 'Radiosynthesis and in Vivo Evaluation of Novel Radioligands for Pet Imaging of Cerebral 5-HT<sub>7</sub> Receptors', *Journal of Nuclear Medicine*, 55 (2014), 640-46.

**V. L. Andersen**, H. D. Hansen, M. M. Herth, G. M. Knudsen, and J. L. Kristensen, '<sup>11</sup>C-Labeling and Preliminary Evaluation of Vortioxetine as a Pet Radioligand', *Bioorganic & Medicinal Chemistry Letters*, 24 (2014), 2408-11.

M. M. Herth, **V. L. Andersen**, H. D. Hansen, N. Stroth, B. Volk, A. Ettrup, S. Lehel, P. Svenningsson, G. M. Knudsen and J. L. Kristensen, 'Evaluation of 3-Ethyl-3-(phenylpiperazinylbutyl)oxindoles as PET ligands for the 5-HT<sub>7</sub> Receptor – Synthesis, pharmacology, radiolabeling and in vivo Brain Imaging', *Journal of Medicinal Chemistry* (To be submitted).

Furthermore, work during the Ph.D has led to the following publication. It has not been touched upon in the thesis on account of being outside the scope of the thesis (attached as appendix 5).

M. M. Herth, **V. L. Andersen**, S. Lehel, J. Madsen, G. M. Knudsen, and J. L. Kristensen, 'Development of a C-11-Labeled Tetrazine for Rapid Tetrazine-Trans-Cyclooctene Ligation', *Chemical Communications*, 49 (2013), 3805-07.

## Abbreviations

5-HIAA:	5-hydroxyindoleacetic acid
5-HT:	5-hydroxytryptamine, serotonin
5-HTP:	5-hydroxytryptophan
5-HTT:	Serotonin transporter (SERT)
AADC:	Aromatic aminoacid decarboxylase
Ac:	Acetyl
AC:	Adenylate cyclase
Ar:	Aryl
A <sub>s</sub> :	Specific activity
BBB:	Blood brain barrier
Boc:	<i>Tert</i> -butyloxycarbonyl
B <sub>max</sub> :	Receptor density
BP:	Binding potential
BP <sub>ND</sub> :	Binding potential related to nondisplaceable radioligand in tissue
BP <sub>F</sub> :	Binding potential related to free radioligand in tissue
BP <sub>P</sub> :	Binding potential related to plasma concentration of radioligand
cAMP:	Cyclic adenosine monophosphate
CNS:	Central nervous system
COX-2:	Cyclooxygenase-2
Dbz:	Dibenzylideneacetone
DAG:	Diacylglycerol
DEA:	Diethylamine
DME:	1,2-dimethoxyethane
DMF:	Dimethylformamide
DOTA:	1,4,7,10-tetraazacyclododecane-1,4,7,10-tetraacetic acid
Et:	Ethyl
FST:	Forced swim test
GC:	Gas chromatography
GPCR:	G-protein coupled receptor
IP <sub>3</sub>	Inositol 1,4,5-triphosphate
HPLC:	High-performance liquid chromatography

iPA:	Isopropyl alcohol
K <sub>D</sub> :	Dissociation constant
K <sub>i</sub> :	Inhibition constant
LAH:	Lithium aluminium hydride
MAO:	Monoamine oxidase
MDD:	Major Depressive Disorder
Me:	Methyl
MRP:	Multidrug resistance-associated protein
MW:	Microwave
NMR:	Nuclear magnetic resonance
OATP:	Organic anion-transporting polypeptide
PET:	Positron Emission Tomography
Ph:	Phenyl
PIB:	Pittsburg compound b
PIP <sub>2</sub> :	Phosphatidylinositol-4,5-bisphosphate
Py:	Pyridyl
RCP:	Radiochemical purity
RCY:	Radiochemical yield
SERT:	Serotonin transporter (5-HTT)
SPECT:	Single photon emission computed tomography
SSRI:	Selective serotonin reuptake inhibitor
Tf:	Trifluoromethylsulfonyl
TFA:	Trifluoroacetic acid
TH:	Tryptophan hydroxylase
THF:	Tetrahydrofuran
TLC:	Thin layer chromatography
TRYP:	Tryptophane
TST:	Tail suspension test

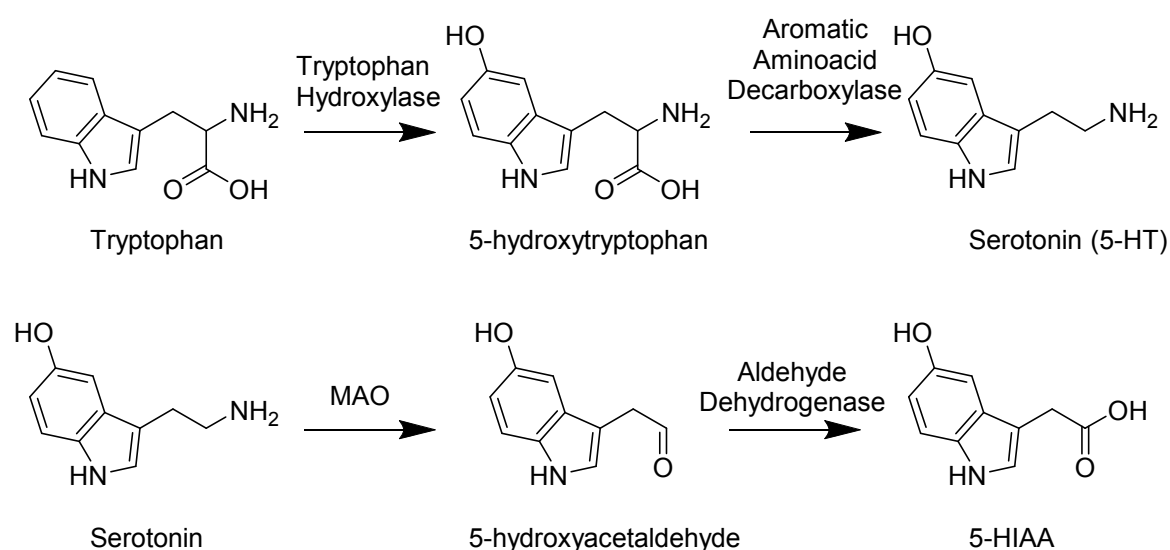
# Table of contents

1	Introduction .....	11
1.1	The serotonergic system .....	11
1.2	5-HT receptors.....	13
1.3	The 5-HT <sub>7</sub> receptor .....	13
1.4	Positron Emission Tomography.....	15
1.5	PET in research .....	18
1.6	Development of PET-tracers .....	20
1.7	PET-ligands for the 5-HT <sub>7</sub> receptor.....	22
1.8	Organic chemistry VS radiochemistry .....	24
1.9	Primary and secondary <sup>11</sup> C-building blocks in radiochemistry .....	25
1.10	Cross-couplings in <sup>11</sup> C-radiochemistry .....	26
2	Aims .....	30
3	Results and discussion .....	32
3.1	Labeling of amine containing model compounds.....	32
3.2	[ <sup>11</sup> C]Vortioxetine .....	35
3.3	[ <sup>11</sup> C]Cimbi-712, [ <sup>11</sup> C]Cimbi-772 and [ <sup>11</sup> C]Cimbi-775.....	39
3.4	[ <sup>11</sup> C]E-55888 .....	45
4	Conclusion and perspectives .....	48
5	Experimental.....	50
7	References .....	67
8	Appendices .....	75

# 1 Introduction

## 1.1 The serotonergic system

Since the discovery of serotonin (5-hydroxytryptamine, 5-HT) in the gastrointestinal tract<sup>1</sup> and subsequent discovery in the central nervous system (CNS),<sup>2</sup> the serotonergic system has grown to be a subject of extensive research.<sup>3</sup> Even though the majority of 5-HT is found outside the CNS<sup>4</sup>, 5-HT plays an important role in many behavioral and psychological processes such as mood, aggression, appetite, sleep and memory.<sup>5</sup>



**Scheme 1.** Top: Biosynthesis of 5-HT from tryptophan. Bottom: Metabolism of 5-HT into 5-HIAA.

Inside the CNS, 5-HT is stored and synthesized within the neurons originating from the raphe nuclei. These neurons radiate throughout CNS in such an extent that most cells within the brain is in proximity to a serotonergic fiber.<sup>5</sup> As 5-HT cannot cross the blood brain barrier (BBB), it has to be synthesized within the brain. 5-HT is synthesized from tryptophan (TRYP) in a two-step biosynthesis. Tryptophan hydroxylase (TH) converts tryptophan into 5-hydroxytryptophan (5-HTP) which is subsequently converted into 5-HT via the enzyme aromatic amino acid decarboxylase (AADC) (scheme 1).<sup>6</sup> Once synthesized 5-HT is stored in vesicles from which it can be released into the synaptic cleft upon neuronal stimulation. When released into the synaptic cleft, 5-HT can either bind to receptors, both pre and post-synaptic, or it can be taken up into the pre-synaptic neuron via the serotonin transporter (SERT) (Figure 1). After reuptake, 5-HT can be incorporated into vesicles for reuse or it can be broken down by monoamine oxidase (MAO). The resulting

compound, 5-hydroxyindoleacetaldehyde, can be further metabolised by aldehyde dehydrogenase to give 5-hydroxyindoleacetic acid (5-HIAA) which is excreted through urine (scheme 1).<sup>3</sup>

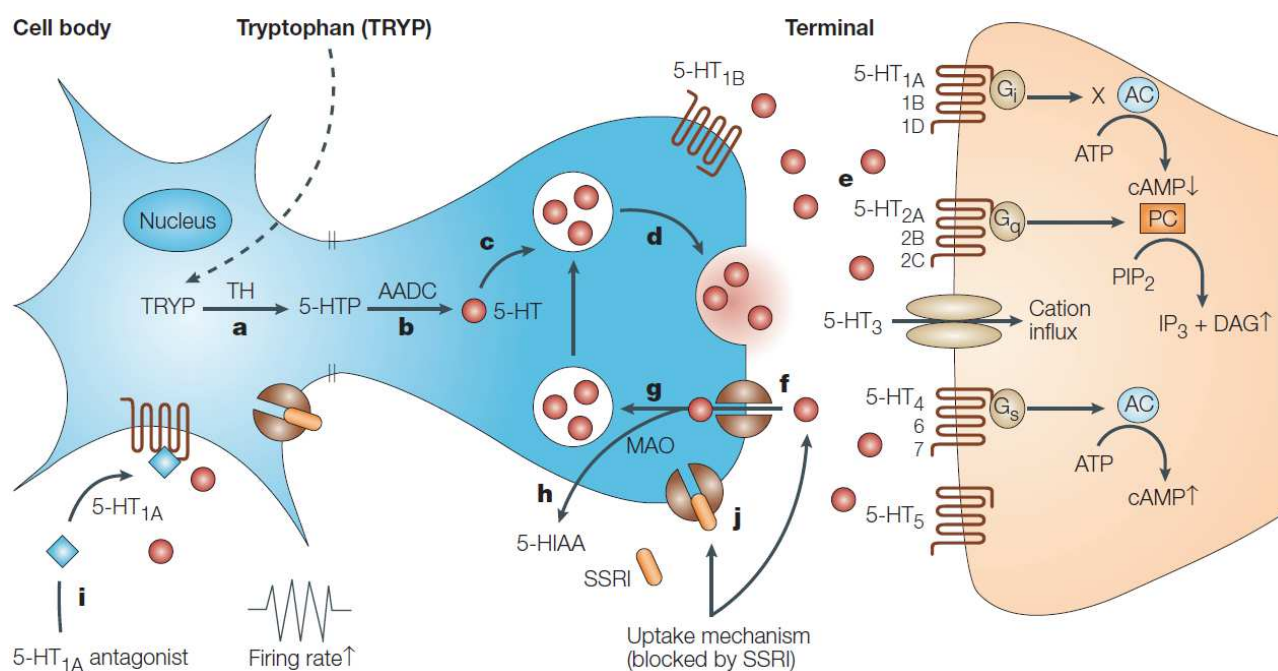


**Figure 1.** Diagram of serotonergic neurotransmission. **a)** TH catalyses the conversion of TRYP to 5-HTP. **b)** AADC catalyses the conversion of 5-HTP to 5-HT. **c)** 5-HT is stored in vesicles. **d)** release of 5-HT from storage vesicles into the synaptic cleft. **e)** 5-HT can activate subtypes of the seven 5-HT receptor families, which couple with their respective system of signal transduction inside the postsynaptic neuron. **f)** Reuptake of 5-HT into the presynaptic neuron by SERT. **g,h)** Within the presynaptic neuron 5-HT can either be stored in vesicles or degraded by MAO. **i)** Activation of presynaptic 5-HT<sub>1A</sub> autoreceptor by 5-HT, which can be blocked by selective 5-HT<sub>1A</sub> antagonists. **j)** Selective serotonin reuptake inhibitors (SSRIs) block SERT. Modified from: Wong et al. 2005<sup>7</sup>

Dysfunction in the 5-HT system has been linked to a variety of CNS related disorders such as depression,<sup>8</sup> parkinsons disease (PD),<sup>9</sup> migraine<sup>10</sup> and anxiety.<sup>11</sup> In PD a loss of serotonergic neruons<sup>12,13</sup> as well as decreased levels of 5-HT<sup>14,15</sup> has been reported. Additionally, PET studies have shown a decrease in 5-HT<sub>1A</sub> and SERT in patients with PD.<sup>9</sup> The 5-HT<sub>1A</sub> receptor has also been implicated in anxiety. 5-HT<sub>1A</sub> agonists have been shown to have anxiolytic effect<sup>16</sup> whereas 5-HT<sub>1a</sub> knockout mice have been shown to have increased anxiety. The 5-HT<sub>7</sub> receptor has likewise been linked to disorders, as further described in chapter 1.3. A way of investigating this could be through the use of positron emission tomography (PET). The basis and applications of PET are described in chapter 1.4 and 1.5

## 1.2 5-HT receptors

The family of 5-HT receptors encompasses 14 receptor classes,<sup>3</sup> 13 of which are expressed in humans. The receptors can be divided into seven subfamilies 5-HT<sub>1-7</sub>.<sup>17</sup> With the exception of the 5-HT<sub>3</sub> receptor, a ligand gated ion-channel, all of these receptors are G-protein coupled receptors (GPCR's) of the "type A"-family known as rhodopsin-like receptors.<sup>6</sup> All GPCRs are characterized by having an extracellular N-terminus, seven helical transmembrane regions, connected by three intracellular and three extracellular loops, and an intracellular C-terminus. At the intracellular region the receptor is coupled to various G-proteins. The coupling to these proteins, as well as their amino acid sequence and pharmacological properties distinguish the six 5-HT GPCR subfamilies from each other. Activation of the receptor mediates structural changes within the G-protein which in turn regulate the activity of secondary messenger generating enzymes such as adenylate cyclase. The six 5-HT GPCR sub-families can be divided as such: 5-HT<sub>1a-f</sub> and 5-HT<sub>5a</sub> are coupled to G<sub>i/o</sub> and inhibits adenylate cyclase, thus reducing cAMP levels.<sup>6</sup> Although 5-HT<sub>5B</sub> genes are present in humans, the 5-HT<sub>5B</sub> gene does not produce a functional protein on account of interrupting stop codons.<sup>18</sup> 5-HT<sub>2a-c</sub> couples to G<sub>q</sub> which activates phospholipase C and thereby increases IP<sub>3</sub> levels.<sup>6</sup> 5-HT<sub>4</sub>, 5-HT<sub>6</sub> and 5-HT<sub>7</sub> couples to G<sub>s</sub> activating adenylate cyclase resulting in increasing cAMP levels.<sup>6</sup> cAMP is responsible for intracellular signalling, primarily through activation of the enzyme phosphokinase A. The 5-HT<sub>3</sub> receptor mediate rapid activating as well as desensitizing inward currents. These are primarily carried by Na<sup>+</sup> and K<sup>+</sup> but the receptor also shows permeability for Ca<sup>2+</sup>.<sup>19</sup>

## 1.3 The 5-HT<sub>7</sub> receptor

The 5-HT<sub>7</sub> receptor is the most recently discovered 5-HT receptor, and until its cloning from several animals including humans in 1993,<sup>20-22</sup> it was described as a 5-HT<sub>1</sub> like receptor.<sup>23,17</sup> In peripheral tissue it is found in the smooth muscle cells of blood vessels<sup>24</sup> as well as in the gastrointestinal tract.<sup>25</sup> A study by Varnas et al. established 5-HT<sub>7</sub> receptor distribution throughout the human CNS using the 5-HT<sub>7</sub> antagonist [<sup>3</sup>H]SB-269970.<sup>26</sup> Thalamus was found to have the highest binding. Intermediate binding was found in hypothalamus, amygdala and hippocampus and low binding in the striatum and cerebellum. Another study using [<sup>3</sup>H]SB-269970 in rats have reported a similar

distribution: highest binding in thalamus, intermediate to high binding in hypothalamus, amygdala and hippocampus and no binding in striatum and cortex.

The 5-HT<sub>7</sub> receptor has been linked to the pathophysiology of depression.<sup>27</sup> The forced swim test (FST) and tail suspension test (TST) have both been used to show an antidepressant effect of reduced 5-HT<sub>7</sub> receptor activity, either by pharmacological means<sup>28-30</sup> or by the use of knockout mice.<sup>31,32</sup> The FST and TST have likewise been used to show the role of 5-HT<sub>7</sub> receptor in depression through the use of amisulpride and lurasidone, two atypical antipsychotics with antidepressant effect. In wildtype mice they would elicit an antidepressant-like effect but none in knockout mice.<sup>33,34</sup> Additionally, Vortioxetine, (Brintellix®) a new drug for the treatment for of major depressive disorder (MDD), is a multimodal drug with affinities for 5-HT<sub>1A</sub>, 5-HT<sub>1B</sub>, 5-HT<sub>3</sub>, 5-HT<sub>7</sub> and SERT.<sup>35</sup> As of yet the exact mode of action has yet to be determined.

Attempts to establish a link between the 5-HT<sub>7</sub> receptor and anxiety have yet been inconclusive. The effect of SB-269970 (Figure 2) has been investigated in both mice and rats. In rats, SB-269970 elicited an anxiolytic effect in both the Vogel drinking test and the elevated plus maze models of anxiety.<sup>30</sup> SB-269970 was found to elicit a lesser anxiolytic effect than the reference anxiolytic diazepam though. Furthermore, the marble burying test, another model used for anxiety, has shown anxiolytic effect in 5-HT<sub>7</sub> receptor knockout mice as well as in mice injected with SB-269970.<sup>36</sup> In contrast, studies using 5-HT<sub>7</sub> receptor knockout mice in the light-dark transfer test and in the elevated plus maze have found no difference between knock-out and wild-type mice.<sup>32,37</sup> Furthermore, a range of 5-HT<sub>7</sub> selective compounds developed by Volk et al. have displayed anxiolytic effect in both the Vogel drinking test and the light-dark transfer test.<sup>38</sup>

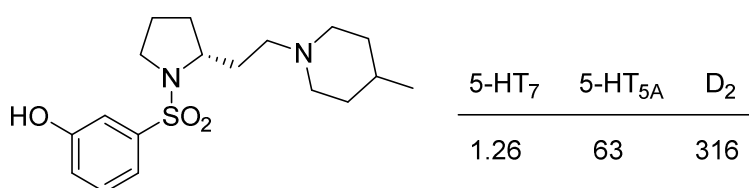


**Figure 2.** Structure of SB-269970 and the three highest affinities of SB-269970, affinities of other targets >316 nM. Values recalculated into nM from pKi values reported in Lovell et al.<sup>39</sup>

As with the link between the 5-HT<sub>7</sub> receptor and anxiety the endeavors to link the 5-HT<sub>7</sub> receptor to epilepsy has been inconclusive. The first study linking the 5-HT<sub>7</sub> receptor to epilepsy was conducted before the availability of selective antagonists. A correlation was shown between the affinity of a range of compounds for the 5-HT<sub>7</sub> receptor and their ability to protect against



audiogenic seizure in mice.<sup>40</sup> Yang et al. have shown that 5-HT<sub>7</sub> receptor activation increases the number seizures in epileptic rats and 5-HT<sub>7</sub> receptor antagonists decreases the number of seizures. Furthermore they report that 5-HT<sub>7</sub> receptor expression is higher in epileptic than in non-epileptic subjects in rats and humans.<sup>41</sup> In contrast, a study by Witkin et al. using chemical and electrical induced seizures in 5-HT<sub>7</sub> receptor knockout mice, showed a lowering in seizure thresholds.<sup>42</sup>

As the 5-HT<sub>7</sub> receptor is indicated in several disorders a 5-HT<sub>7</sub> receptor PET-ligand could be valuable tool in the further elucidation of the receptors role in these. The use of PET combined with a 5-HT<sub>7</sub> selective PET-ligand would allow the quantification of receptor densities within the brain and changes therein in relation to these disorders.

## 1.4 Positron Emission Tomography

Medical imaging is a still expanding field in which the techniques can be divided into structural and functional imaging. Both fields have inherent advantages and disadvantages. Structural imaging techniques such as magnetic resonance imaging, x-ray computed tomography or ultrasound gives valuable anatomical information but little to no information regarding ongoing processes in the body. Functional imaging techniques such as PET or single photon emission computed tomography (SPECT) provide information about physiological processes in a manner that can be quantified.

PET is based on the use of radioactive isotopes. To be eligible for use in PET an isotope has to decay via positron emission (also known as  $\beta^+$ -decay). Once emitted, a positron will travel until its kinetic energy is sufficiently low to collide with an electron. The collision of positron and electron initially forms positronium, with a half-life of 125 picoseconds, which then annihilates yielding two 511 keV photons emitted in almost opposite directions (Figure 3).<sup>43</sup> It is the coinciding detection of such photon-pairs which forms the basis of PET. If two photons are detected within a narrow time frame they are deemed coincident. At a coincidence event a line of response is drawn between the two involved detectors. By registering vast multitudes of such photon-pairs and reconstructing the resulting dataset, it is possible to pinpoint the location(s) of the tracer in the body as well as gain information about changes in tracer concentration over time.

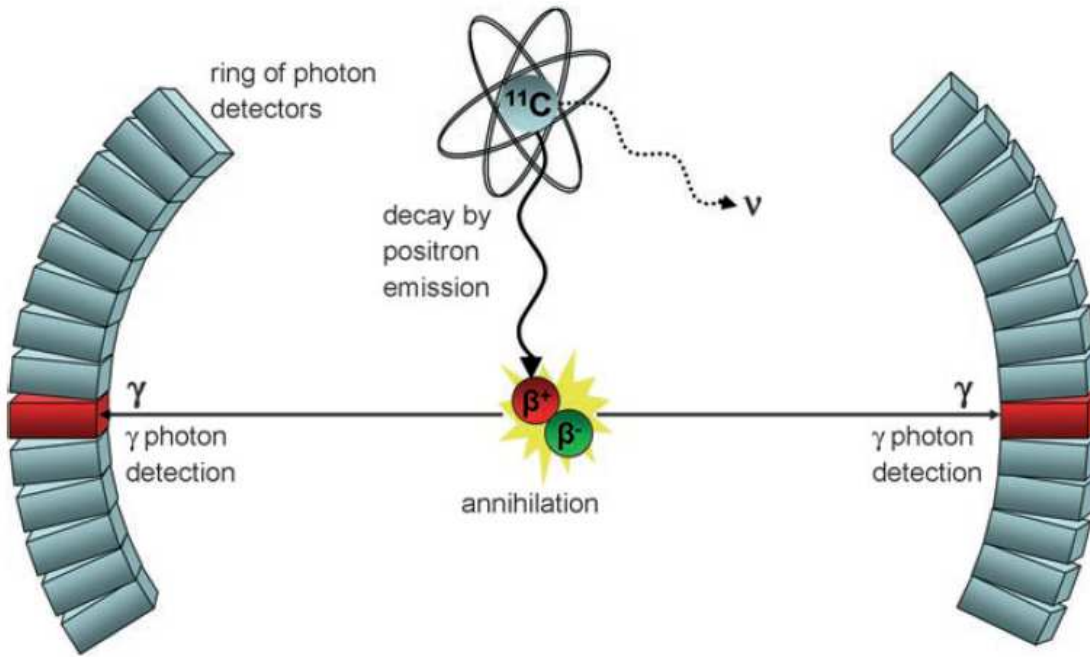


**Figure 3.** PET exemplified by decay of  $^{11}\text{C}$ . Source: Miller et al.<sup>44</sup>

The straight line from the radionuclide to the point of collision is known as the positron range and depends on the kinetic energy of the emitted positron. This energy is dictated by the isotope from which the positron is emitted which for  $\beta^+$ -decay is a continuous spectrum (Figure 4).

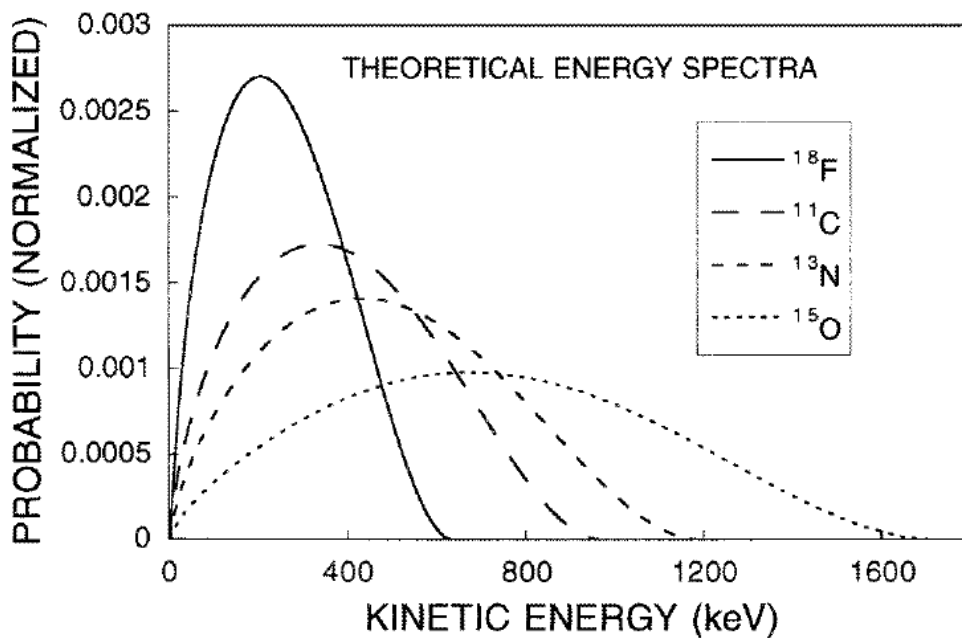


**Figure 4.** Theoretical positron kinetic energy spectra for  $^{18}\text{F}$ ,  $^{11}\text{C}$ ,  $^{13}\text{N}$  and  $^{15}\text{O}$  (normalized to have equal area under the curve). Source: Levin et al. 1999<sup>45</sup>

As such the maximum positron range is defined by the maximum energy. Furthermore, the collision of positron and electron is not dependent on the complete expenditure of kinetic energy.<sup>46</sup> Thus the collision can occur at a lower range than the maximum range. Indeed most collisions occur at a shorter range than the maximum range which gives rise to another important range: The average positron range. It is the transferal of the residual kinetic energy which distorts the angle of the annihilation photons away from 180°. Additionally, as the energy spectrum of the positron differs from isotope to isotope, the use of differing isotopes will result in differences in the resolution achieved in a PET-scan (Table 1).

**Table 1.** Different isotopes used in PET-tracers. Modified from Brown et al. and Miller et al.<sup>47,44</sup>

<b>Isotope</b>	<b>Production method</b>	<b>Product</b>	<b>Half-life (min)</b>	<b><math>E_{\beta^+,max}</math> (KeV)</b>	<b>Max. <math>\beta^+</math>-range (mm) in water</b>	<b>Avg. <math>\beta^+</math>-range (mm) in water</b>
<b><sup>15</sup>O</b>	Cyclotron <sup>15</sup> N(d,n) <sup>15</sup> O	[ <sup>15</sup> O]O <sub>2</sub>	2.04	1740	8.0	1.80
<b><sup>13</sup>N</b>	Cyclotron <sup>16</sup> O(p, $\alpha$ ) <sup>13</sup> N	[ <sup>13</sup> N]NH <sub>3</sub> or [ <sup>13</sup> N]NO <sub>x</sub>	9.97	1200	5.0	1.15
<b><sup>11</sup>C</b>	Cyclotron <sup>14</sup> N(p, $\alpha$ ) <sup>11</sup> C	[ <sup>11</sup> C]CO <sub>2</sub> or [ <sup>11</sup> C]CH <sub>4</sub>	20.4	970	3.8	0.85
<b><sup>18</sup>F</b>	Cyclotron <sup>18</sup> O(p,n) <sup>18</sup> F	[ <sup>18</sup> F]F <sup>-</sup>	110	640	2.2	0.46

The isotopes used in PET are dominated by short lived isotopes. These include isotopes such as <sup>15</sup>O, <sup>13</sup>N, <sup>11</sup>C and <sup>18</sup>F (Table 1). On account of their short half-lives <sup>15</sup>O and <sup>13</sup>N are usually impractical when it comes to incorporation into larger biologically active molecules. As such they are primarily used in special applications such as measuring cerebral blood flow using [<sup>15</sup>O]H<sub>2</sub>O<sup>44</sup> or measuring myocardial blood flow using [<sup>13</sup>N]NH<sub>3</sub>.<sup>48</sup> <sup>11</sup>C and <sup>18</sup>F are the most widely used radioisotopes, both with inherent advantages and disadvantages. Carbon is in vast abundance in the library of potential PET-tracers when compared to fluorine. As such, finding a labelable candidate is more likely, when aiming for <sup>11</sup>C-labeling rather than <sup>18</sup>F-labeling. The abundance of carbon in biologically active compounds and in chemistry in general also means that a wider array of reactions is applicable.

The short half-life of  $^{11}\text{C}$  makes the use of an onsite cyclotron as well as rapid radiosynthesis a necessity yet also has an advantage. As most of the activity will be gone after six half-lives ( $6t_{1/2} \rightarrow 1,5\%$ ), the half-life of  $^{11}\text{C}$  makes consecutive experiments within two hours of each other a possibility ( $6 \cdot 20\text{min} = 120\text{min}$ ). As such, multiple experiments within the same subject can be conducted also known as test-retest studies.  $^{18}\text{F}$  has a longer half-life and a shorter positron range than  $^{11}\text{C}$ . The longer half-life makes test-retest studies in the course of one day problematic ( $6 \cdot 110\text{min} = 11\text{hour}$ ) but also makes multistep radiosynthesis more feasible as well as opening up the possibility of shipping the  $^{18}\text{F}$ -labeled tracer to sites without access to a cyclotron.

## 1.5 PET in research

The use of PET-tracers enables the targeting of specific tissues, cells or even proteins. PET-tracers are administered in minute doses as not to occupy more than 5-10% of the total receptor population.<sup>49</sup> This serves the purpose of allowing the imaging of the desired receptor without having a marked impact on the total availability of the receptor, also known as the tracer principle. Combined with compartmental modelling or reference tissue modelling this allows for the quantification of data obtained through PET imaging.

A typical measure used in the quantification of PET data is the binding potential (BP). *In vitro* BP is defined as  $BP = \frac{B_{max}}{K_D}$  where  $B_{max}$  is the total concentration of receptor and  $K_D$  is the dissociation constant of the ligand.<sup>49</sup> Assuming that at tracer doses  $F \ll K_D$  applying the michaelis-menten equation adapted for receptor purposes ( $B = \frac{B_{max}F}{K_D + F}$ ) can be rewritten:  $\frac{B}{F} = \frac{B_{max}}{K_D} = BP$ . It is this assumption that is the basis of the tracer principle. *In vivo* BP can be measured by comparison to one of three reference concentration:  $BP_F$  which is the ratio at equilibrium of the tissue bound radioligand concentration against free ligand concentration,  $BP_P$ , the ratio at equilibrium of the tissue bound radioligand concentration against the concentration of total parent radioligand in plasma and  $BP_{ND}$ , the ratio at equilibrium of tissue bound radioligand concentration against the concentration of non-displaceable tissue bound radioligand.

PET has seen increased use in pharmaceutical drug development. By using receptor specific PET-ligands it has been possible to evaluate receptor occupancy at effective doses in both antipsychotics

and antidepressants. The use of [ $^{11}\text{C}$ ]DASB has thus been used in subjects under treatment with the selective reuptake inhibitors paroxetine and citalopram. The study found an 80% SERT occupancy at effective clinical doses.<sup>50</sup> Additionally PET can be utilised as a proof of concept in drug development. Through the use of drug candidate identical PET-ligands it is possible to determine biological parameters of the drug candidate such as: BBB penetration, receptor binding, non-specific binding and metabolism.<sup>46</sup> Examples hereof is the labeling and comparison of two neurokinin 1 receptor antagonists, [ $^{11}\text{C}$ ]GR203040 and [ $^{11}\text{C}$ ]GR205171. On account of a higher brain uptake and a lower non-specific binding, [ $^{11}\text{C}$ ]GR205171 was chosen as the preferred candidate.<sup>51</sup>

PET-imaging has been widely utilised in the investigation of various brain functions, such as glucose metabolism in the brain<sup>52,53</sup> and BBB transport,<sup>54,55</sup> and disorders such as imaging beta-amyloid plaques, using [ $^{11}\text{C}$ ]PIB, in connection with alzheimers.<sup>56</sup> On account of its role in various disorders the serotonergic system has received extensive attention in the field of PET-imaging. PET-ligands for various 5-HT targets have already been applied in humans, to test their role in different disorders, examples are: [ $^{11}\text{C}$ ]WAY-100635 (5-HT<sub>1A</sub>), [ $^{11}\text{C}$ ]P943 (5-HT<sub>1B</sub>), [ $^{18}\text{F}$ ]altanserin (5-HT<sub>2A</sub>), [ $^{11}\text{C}$ ]DASB (SERT) or [ $^{11}\text{C}$ ]AMT (5-HT synthesis). [ $^{11}\text{C}$ ]WAY-100635 has for example been used to show a decreased 5-HT<sub>1A</sub> binding in patients suffering from panic disorder.<sup>57</sup> [ $^{11}\text{C}$ ]AMT has been used to show changes in 5-HT synthesis rate during acute mood changes<sup>58</sup> and during treatment with antidepressants.<sup>59</sup> [ $^{11}\text{C}$ ]DASB has been used to show a reduced availability of SERT in patients suffering from unipolar depressive disorder compared to healthy subjects.<sup>60</sup> [ $^{18}\text{F}$ ]altanserin has been used to show an age-related reduced 5-HT<sub>2A</sub> binding.<sup>61</sup> Furthermore, studies using [ $^{11}\text{C}$ ]P943 have begun to appear investigating the role of 5-HT<sub>1B</sub> in alcohol dependence<sup>62</sup> and depression.<sup>63</sup> The use of [ $^{11}\text{C}$ ]WAY-100635 and [ $^{11}\text{C}$ ]AMT are examples of two of the applications of PET: Measuring changes in receptor densities and changes in metabolism. A 5-HT<sub>7</sub> receptor PET-ligand could thus be a valuable tool in quantifying 5-HT<sub>7</sub> receptor densities within the brain.

A goal within the field of serotonergic PET-ligands has been the development of a ligand sensitive to changes in endogenous 5-HT. Such a PET-ligand would be an invaluable tool in determining the role of 5-HT in various disorders. Currently several different PET-ligands for different targets have been evaluated in regards to their sensitivity to endogenous 5-HT. [ $^{11}\text{C}$ ]DASB (SERT), [ $^{11}\text{C}$ ]WAY-100635 (5-HT<sub>1A</sub>), [ $^{18}\text{F}$ ]WAY-analogues (5-HT<sub>1A</sub>), [ $^{18}\text{F}$ ]MPPF (5-HT<sub>1A</sub>), [ $^{11}\text{C}$ ]CUMI-101 (5-HT<sub>1A</sub>),

[<sup>11</sup>C]AZ10419369 (5-HT<sub>1B</sub>) [<sup>11</sup>C]MDL-100907 (5-HT<sub>2A</sub>), [<sup>18</sup>F]setoperone (5-HT<sub>2A</sub>) and [<sup>18</sup>F]altanserin (5-HT<sub>2A</sub>) have all been found to be insensitive to 5-HT changes or results have been conflicting.<sup>64-66</sup> 5-HT shows the highest affinity for the 5-HT<sub>7</sub> receptor ( $K_i = 0.3-8$  nM) with the closest contenders being 5-HT<sub>1A</sub> ( $K_i = 0.2-400$  nM) and 5-HT<sub>1B</sub> ( $K_i = 1-40$  nM).<sup>64</sup> Paterson et al. reports that if a PET-ligand is assumed to compete with a neurotransmitter for occupation of a shared target then an increase in concentration of the neurotransmitter will result in a reduced availability of the target, giving rise to a reduction in the observed binding of the PET-ligand.<sup>64</sup> A 5-HT<sub>7</sub> receptor PET-ligand could thus have potential as a tool to measure endogenous levels of 5-HT and fluctuations herein.

## 1.6 Development of PET-tracers

The search for new PET-tracers is a multidisciplinary undertaking involving fields of research such as: Medicinal chemistry, pharmacology, radiochemistry, biology, physics and image analysis. Despite ongoing advancements in the fields of radiochemistry and PET-tracers the development of PET-tracers is still largely dependent on a trial and error approach. The development of a PET-tracer from initial medicinal chemistry and *in vitro* assays through initial labeling experiments and animal *in vivo* experiments to actual clinical testing is an expensive and time consuming process.

To develop a PET-tracer, a target first has to be identified and candidate compounds have to be found. These are often based on commercially available compounds or compounds found in literature. Ideally these should contain sites viable for labeling yet introduction of such a site can be a necessity, preferably in a position that affects affinity and selectivity minimally. Additionally, a precursor for commercially available candidates is not always available and will have to be synthesised. A number of criteria must be met for a PET-tracer to be useful for quantitative PET-imaging of a target.

1. The labeling of a tracer candidate should be efficient and reliable. For clinical applications the labeling should preferably be carried out as the last step in the tracer synthesis. Despite this a labeling procedure of more than one step can often be necessary. The labeling should be swift as not to lose more activity than necessary. This timeframe is governed by the half-life of the used radionuclide, the shorter the half-life, the faster the labeling process should

be. One should aim to keep the process of labeling, purification and formulation of PET-tracer under three half-lives of the radionuclide in use to ensure a sufficient amount of activity is obtained for administration.<sup>44</sup>

2. Care should be taken to ensure high specific activity ( $A_s$ ), which is defined as the amount of radioactivity per total amount of compound, typically given as a molar unit (GBq/ $\mu$ mol). As administered amounts in PET-scans are described in amount of activity,  $A_s$  directly affects the total molar amount that is administered. Thus a high  $A_s$  lowers the molar amount, reducing the risk of violating the assumption that the tracer only occupies a small fraction of the receptors.
3. Candidates should have a high affinity and selectivity for the desired target. The necessary affinity, usually in the nM range, depends on the target tissue and the receptor density therein. The lower the density the higher the affinity, of the candidate ligand, needs to be in order to ensure sufficient signal to background ratios. The relative density of the target receptor to receptors, to which the candidate has competing affinity, greatly affects the need for selectivity. The relation between relative receptor densities and selectivity can be described as  $receptor\ binding = \frac{K_D\ off\ target}{K_D\ target} \cdot \frac{B_{max\ target}}{B_{max\ off\ target}}$ . Thus, a compound, that shows a 100-fold selectivity towards target A over target B, evaluated in a tissue where target B is ten times more prominent would only show a ten-fold difference in signal between the two targets. Ideally, a tracer candidate would be completely selective towards the desired receptor in the target tissue but this is rarely the case.
4. A tracer candidate for the CNS has to be able to cross the BBB. If the candidate relies on passive diffusion to enter the brain this is often dependent on lipophilicity of the candidate. LogP values of 2.0-3.5 are generally desirable.<sup>67</sup> A low lipophilicity will makes entry into the brain unlikely whereas a high lipophilicity can result in non-specific binding of the candidate.
5. Metabolites of the labelled candidate have to be taken into account as well. Radioactive lipophilic metabolites might enter the brain. This might lead to a contamination of the signal. Additionally, the metabolite can potentially bind to the target in a similar fashion as the parent compound giving rise to a signal that is the combined of both. This complicates the data analysis as the relative amount of bound parent compound vs metabolite is unknown.

6. Finally a candidate should display reversible kinetics within the timeframe of the PET experiment to ease the kinetic modelling of the achieved data. Additionally, a lack of reversible binding can present a problem if the purpose of the tracer is to evaluate competing compounds at the receptor. Furthermore, it should also be displaceable by a competing ligand as to ascertain specific binding at the receptor. The ability to be displaced can also be shown by using cold PET-ligand as a blocking agent. Whereas this approach will show whether or not the PET-ligand is displaceable it does not give information in regards to the actual binding site.

## 1.7 PET-ligands for the 5-HT<sub>7</sub> receptor

The first 5-HT<sub>7</sub> receptor PET-ligand, [<sup>11</sup>C]DR4446 (Figure 5), was published in 2002 by Zhang et al.<sup>68</sup> As a tetrahydrobenzindole it was labeled from its corresponding desmethyl-precursor using [<sup>11</sup>C]MeI. The ligand showed good BBB brain permeability and was metabolically stable. Limited specific binding was observed. The 5-HT<sub>7</sub> receptor antagonist SB-269970 has been derivatised to give potential 5-HT<sub>7</sub> PET-ligands. This has led to the compounds [<sup>18</sup>F]-1-(2-((2S)-1-(phenylsulfonyl)pyrrolidin-2-yl)ethyl)piperidin-4-yl 4-fluorobenzoate, shown in Figure 5 as [<sup>18</sup>F]SB-269970 derivative, and [<sup>18</sup>F]2FP3 (Figure 5) which were both labeled from their respective nitro-precursors.<sup>69,70</sup> The first tracer was found to bind homogenously throughout the brain with no specific 5-HT<sub>7</sub> receptor binding<sup>69</sup> and [<sup>18</sup>F]2FP3 showed some promise in *in vivo* experiments in cats.<sup>71</sup> Blocking with SB-269970 found the [<sup>18</sup>F]2FP3 to be displaceable yet a lack of arterial input function ruled out quantification of the data.

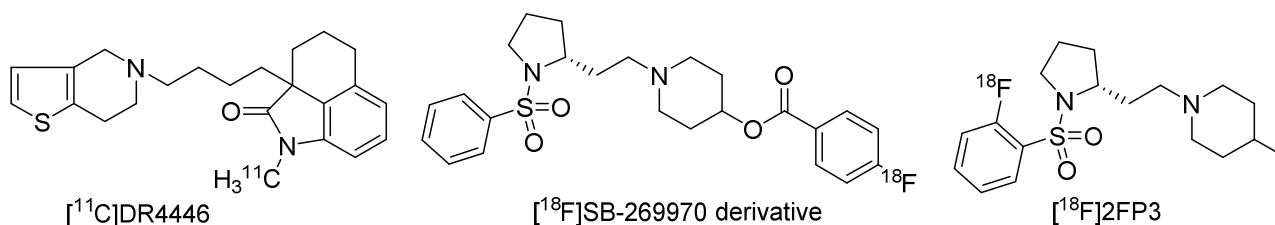


**Figure 5.** Structures of [<sup>11</sup>C]DR4446, [<sup>18</sup>F]SB-269970 derivative and [<sup>18</sup>F]2FP3.

Seven analogues of 2FP3 have likewise been synthesized. Their general structure is shown in Figure 6. [<sup>18</sup>F]4F3P3 and [<sup>18</sup>F]2F3P3 (Figure 6), the two compounds with the most promising in



in vitro profiles thereof, did not show brain uptake.<sup>72</sup> This is suspected to be on account of the tracers being substrate to efflux pumps in the brain.

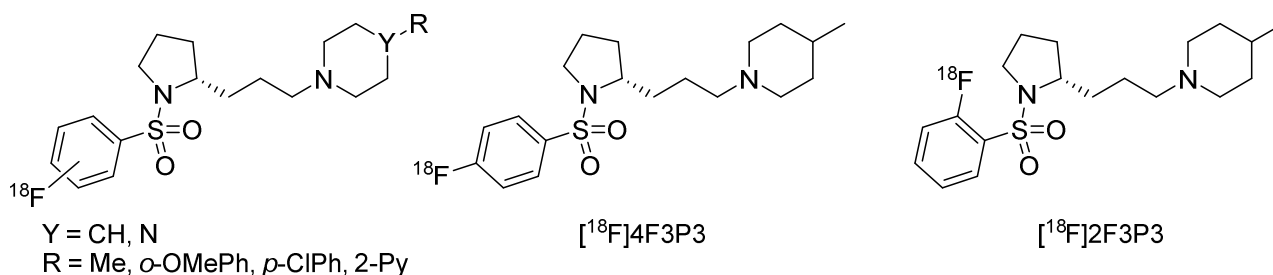


**Figure 6.** General structure of 2FP3 analogues and structures of [<sup>18</sup>F]4F3P3 and [<sup>18</sup>F]2F3P3.

Recently three Arylpiperazine (Figure 7) based ligands have been evaluated. Despite showing promising in vitro characteristics, two of the ligands did not exhibit sufficient brain penetration.<sup>73</sup> The last arylpiperazine crosses the BBB and displayed reversible tracer kinetics. Attempts at displacement with SB-269970 revealed limited displacement suggesting that the PET-ligand binds non-specifically.<sup>74</sup>

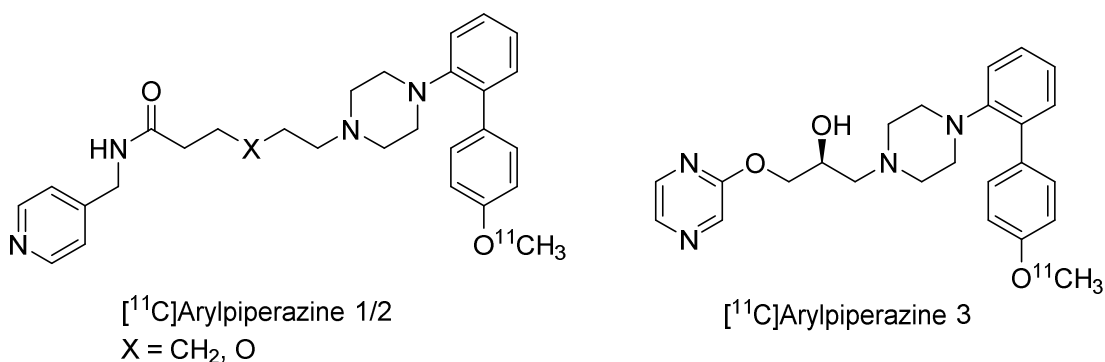


**Figure 7.** Structures of the three arylpiperazines.

In 2013, Shimoda et al reported the synthesis and evaluation of [<sup>11</sup>C]1-(2-(4-methoxyphenyl)phenyl)piperazine (Figure 8). Labeled from its desmethyl-precursor using [<sup>11</sup>C]MeI it enters the brain and has reversible kinetics but no specific binding was observed.<sup>75</sup>

A ligand developed in our group, [<sup>11</sup>C]Cimbi-806 (Figure 8), was likewise observed to enter the brain and displayed reversible kinetics yet lacked displacement when blocking with SB-269970 was attempted.<sup>76</sup> Finally, [<sup>11</sup>C]Cimbi-717 (Figure 8), a (phenylpiperazinyl-butyl)oxindole, has been evaluated. With penetration into the brain, reversible kinetics and displaceability it is to this date one of the promising candidates for a viable 5-HT<sub>7</sub> receptor PET-ligand.<sup>77</sup>

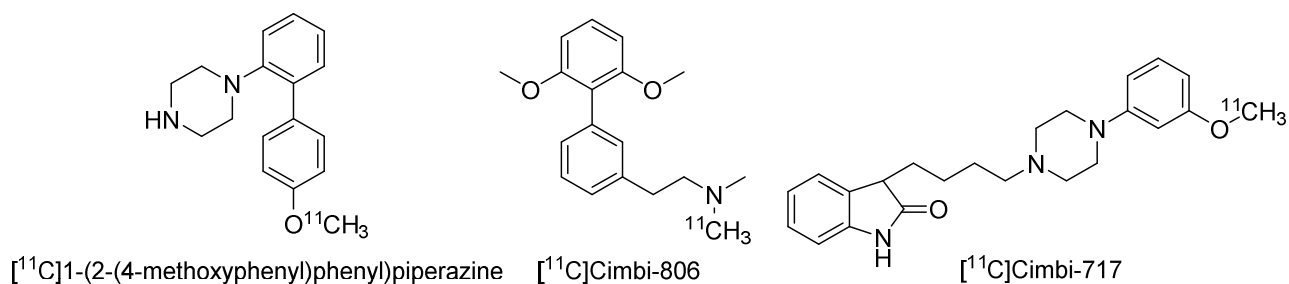


**Figure 8.** Structures of  $[^{11}\text{C}]1-(2-(4\text{-methoxyphenyl})\text{phenyl})\text{piperazine}$ ,  $[^{11}\text{C}]\text{Cimbi-806}$  and  $[^{11}\text{C}]\text{Cimbi-717}$ .

## 1.8 Organic chemistry VS radiochemistry

Several considerations have to be made when moving from synthesising precursors and references in the organic chemistry lab to the labeling of the radioactive tracer in the radiochemistry lab. Many of these revolve around the difference in scale on which one works in the two respective labs. The amount of radionuclide present when conducting the labeling of a tracer is typically in the pico to nano mole range. Therefore the precursor being labeled as well as any catalyst or reagents will be present in a vast excess. This has several implications. Minute amounts of impurities in precursor, reagents etc. which would normally have no significant impact on yields, can be detrimental if the impurity proves to be more reactive towards the radioactive synthon. The stoichiometric conditions during radiochemical experiments mean that most conditions can be considered pseudo first order. This makes optimisation of reaction conditions, before carrying out radioactive experiments, problematic. Finally the small amounts of product obtained, as well as safety concerns, usually rules out identification of the product via NMR spectroscopy. As such the identification is carried out through chromatographic means, either by high performance liquid chromatography (HPLC), gas chromatography (GC) or thin layer chromatography (TLC), using a cold (non-radioactive) reference compound (Figure 9).

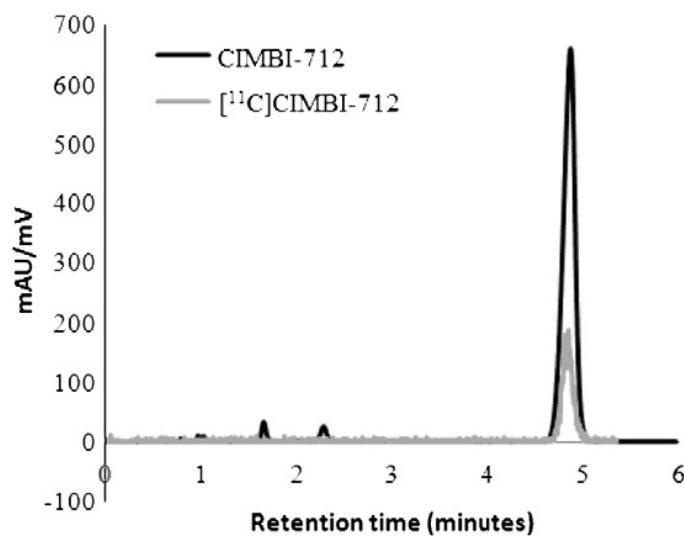


**Figure 9.** Example of identification of  $[^{11}\text{C}]$ Cimbi-712 by the use of HPLC and cold Cimbi-712. Source: Paper 1<sup>78</sup>

## 1.9 Primary and secondary $^{11}\text{C}$ -building blocks in radiochemistry

As shown in Table 1, cyclotron-generated Carbon-11 is primarily produced in the form of  $[^{11}\text{C}]\text{CO}_2$  and  $[^{11}\text{C}]\text{CH}_4$ . These primary  $^{11}\text{C}$ -building blocks will often have to be converted into a more reactive species to be viable for incorporation into a larger molecule. Of these the most common species is  $[^{11}\text{C}]\text{MeI}$ .<sup>79</sup>  $[^{11}\text{C}]\text{MeI}$  can be generated through two methods, known as the wet and gas-phase method respectively. The wet method utilises a two-step synthesis. First a reduction of  $[^{11}\text{C}]\text{CO}_2$  with LAH produces  $[^{11}\text{C}]\text{MeOH}$ , which can then be converted into  $[^{11}\text{C}]\text{MeI}$  using HI.<sup>80</sup> Finally it is dried and separated from side products. The gas phase method uses a radical reaction between  $[^{11}\text{C}]\text{CH}_4$  and  $\text{I}_2$  at 700-750 °C.<sup>81</sup>  $[^{11}\text{C}]\text{MeI}$  can be further converted into  $[^{11}\text{C}]\text{MeOTf}$  using AgOTf at 200 °C.<sup>44</sup> Despite being the most commonly used secondary  $^{11}\text{C}$ -building blocks,  $[^{11}\text{C}]\text{MeI}$  and  $[^{11}\text{C}]\text{MeOTf}$  are not the only secondary building blocks that can be formed from  $[^{11}\text{C}]\text{CO}_2$  and  $[^{11}\text{C}]\text{CH}_4$  (Figure 10). Through treatment with Grignard reagents it is possible to form  $^{11}\text{C}$ -carboxylic acids from  $[^{11}\text{C}]\text{CO}_2$  which can be further converted into acyl chlorides.<sup>44</sup>  $[^{11}\text{C}]\text{CO}$  can be formed from  $[^{11}\text{C}]\text{CO}_2$  by reduction of  $[^{11}\text{C}]\text{CO}_2$  over zinc at 380-400 °C or over molybdenum at 850 °C.<sup>82</sup>  $[^{11}\text{C}]\text{CH}_4$  can be converted into  $[^{11}\text{C}]\text{HCN}$  by reaction with  $\text{NH}_3$  over platinum.<sup>83</sup>

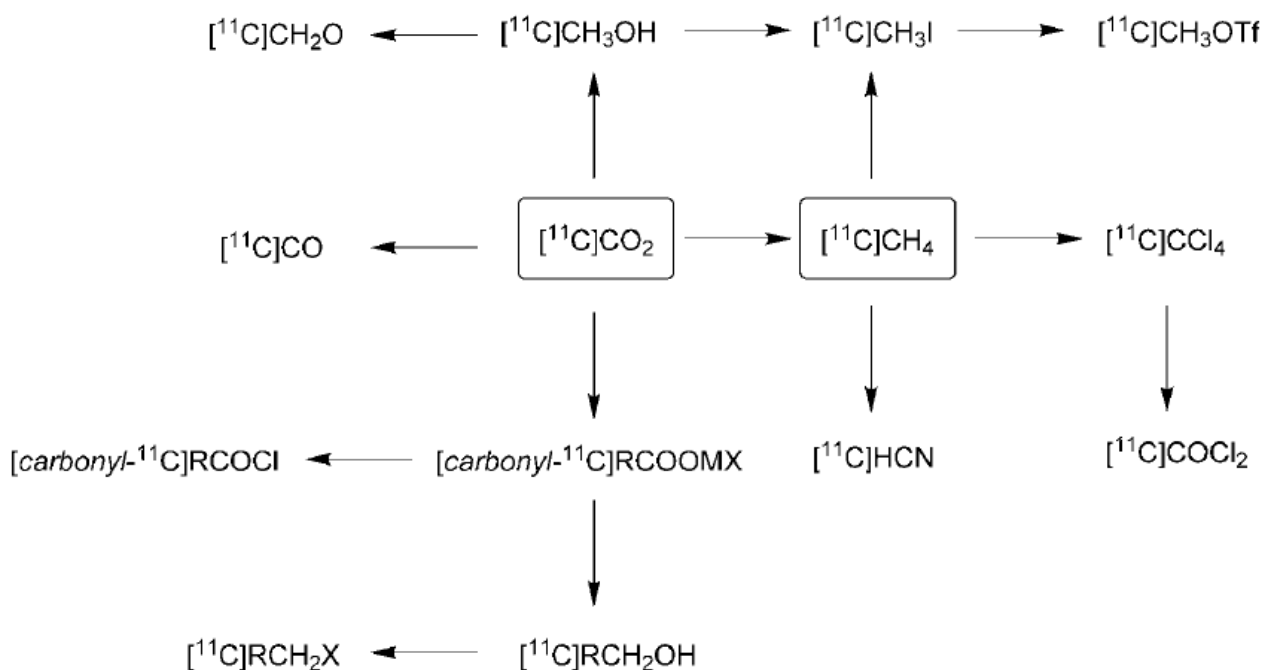


**Figure 10.** Various  $^{11}\text{C}$ -building blocks which can be formed from  $[^{11}\text{C}]\text{CO}_2$  or  $[^{11}\text{C}]\text{CH}_4$ . Source: Miller et al. 2008<sup>44</sup>

## 1.10 Cross-couplings in $^{11}\text{C}$ -radiochemistry

The most commonly applied method in  $^{11}\text{C}$ -labeling is the  $^{11}\text{C}$ -methylation of nucleophiles, such as alcohols, amines and thiols, using  $[^{11}\text{C}]\text{MeI}$  or  $[^{11}\text{C}]\text{MeOTf}$ . This approach has certain advantages and disadvantages. On account of its extensive usage, the reaction methodology is well established and a set of successful labeling conditions can usually be found easily. The ease with which amines, alcohols and thiols can be labeled often makes the use of protection groups a necessity to avoid side-reactions. This on the other hand introduces another step in the radiosynthesis of the labeled compound thereby increasing the overall synthesis time as well as introducing another point at which the labeling procedure can fail. As with any approach, the existence of a compound with a suitable motif, in this case O-, N- or S-methyl, is a prerequisite for the development of a PET-tracer. In the pursuit of a larger range of possible motifs, a multitude of other reactions have been investigated to evaluate their applicability in radiochemistry. Several of these reactions belong to the same reaction type: cross-couplings. The first application of cross-couplings in radiochemistry was reported in 1995. Andersson et al. reported the synthesis of  $[^{11}\text{C}]\text{toluene}$ , methyl 4- $[^{11}\text{C}]\text{methylbenzoate}$  and 3- $[^{11}\text{C}]\text{propene}$  from stannyl precursors as well as the synthesis of

[ $^{11}\text{C}$ ]heptane from a trialkylborane precursor.<sup>84</sup> Following this publication the Stille reaction has received the most attention of the two. Two years later a general method was published using  $\text{Pd}_2\text{dba}_3$  and  $\text{P}(o\text{-tolyl})_3$  in DMF with  $\text{CuCl}$  and  $\text{K}_2\text{CO}_3$ .<sup>85</sup> The Stille reaction has also been shown to be applicable when the introduction of a [ $^{11}\text{C}$ ]carbonyl group is desirable.<sup>86,87</sup> The Stille reaction has been used to label several biologically active compounds such as: [ $^{11}\text{C}$ ]CHIBA-1001 an  $\alpha_7$  ligand, [ $p\text{-}^{11}\text{C}\text{-methyl}$ ]MADAM a SERT ligand and [ $^{11}\text{C}$ ]celecoxib a COX-2 ligand (Figure 11).<sup>88-90</sup>

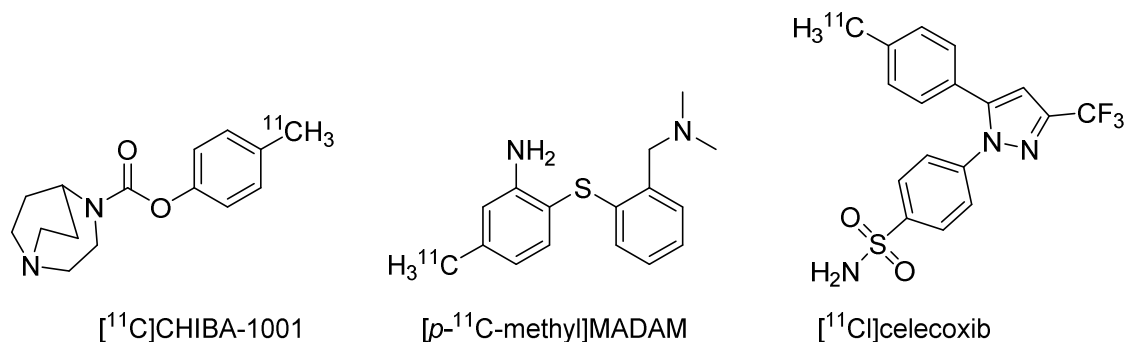


**Figure 11.** Structures of [ $^{11}\text{C}$ ]CHIBA-1001, [ $p\text{-}^{11}\text{C}\text{-methyl}$ ]MADAM and [ $^{11}\text{C}$ ]celecoxib.

The Suzuki reaction has received less attention than the Stille reaction following the initial publication in 1995. None the less two groups have published approaches to a general procedure, one utilising microwave heating, one using conventional heating, with the latter getting the best overall yields.<sup>91,92</sup> Like the Stille reaction, the reaction was found to give high yields when using  $\text{Pd}_2\text{dba}_3$ ,  $\text{P}(o\text{-tolyl})_3$  and  $\text{K}_2\text{CO}_3$  in DMF. Both publications found the reaction tolerates a wide array of functional groups but also that the performing the oxidative addition to palladium before adding boronic species was crucial to ensuring high and reproducible radiochemical yields (RCY's). Furthermore the Suzuki reaction has been utilised in the introduction [ $^{11}\text{C}$ ]carbonyl groups.<sup>93</sup> The Suzuki reaction has also been applied to several biologically active compounds. Examples are: [ $^{11}\text{C}$ ]dehydropravastatin a ligand for OATP1B1 and MRP2 in the liver and [ $^{11}\text{C}$ ]MENET a ligand for the norepinephrine transporter (Figure 12).<sup>94,95</sup>

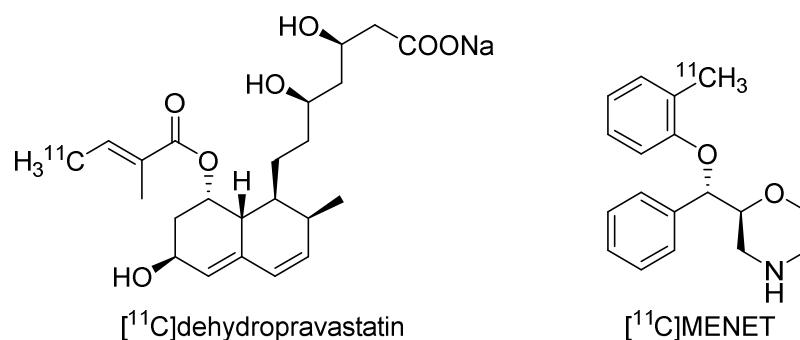


**Figure 12.** Structures of  $[^{11}\text{C}]$ dehydropravastatin and  $[^{11}\text{C}]$ MENET.

In 2000 Björkman and Långström added the Heck reaction to the roster of cross-couplings used in radiochemistry. By reacting benzaldehyde with  $[^{11}\text{C}]\text{CH}_3\text{I}$  in a Wittig reaction followed by Heck reaction with a series of arylhalides they were able to synthesize a range of  $^{11}\text{C}$ -labeled functionalised olefins.<sup>96</sup>

The labeling of  $17\alpha$ -(3'- $[^{11}\text{C}]$ prop-1-yn-1-yl)-3-methoxy- $3,17\beta$ -estradiol displayed the use of the Sonogashira reaction in radiochemistry. By using  $\text{Pd}_2\text{dba}_3$ ,  $\text{AsPh}_3$  and TBAF in THF at  $60^\circ\text{C}$  it was possible to label the  $17\alpha$ -estradiol analogue in 49-64% RCY.<sup>97</sup>

Finally in 2013 Kealey et al. were the first to apply the Negishi reaction. Using rieke zinc they were able to label a variety of arylhalides as well as the metabotropic glutamate receptor subtype 5 ligand MPEP (Figure 13). Interestingly they found that, in contrast to what was observed by Hostetler et al. and Doi et al. in the Suzuki reaction, addition of  $[^{11}\text{C}]\text{MeI}$  before adding the zinc species had a negative effect on RCY's.<sup>98</sup>

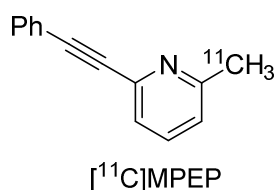


**Figure 13.** Structure of  $[^{11}\text{C}]$ MPEP.

A common denominator between the various cross-couplings described herein is that they are all Pd-mediated rather than catalyzed. For example, the Suzuki reaction has a circular mechanism with three key steps: Oxidative addition, transmetalation and reductive elimination (Figure 14). By the end of the cycle Pd has been regenerated and can thus undergo reaction once more. This allows the use of Pd in catalytic amounts. When utilized in radiochemistry, the stoichiometric ratios mentioned

in chapter 1.8 means that Pd will be present in excess compared to  $[^{11}\text{C}]\text{MeI}$ . Therefore the mechanism has to be thought of as step by step rather than circular (Figure 14). Thus giving rise to the reactions being Pd-mediated rather than catalyzed.

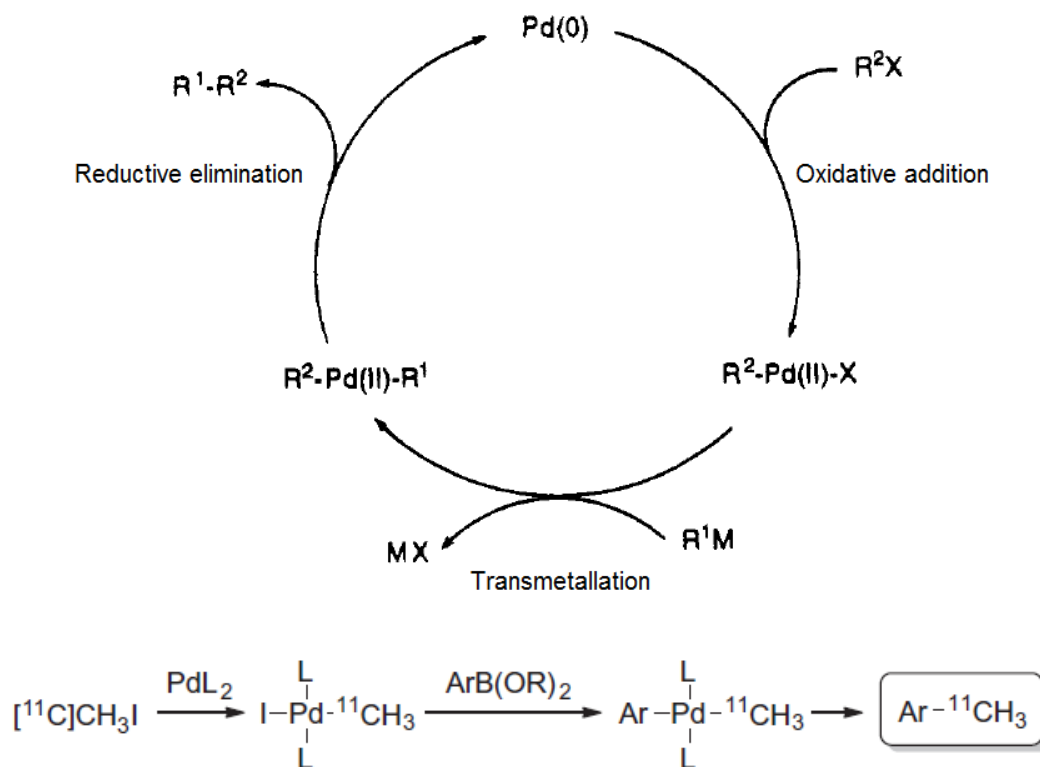


**Figure 14.** Top: Classical catalytic cycle. Modified from Miyaura et al.<sup>99</sup> Bottom: Step by step mechanism of Pd-mediated Suzuki reaction. Source: Paper I<sup>78</sup>

## 2 Aims

The aims of this thesis have been twofold.

1. To synthesise and label potential 5-HT<sub>7</sub> receptor PET-ligands for *in vivo* evaluation.

This aim can furthermore be split up in accordance with the potentials of a 5-HT<sub>7</sub> receptor PET-ligand: As a tool for receptor quantification or as a tool for measuring endogenous 5-HT.

A compound group of interest is the (phenylpiperazinyl-butyl)oxindoles, on account of their affinity and selectivity for the 5-HT<sub>7</sub> receptor. Herein three interesting compounds have been identified, Cimbi-712, Cimbi-772 and Cimbi-775 (Figure 15).

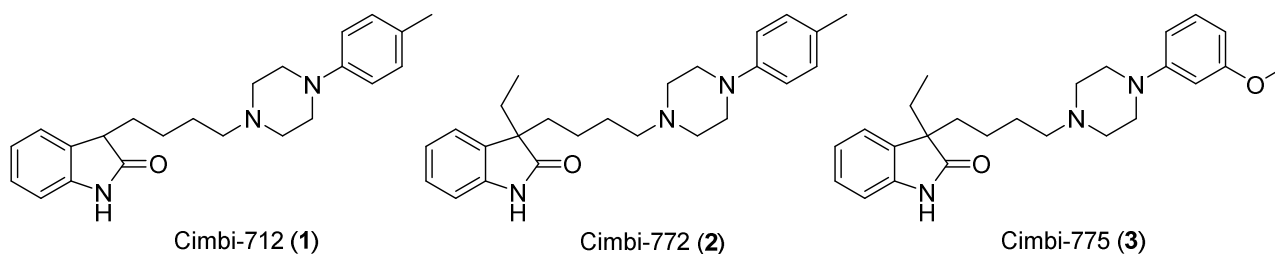


**Figure 15.** Structures of Cimbi-712, Cimbi-772 and Cimbi-775.

Furthermore the agonist E-55888 (Figure 16) shows a high affinity and selectivity for the 5-HT<sub>7</sub> receptor and could thus potentially be suitable as a PET-ligand.

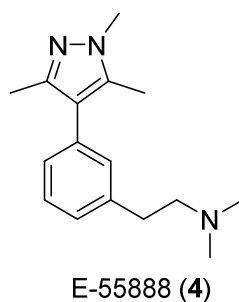


**Figure 16.** Structure of E-55888.

Cimbi-712, Cimbi-772 and E-55888 all contain methyl-groups, inaccessible via conventional O-, N- or S-methylation. These methyl groups could potentially be labeled via the Suzuki reaction. At the current time it was uncertain whether the Suzuki reaction tolerated amine motifs in its substrates when applied in radiochemistry, giving rise to the second aim of this thesis.



2. To investigate and develop a method by which the Suzuki reaction can be applied to amine containing compounds and furthermore to apply this method in the labeling of biologically active compounds and potential 5-HT<sub>7</sub> receptor PET-ligands.

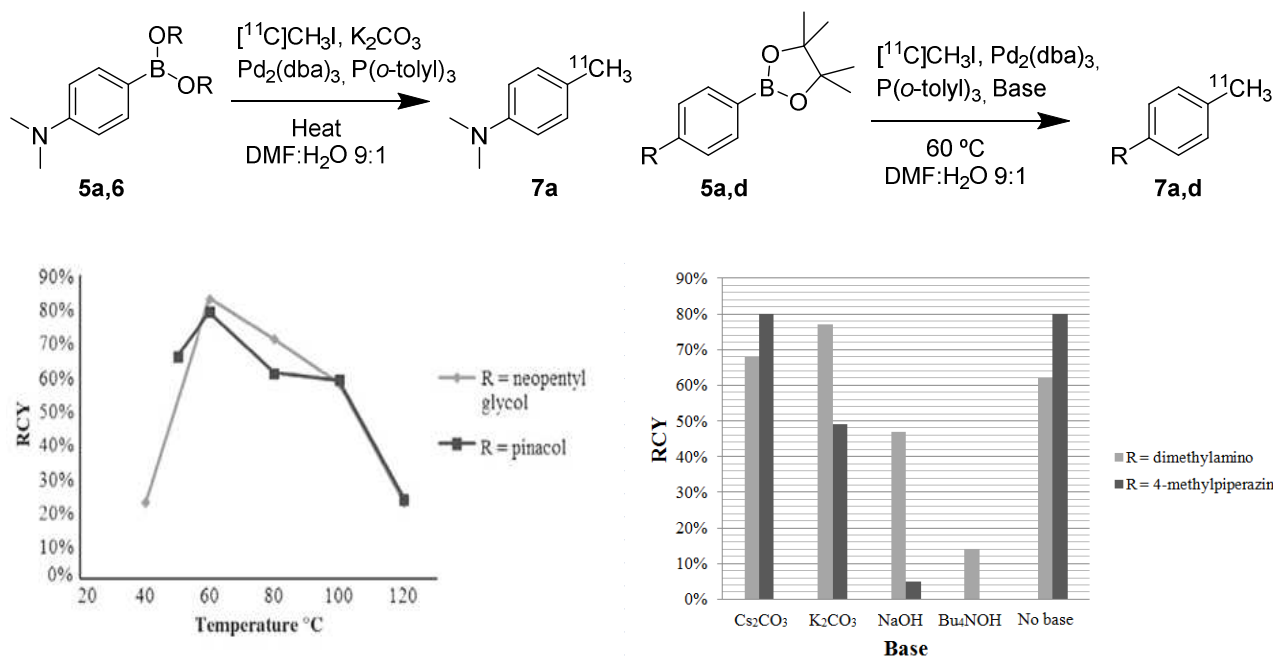
As the labeling method described in aim two was instrumental in the labeling of several compounds in this thesis it is described as the first chapter in the results and discussion.

## 3 Results and discussion

### 3.1 Labeling of amine containing model compounds

Cimbi-712 and Cimbi-772 are compounds with potential as 5-HT<sub>7</sub> receptor PET-ligands. They contain a tolyl motif, tertiary amines and no motifs viable for conventional O-, N- or S-methylation. They could thus potentially be labeled via the Suzuki reaction. At the current time the applicability of the Suzuki reaction to compounds containing amines was uncertain. Hostetler et al. and Doi et al. have both reported that reaction between [<sup>11</sup>C]CH<sub>3</sub>I and palladium catalyst, before addition of boronic precursor to the reaction, is crucial to ensure successful labeling.<sup>92,91</sup> As described in chapter 1.10 the stoichiometric ratio between [<sup>11</sup>C]CH<sub>3</sub>I and palladium catalyst means that the reaction has to be thought of as palladium-mediated rather than catalysed. As such the regular steps in the catalytic cycle can be considered as individual steps (Figure 14). This led to the hypothesis that by “trapping” [<sup>11</sup>C]CH<sub>3</sub>I as an [<sup>11</sup>C]CH<sub>3</sub>-Pd-I complex it should be possible to carry out Suzuki reactions in the presence of free amines. To test this hypothesis a set of standard conditions was devised through experimentation with different reaction variables such as temperature, base, palladium catalyst and the use of conventional heating versus heating by microwave. These standard conditions would then be used to label a series of model compounds containing different amine motifs.

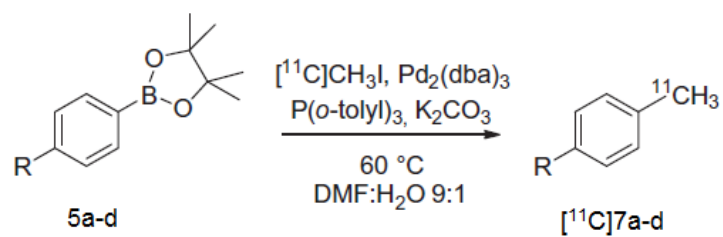
Investigating the impact of the chosen palladium catalysts found a combination of Pd<sub>2</sub>dba<sub>3</sub> and P(*o*-tolyl)<sub>3</sub> 1:2 to be the only system that gave any significant yields. The reaction temperature had a large impact on the reaction yields, with a reaction temperature of 60 °C being optimal, whereas the choice of boronic ester was found to be largely irrelevant (Figure 15).

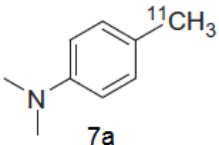
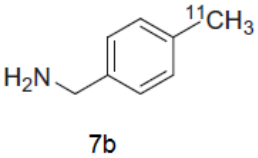
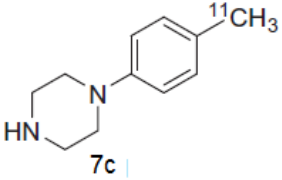
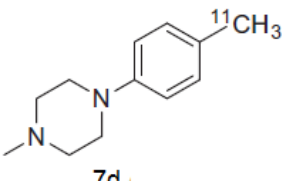


**Figure 15.** Left: Impact of temperature and boronic ester species on yield. Right: Impact of base on yield. Modified from paper I<sup>78</sup>

Just like temperature, base was found to have a large effect on the yield. In general weak bases gave higher yields than strong bases with the optimal setup being very substrate dependent. In this range of experiments it was also discovered that the labeling could be carried out without adding any additional base showing that the precursor can act as its own base, likely on account of the large excess of precursor compared to the amount of [<sup>11</sup>C]CH<sub>3</sub>I. Thus Cs<sub>2</sub>CO<sub>3</sub>, K<sub>2</sub>CO<sub>3</sub> and no added base gave highest yields. Of these K<sub>2</sub>CO<sub>3</sub> was used as the standard base making the standard conditions: 60 °C, Pd<sub>2</sub>dba<sub>3</sub> + P(*o*-tolyl)<sub>3</sub> and K<sub>2</sub>CO<sub>3</sub>. Using these standards a series of compounds, containing various amine motifs. In this setup conventional heating was compared to heating by microwave. Yields were very substrate dependent with conventional heating giving RCY's of 49-82% and microwave heating giving RCY's of 5-86% (Table 2). Substrate reactivities for conventional heating were **7b** > **7a** > **7c** > **7d** whereas heating by microwave showed the reverse order of reactivity.

**Table 2.** Labeling of model compounds containing varying amine motifs. Modified from Paper I<sup>78</sup>



Entry	Product	RCY (%) conventional heating	RCY (%) MW heating
1	 7a	77	54
2	 7b	82	5
3	 7c	64	77
4	 7d	49	86

## 3.2 [<sup>11</sup>C]Vortioxetine

The drug vortioxetine (Brintellix®) is marketed in its cold form as a treatment for MDD. Vortioxetine contains a 2,4-dimethylbenzene motif and could thus potentially be labeled via the method devised in the previous chapter (Figure 16). Potential labeling sites are ortho and para to the thioether (Figure 16). Vortioxetine contains a secondary amine in the piperazine moiety which could cause problems with side reactions in the form of N-methylation. If [<sup>11</sup>C]MeI is not sufficiently “trapped” in an [<sup>11</sup>C]-Pd-I complex residual amounts of [<sup>11</sup>C]MeI would result in a <sup>11</sup>C-N-methylated byproduct.

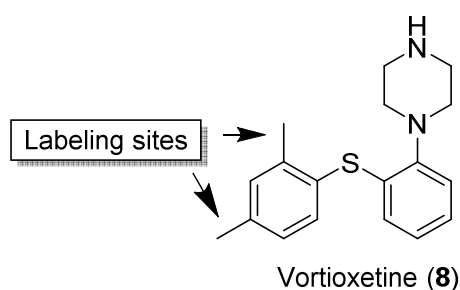
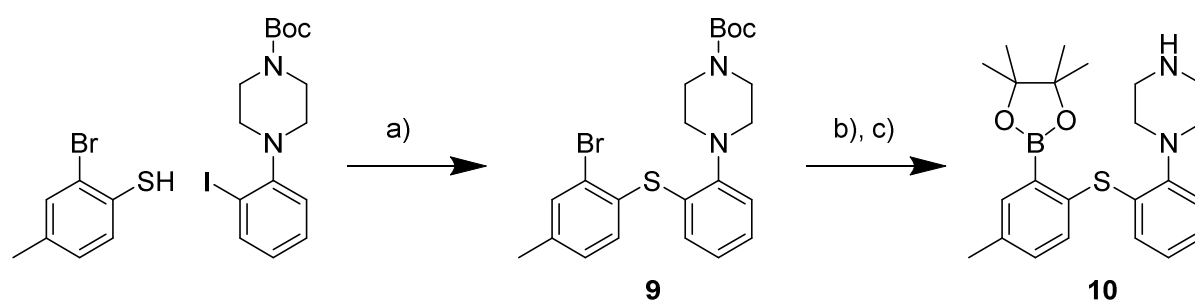


**Figure 16.** Structure of vortioxetine (**8**) and possible labeling sites.

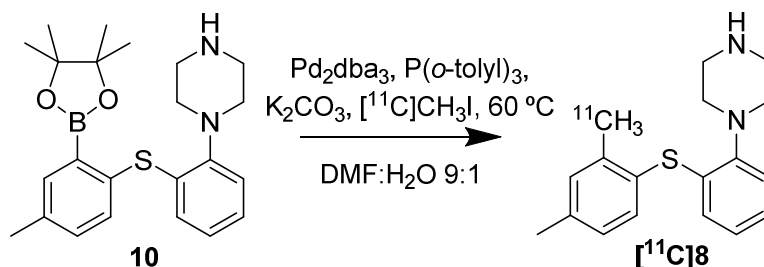
On account of problematic precursor synthesis, labeling of the ortho position was chosen. The precursor was synthesized in a three step synthesis (scheme 2).



**Scheme 2.** Synthesis of **10**. a) Pd2dba3, DPEphos, t-BuOK, toluene, 100 °C (MW), 30 min, 81%; b) bis(pinacolato)diboron, Pd(dppf)Cl<sub>2</sub>, KOAc, 1,4-dioxane, 100 °C, 12 h; c) TFA, CH<sub>2</sub>Cl<sub>2</sub>. Yield of b,c) combined: 32%.

Starting from 2-bromo-4-methylbenzenethiol and tert-butyl 4-(2-iodophenyl)piperazine-1-carboxylate a thioether was formed via a palladium mediated reaction. Palladium catalyzed insertion of a boronic pinacol ester followed by liberation of the free amine by boc-deprotection yielded the precursor (**10**) in an overall yield of 25.9%. The two initial steps were to varying extent

hampered by a tendency towards debromination. Dry solvents and rigorous degassing was found to be crucial in preventing this side reaction. Labeling of the compound was carried out with the conditions from chapter 3.1 (scheme 3).



**Scheme 3.** Labeling of [ $^{11}\text{C}$ ]Vortioxetine.

RCY's, as determined by analytical high performance liquid chromatography (HPLC), was in the range of 40%. Synthesis and purification by preparative HPLC gave an isolated RCY's of 161.4-346 MBq with an  $A_s$  of 8-478 GBq/ $\mu\text{mol}$  ( $n = 2$ ) and radiochemical purity (RCP) of >97% from a 40 min irradiation. During the labeling process it was discovered that the state of the Pd- and ligand-source is crucial. In several cases a second product was formed, presumably the N-methylated species rather than the cross-coupled product. This was investigated by carrying out the reaction without palladium thus making N-methylation the only possible reaction (Figure 17). Acquisition of new Pd-source as well as new ligand re-established the cross-coupled product as the product.

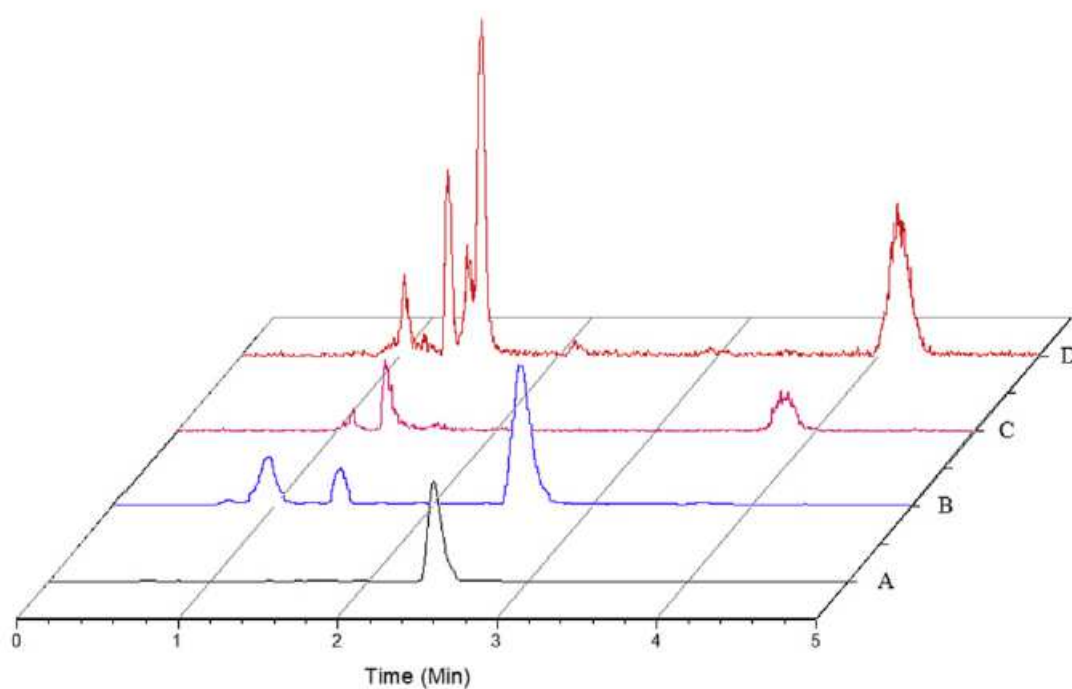


**Figure 17.** Effect of the state of the palladium ligand combination on the amount of N-methylation. (A) Reference spectrum of **8** (with UV-detection). (B) Successful  $^{11}\text{C}$ -labeling of **8**. (C) Unsuccessful  $^{11}\text{C}$ -labeling of **8** – product with retention time ~4 min presumably the N-methylated precursor. (D) No Pd catalyst added – product with retention time ~4 min presumably the N-methylated precursor. Conditions: MeCN: Borax buffer 0.01 M 80:20, Luna 5  $\mu\text{m}$  C18 100  $\text{\AA}$  column (150 x 4.6 mm.), flowrate: 2 mL/min. Modified from: Paper III<sup>100</sup>

$^{[11}\text{C}]$ Vortioxetine's potential as a PET-ligand was evaluated in a Danish landrace pig. From the affinity profile of vortioxetine (Table 3) one would expect to observe binding in striatum, cortex, hippocampus and thalamus.<sup>77,101</sup> The PET-scan revealed a rapid brain uptake with slow tracer washout and binding in thalamus, cortex, hippocampus, striatum and cerebellum (Figure 18). Binding in cerebellum was unexpected as none of the compounds' targets are reported as having high densities in this part of the brain. A possible explanation could be binding of metabolites. Determination of radioactive metabolites was hampered by low amounts of activity. As such the involvement of metabolites is uncertain.

**Table 3.** Affinities of vortioxetine towards various 5-HT targets. Source: Paper 3<sup>100</sup>

Target	Mode of action	Affinity ( $K_i$ , nM)
5-HTT	inhibitor	1.6
5-HT <sub>1A</sub>	agonist	15
5-HT <sub>1B</sub>	partial agonist	33
5-HT <sub>3A</sub>	antagonist	3.7
5-HT <sub>7</sub>	antagonist	19

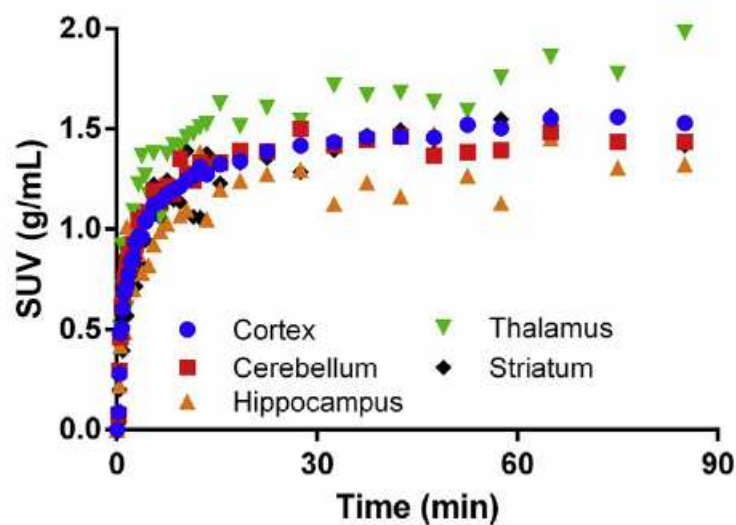
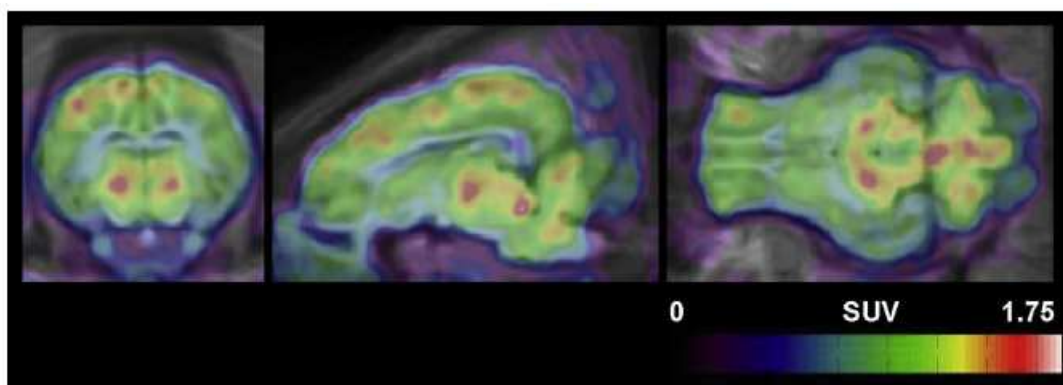


**Figure 18.** Top: Coronal, sagittal and transverse (left to right) Summed PET images (0-90 min, 3 mm Gaussian filtering) of [<sup>11</sup>C]Vortioxetine in the pig brain. Bottom: Time-activity curves showing absolute radioligand uptake for the indicated brain regions. SUV: standardized uptake value. Source: Paper III<sup>100</sup>

The wide range of different targets as well as slow tracer kinetics makes [<sup>11</sup>C]Vortioxetine unsuitable as a tracer for the imaging of the 5-HT<sub>7</sub> receptor. Despite being unsuitable as a 5-HT<sub>7</sub>



receptor PET-ligand, [ $^{11}\text{C}$ ]vortioxetine could be a valuable tool in the further elucidation of Vortioxetines effect on MDD.

### 3.3 [ $^{11}\text{C}$ ]Cimbi-712, [ $^{11}\text{C}$ ]Cimbi-772 and [ $^{11}\text{C}$ ]Cimbi-775

In 2008 Volk et al. published a series of compounds, (phenylpiperazinyl-butyl)oxindoles, displaying high affinity for the 5-HT<sub>7</sub> receptor.<sup>38</sup> These compounds were reported as showing antagonistic properties. Previous work in our group by Herth et al.<sup>102</sup> endeavored to introduce labelable moieties into this group of compounds whilst maintaining a high affinity for the 5-HT<sub>7</sub> receptor. Two compounds with particular promise were identified, **1** and **11** also known as Cimbi-712 and Cimbi-717 respectively (Figure 19). Cimbi-717 had already been tested *in vivo* and displayed a rapid brain uptake as well as reversible kinetics and decrease in binding under pretreatment with the antagonist SB-269970. As Cimbi-712 displays a slightly higher affinity towards the 5-HT<sub>7</sub> receptor than Cimbi-717<sup>102</sup> it ought to show promise as a PET-tracer.

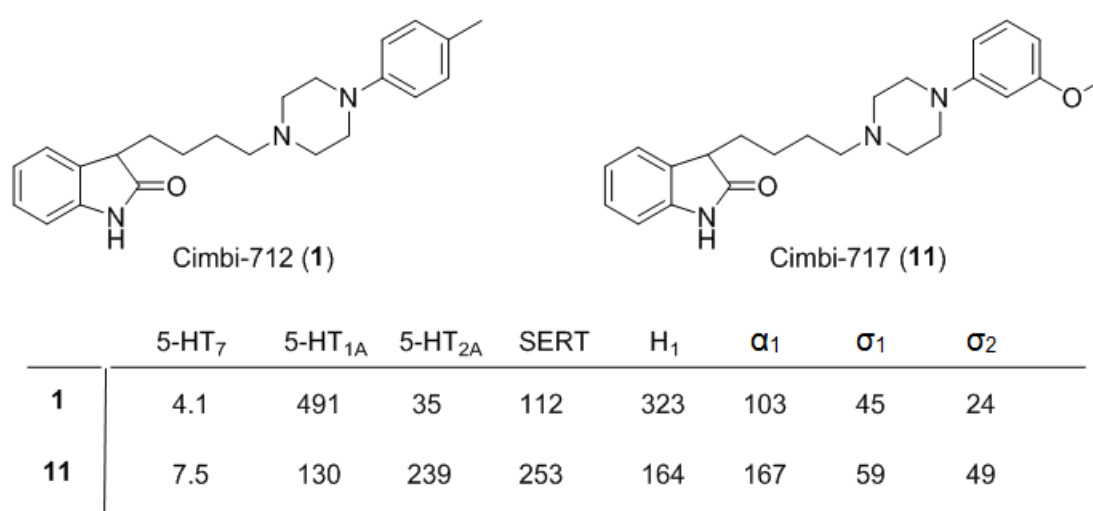
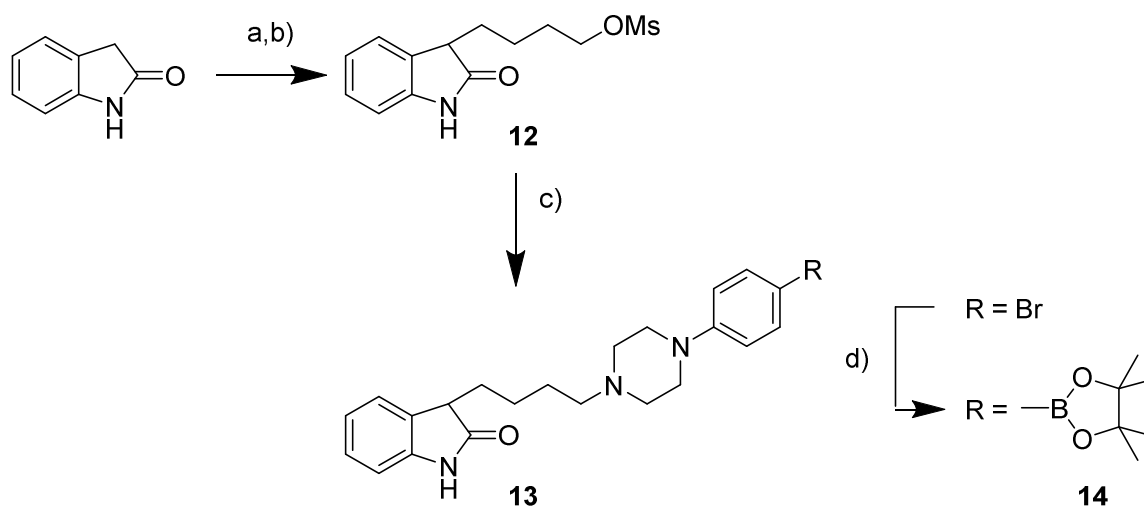


**Figure 19.** Structures of Cimbi-712 and Cimbi-717 and their affinities as K<sub>i</sub> in nM. H<sub>1</sub>: Histamine-1 receptor, α<sub>1</sub>: Alpha-1 adrenergic receptor, α<sub>2</sub>: Alpha-2 adrenergic receptor, σ<sub>1</sub>: Sigma-1 receptor.

Cimbi-712 is with its 4-methyl group viable for labeling via the Suzuki reaction. Synthesis of precursor were based on the formation of 4-(2-oxindolin-3-yl)butyl methanesulfonate (**12**). By reacting **12** with 1-(4-bromophenyl)piperazine **13** was formed. **13** could then be converted into the precursor (**14**) using a palladium catalyzed boronic ester insertion (Scheme 4).



**Scheme 4.** Synthesis of precursor of Cimbi-712. a) 1,4-butanediol, Raney-Nickel, 200 °C, 12 h, 70%; b) MeSO<sub>2</sub>Cl, Et<sub>3</sub>N, THF, -78 °C to rt, 2 h; c) 1-(4-bromophenyl)piperazine, Na<sub>2</sub>CO<sub>3</sub>, 130 °C, 55%; d) bis(pinacolato)diboron, Pd(dppf)Cl<sub>2</sub>, KOAc, 1,4-dioxane, 100 °C, 12 h, 54%.

Labeling of the corresponding boronic precursor, via the Suzuki reaction, yielded [<sup>11</sup>C]Cimbi-712 with a RCY of 30% as determined by HPLC-analysis. Synthesis followed by HPLC purification yielded 0.3-0.5 GBq with an A<sub>s</sub> of 57-224 GBq/μmol and a RCP >98% from a 40 min irradiation. [<sup>11</sup>C]Cimbi-712 was evaluated in Danish landrace pigs. Following i.v. injection, high brain uptake was observed with slow tracer kinetics. The highest uptake was observed in thalamus and the lowest in cerebellum. This binding profile is in accordance with [<sup>3</sup>H]SB-269970 determination of 5-HT<sub>7</sub> receptor densities in the pig brain.<sup>77</sup> A blocking study using the compound SB-269970 showed a decreased binding in both thalamus and cerebellum (Figure 20). As such Cimbi-712 was found to be inferior to Cimbi-717 as candidate for a 5-HT<sub>7</sub> receptor PET-ligand on account of its slow kinetics.

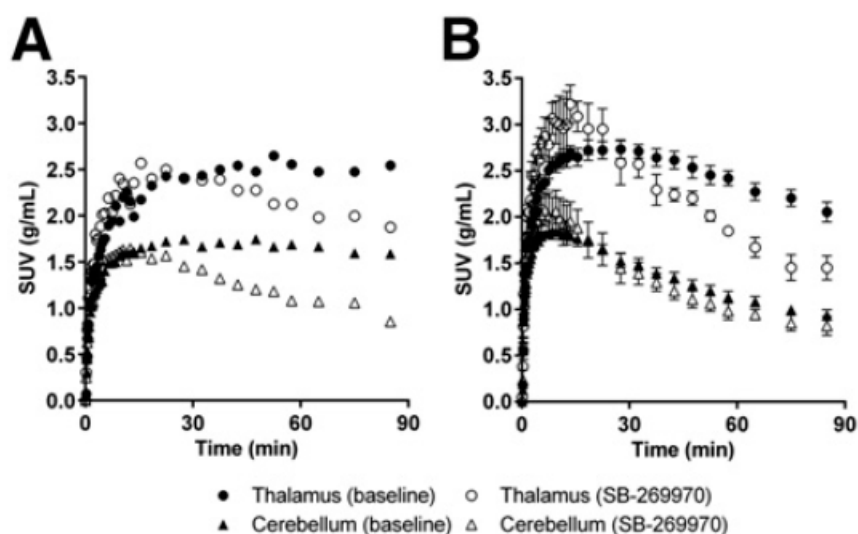


**Figure 20.** (A) Time-activity curves for [ $^{11}\text{C}$ ]Cimbi-712 at baseline ( $\bullet$  and  $\blacktriangle$ ,  $n = 2$ ) and after blocking with 1.0 mg/kg/h SB-269970 ( $\circ$  and  $\triangle$ ,  $n = 2$ ). (B) Time-activity curves for [ $^{11}\text{C}$ ]-Cimbi-717 at baseline ( $\bullet$  and  $\blacktriangle$ ,  $n = 6$ ) and after blocking with 1.0 mg/kg/h SB-269970 ( $\circ$  and  $\triangle$ ,  $n = 6$ ). Modified from Paper II<sup>77</sup>

Cimbi-712 has a chiral center at the oxindole 3-position, making the evaluated [ $^{11}\text{C}$ ]Cimbi-712 a racemate and thus technically two different compounds mixed together. To evaluate any potential difference between the R- and S-form the racemate of Cimbi-712 were separated into its enantiomers (Figure 21). Upon purification, the enantiomers were found to racemise within 5 minutes making evaluation of the different enantiomers impossible. The racemization could be explained by the acidity of the proton in the oxindole 3-position. Deprotonation will leave a planar carbanion which can be reprotonated from either side yielding either the R- or S-enantiomer.

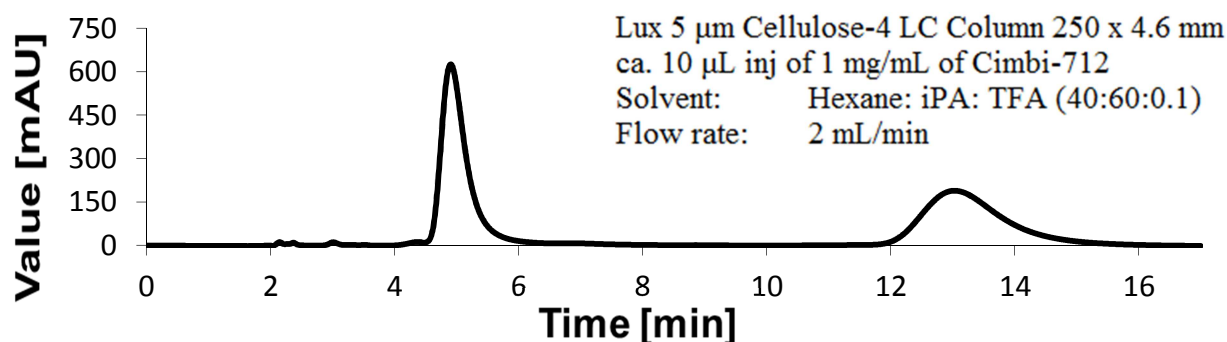


**Figure 21.** Enantiomeric separation of Cimbi-712. Racemization was observed upon immediate reinjection of an isolated peak.

By blocking the oxindole 3-position with an aliphatic side-chain this racemization should be preventable as the formation of a carbanion is no longer possible. With this intent the ethyl substituted derivatives, Cimbi-772 (**2**) and Cimbi-775 (**3**), were chosen for labeling and *in vivo* evaluation (Figure 22).

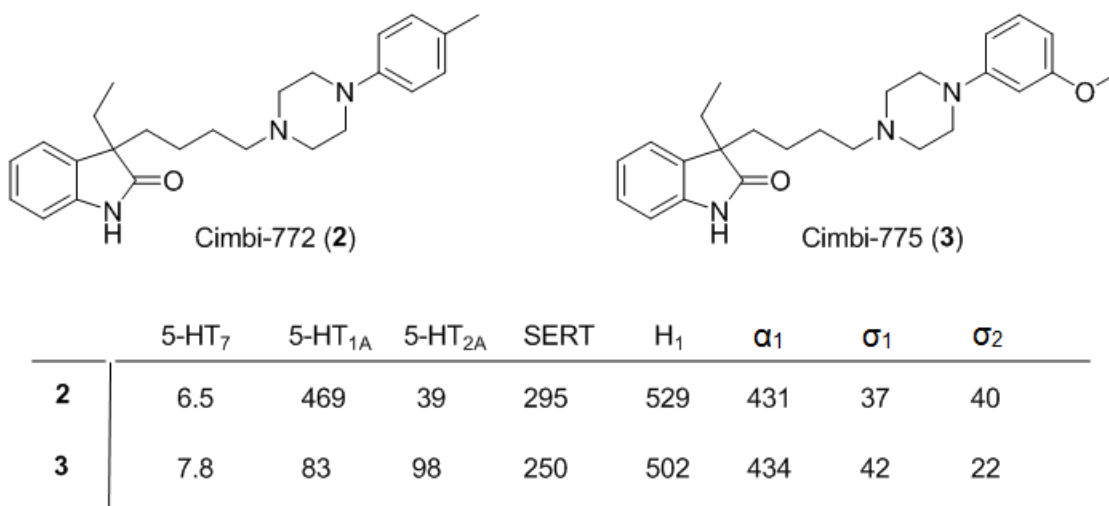
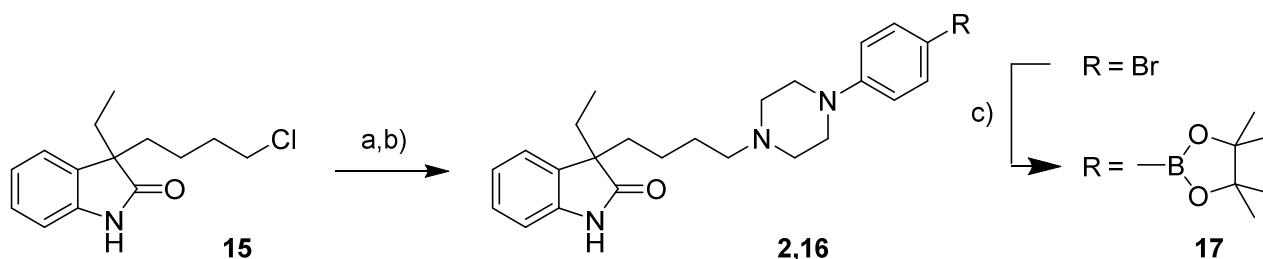


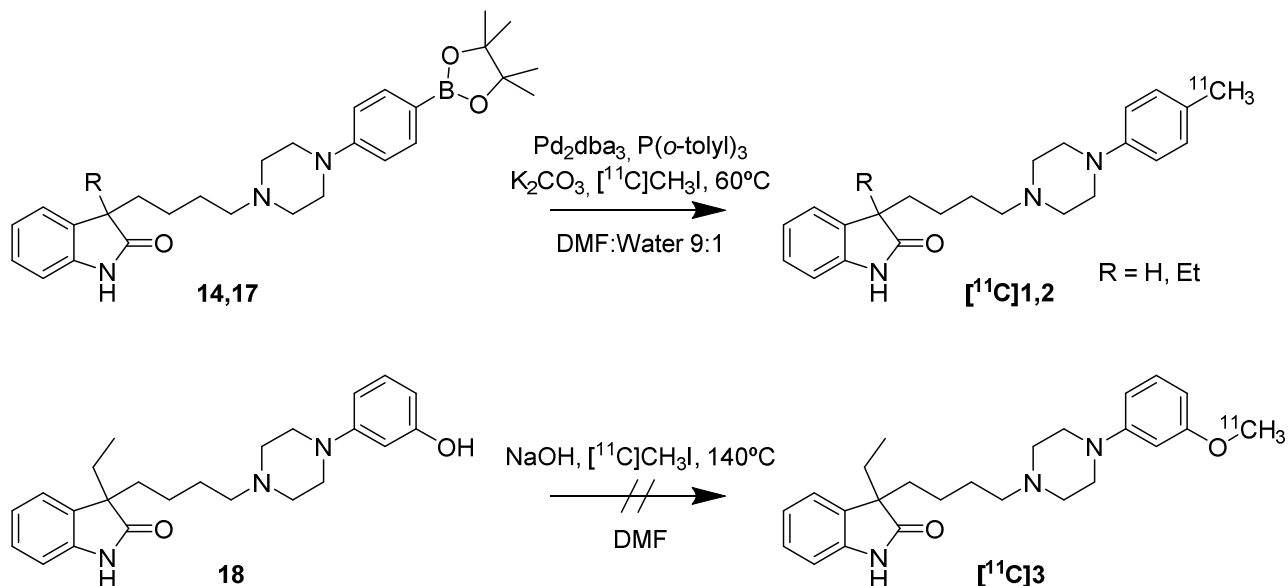
**Figure 22.** Structures of Cimbi-772 and Cimbi-775 and their affinities as  $K_i$  in nM. H<sub>1</sub>: Histamine-1 receptor, α<sub>1</sub>: Alpha-1 adrenergic receptor, α<sub>2</sub>: Alpha-2 adrenergic receptor, σ<sub>1</sub>: Sigma-1 receptor.

Precursor and reference of Cimbi-772 were synthesized from 3-(4-chlorobutyl)-3-ethylindolin-2-one (**15**) in a two and one step reaction respectively. By reacting **15** with 1-(4-bromophenyl)piperazine, 3-(4-(4-(4-bromophenyl)piperazin-1-yl)butyl)-3-ethylindolin-2-one (**16**) could be formed. Palladium catalyzed boronic ester insertion would then yield the precursor (**17**). Reaction between **15** and 1-(*p*-tolyl)piperazine yielded the reference compound (**2**) (Scheme 5).



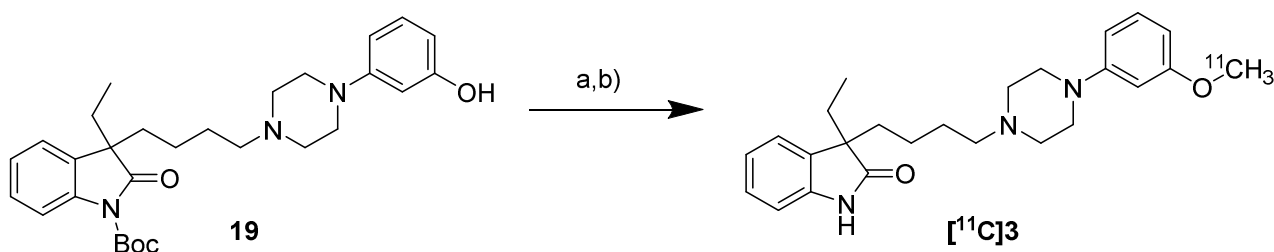
**Scheme 5.** Synthesis of Cimbi-772 and its precursor. a) 1-(*p*-tolyl)piperazine, Na<sub>2</sub>CO<sub>3</sub>, 130 °C, 66.9%; b) 1-(4-bromophenyl)piperazine, Na<sub>2</sub>CO<sub>3</sub>, 130 °C, 61.5%; c) bis(pinacolato)diboron, Pd(dppf)Cl<sub>2</sub>, KOAc, 1,4-dioxane, 100 °C, 12 h, 50.6%.

Cimbi-772 contains the same tolyl motif as Cimbi-712 and should thus be possible to label from its corresponding boronic precursor via the Suzuki reaction. [ $^{11}\text{C}$ ]Cimbi-775 contains a methoxy group, making labeling from the corresponding phenolic precursor (**18**) a possibility (Scheme 6).



**Scheme 6.** Top: Labeling of [ $^{11}\text{C}$ ]Cimbi-712 and [ $^{11}\text{C}$ ]Cimbi-772. Bottom: Failed labeling of [ $^{11}\text{C}$ ]Cimbi-775.

Labeling of [ $^{11}\text{C}$ ]Cimbi-772 was successful with a RCY of 30% as determined by HPLC. Synthesis followed by HPLC purification gave isolated yields of 122-230 MBq with a RCP of  $>97\%$  and an  $A_s$  of 183-542 GBq/ $\mu\text{mol}$  from a 40 min irradiation. Labeling of [ $^{11}\text{C}$ ]Cimbi-775 turned out to be problematic. Labeling as shown in scheme 6 resulted in another labeled product than [ $^{11}\text{C}$ ]Cimbi-775, possibly in the oxindole N-position. As such the labeling was attempted from a boc-protected precursor in a two-step radiosynthesis consisting of an O-methylation followed by boc-deprotection (Scheme 7).



**Scheme 7.** a) [ $^{11}\text{C}$ ]CH $_3\text{I}$ , 2M NaOH, DMF,  $140^\circ\text{C}$ , 5 min. b)  $\text{CH}_2\text{Cl}_2/\text{TFA}$  (1:1),  $80^\circ\text{C}$ , 5 min.

Using this approach it was possible to label [ $^{11}\text{C}$ ]Cimbi-775. Synthesis followed by HPLC purification it was possible to isolate 152-211 MBq with a RCP of  $>97\%$  and an  $A_s$  of 78-331

GBq/ $\mu\text{mol}$  from a 40 min irradiation. Chiral resolution of both Cimbi-772 (Figure 23) and Cimbi-775 yielded enantiomerically pure compounds which showed no tendency towards racemization.

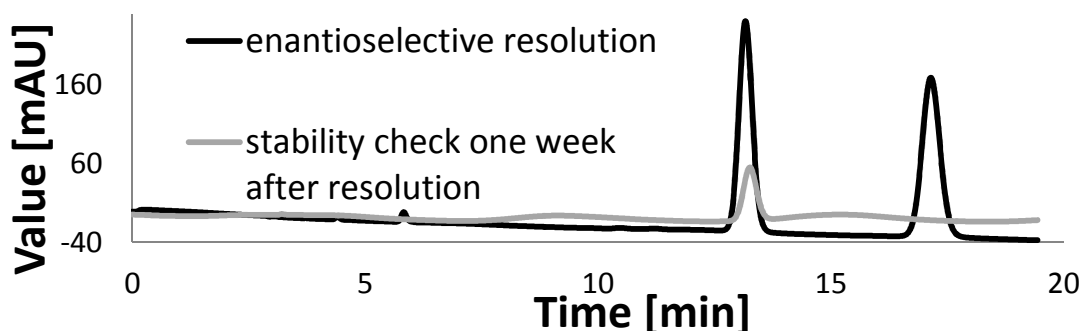


**Figure 23.** Chiral resolution of Cimbi-772 and stability check.

*In vivo* evaluation in Danish landrace pigs showed that [ $^{11}\text{C}$ ]Cimbi-772 and [ $^{11}\text{C}$ ]Cimbi-775 enters the brain. The highest binding was found in the thalamus and the lowest binding in the cerebellum which is according to the 5-HT<sub>7</sub> receptor distribution in pigs determined with [ $^3\text{H}$ ]SB-269970. The tracers showed slow yet reversible kinetics however there was no reduction in signal after blockage with SB-269970 (Figure 24). As such neither [ $^{11}\text{C}$ ]Cimbi-772 or [ $^{11}\text{C}$ ]Cimbi-775 are deemed suitable as PET-ligands for the 5-HT<sub>7</sub> receptor.

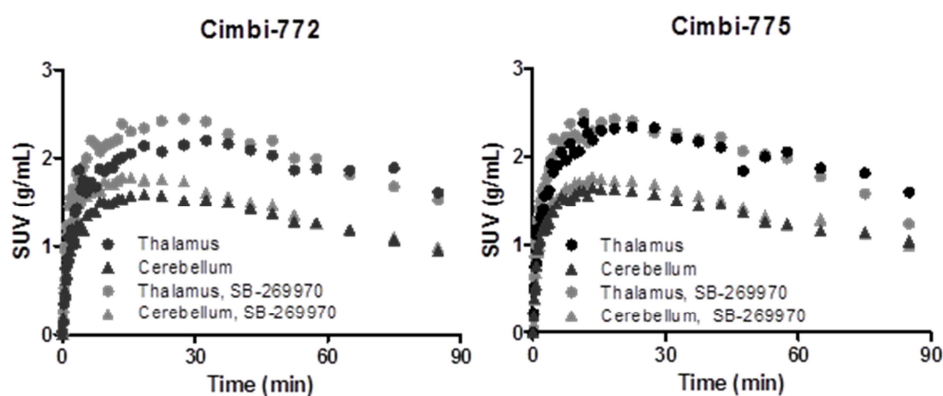


**Figure 24.** Time-activity curves of [ $^{11}\text{C}$ ]Cimbi-772 and [ $^{11}\text{C}$ ]Cimbi-775.

*In vitro* evaluation of the enantiomers of Cimbi-772 (**2**) and Cimbi-775 (**3**) revealed promising affinity and selectivity profiles of (+)-**2** and (+)-**3** (Table 3). Despite this they were not tested *in vivo* on account of the discouraging results from racemic [ $^{11}\text{C}$ ]Cimbi-772 and [ $^{11}\text{C}$ ]Cimbi-775.

**Table 3.** Affinities of Cimbi-712 (**1**), Cimbi-717 (**11**), Cimbi-772 (**2**) Cimbi-775 (**3**) as  $K_i$  in nM.  $H_1$ : Histamine-1 receptor,  $\alpha_1$ : Alpha-1 adrenergic receptor,  $\alpha_2$ : Alpha-2 adrenergic receptor,  $\sigma_1$ : Sigma-1 receptor.

	<b>1</b>	<b>2</b>	<b>(+)-2</b>	<b>(-)-2</b>	<b>11</b>	<b>3</b>	<b>(+)-3</b>	<b>(-)-3</b>
5-HT <sub>7</sub>	4.1	6.5	5.6	82	7.5	7.8	11	56
5-HT <sub>1A</sub>	491	469	787	633	130	83	192	151
5-HT <sub>2A</sub>	35	39	94	110	239	98	352	66
5-HTT	112	295	271	827	253	250	376	1439
H <sub>1</sub>	323	529	135	61	164	502	42	2405
$\alpha_1$	103	431	951	487	167	434	>10k	794
$\sigma_1$	45	37	33	390	59	42	46	249
$\sigma_2$	24	40	347	61	49	22	152	16

### 3.4 [<sup>11</sup>C]E-55888

A highly selective compound for the 5-HT<sub>7</sub> receptor is E-55888 (Figure 25) developed by the pharmaceutical company Esteve. It is a full agonist and shows a 280 fold selectivity for the 5-HT<sub>7</sub> receptor, compared to 5-HT<sub>1A</sub>, the only other identified target.<sup>103</sup> As the compound contains several methylgroups it allows for labeling in four different positions utilising two different reactions: Cross-coupling and N-methylation. As such the labeling method devised in chapter 3.1 could potentially be applied to the labeling of the compound.

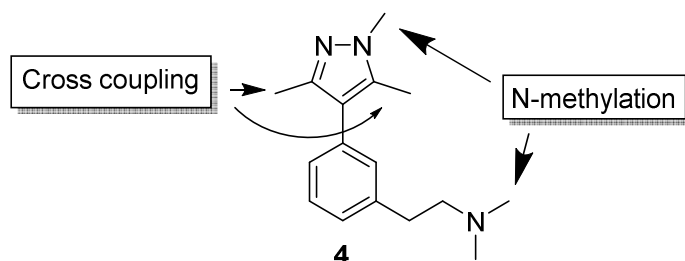
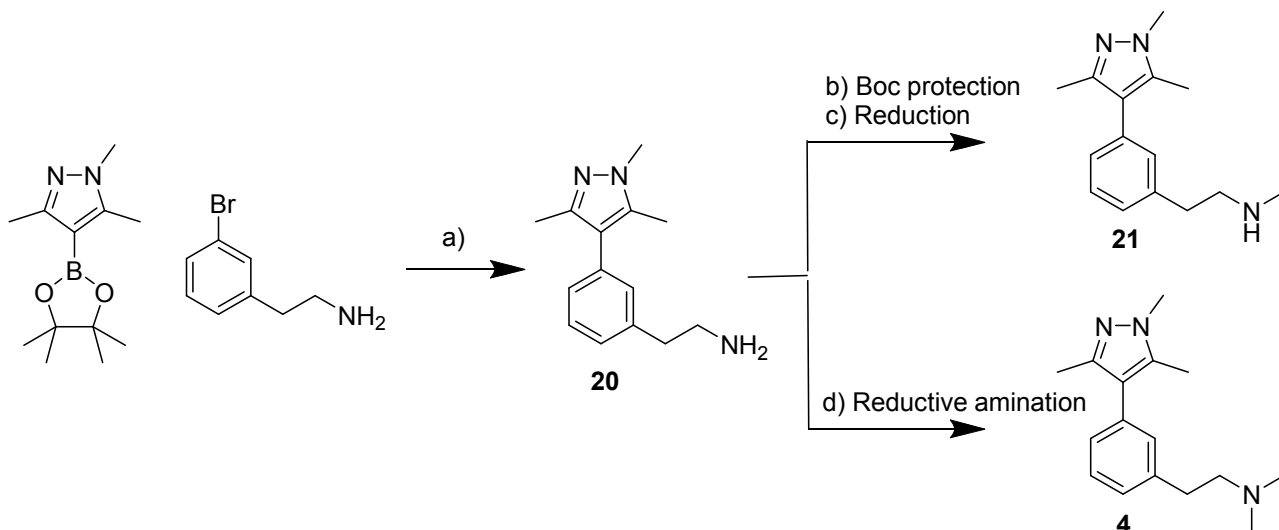


**Figure 25.** Structure of E-55888 and potential labeling sites.

Initially labeling via N-methylation was chosen as reference and precursor could be synthesized through either a two or a three step synthesis (Scheme 8). Furthermore labeling via N-methylation ought to provide a simple labeling route to [ $^{11}\text{C}$ ]E-55888.

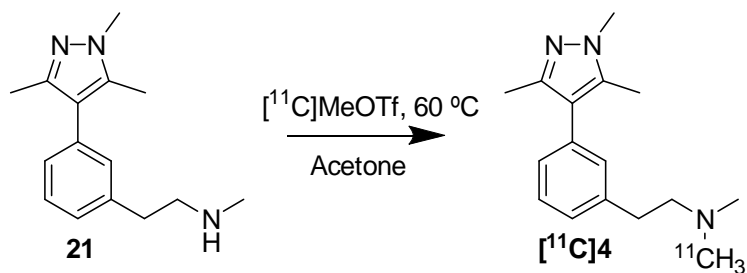


**Scheme 8.** Synthesis of precursor and reference for E-55888. a)  $\text{K}_2\text{CO}_3$ ,  $\text{Pd}(\text{PPh})_4$ , DME:water 1:1, 100 °C (MW), 30 min, 74.8%; b)  $\text{Boc}_2\text{O}$ ,  $\text{Na}_2\text{CO}_3$ , THF:water 2:5, reflux, 15 h; c)  $\text{LiAlH}_4$ , THF, reflux, 5 h, 31.6% (b,c combined); d)  $\text{NaCNBH}_3$ ,  $\text{ZnCl}_2$ ,  $\text{CH}_2\text{O}$ , MeOH, rt, 2 h, 81%.

A cross-coupling between 1,3,5-trimethyl-4-(4,4,5,5-tetramethyl-1,3,2-dioxaborolan-2-yl)-1H-pyrazole and 3-bromophenethylamine yielded 2-(3-(1,3,5-trimethyl-1H-pyrazol-4-yl)phenyl)ethanamine (**20**) from which both precursor and reference could be synthesized. A boc protection followed by reduction with LAH gave the precursor (**21**) and reductive amination using  $\text{NaCNBH}_3$  and formaldehyde gave the reference compound (**4**).

Labeling of [ $^{11}\text{C}$ ]E-55888 was achieved using [ $^{11}\text{C}$ ]MeOTf in acetone at 60 °C (Scheme 9) with a RCY of 80-90% as determined by HPLC. Radiosynthesis followed by purification gave isolated yields of 1743-2433 MBq, RCP of >97% and an  $A_s$  of 303-346 GBq/ $\mu\text{mol}$  from a 40 min irradiation.





**Scheme 9.** Labeling of [<sup>11</sup>C]E-55888.

Evaluation of the radiolabeled compound, in Danish landrace pigs, showed a rapid brain uptake with reversible kinetics. As expected, thalamus had the highest binding and cerebellum the lowest, however the ratio of binding between thalamus and cerebellum is low indicating a low specific binding. Two blocking studies were conducted: A study using SB-269970 and a study using the closely related compound SB-258719. Blocking with SB-258719 and SB-269970 was unable to reduce the binding of [<sup>11</sup>C]E-55888 (Figure 26). Surprisingly both blocking agents resulted in an increased uptake. The increased binding still has to be explained. These are preliminary data and will thus have to be investigated further. Both the low amount of specific binding at baseline and the lack of displacement by SB-258719 and SB-269970 indicates that [<sup>11</sup>C]E-55888 is unsuitable as a PET-ligand for the 5-HT<sub>7</sub> receptor.

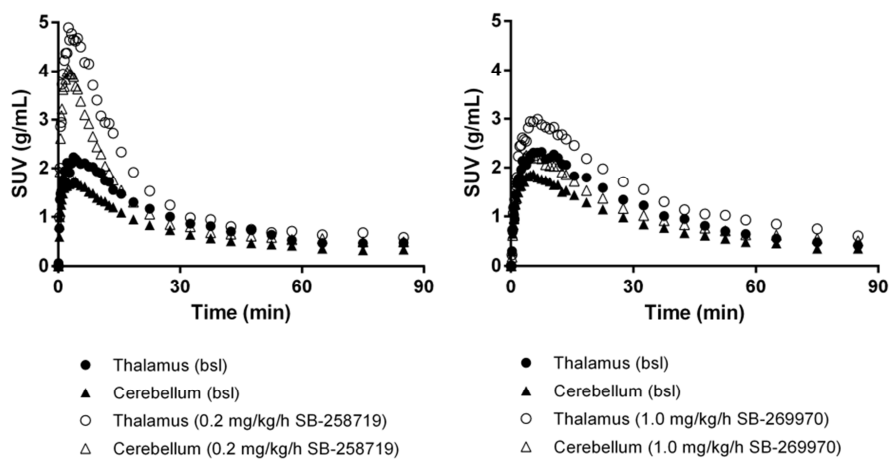


**Figure 26.** Time-activity curves of [<sup>11</sup>C]E-55888 using either SB-258719 (left) or SB-269970 (right).

## 4 Conclusion and perspectives

In conclusion one general labeling method has been established and five PET-ligands have been synthesised, labeled and evaluated in Danish landrace pigs.

In chapter 3.1 a general labeling method for the labeling of amine containing compounds via the Suzuki reaction was described. By trapping [ $^{11}\text{C}$ ]MeI as a [ $^{11}\text{C}$ ]Me-Pd-I complex before adding boronic precursor it was possible to label compounds containing amines, a functional group that would normally require a protection-group to avoid competing N-methylation. Additionally the effects of variations in reaction temperature, base, Pd-catalyst and boronic ester species were investigated. A general procedure was devised and used to label several model compounds. In this context the effects of conventional heating versus microwave heating was investigated. RCY's were found to be highly substrate specific with conventional heating giving higher overall yields.

A general labeling method which allows for amines should widen the library of compounds with labeling potential. Furthermore, application of a similar approach in the other cross-couplings utilised in radiochemistry could potentially widen the scope of these reactions as well.

In chapter 3.2 the method devised in chapter 3.1 was applied to the labeling of [ $^{11}\text{C}$ ]vortioxetine, a new drug for the treatment of MDD. The compound was labeled in sufficient yields to investigate its *in vivo* distribution in a Danish landrace pig. Binding was observed in cortex, thalamus, striatum, hippocampus and cerebellum. With the exception of binding in cerebellum this was in accordance with what would be expected from the affinity profile of the compound. On account of its multiple affinities it is not a suitable PET-ligand for the 5-HT<sub>7</sub> receptor.

As [ $^{11}\text{C}$ ]vortioxetine could be labeled without competing N-methylation it shows that protection groups are unnecessary when labeling through the method developed in chapter 3.1. As such the method has the potential of reducing the necessary steps in the radiosynthesis of future radiotracers. Despite being unsuitable as a 5-HT<sub>7</sub> receptor PET-ligand, [ $^{11}\text{C}$ ]vortioxetine could have other applications. As the mode of action of vortioxetine has not yet been determined, [ $^{11}\text{C}$ ]vortioxetine could be a valuable tool in its elucidation. Furthermore, as a treatment for MDD [ $^{11}\text{C}$ ]vortioxetine could be a tool to gain further knowledge about the disorder itself. Finally it is known that several drug treatments against depression have responders and non-responders.<sup>104</sup> If this is the case with

vortioxetine as well the radiolabeled equivalent could potentially be used to investigate differences between these patient groups.

In chapter 3.3 the synthesis, labeling and evaluation of the potential 5-HT<sub>7</sub> receptor PET-ligands [<sup>11</sup>C]Cimbi-712, [<sup>11</sup>C]Cimbi-772 and [<sup>11</sup>C]Cimbi-775 was described. [<sup>11</sup>C]Cimbi-712 and [<sup>11</sup>C]Cimbi-772 was labeled via the method described in chapter 3.1 and [<sup>11</sup>C]Cimbi-775 via O-methylation. *In vivo* evaluation revealed that all three ligands enter the brain. [<sup>11</sup>C]Cimbi-712 had slow tracer kinetics but was displaceable by SB-269970. [<sup>11</sup>C]Cimbi-772 and [<sup>11</sup>C]Cimbi-775 both displayed slow yet reversible tracer kinetics and a lack *in vivo* specificity. None of the compounds were found to be viable as a 5-HT<sub>7</sub> receptor PET-ligand.

In chapter 3.4 the synthesis, labeling and evaluation of the agonist [<sup>11</sup>C]E-55888 as a potential 5-HT<sub>7</sub> receptor PET-ligand was described. [<sup>11</sup>C]E-55888 was labeled via N-methylation. The PET-ligand enters the brain and displayed reversible tracer kinetics yet is not displaceable by the use of SB-258719 or SB-269970. As such [<sup>11</sup>C]E-55888 was not found to be viable as a 5-HT<sub>7</sub> receptor PET-ligand. Furthermore a self-block study is planned to ascertain if [<sup>11</sup>C]E-55888 is can be displaced at all.

A PET-ligand for the 5-HT<sub>7</sub> receptor is still a desirable tool. As the receptor where 5-HT shows the highest affinity, a PET-ligand for the 5-HT<sub>7</sub> receptor could provide a tool to measure endogenous serotonin within the brain. Additionally, the 5-HT<sub>7</sub> receptor has been linked to various processes and disorders. Thus a PET-ligand could be a tool to quantify 5-HT<sub>7</sub> receptor levels and thus help elucidate its role in these disorders. As of yet the most promising candidate for a 5-HT<sub>7</sub> receptor PET-ligand is the previously developed [<sup>11</sup>C]Cimbi-717.

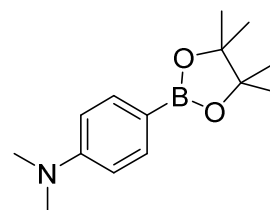
## 5 Experimental

### General information:

Chemicals were purchased from Sigma or Merck. Unless otherwise stated, all chemicals were used without further purification. GC–MS analysis was performed on a Shimadzu. LC-MS analysis was performed on an Agilent 1100 system with a Hewlett Packard series 1100 MS detector. For Solid Phase Extraction (SPE), Sep-Pak®-C18-cartridges (Waters, USA) were used. Thin Layer Chromatography (TLC) was performed using plates from Merck (Silicagel 60 F254). <sup>1</sup>H-NMR spectra and <sup>13</sup>C-NMR spectra were recorded using a Bruker AC 300 spectrometer or a Bruker AC 400 spectrometer. Chemical shifts are quoted as  $\delta$ -values (ppm) downfield from tetramethylsilane (TMS). Preparative high performance liquid chromatography (HPLC) were performed on a Dionex system consisting of a pump P680A pump, a UVD 170U detector and a Scansys radiodetector. Analytical HPLC was performed on a Dionex system consisting of a pump P680A pump, a UVD 170U detector and a Scansys radiodetector, an ultimate3000 system with a Scansys radiodetector or a Waters system comprised of a 2795 separation unit, a 2996 diode array and a Scansys radiodetector. [<sup>11</sup>C]Methane was produced via the <sup>14</sup>N(p, $\alpha$ )<sup>11</sup>C reaction by bombardment of an [<sup>14</sup>N]N<sub>2</sub> containing 10% H<sub>2</sub> target with a 17 MeV proton beam in a Scanditronix MC32NI cyclotron. Microwave-assisted syntheses were carried out in a Scansys PET-SYN apparatus operating in single mode; the microwave cavity producing controlled irradiation at 2.45 GHz. The temperature was monitored by an IR sensor focused on a point on the reactor vial glass. The reactions were run in sealed vials (1 mL). Desired temperatures were obtained using variable power monitored by PID regulation.

### 4-(4,4,5,5-tetramethyl-1,3,2-dioxaborolan-2-yl)-N,N-dimethylaniline (5a)

4-(dimethylamino)phenylboronic acid (1 g, 6.06 mmol) was dissolved in 25 ml of CH<sub>2</sub>Cl<sub>2</sub> and added pinacol (718.7 mg, 6.08 mmol). This mixture was stirred for 15 h. The mixture was washed with 2x5 mL of brine and 3x5 mL of water. The organic phase was dried and concentrated *in vacuo*. Yield: 1.50 g (6.04 mmol, 99.7 %). <sup>1</sup>H-NMR (CDCl<sub>3</sub>, 300MHz)  $\delta$ : 7.67

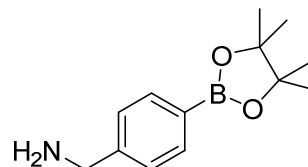


(m, 2H), 6.68 (m, 2H), 2.9 (s, 6H), 1.32 (s, 12H). GC-MS: 247 m/z. Analytical data corresponds with data found in literature.<sup>105</sup>

#### (4-(4,4,5,5-tetramethyl-1,3,2-dioxaborolan-2-yl)phenyl)methanamine (5b)

*p*-bromobenzamine (1 g, 5.37 mmol) was dissolved in THF:Water 2:5.

Boc<sub>2</sub>O (1.41 g, 6.45 mmol) and Na<sub>2</sub>CO<sub>3</sub> (1.67 g, 12.09 mmol) were then added and the mixture was refluxed for 12 h. Extraction was performed with 3x50 mL of EtOAc. The organic phase was dried with



Na<sub>2</sub>SO<sub>4</sub> and concentrated *in vacuo*. The residue was purified by flash chromatography using heptane : EtOAc 10:1. Yield: 1.36 g (89%, 4.79 mmol). <sup>1</sup>H-NMR (CDCl<sub>3</sub>, 400MHz) δ: 7.74 (dt, 2H), 7.18 (d, 2H), 4.28 (d, 2H), 1.48 (s, 9H). <sup>13</sup>C-NMR (CDCl<sub>3</sub>, 100MHz) δ: 156, 138, 132, 129,

121, 80, 44, 28. GC-MS: 285 m/z. Analytical data can be found in literature.<sup>106</sup> Tert-butyl-4-

bromobenzylcarbamate (400 mg, 1.40 mmol) was dissolved in 10 mL of dry dioxane, potassium acetate (165 mg, 1.68 mmol), bis(pinacolato)diboron (426 mg, 1.68 mmol) and Pd(dppf)Cl<sub>2</sub> (10 mg,

0.01 mmol) were added and the reaction was stirred at 100 °C for 12 h. The mixture was stirred with 10 mL of sat. NaCl aqueous solution for 10 min. and extracted with 3x50 mL EtOAc. The combined organic phases were dried with Na<sub>2</sub>SO<sub>4</sub> and concentrated *in vacuo*. The resulting residue

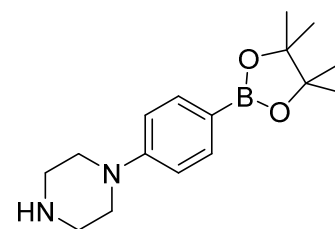
was purified by flash chromatography using heptane : EtOAc 10:1. The pure compound was treated with 2.0 M HCl in diethyl ether and the resulting deprotected HCl salt was filtered off. Yield: 276

mg (73%, 1.039 mmol). <sup>1</sup>H-NMR (CDCl<sub>3</sub> 400MHz) δ: 7.69 (d, 2H), 7.48 (d, 2H), 4.03 (s, 2H), 1.29

(s, 12H). Analytical data corresponds with data found in literature.<sup>107</sup>

#### 1-(4-(4,4,5,5-tetramethyl-1,3,2-dioxaborolan-2-yl)phenyl)piperazine (5c)

phenyl-piperazine (6.32 mL, 41.37 mmol) was dissolved in 75 mL of ethanol. This was slowly added 90 mL of a 1M Br<sub>2</sub> in EtOH solution (90 mmol). The reaction mixture was stirred at room temperature for 15 h. The mixture was added 140 mL of water and basified using 15% aqueous NaOH. 200 mL of EtOAc was added to achieve phase



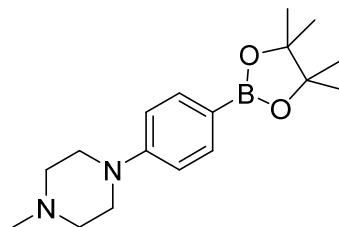
separation. Afterwards the water phase was extracted with 3x75 mL EtOAc and the combined organic phases were dried and concentrated *in vacuo* yielding 12.99 g of crude 1-(4-

bromophenyl)piperazine. When necessary the product was purified by flash chromatography using CH<sub>2</sub>Cl<sub>2</sub>:MeOH:Et<sub>3</sub>N 10:1:0.01 and concentrated *in vacuo*. IR: 1493, 1236, 814 cm<sup>-1</sup>. <sup>1</sup>H-NMR

(CDCl<sub>3</sub>, 300 MHz)  $\delta$ : 7.32 (m, 2H), 6.77 (m, 2H), 3.11 (m, 4H), 3.03 (m, 4H). <sup>13</sup>C-NMR (CDCl<sub>3</sub>, 300MHz)  $\delta$ : 150.9, 132.0, 117.8, 111.9, 50.3, 46.2. GC-MS: 240 m/z. Mp: 121-122°C. 1-(4-bromophenyl)piperazine (2 g, 8.29 mmol), Boc<sub>2</sub>O (1.9 g, 8.71 mmol), and sodium carbonate (1.97 g, 18.6 mmol) was dissolved in THF:Water 5:2 and refluxed for 12 h. Extraction was performed with 3x50 mL EtOAc. The combined organic phases were washed with 2x50 mL brine, dried and concentrated in vacuo. The resulting solid was purified by flash chromatography (EtOAc:Heptane 1:1) Yield: 2.04 g (72%, 5.98 mmol). <sup>1</sup>H-NMR (CDCl<sub>3</sub>, 300 MHz)  $\delta$ : 7.33 (m, 2H), 6.78 (m, 2H), 3.56 (m, 4H), 3.09 (m, 4H), 1.48 (s). <sup>13</sup>C-NMR (CDCl<sub>3</sub>, 400 MHz)  $\delta$ : 154.7, 150.2, 132.0, 118.2, 80.0, 49.3, 28.5. tert-butyl 4-(4-bromophenyl)piperazine-1-carboxylate (250 mg, 0.733 mmol), Potassium acetate (86 mg, 0.879 mmol) and Pd(dppf)Cl<sub>2</sub> (10 mg) was dissolved in 1,4-dioxane and heated to 100 °C with stirring. 4,4,4',4',5,5,5',5'-octamethyl-2,2'-bi(1,3,2-dioxaborolane) (223 mg, 0.879 mmol) was then added and stirring was continued for 12 h. A crude sample was analyzed on GCMS, if the reaction was not finished a small amount of 4,4,4',4',5,5,5',5'-octamethyl-2,2'-bi(1,3,2-dioxaborolane) was added and stirring was continued for 2 hours. The reaction was then cooled to room temperature and stirred with 10 mL of brine for 10 min. The combined phases was extracted with 3x50 mL of EtOAc. The combined organic phases were dried and concentrated *in vacuo*. The crude product was purified by flash chromatography using EtOAc:Heptane 1:2. The pure compound was treated with 2.0 M HCl in diethyl ether and the resulting deprotected HCl salt was filtered off. Yield: 120.1 mg (50%, 0.370 mmol) <sup>1</sup>H-NMR (CDCl<sub>3</sub>, 400 MHz)  $\delta$ : 7.72 (d, 2H), 6.90 (d, 2H), 3.23 (m, 4H), 3.03 (m, 4H), 1.33 (s, 12H). <sup>13</sup>C-NMR (CDCl<sub>3</sub>, 400 MHz)  $\delta$ : 153.8, 136.1, 114.5, 83.4, 49.3, 45.9, 24.8. LC-MS (m+1): 289.2 m/z.

### 1-methyl-4-(4-(4,4,5,5-tetramethyl-1,3,2-dioxaborolan-2-yl)phenyl)piperazine (5d)

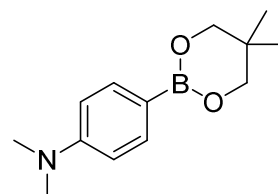
1.39 M t-BuLi (1.4 mL, 1.95 mmol) was dissolved in 10 mL dry THF at -78 °C. 1-(4-bromophenyl)-4-methylpiperazine (201.7 mg, 0.79 mmol) dissolved in 3 mL dry THF was added dropwise whilst the solution was stirred. The reaction was stirred for 15 min afterwards. B(Oi-Pr)<sub>3</sub> (0.36 mL, 2.35 mmol) was added dropwise and heated to room temperature. After reaching room temperature the reaction was stirred for one hour. Pinacol (141.2 mg, 1.19 mmol) was added and stirring was continued for two hours. The mixture was washed with 3x10 mL saturated aqueous NH<sub>4</sub>Cl:water 1:1, 2x10 mL saturated aqueous NaHCO<sub>3</sub> and 2x10 mL water. The organic phase was dried and evaporated *in vacuo*. The resulting



residue was purified by flash chromatography using EtOAc:MeOH:Et<sub>3</sub>N (10:1:0.02). Yield: 107.5 mg (0.36 mmol, 45%). IR: 1361, 1237, 1140 cm<sup>-1</sup>. <sup>1</sup>H-NMR (CDCl<sub>3</sub>, 300 MHz) δ: 7.70 (m, 2H), 6.89 (m, 2H), 3.29 (t, 4H), 2.57 (t, 4H), 2.36 (s, 3H). <sup>13</sup>C-NMR (CDCl<sub>3</sub>, 300MHz) δ: 136.3, 114.5, 83.5, 55.1, 48.2, 46.3, 24. GC-MS: 302 m/z. Mp: 113-115 °C.

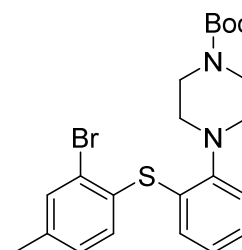
#### 4-(5,5-dimethyl-1,3,2-dioxaborinan-2-yl)-N,N-dimethylaniline (6)

4-(dimethylamino)phenylboronic acid (0.99 g, 6.00 mmol) was dissolved in 25 mL of CH<sub>2</sub>Cl<sub>2</sub> and added neopentyl glycol (635 mg, 6.10 mmol). This mixture was stirred for 15 h. The mixture was washed with 2x5 mL of brine and 3x5 mL of water. The organic phase was dried and concentrated *in vacuo*. Yield: 1.34 g (5.77 mmol, 96.2 %). <sup>1</sup>H-NMR (CDCl<sub>3</sub>, 300MHz) δ: 7.66 (m, 2H), 6.68 (m, 2H), 3.73 (s, 4H), 2.97 (s, 6H), 1.00 (s, 6H). GC-MS: 233 m/z. Analytical data corresponds with data found in literature.<sup>105</sup>

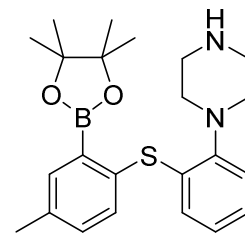


#### tert-butyl 4-(2-((2-bromo-4-methylphenyl)thio)phenyl)piperazine-1-carboxylate (9)

tert-BuOK (311 mg, 2.78 mmol), Pd<sub>2</sub>dba<sub>3</sub> (57.8 mg, 0.063 mmol), DPEphos (136 mg, 0.252 mmol), 2-bromo-4-methylbenzenethiol (512 mg, 2.52 mmol) and tert-butyl 4-(2-iodophenyl)piperazine-1-carboxylate (980 mg, 2.52 mmol) was dissolved in dry toluene (4 mL), kept under nitrogen and degassed using a stream of nitrogen for 10 min. The mixture was then heated to 100 °C (MW). The resulting crude was purified by dry column vacuum chromatography using heptane to heptane/EtOAc 10:1 (rf = 0.48 heptane/EtOAc 3:1) yielding 950 mg as a slightly yellow oil (81%). <sup>1</sup>H NMR (CDCl<sub>3</sub>, 400 MHz) δ: 1.49 (s, 9H) 2.35 (s, 3H) 2.97–3.03 (m, 4 H) 3.50–3.55 (m, 4 H) 6.85 (dd, J = 7.78, 1.51 Hz, 1H) 6.95–6.99 (m, 1H) 7.04–7.08 (m, 2H) 7.17–7.23 (m, 2H) 7.51 (d, J = 1.00 Hz, 1H). <sup>13</sup>C NMR (CDCl<sub>3</sub>, 400 MHz) d: 20.8, 28.5, 51.6, 79.7, 120.4, 124.6, 127.3, 127.7, 129.0, 129.6, 131.7, 132.1, 134.0, 134.2, 139.6, 150.4, 154.9. LC-MS (m+1): 464 m/z.

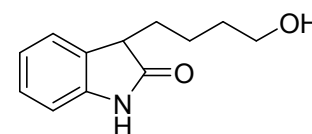


**1-(2-((4-Methyl-2-(4,4,5,5-tetramethyl-1,3,2-dioxaborolan-2-yl)phenyl)thio)phenyl)piperazine (10)**



Pd(dppf)Cl<sub>2</sub> (13.3 mg, 0.018 mmol), bis(pinacolato)diboron (169 mg, 0.665 mmol), KOAc (178 mg, 1.81 mmol) and **4** (280 mg, 0.604 mmol) was dissolved in dry 1,4-dioxane (10 mL), degassed with nitrogen for 10 min and heated to 100 °C for 18 h. The resulting crude was purified by dry column vacuum chromatography using heptane to heptane/EtOAc 10:1 (rf = 0.55 heptane/EtOAc 3:1). Yielding 124 mg of Boc-protected **10** as a slightly yellow oil (40%). <sup>1</sup>H NMR (CDCl<sub>3</sub>, 400 MHz) δ: 1.15 (s, 12H) 1.50 (s, 9H) 2.38 (s, 3H) 3.05 (br s, 4H) 3.58 (br s, 4H) 6.74 (d, J = 7.83 Hz, 1H) 6.88 (t, J = 7.46 Hz, 1H) 7.00 (m, 1H) 7.06 (m, 1H) 7.22 (d, J = 7.82 Hz, 1H) 7.35 (d, J = 7.83 Hz, 1H) 7.63 (s, 1H). <sup>13</sup>C NMR (CDCl<sub>3</sub>, 400 MHz) δ: 21.1, 24.6, 28.5 51.4, 79.6, 83.8, 119.5, 124.5, 125.6, 127.2, 132.3, 134.6, 134.8, 136.4, 137.1, 137.4, 155.0. LC-MS (m+1): 511 m/z. This material was deprotected in the following way: 90 mg (0,176 mmol) was dissolved in CH<sub>2</sub>Cl<sub>2</sub> (10 mL) and TFA (0.5 mL) was added and the mixture was stirred for 30 min. The resulting mixture was then washed with saturated aqueous NaHCO<sub>3</sub> (3x10 mL) and the organic phase was evaporated to dryness yielding 57 mg of **10** as a slightly yellow oil, 0,14 mmol, 79%) <sup>1</sup>H NMR (CDCl<sub>3</sub>, 400 MHz) δ: 1.13 (s, 10H) 2.38 (s, 3H) 3.37 (d, J = 12.23 Hz, 8H) 6.77 (d, J = 7.58 Hz, 1H) 6.93 (s, 1H) 7.02–7.05 (m, 1H) 7.09 (d, J = 7.09 Hz, 1H) 7.23 (d, J = 6.36 Hz, 1H) 7.34 (d, J = 7.82 Hz, 1H) 7.66 (s, 1H). <sup>13</sup>C NMR (CDCl<sub>3</sub>, 400 MHz) δ: 21.0, 24.5, 44.2, 48.3, 83.9, 119.8, 125.5, 125.9, 127.4, 132.5, 134.1, 134.7, 136.5, 137.6, 147.2. LC-MS (m+1): 411 m/z.

**3-(4-hydroxybutyl)indolin-2-one**

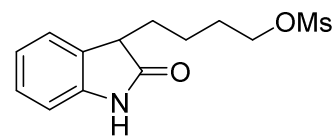


Oxindole (5.32 g, 40 mmol), 1,4-butanediol (40 ml, 489 mmol) and 2 g of raney nickel in water slurry were heated to 200 °C in a pressurized container for 12 h. The resulting mixture was diluted using acetone and flushed through a pad of celite and concentrated *in vacuo*. Excess butane-1,4-diol was removed by kugelrohr distillation at 170 °C leaving a brown oil. The oil was purified by flash chromatography using EtOAc. Yield: 5.72 g (27.9 mmol, 69.8 %). <sup>13</sup>C-NMR (CDCl<sub>3</sub>, 400MHz) δ: 180.9, 141.8, 129.8, 128.1, 124.2, 122.4, 110.0, 62.6, 46.2, 32.7, 30.2, 22.2. Data corresponds to reported data in.<sup>108</sup>



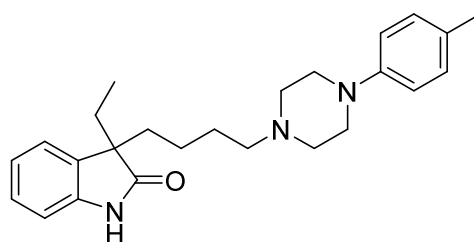
### 4-(2-oxindolin-3-yl)butyl methanesulfonate (**12**)

3-(4-hydroxybutyl)indolin-2-one (5.7205 g, 27.9 mmol) and Et<sub>3</sub>N (7.77 ml, 55.7 mmol) was dissolved in 50 ml of dry THF and cooled to -78°C. Mesyl chloride was added dropwise with stirring and the temperature was raised to rt. Upon reaching rt. the reaction was stirred for 1h. The crude was stored for further use.



### 3-ethyl-3-(4-(4-(p-tolyl)piperazin-1-yl)butyl)indolin-2-one (**2**)

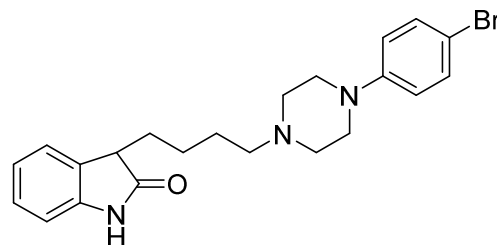
1-(4-Methylphenyl)-piperazine (210 mg, 1.192 mmol), sodium carbonate (126 mg, 1.192 mmol) and 3-ethyl-3-( $\omega$ -chlorobutyl)oxindole (300 mg, 1.192 mmol) yielded in **2** (312 mg, 0.797 mmol, 66.9%) as a white solid. **2** was purified by flash chromatography using



EtOAc (rf = 0.12). Mp 127.8-128.3 °C; <sup>1</sup>H-NMR (CDCl<sub>3</sub>, 400 MHz)  $\delta$ : 9.28 (1H, s), 7.19 (1H, m), 7.12 (1H, m), 7.05 (3H, m), 6.91 (1H, d, J= 7.8 Hz), 6.82 (2H, m), 3.10 (4H, m), 2.52 (4H, m), 2.26 (5H, m), 1.94 (2H, m), 1.80 (2H, m), 1.43 (2H, m) 1.13 (1H, m), 0.93 (1H, m), 0.64 (3H, t, J= 7.4 Hz); <sup>13</sup>C-NMR (CDCl<sub>3</sub>, 100 MHz)  $\delta$ : 182.8, 149.1, 141.5, 132.5, 129.5, 129.0, 127.5, 122.9, 122.2, 116.2, 109.5, 58.2, 54.2, 53.1, 49.5, 37.5, 30.9, 26.8, 22.2, 20.3, 8.0; LCMS (ESI) RT: 5.36 min, m/z 392.1 [M+H]<sup>+</sup> at 210 and 254 nm; R<sub>f</sub>: 0.12 (EtOAc); HRMS (ESI) [MH<sup>+</sup>] cald. for C<sub>25</sub>H<sub>34</sub>N<sub>3</sub>O 392.269, found 392.2710

### 3-(4-(4-(4-bromophenyl)piperazin-1-yl)butyl)indolin-2-one (**13**)

1-(4-bromophenyl)piperazine (425 mg, 1.763 mmol) was melted at 130 °C, Na<sub>2</sub>CO<sub>3</sub> (187 mg, 1.763 mmol) and **12** (499 mg, 1.763 mmol) was and stirred until the mixture turned solid. The solid was dissolved in a mixture of EtOAc and water. The organic phase was concentrated *in*

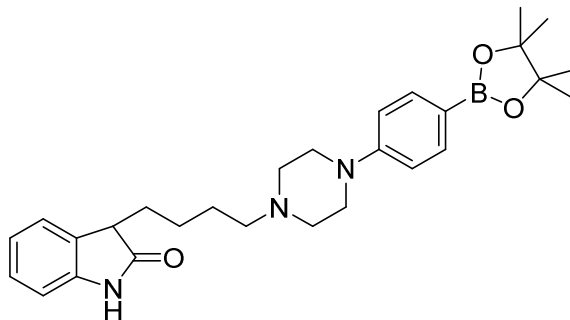


*vaquo* and purified using flash chromatography (EtOAc). Yield: 416.2 mg (55.1%, 0.972 mmol) IR: 1703, 1589, 1493, 815 cm<sup>-1</sup>. <sup>1</sup>H-NMR (CDCl<sub>3</sub>, 300MHz)  $\delta$ : 7.77 (s, 1H), 7.31 (m, 2H), 7.20 (m, 2H), 7.02 (m, 1H), 6.86 (d, 1H, J = 7.3 Hz) 6.76 (m, 2H), 3.48 (t, 1H, J = 5.9 Hz) 3.17 (t, 4H, J = 4.7), 2.59 (m, 4H), 2.39 (t, 2H, J = 7.8 Hz), 2.00 (m, 2H), 1.57 (m, 2H), 1.41 (m, 2H). <sup>13</sup>C-NMR

(CDCl<sub>3</sub>, 300MHz)  $\delta$ : 180.4, 150.3, 141.7, 131.9, 129.7, 128.0, 124.4, 122.4, 117.7, 111.9, 109.8, 58.3, 53.1, 48.9, 46.8, 30.4, 26.8, 23.8. LC-MS: 429 m/z (M+1). Mp: 132-134°C.

### 3-(4-(4-(4-(4,4,5,5-tetramethyl-1,3,2-dioxaborolan-2-yl)phenyl)piperazin-1-yl)butyl)indolin-2-one (14)

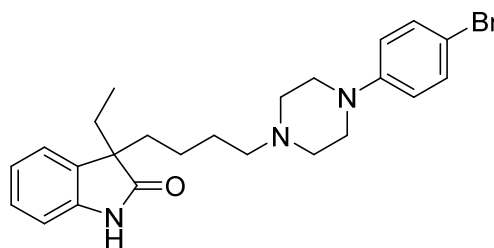
**13** (50 mg, 0.12 mmol), KOAc (22.9 mg, 0.23 mmol), Bis(pinacolato)diboron (35.6 mg, 0.14 mmol) and Pd(dddpf)Cl<sub>2</sub> (10 mg, 0.01 mmol) was dissolved in 10 mL of dry Dioxane, heated to 100 °C and stirred for 12 h. The reaction was then cooled to r.t, stirred with 10 mL of brine for 10 min and extracted with 3x50 mL EtOAc. The combined



organic phases were dried, concentrated *in vacuo* and purified by flash chromatography (EtOAc). Yield: 30 mg (54 %, 0.06 mmol). <sup>1</sup>H-NMR (CDCl<sub>3</sub>, 300MHz)  $\delta$ : 8.62 (s b, 1H), 7.70 (d, 2H, J = 8.8 Hz) 7.22 (t, 2H, J = 7, 8.2 Hz ), 7.03 (m, 1H), 6.88 (m, 3H), 3.50 (t, 1H, J = 5.9 Hz) 3.31 (t, 4H, J = 5.3), 2.64 (t, 4H, J = 4.7 Hz), 2.42 (t, 2H, J = 7.9 Hz), 2.02 (m, 2H), 1.61 (m, 2H), 1.44 (m, 2H), 1.34 (s, 12H). <sup>13</sup>C-NMR (CDCl<sub>3</sub>, 400MHz)  $\delta$ : 189.8, 153.1, 141.4, 136.2, 129.6, 127.9, 124.2, 122.3, 114.5, 109.6, 83.4, 58.1, 52.8, 47.7, 45.8, 30.2, 26.2, 24.9, 23.6. High-res MS: 476.3094 (M+1)

### 3-(4-(4-(4-bromophenyl)piperazin-1-yl)butyl)-3-ethylindolin-2-one (16)

1-(4-bromophenyl)piperazine (479 mg, 1.986 mmol), 3-(4-chlorobutyl)-3-ethylindolin-2-one (500 mg, 1.98 mmol), and Na<sub>2</sub>CO<sub>3</sub> (211 mg, 1.986 mmol) was heated to 180 °C and stirred for 3 h. After cooling to rt. the resulting solid was dissolved in a mixture of EtOAc and water. The organic phase was concentrated *in vacuo* and purified by

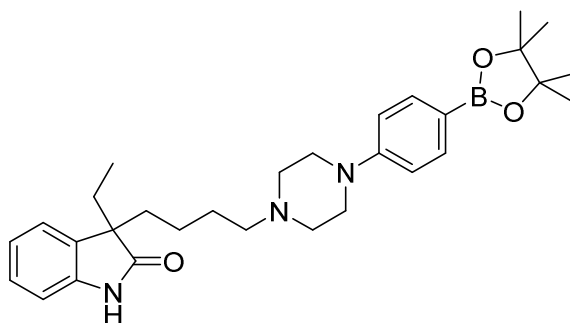


flash chromatography using EtOAc (rf = 0.18). Yield: 557.2 mg (61.5%). 145-145.5 °C; <sup>1</sup>H-NMR (CDCl<sub>3</sub>, 400 MHz)  $\delta$ : 7.73 (1H, s), 7.33 (2H, m), 7.21 (1H, td, J = 7.59, 1.38 Hz), 7.12 (1H, m), 7.06 (1H, m), 6.88 (1H, d, J = 7.78 Hz), 6.76 (2H, m), 3.16 (4H, m), 2.56 (4H, brs), 2.31 (2H, t, J =

7.65 Hz), 1.93 (2H, m), 1.79 (2H, m), 1.45 (2H, m), 1.12 (1H, m), 0.93 (1H, m), 0.64 (3H, t, J = 7.40 Hz);  $^{13}\text{C-NMR}$  ( $\text{CDCl}_3$ , 100 MHz)  $\delta$ : 181.8, 150.2, 141.1, 132.5, 131.8, 127.6, 123.2, 122.5, 117.6, 109.3, 58.1, 52.8, 48.7, 37.5, 31.1, 26.9, 22.2, 8.5; LCMS (ESI): RT: 5.97 min, m/z: 457.2  $[\text{M}+\text{H}]^+$  at 210 and 254 nm;  $R_f = 0.18$  (EtOAc); HRMS (ESI)  $[\text{MH}]$  calcd. for  $\text{C}_{24}\text{H}_{31}\text{BrN}_3\text{O}$  456.1645, found 456.1657

### 3-ethyl-3-(4-(4-(4-(4,4,5,5-tetramethyl-1,3,2-dioxaborolan-2-yl)phenyl)piperazin-1-yl)butyl)indolin-2-one (17)

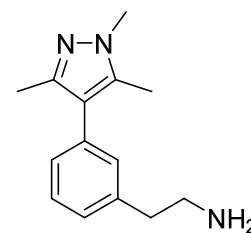
24 (77 mg, 0.169 mmol), KOAc (19.8 mg, 0.202 mmol), Bis(pinacolato)diboron (86 mg, 0.337 mmol) and  $\text{Pd}(\text{ddpf})\text{Cl}_2$  (10 mg, 0.01 mmol) was dissolved in 10 mL of dry Dioxane, heated to 100  $^\circ\text{C}$  and stirred for 12 h. The reaction was then cooled to r.t, stirred with 10 mL of brine for 10 min



and extracted with 3x50 mL EtOAc. The combined organic phases were dried, concentrated *in vacuo* and purified by column chromatography using pure heptane to pure ethyl acetate yielding 43 mg (50.6%) as a dark yellow oil.  $^1\text{H-NMR}$  ( $\text{CDCl}_3$ , 400 MHz)  $\delta$ : 7.70 (2H, d, J = 8.78 Hz), 7.59 (1H, s), 7.20 (1H, td, J = 7.65, 1.38 Hz), 7.13 (1H, m), 7.07 (1H, td, J = 7.40, 0.88 Hz), 6.87 (3H, m), 3.24 (4H, t, J = 4.77 Hz), 2.52 (4H, brs), 2.27 (2H, t, J = 7.53 Hz), 1.93 (2H, m), 1.79 (2H, m), 1.44 (2H, m), 1.33 (12H, s), 1.12 (1H, m), 0.92 (1H, m), 0.64 (3H, t, J = 7.40 Hz);  $^{13}\text{C-NMR}$  ( $\text{CDCl}_3$ , 75 MHz)  $\delta$ : 181.7, 141.0, 136.1, 132.6, 127.6, 123.2, 122.5, 114.3, 109.3, 83.4, 77.2, 58.2, 54.1, 52.9, 48.0, 37.6, 31.1, 24.9, 22.3, 8.55; LC-MS (ESI): RT: 7.00 min, m/z: 504.3  $[\text{M}+\text{H}]^+$  at 210 and 254 nm;  $R_f = 0.73$  (EtOAc); HRMS (ESI)  $[\text{MH}^+]$  calcd. for  $\text{C}_{30}\text{H}_{43}\text{BN}_3\text{O}_3$  504.3397, found 504.3420

### 2-(3-(1,3,5-trimethyl-1H-pyrazol-4-yl)phenyl)ethanamine (20)

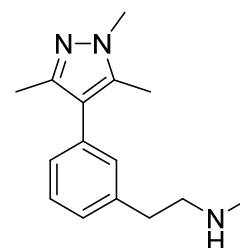
1,3,5-trimethyl-4-(4,4,5,5-tetramethyl-1,3,2-dioxaborolan-2-yl)-1H-pyrazole (610 mg, 2.58 mmol), 2-(3-bromophenyl)ethanamine (345 mg, 1.722 mmol),  $\text{K}_2\text{CO}_3$  (262 mg, 1.895 mmol) and tetrakis(triphenylphosphine)palladium (199 mg, 0.172 mmol) was dissolved in 12 ml DME:Water 1:1 and degassed with nitrogen for 10 min. The reaction mixture was then reacted at 100  $^\circ\text{C}$



(MW) for 30 min under nitrogen. Purified by dry column vacuum chromatography using EtOAc to EtOAc:Et<sub>3</sub>N 10:1. Yield: 295.6 mg (74.8%) Rf: 0.2 (EtOAc:MeOH:Et<sub>3</sub>N 10:1:1). <sup>1</sup>H NMR (CDCl<sub>3</sub>, 400 MHz) δ: 2.20 - 2.26 (m, 6 H) 2.75 - 2.81 (m, 2 H) 2.97 - 3.03 (m, 2 H) 3.77 (s, 3 H) 7.05 - 7.15 (m, 3 H) 7.33 (t, *J*=7.46 Hz, 1 H). <sup>13</sup>C NMR (CDCl<sub>3</sub>, 100 MHz) δ: 10.3, 12.5, 36.0, 39.9, 43.6, 119.1, 126.6, 127.3, 128.5, 129.9, 134.4, 136.2, 139.8, 145.0. LC-MS (m+1): 230.1 m/z

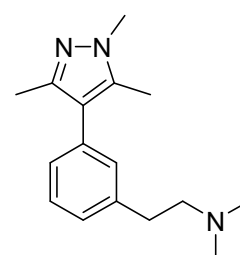
#### **N-methyl-2-(3-(1,3,5-trimethyl-1H-pyrazol-4-yl)phenyl)ethanamine (21)**

2-(3-(1,3,5-trimethyl-1H-pyrazol-4-yl)phenyl)ethanamine (126 mg, 0.549 mmol), Boc<sub>2</sub>O (132 mg, 0.604 mmol) and Na<sub>2</sub>CO<sub>3</sub> (146 mg, 1.374 mmol) was dissolved in 20 ml of THF and 50 ml of water and refluxed for 15h. The reaction mixture was then cooled to rt and extracted with 3x40 ml of EtOAc. The combined organic phases were evaporated, dissolved in 50 ml of dry THF and added LiAlH<sub>4</sub> (25mg, 0.659 mmol) and refluxed for 5h. The resulting mixture was quenched using 10 ml of 1M NaOH and extracted using 3x40 ml of EtOAc. The combined organic phases were evaporated and purified by dry column vacuum chromatography using EtOAc to EtOAc:Et<sub>3</sub>N 10:1. Yield: 42.2 mg (31.6%) Rf: 0.14 (EtOAc:MeOH:Et<sub>3</sub>N 10:1:1). <sup>1</sup>H NMR (CDCl<sub>3</sub>, 400 MHz) δ: 2.21 - 2.28 (m, 6 H) 2.48 (s, 3 H) 2.82 - 2.93 (m, 4 H) 3.79 (s, 3 H) 7.07 - 7.16 (m, 3 H) 7.31 - 7.37 (m, 1 H). <sup>13</sup>C NMR (CDCl<sub>3</sub>, 100 MHz) δ: 10.3, 12.5, 36.0, 36.1, 36.3, 53.2, 119.1, 126.5, 127.3, 128.5, 129.8, 134.4, 136.2, 140.0. LC-MS (m+1): 244.1 m/z



#### **N,N-dimethyl-2-(3-(1,3,5-trimethyl-1H-pyrazol-4-yl)phenyl)ethanamine (4)**

2-(3-(1,3,5-trimethyl-1H-pyrazol-4-yl)phenyl)ethanamine (140.9 mg, 0.614 mmol), NaCNBH<sub>3</sub> (85 mg, 1.352 mmol), ZnCl<sub>2</sub> (41.9 mg, 0.307 mmol) and 37% formaldehyde (250 μl, 3.08 mmol) was dissolved in 25 ml MeOH and stirred at rt for 2h. The mixture was evaporated and purified by dry column vacuum chromatography using EtOAc to EtOAc:Et<sub>3</sub>N 10:1. Yield: 131.2 mg (83%) Rf: 0.22 (EtOAc:MeOH:Et<sub>3</sub>N 10:1:1). <sup>1</sup>H NMR (CDCl<sub>3</sub>, 400 MHz) δ: 2.24 (d, *J*=2.45 Hz, 6 H) 2.31 (s, 6 H) 2.54 - 2.61 (m, 2 H) 2.78 - 2.85 (m, 2 H) 3.78 (s, 3 H) 7.05 - 7.14 (m, 3 H) 7.29 - 7.35 (m, 1 H). <sup>13</sup>C NMR (CDCl<sub>3</sub>, 100 MHz) δ: 10.3, 12.5, 34.5, 36.0, 45.5, 60.4, 61.6, 119.2, 126.4, 127.1, 128.4, 129.8, 134.3, 136.1, 140.5, 145.0. LC-MS (m+1): 258.2 m/z



## **General labeling procedure for developing a standard procedure for the labeling of amine containing compounds**

Aryl boronic ester, palladium-catalyst and base were used in a ratio of 40:1:4. [ $^{11}\text{C}$ ]MeI was trapped in 300  $\mu\text{L}$  DMF. To the trapped [ $^{11}\text{C}$ ]MeI was added Pd-catalyst dissolved in 300  $\mu\text{L}$  of DMF:water 9:1 and heated to 60  $^{\circ}\text{C}$ . [ $^{11}\text{C}$ ]MeI was allowed to react for 2 min and the temperature was then adjusted to a predetermined temperature between 40 and 120  $^{\circ}\text{C}$ . Aryl boronic ester and the base of choice dissolved in 150  $\mu\text{L}$  of DMF:water 9:1 was added and allowed to react for 5 min. Results were analysed by HPLC using a Luna 5  $\mu\text{m}$  C18 100  $\text{\AA}$  column (150 x 4.6 mm. 50:50 0.01 M Borax buffer : MeCN flowrate 2 mL/min).

### **Standard labeling procedure:**

Aryl boronic ester,  $\text{Pd}_2(\text{dba})_3$ ,  $\text{P}(o\text{-tolyl})_3$  and base were used in a ratio of 40:1:2:4 with appropriate masses calculated from the use of 0.1 mg of  $\text{P}(o\text{-tolyl})_3$ . [ $^{11}\text{C}$ ]MeI was trapped in 300  $\mu\text{L}$  DMF. To the trapped [ $^{11}\text{C}$ ]MeI was added Pd-catalyst dissolved in 300  $\mu\text{L}$  of DMF:water 9:1 and heated to 60  $^{\circ}\text{C}$ . [ $^{11}\text{C}$ ]MeI was allowed to react for 2 min. Aryl boronic ester was added along with 0.5 M  $\text{K}_2\text{CO}_3$  dissolved in 150  $\mu\text{L}$  of DMF:water 9:1 and allowed to react for 5 min. Results were analysed by HPLC using a Luna 5  $\mu\text{m}$  C18 100  $\text{\AA}$  column (150 x 4.6 mm. 50:50 0.01 M Borax buffer : MeCN flowrate: 2 mL/min).

### **Labeling procedure utilizing Microwave:**

Aryl boronic ester,  $\text{Pd}_2(\text{dba})_3$ ,  $\text{P}(o\text{-tolyl})_3$  and base were used in a ratio of 40:1:2:4 with appropriate masses calculated from the use of 0.1 mg of  $\text{P}(o\text{-tolyl})_3$ . [ $^{11}\text{C}$ ]MeI was trapped in 300  $\mu\text{L}$  DMF. To the trapped [ $^{11}\text{C}$ ]MeI was added Pd-catalyst dissolved in 300  $\mu\text{L}$  of DMF:water 9:1 and the reaction was then heated to 60  $^{\circ}\text{C}$ . [ $^{11}\text{C}$ ]MeI was allowed to react for 2 min. Aryl boronic ester was added along with 0.5 M  $\text{K}_2\text{CO}_3$  dissolved in 150  $\mu\text{L}$  of DMF:water 9:1 and microwave irradiated for 3 min at 100 Mhz. Results were analysed by HPLC using a Luna 5  $\mu\text{m}$  C18 100  $\text{\AA}$  column (150 x 4.6 mm. 50:50 0.01 M Borax buffer : MeCN flowrate: 2 mL/min).

### Labeling of [<sup>11</sup>C]Cimbi-712:

**14**, Pd<sub>2</sub>(dba)<sub>3</sub>, P(*o*-tolyl)<sub>3</sub> and base were used in a ratio of 40:1:2:4 with appropriate masses calculated from the use of 0.1 mg of P(*o*-tolyl)<sub>3</sub>. [<sup>11</sup>C]MeI was trapped in 300 μL DMF. To the trapped [<sup>11</sup>C]MeI was added Pd-catalyst and base dissolved in 300 μL of DMF:water 9:1 and heated to 60 °C. [<sup>11</sup>C]MeI was allowed to react for 2 min. **8** was added along with 0.5 M K<sub>2</sub>CO<sub>3</sub> dissolved in 150 μL of DMF:water 9:1 and allowed to react for 5 min. Purification was performed by preparative HPLC using a Luna 5 μm C18 100 Å coloumn (Phenomenex Inc.) (250 x 10 mm, 50:50 0.01 M Borax buffer : MeCN, flowrate: 9 mL/min). The collected fraction was trapped on a solid-phase C18 sep-pack extraction coloumn and eluted with 3 ml EtOH. Results were analysed by HPLC using a Luna 5 μm C18 100 Å coloumn (Phenomenex Inc.) (150 x 4.6 mm. 50:50 0.01 M Borax buffer : MeCN, flowrate 2 mL/min). Total synthesis time: 40-50 min.

### Labeling of [<sup>11</sup>C]vortioxetine

**10**, Pd<sub>2</sub>(dba)<sub>3</sub>, P(*o*-tolyl)<sub>3</sub> and base were used in a ratio of 40:1:2:4 with appropriate masses calculated from the use of 0.1 mg of P(*o*-tolyl)<sub>3</sub>. [<sup>11</sup>C]MeI was trapped in 300 μL DMF. To the trapped [<sup>11</sup>C]MeI was added Pd-catalyst and K<sub>2</sub>CO<sub>3</sub> dissolved in 300 μL of DMF/water 9:1 and heated to 60 °C. [<sup>11</sup>C]MeI was allowed to react for 2 min. **10** was added dissolved in 150 μL of DMF/water 9:1 and allowed to react for 5 min. Purification was performed by preparative HPLC using a Luna 5 μm C18 100 Å column (Phenomenex Inc.) (250 x 10 mm, 50:50 citrate buffer pH 4.62: MeCN, flowrate: 9 mL/min). The collected fraction was trapped on a solid-phase C18 sep-pack extraction column and eluted with 3 ml EtOH. Results were analyzed by HPLC using a Luna 5 μm C18 100 Å column (Phenomenex Inc.) (150 x 4.6 mm. 50:50 citrate buffer pH 4.62: MeCN, flowrate 2 mL/min). Starting activities around 100 GBq EOB as [<sup>11</sup>C]CH<sub>4</sub>. Yields as determined by HPLC: 40%. Isolated yields: 161.4–346 MBq. Specific activities: 8–478 GBq/μmol. Total synthesis time: 55 min.

### Labeling of [<sup>11</sup>C]Cimbi-772

[<sup>11</sup>C]methyl iodide ([<sup>11</sup>C]MeI) produced using a fully automated system was transferred in a stream of helium to a 1.1-mL vial containing DMF (300 μL). To this vial was added Pd<sub>2</sub>(dba)<sub>3</sub> (0.3 mg), P(*o*-tolyl)<sub>3</sub>, and 2,6 μL of a 0,5M K<sub>2</sub>CO<sub>3</sub> solution dissolved in DMF:H<sub>2</sub>O 9:1 (150 μL). The resulting mixture was heated at 60 °C for 2 min. Afterwards, precursor dissolved in DMF:H<sub>2</sub>O 9:1

(150  $\mu$ L) was added and the mixture was heated at 60  $^{\circ}$ C for another 5 min. Purification of the crude product was accomplished using HPLC (Luna 5 $\mu$  C<sub>18</sub>(2) 100  $\text{\AA}$ , 250 x 10.00 mm 5 micron; 0.01M Borax buffer: MeCN (30:70, flow rate: 9 mL/min, RT: 475 sec ([<sup>11</sup>C]Cimbi-772). The fraction corresponding to the labeled product was collected in sterile water (150 mL), and the resulting solution was passed through a solid-phase C18 Sep-Pak extraction column (Waters Corp.), which had been preconditioned with ethanol (10 mL), followed by *isotonic* sodium chloride solution (20 mL). The column was flushed with sterile water (3 mL). Then, the trapped radioactivity was eluted with ethanol (3 mL) into a 20-mL vial containing phosphate buffer (9 mL, 100 mM, pH 7), giving a 12 mL solution of [<sup>11</sup>C]Cimbi-772. In a total synthesis time of 45–50 min, 0.1–0.2 GBq of [<sup>11</sup>C]Cimbi-772 was produced.

### **Labeling of [<sup>11</sup>C]Cimbi-775**

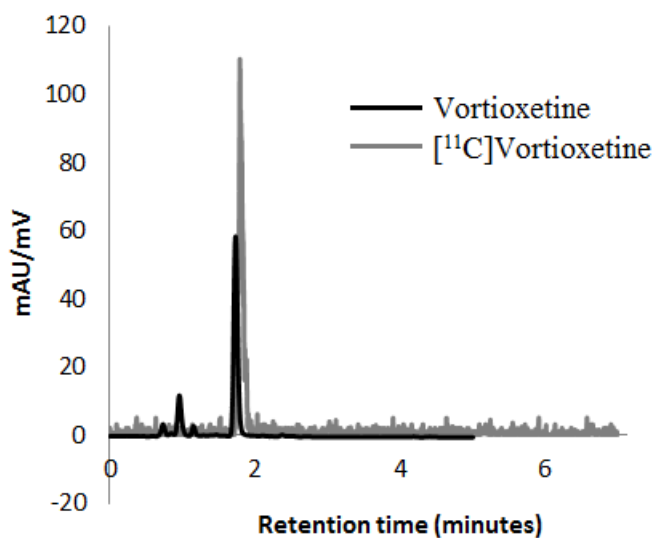
[<sup>11</sup>C]methyl iodide ([<sup>11</sup>C]MeI) produced using a fully automated system was transferred in a stream of helium to a 1.1-mL vial containing the labeling precursor 21 (0.3–0.4 mg), DMF (300  $\mu$ L) and 4  $\mu$ L of a 2N NaOH solution. The resulting mixture was heated at 140  $^{\circ}$ C for 5 min. Afterwards, the solution was subsequently cooled to 80  $^{\circ}$ C by nitrogen cooling before 500  $\mu$ L of a TFA:CH<sub>2</sub>Cl<sub>2</sub> solution (1:1) was added. The solution was stirred for further 5 min at this temperature and then quenched with 3.5 mL of HPLC eluent. Purification of the crude product was accomplished using HPLC (Luna 5 $\mu$  C18 100  $\text{\AA}$ , 250 x 10.00 mm 5 micron; EtOH/0.1 H<sub>3</sub>PO<sub>4</sub> (20:80, flow rate: 6 mL/min, RT: 650 sec ([<sup>11</sup>C]Cimbi-775). The fraction corresponding to the labeled product was collected in sterile water (150 mL), and the resulting solution was passed through a solid-phase C18 Sep-Pak extraction column (Waters Corp.), which had been preconditioned with ethanol (10 mL), followed by *isotonic* sodium chloride solution (20 mL). The column was flushed with sterile water (3 mL). Then, the trapped radioactivity was eluted with ethanol (3 mL), followed by *isotonic* sodium chloride solution (3 mL) into a 20-mL vial containing phosphate buffer (9 mL, 100 mM, pH 7), giving a 15 mL solution of [<sup>11</sup>C]Cimbi-775 with a pH of approximately 7. In a total synthesis time of 45–50 min, 0.4–0.5 GBq of [<sup>11</sup>C]Cimbi-775 was produced.

## Labeling of [<sup>11</sup>C]E55888

0.3 mg of **21** was dissolved in 300 µl of actone. After the trapping of [<sup>11</sup>C]MeOTf the reaction was heated to 60°C for 90 sec. Purification was performed by semi-preparative HPLC using a Luna 5 µm C18 100 Å column (Phenomenex Inc.) (250 x 10 mm), 80:20 0,1% TFA in water : MeCN, flowrate: 6 mL/min). The collected fraction was trapped on a solid-phase C18 sep-pack extraction column and eluted with 3 ml EtOH. Results were analyzed by HPLC using a Luna 5 µm C18 100 Å column (Phenomenex Inc.) (150 x 4.6 mm), 85:15 0,1% TFA in water : MeCN, flowrate 2 mL/min). Isolated yields: 1743-2433 MBq. Specific activities: 303-346 GBq/µmol. Total synthesis time: 37-42 min.

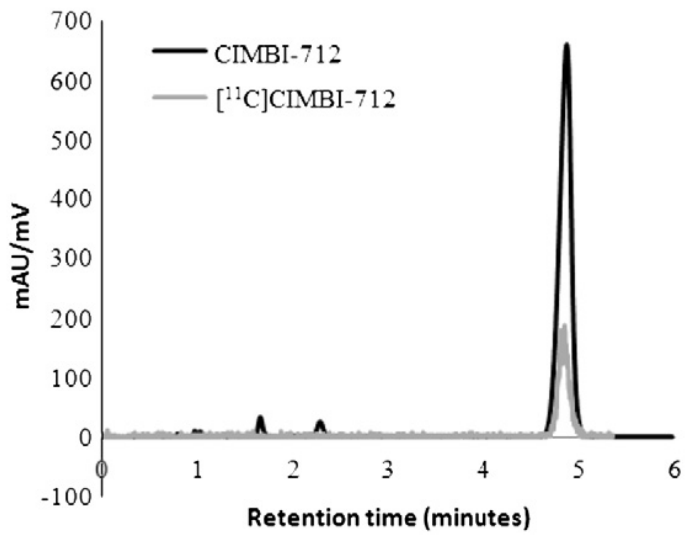
## Analytical HPLC chromatograms of purified radioactive products

### [<sup>11</sup>C]Vortioxetine

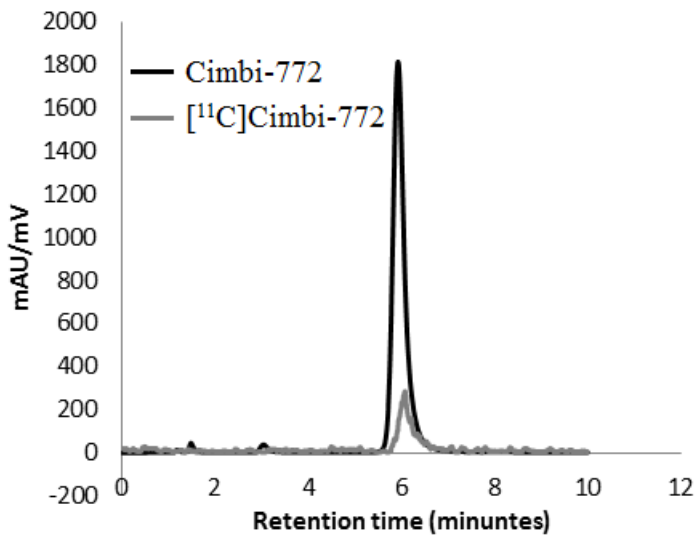




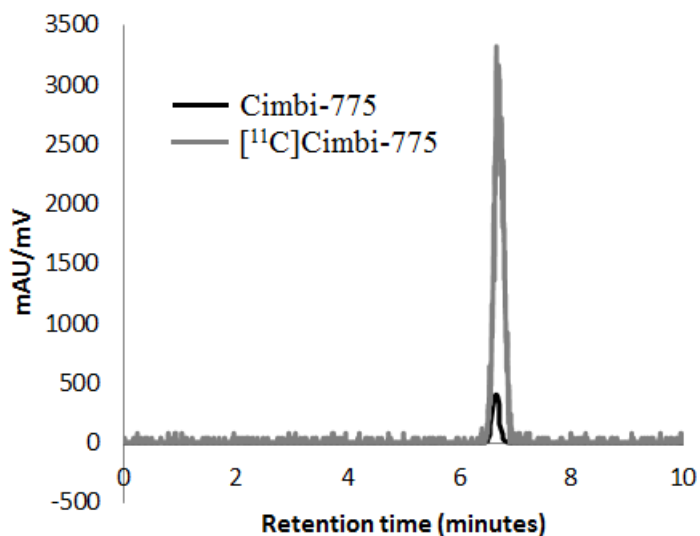
### [<sup>11</sup>C]Cimbi-712



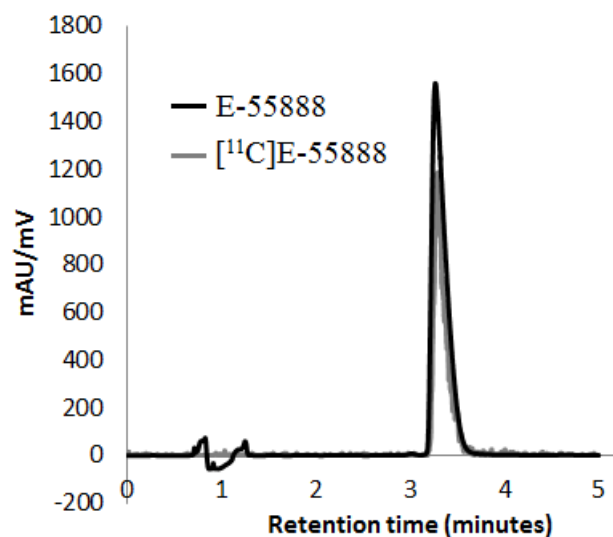
### [<sup>11</sup>C]Cimbi-772



### [<sup>11</sup>C]Cimbi-775



### [<sup>11</sup>C]E-55888



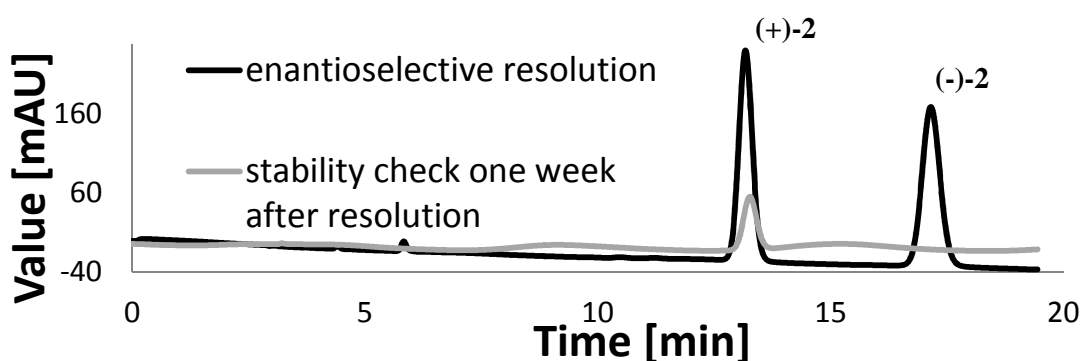
### Chiral resolution of Cimbi-712, and Cimbi-772 and Cimbi-775

Analytic resolution of Cimbi-712: 5  $\mu$ L of the desired racemate (1 mg/1 mL MeCN) were injected on a Lux 5  $\mu$ m Cellulose-4 LC Column 250 x 4.6 mm. The sample was eluted with Hexane:iPA:DEA (40:60:0.1) with a flowrate of 1 mL/min. Retention time (RT) of the separated enantiomers of Cimbi-712: a) 4.91 min b) 13.03 min

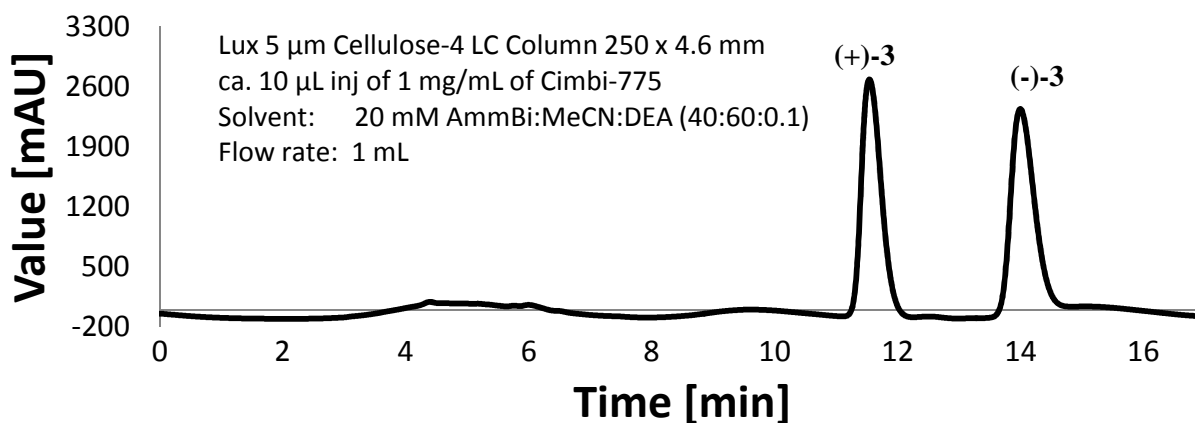
Analytic resolution of Cimbi-772 and Cimbi-775: 5  $\mu$ L of the desired racemate (1 mg/1 mL MeCN) were injected on a Lux 5  $\mu$ m Cellulose-4 LC Column 250 x 4.6 mm. The sample was eluted with 20 mM AmmBi: MeCN:DEA (40:60:0.1) with a flowrate of 1 mL/min. 1) Retention time (RT) of the separated enantiomers of Cimbi-772: a) 12.45 min b) 16.81 min 2) RT of the enantiomers of Cimbi-775: a) 11.956 min b) 14.13 min;

Chiral separation was carried out using a Jasco PU 880 pump, a spectraseries UV100 detector connected to a Merck Hitachi D-2000 chromato-integrator and a Diacel Chiralpak IF (5  $\mu$ m 10 mm x 250 mm) column. Cimbi-772 was separated using heptane:IPA:DEA 90:10:0.1 at 4.5 ml/min and Cimbi-775 was separated using heptane:IPA:DEA 80:20:0.1 at 4.5 ml/min.

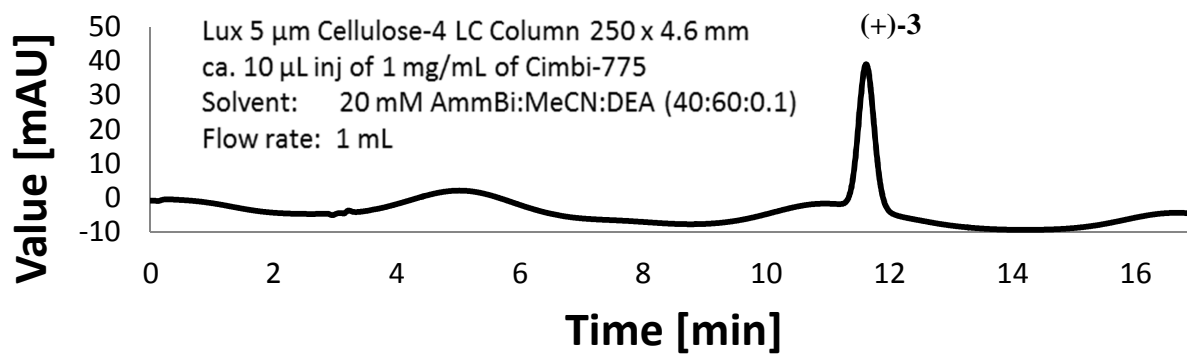
#### Chiral resolution of Cimbi-772 (2) and stability test



#### Chiral resolution of Cimbi-775 (3)



### Stability test of (+)-3



### Optical Rotation

Optical rotation was measured on a Bellingham + stanley ADP410 polarimeter at 689 nm.

(-) - 2:  $[\alpha]_D^{20} = -16$  (c = 0.5, CHCl<sub>3</sub>)

(+) - 2:  $[\alpha]_D^{20} = +16$  (c = 0.5, CHCl<sub>3</sub>)

(-) - 3:  $[\alpha]_D^{20} = -16$  (c = 0.5, CHCl<sub>3</sub>)

(+) - 3:  $[\alpha]_D^{20} = +16$  (c = 0.5, CHCl<sub>3</sub>)

## 7 References

1. Erspamer, V.; Asero, B. *Nature* 1952, **169**, 800-801.
2. Twarog, B. M.; Page, I. H.; Bailey, H. *American Journal of Physiology* 1953, **175**, 157-161.
3. Saulin, A.; Savli, M.; Lanzenberger, R. *Amino Acids* 2012, **42**, 2039-2057.
4. Gershon, M. D.; Tack, J. *Gastroenterology* 2007, **132**, 397-414.
5. Berger, M.; Gray, J. A.; Roth, B. L. *Annual Review of Medicine* 2009, **60**, 355-366.
6. Nichols, D. E.; Nichols, C. D. *Chemical Reviews* 2008, **108**, 1614-1641.
7. Wong, D. T.; Perry, K. W.; Bymaster, F. P. *Nature Reviews Drug Discovery* 2005, **4**, 764-774.
8. Lucki, I. *Biological Psychiatry* 1998, **44**, 151-162.
9. Huot, P.; Fox, S. H. *Experimental Brain Research* 2013, **230**, 463-476.
10. Dussor, G. *Current Opinion in Supportive and Palliative Care* 2014, **8**, 137-142.
11. Lacivita, E.; Di Pilato, P.; De Giorgio, P.; Colabufo, N. A.; Berardi, F.; Perrone, R.; Leopoldo, M. *Expert Opinion on Therapeutic Patents* 2012, **22**, 887-902.
12. Halliday, G. M.; Li, Y. W.; Blumbergs, P. C.; Joh, T. H.; Cotton, R. G. H.; Howe, P. R. C.; Blessing, W. W.; Geffen, L. B. *Annals of Neurology* 1990, **27**, 373-385.
13. Halliday, G. M.; Blumbergs, P. C.; Cotton, R. G. H.; Blessing, W. W.; Geffen, L. B. *Brain Research* 1990, **510**, 104-107.
14. Kish, S. J.; Tong, J. C.; Hornykiewicz, O.; Rajput, A.; Chang, L. J.; Guttman, M.; Furukawa, Y. *Brain* 2008, **131**, 120-131.
15. Scatton, B.; Javoyagid, F.; Rouquier, L.; Dubois, B.; Agid, Y. *Brain Research* 1983, **275**, 321-328.

16. Devry, J. *Psychopharmacology* 1995, **121**, 1-26.
17. Hannon, J.; Hoyer, D. *Behavioural Brain Research* 2008, **195**, 198-213.
18. Grailhe, R.; Grabtree, G. W.; Hen, R. *European Journal of Pharmacology* 2001, **418**, 157-167.
19. Lummis, S. C. R. *Journal of Biological Chemistry* 2012, **287**, 40239-40245.
20. Bard, J. A.; Zgombick, J.; Adham, N.; Vaysse, P.; Brancheck, T. A.; Weinshank, R. L. *Journal of Biological Chemistry* 1993, **268**, 23422-23426.
21. Plassat, J. L.; Amlaiky, N.; Hen, R. *Molecular Pharmacology* 1993, **44**, 229-236.
22. Shen, Y.; Monsma, F. J.; Metcalf, M. A.; Jose, P. A.; Hamblin, M. W.; Sibley, D. R. *Journal of Biological Chemistry* 1993, **268**, 18200-18204.
23. Gellynck, E.; Heyninck, K.; Andressen, K. W.; Haegeman, G.; Levy, F. O.; Vanhoenacker, P.; Van Craenenbroeck, K. *Experimental Brain Research* 2013, **230**, 555-568.
24. Schoeffter, P.; Ullmer, C.; Bobirnac, I.; Gabbiani, G.; Lubbert, H. *British Journal of Pharmacology* 1996, **117**, 993-994.
25. Irving, H. R.; Tan, Y. Y.; Tochon-Danguy, N.; Liu, H. H.; Chetty, N.; Desmond, P. V.; Pouton, C. W.; Coupar, I. A. *Life Sciences* 2007, **80**, 1198-1205.
26. Varnas, K.; Thomas, D. R.; Tupala, E.; Tiihonen, J.; Hall, H. *Neuroscience Letters* 2004, **367**, 313-316.
27. Hedlund, P. B. *Psychopharmacology* 2009, **206**, 345-354.
28. Bonaventure, P.; Kelly, L.; Aluisio, L.; Shelton, J.; Lord, B.; Galici, R.; Miller, K.; Atack, J.; Lovenberg, T. W.; Dugovic, C. *Journal of Pharmacology and Experimental Therapeutics* 2007, **321**, 690-698.
29. Sarkisyan, G.; Roberts, A. J.; Hedlund, P. B. *Behavioural Brain Research* 2010, **209**, 99-108.
30. Wesolowska, A.; Nikiforuk, A.; Stachowicz, K.; Tatarczynska, E. *Neuropharmacology* 2006, **51**, 578-586.

31. Hedlund, P. B.; Huitron-Resendiz, S.; Henriksen, S. J.; Sutcliffe, J. G. *Biological Psychiatry* 2005, **58**, 831-837.
32. Guscott, M.; Bristow, L. J.; Hadingham, K.; Rosahl, T. W.; Beer, M. S.; Stanton, J. A.; Bromidge, F.; Owens, A. P.; Huscroft, I.; Myers, J.; Rupniak, N. M.; Patel, S.; Whiting, P. J.; Hutson, P. H.; Fone, K. C.; Biello, S. M.; Kulagowski, J.; McAllister, G. *Neuropharmacology* 2005, **48**, 492-502.
33. Cates, L. N.; Roberts, A. J.; Huitron-Resendiz, S.; Hedlund, P. B. *Neuropharmacology* 2013, **70**, 211-217.
34. Abbas, A. I.; Hedlund, P. B.; Huang, X. P.; Tran, T. B.; Meltzer, H. Y.; Roth, B. L. *Psychopharmacology* 2009, **205**, 119-128.
35. Bang-Andersen, B.; Ruhland, T.; Jorgensen, M.; Smith, G.; Frederiksen, K.; Jensen, K. G.; Zhong, H. L.; Nielsen, S. M.; Hogg, S.; Mork, A.; Stensbol, T. B. *Journal of Medicinal Chemistry* 2011, **54**, 3206-3221.
36. Hedlund, P. B.; Sutcliffe, J. G. *Neuroscience Letters* 2007, **414**, 247-251.
37. Roberts, A. J.; Krucker, T.; Levy, C. L.; Slanina, K. A.; Sutcliffe, J. G.; Hedlund, P. B. *European Journal of Neuroscience* 2004, **19**, 1913-1922.
38. Volk, B.; Barkoczy, J.; Hegedus, E.; Udvari, S.; Gacsalyi, I.; Mezei, T.; Pallagi, K.; Kompagne, H.; Levay, G.; Egyed, A.; Harsing, L. G.; Spedding, M.; Simig, G. *Journal of Medicinal Chemistry* 2008, **51**, 2522-2532.
39. Lovell, P. J.; Bromidge, S. M.; Dabbs, S.; Duckworth, D. M.; Forbes, I. T.; Jennings, A. J.; King, F. D.; Middlemiss, D. N.; Rahman, S. K.; Saunders, D. V.; Collin, L. L.; Hagan, J. J.; Riley, G. J.; Thomas, D. R. *Journal of Medicinal Chemistry* 2000, **43**, 342-345.
40. Bourson, A.; Kapps, V.; Zwingelstein, C.; Rudler, A.; Boess, F. G.; Sleight, A. J. *Naunyn-Schmiedeberg's Archives of Pharmacology* 1997, **356**, 820-826.
41. Yang, Z. Y.; Liu, X. J.; Yin, Y. P.; Sun, S. G.; Deng, X. J. *European Journal of Pharmacology* 2012, **685**, 52-58.
42. Witkin, J. M.; Baez, M.; Yu, J. L.; Barton, M. E.; Shannon, H. E. *Epilepsy Research* 2007, **75**, 39-45.
43. Ache, H. J. *Angewandte Chemie-International Edition* 1972, **11**, 179-&.

44. Miller, P. W.; Long, N. J.; Vilar, R.; Gee, A. D. *Angewandte Chemie-International Edition* 2008, 47, 8998-9033.
45. Levin, C. S.; Hoffman, E. J. *Physics in Medicine and Biology* 1999, 44, 781-799.
46. Piel, M.; Vernaleken, I.; Rösch, F. *Journal of Medicinal Chemistry* 2014.
47. Brown, T. F.; Yasillo, N. J. *Journal of Nuclear Medicine Technology* 1997, 25, 98-102.
48. Stabin, M. G. *Journal of Nuclear Medicine* 2008, 49, 1555-1563.
49. Innis, R. B.; Cunningham, V. J.; Delforge, J.; Fujita, M.; Giedde, A.; Gunn, R. N.; Holden, J.; Houle, S.; Huang, S. C.; Ichise, M.; Lida, H.; Ito, H.; Kimura, Y.; Koeppe, R. A.; Knudsen, G. M.; Knuuti, J.; Lammertsma, A. A.; Laruelle, M.; Logan, J.; Maguire, R. P.; Mintun, M. A.; Morris, E. D.; Parsey, R.; Price, J. C.; Slifstein, M.; Sossi, V.; Suhara, T.; Votaw, J. R.; Wong, D. F.; Carson, R. E. *Journal of Cerebral Blood Flow and Metabolism* 2007, 27, 1533-1539.
50. Meyer, J. H.; Wilson, A. A.; Ginovart, N.; Goulding, V.; Hussey, D.; Hood, K.; Houle, S. *American Journal of Psychiatry* 2001, 158, 1843-1849.
51. Bergstrom, M.; Fasth, K. J.; Kilpatrick, G.; Ward, P.; Cable, K. M.; Wipperfman, M. D.; Sutherland, D. R.; Langstrom, B. *Neuropharmacology* 2000, 39, 664-670.
52. Phelps, M. E.; Huang, S. C.; Hoffman, E. J.; Selin, C.; Sokoloff, L.; Kuhl, D. E. *Annals of Neurology* 1979, 6, 371-388.
53. Hasselbalch, S. G.; Knudsen, G. M.; Videbaek, C.; Pinborg, L. H.; Schmidt, J. F.; Holm, S.; Paulson, O. B. *Diabetes* 1999, 48, 1915-1921.
54. Syvanen, S.; Lindhe, O.; Palner, M.; Kornum, B. R.; Rahman, O.; Langstrom, B.; Knudsen, G. M.; Hammarlund-Udenaes, M. *Drug Metabolism and Disposition* 2009, 37, 635-643.
55. Josserand, V.; Pelerin, H.; de Bruin, B.; Jego, B.; Kuhnast, B.; Hinnen, F.; Duconge, F.; Boisgard, R.; Beuvon, F.; Chassoux, F.; Dumas-Duport, C.; Ezan, E.; Dolle, F.; Mabondzo, A.; Tavitian, B. *Journal of Pharmacology and Experimental Therapeutics* 2006, 316, 79-86.
56. Klunk, W. E.; Engler, H.; Nordberg, A.; Wang, Y. M.; Blomqvist, G.; Holt, D. P.; Bergstrom, M.; Savitcheva, I.; Huang, G. F.; Estrada, S.; Ausen, B.; Debnath, M. L.; Barletta, J.; Price, J. C.; Sandell, J.; Lopresti, B. J.; Wall, A.; Koivisto, P.; Antoni, G.; Mathis, C. A.; Langstrom, B. *Annals of Neurology* 2004, 55, 306-319.



57. Nash, J. R.; Sargent, P. A.; Rabiner, E. A.; Hood, S. D.; Argyropoulos, S. V.; Potokar, J. P.; Grasby, P. M.; Nutt, D. J. *British Journal of Psychiatry* 2008, *193*, 229-234.
58. Perreau-Linck, E.; Beauregard, M.; Gravel, P.; Paquette, V.; Soucy, J. P.; Diksic, M.; Benkelfat, C. *Journal of Psychiatry & Neuroscience* 2007, *32*, 430-434.
59. Berney, A.; Nishikawa, M.; Benkelfat, C.; Debonnel, G.; Gobbi, G.; Diksic, M. *Neurochemistry International* 2008, *52*, 701-708.
60. Reimold, M.; Batra, A.; Knobel, A.; Smolka, M. N.; Zimmer, A.; Mann, K.; Solbach, C.; Reischl, G.; Schwarzler, F.; Grunder, G.; Machulla, H. J.; Bares, R.; Heinz, A. *Molecular Psychiatry* 2008, *13*, 606-613.
61. Meltzer, C. C.; Smith, G.; Price, J. C.; Reynolds, C. F.; Mathis, C. A.; Greer, P.; Lopresti, B.; Mintun, M. A.; Pollock, B. G.; Ben-Eliezer, D.; Cantwell, M. N.; Kaye, W.; DeKosky, S. T. *Brain Research* 1998, *813*, 167-171.
62. Hu, J.; Henry, S.; Gallezot, J. D.; Ropchan, J.; Neumaier, J. F.; Potenza, M. N.; Sinha, R.; Krystal, J. H.; Huang, Y. Y.; Ding, Y. S.; Carson, R. E.; Neumeister, A. *Biological Psychiatry* 2010, *67*, 800-803.
63. Murrough, J. W.; Henry, S.; Hu, J. A.; Gallezot, J. D.; Planeta-Wilson, B.; Neumaier, J. F.; Neumeister, A. *Psychopharmacology* 2011, *213*, 547-553.
64. Paterson, L. M.; Tyacke, R. J.; Nutt, D. J.; Knudsen, G. M. *Journal of Cerebral Blood Flow and Metabolism* 2010, *30*, 1682-1706.
65. Nord, M.; Finnema, S. J.; Halldin, C.; Farde, L. *International Journal of Neuropsychopharmacology* 2013, *16*, 1577-1586.
66. Selvaraj, S.; Turkheimer, F.; Rosso, L.; Faulkner, P.; Mouchlianitis, E.; Roiser, J. P.; McGuire, P.; Cowen, P. J.; Howes, O. *Molecular Psychiatry* 2012, *17*, 1254-1260.
67. Waterhouse, R. N. *Molecular Imaging and Biology* 2003, *5*, 376-389.
68. Zhang, M. R.; Haradahira, T.; Maeda, J.; Okauchi, T.; Kida, T.; Obayashi, S.; Suzuki, K.; Suhara, T. *Journal of Labelled Compounds & Radiopharmaceuticals* 2002, *45*, 857-866.
69. Andries, J.; Lemoine, L.; Mouchel-Blaisot, A.; Tang, S.; Verdurand, M.; Le Bars, D.; Zimmer, L.; Billard, T. *Bioorganic & Medicinal Chemistry Letters* 2010, *20*, 3730-3733.

70. Andries, J.; Lemoine, L.; Le Bars, D.; Zimmer, L.; Billard, T. *European Journal of Medicinal Chemistry* 2011, **46**, 3455-3461.
71. Lemoine, L.; Andries, J.; Le Bars, D.; Billard, T.; Zimmer, L. *Journal of Nuclear Medicine* 2011, **52**, 1811-1818.
72. Colomb, J.; Becker, G.; Forcellini, E.; Meyer, S.; Buisson, L.; Zimmer, L.; Billard, T. *Nuclear Medicine and Biology* 2014, **41**, 330-337.
73. Lacivita, E.; Niso, M.; Hansen, H. D.; Di Pilato, P.; Herth, M. M.; Lehel, S.; Ettrup, A.; Montenegro, L.; Perrone, R.; Berardi, F.; Colabufo, N. A.; Leopoldo, M.; Knudsen, G. M. *Bioorganic & Medicinal Chemistry* 2014, **22**, 1736-1750.
74. Hansen, H. D.; Lacivita, E.; Di Pilato, P.; Herth, M. M.; Lehel, S.; Ettrup, A.; Andersen, V. L.; Dyssegaard, A.; De Giorgio, P.; Perrone, R.; Berardi, F.; Colabufo, N. A.; Niso, M.; Knudsen, G. M.; Leopoldo, M. *European Journal of Medicinal Chemistry* 2014, **79**, 152-163.
75. Shimoda, Y.; Yui, J. J.; Xie, L.; Fujinaga, M.; Yamasaki, T.; Ogawa, M.; Nengaki, N.; Kumata, K.; Hatori, A.; Kawamura, K.; Zhang, M. R. *Bioorganic & Medicinal Chemistry* 2013, **21**, 5316-5322.
76. Herth, M. M.; Hansen, H. D.; Ettrup, A.; Dyssegaard, A.; Lehel, S.; Kristensen, J.; Knudsen, G. M. *Bioorganic & Medicinal Chemistry* 2012, **20**, 4574-4581.
77. Hansen, H. D.; Herth, M. M.; Ettrup, A.; Andersen, V. L.; Lehel, S.; Dyssegaard, A.; Kristensen, J. L.; Knudsen, G. M. *Journal of Nuclear Medicine* 2014, **55**, 640-646.
78. Andersen, V. L.; Herth, M. M.; Lehel, S.; Knudsen, G. M.; Kristensen, J. L. *Tetrahedron Letters* 2013, **54**, 213-216.
79. Pretze, M.; Grosse-Gehling, P.; Mamat, C. *Molecules* 2011, **16**, 1129-1165.
80. Langstrom, B.; Antoni, G.; Gullberg, P.; Halldin, C.; Malmberg, P.; Nagren, K.; Rimland, A.; Svard, H. *Journal of Nuclear Medicine* 1987, **28**, 1037-1040.
81. Link, J. M.; Krohn, K. A.; Clark, J. C. *Nuclear Medicine and Biology* 1997, **24**, 93-97.
82. Zeisler, S. K.; Nader, M.; Theobald, A.; Oberdorfer, F. *Applied Radiation and Isotopes* 1997, **48**, 1091-1095.

83. Iwata, R.; Ido, T.; Takahashi, T.; Nakanishi, H.; Iida, S. *Applied Radiation and Isotopes* 1987, **38**, 97-102.
84. Andersson, Y.; Cheng, A. P.; Langstrom, B. *Acta Chemica Scandinavica* 1995, **49**, 683-688.
85. Suzuki, M.; Doi, H.; Bjorkman, M.; Andersson, Y.; Langstrom, B.; Watanabe, Y.; Noyori, R. *Chemistry-a European Journal* 1997, **3**, 2039-2042.
86. Karimi, F.; Barletta, J.; Langstrom, B. *European Journal of Organic Chemistry* 2005, 2374-2378.
87. Arai, T.; Kato, K.; Zhang, M. R. *Tetrahedron Letters* 2009, **50**, 4788-4791.
88. Prabhakaran, J.; Majo, V. J.; Simpson, N. R.; Van Heertum, R. L.; Mann, J. J.; Kumar, J. S. D. *Journal of Labelled Compounds & Radiopharmaceuticals* 2005, **48**, 887-895.
89. Tarkiainen, J.; Vercouille, J.; Emond, P.; Sandell, J.; Hiltunen, J.; Frangin, Y.; Guilloteau, D.; Halldin, C. *Journal of Labelled Compounds & Radiopharmaceuticals* 2001, **44**, 1013-1023.
90. Toyohara, J.; Sakata, M.; Wu, J.; Ishikawa, M.; Oda, K.; Ishii, K.; Iyo, M.; Hashimoto, K.; Ishiwata, K. *Annals of Nuclear Medicine* 2009, **23**, 301-309.
91. Doi, H.; Ban, I.; Nonoyama, A.; Sumi, K.; Kuang, C. X.; Hosoya, T.; Tsukada, H.; Suzuki, M. *Chemistry-a European Journal* 2009, **15**, 4165-4171.
92. Hostetler, E. D.; Terry, G. E.; Burns, H. D. *Journal of Labelled Compounds & Radiopharmaceuticals* 2005, **48**, 629-634.
93. Rahman, O.; Llop, J.; Langstrom, B. *European Journal of Organic Chemistry* 2004, 2674-2678.
94. Zeng, F. X.; Voll, R. J.; Crowe, R. J.; Waldrep, M. S.; Dolph, K. B.; Goodman, M. M. *Journal of Labelled Compounds & Radiopharmaceuticals* 2013, **56**, 307-309.
95. Ijuin, R.; Takashima, T.; Watanabe, Y.; Sugiyama, Y.; Suzuki, M. *Bioorganic & Medicinal Chemistry* 2012, **20**, 3703-3709.
96. Bjorkman, M.; Langstrom, B. *Journal of the Chemical Society-Perkin Transactions 1* 2000, 3031-3034.

97. Wust, F.; Zessin, J.; Johannsen, B. *Journal of Labelled Compounds & Radiopharmaceuticals* 2003, **46**, 333-342.
98. Kealey, S.; Passchier, J.; Huiban, M. *Chemical Communications* 2013, **49**, 11326-11328.
99. Miyaura, N.; Suzuki, A. *Chemical Reviews* 1995, **95**, 2457-2483.
100. Andersen, V. L.; Hansen, H. D.; Herth, M. M.; Knudsen, G. M.; Kristensen, J. L. *Bioorganic & Medicinal Chemistry Letters* 2014, **24**, 2408-2411.
101. Ettrup, A.; Kornum, B. R.; Weikop, P.; Knudsen, G. M. *Synapse* 2011, **65**, 136-145.
102. Herth, M. M.; Volk, B.; Pallagi, K.; Bech, L. K.; Antoni, F. A.; Knudsen, G. M.; Kristensen, J. L. *Acs Chemical Neuroscience* 2012, **3**, 1002-1007.
103. Brenchat, A.; Romero, L.; Garcia, M.; Pujol, M.; Burgueno, J.; Torrens, A.; Hamon, M.; Baeyens, J. M.; Buschmann, H.; Zamanillo, D.; Vela, J. M. *Pain* 2009, **141**, 239-247.
104. Kudlow, P. A.; McIntyre, R. S.; Lam, R. W. *CNS drugs* 2014, **28**, 601-609.
105. Kleeberg, C.; Dang, L.; Lin, Z. Y.; Marder, T. B. *Angewandte Chemie-International Edition* 2009, **48**, 5350-5354.
106. Howell, S. J.; Spencer, N.; Philp, D. *Tetrahedron* 2001, **57**, 4945-4954.
107. Ramalingam, K.; Nowotnik, D. P. *Organic Preparations and Procedures International* 1991, **23**, 729-734.
108. Volk, B.; Mezei, T.; Simig, G. *Synthesis-Stuttgart* 2002, 595-597.

## 8 Appendices

### Appendix 1: Paper I

**V. L. Andersen**, M. M. Herth, S. Lehel, G. M. Knudsen, and J. L. Kristensen, 'Palladium-Mediated Conversion of Para-Aminoarylboronic Esters into Para-Aminoaryl-C-11-Methanes', *Tetrahedron Letters*, 54 (2013), 213-16.

### Appendix 2: Paper II

H. D. Hansen, M. M. Herth, A. Ettrup, **V. L. Andersen**, S. Lehel, A. Dyssegaard, J. L. Kristensen, and G. M. Knudsen, 'Radiosynthesis and in Vivo Evaluation of Novel Radioligands for Pet Imaging of Cerebral 5-HT<sub>7</sub> Receptors', *Journal of Nuclear Medicine*, 55 (2014), 640-46.

### Appendix 3: Paper III

**V. L. Andersen**, H. D. Hansen, M. M. Herth, G. M. Knudsen, and J. L. Kristensen, '<sup>11</sup>C-Labeling and Preliminary Evaluation of Vortioxetine as a Pet Radioligand', *Bioorganic & Medicinal Chemistry Letters*, 24 (2014), 2408-11.

### Appendix 4: Paper IV

M. M. Herth, **V. L. Andersen**, H. D. Hansen, N. Stroth, B. Volk, A. Ettrup, S. Lehel, P. Svenningsson, G. M. Knudsen and J. L. Kristensen, 'Evaluation of 3-Ethyl-3-(phenylpiperazinylbutyl)oxindoles as PET ligands for the 5-HT<sub>7</sub> Receptor – Synthesis, pharmacology, radiolabeling and in vivo Brain Imaging', *Journal of Medicinal Chemistry* (To be submitted).

### Appendix 5

M. M. Herth, **V. L. Andersen**, S. Lehel, J. Madsen, G. M. Knudsen, and J. L. Kristensen, 'Development of a C-11-Labeled Tetrazine for Rapid Tetrazine-Trans-Cyclooctene Ligation', *Chemical Communications*, 49 (2013), 3805-07.



# Appendix 1

## Paper I

Conversion of Para-Aminoarylboronic Esters into Para-Aminoaryl-C-11-Methanes

**V. L. Andersen**, M. M. Herth, S. Lehel, G. M. Knudsen, and J. L. Kristensen

*Tetrahedron Letters*, 54 (2013), 213-16.







## Palladium-mediated conversion of *para*-aminoarylboronic esters into *para*-aminoaryl-<sup>11</sup>C-methanes

Valdemar L. Andersen<sup>a,b,c,d,†</sup>, Matthias M. Herth<sup>a,b,c,d,†</sup>, Szabolcs Lehel<sup>b</sup>, Gitte M. Knudsen<sup>c,d</sup>, Jesper L. Kristensen<sup>a,d,\*</sup>

<sup>a</sup> Department of Drug Design and Pharmacology, School of Pharmaceutical Sciences, Faculty of Health and Medical Sciences, University of Copenhagen, Universitetsparken 2, Copenhagen 2100, Denmark

<sup>b</sup> PET and Cyclotron Unit, Copenhagen University Hospital, Blegdamsvej 9, Copenhagen 2100, Denmark

<sup>c</sup> Neurobiological Research Unit, Copenhagen University Hospital, Juliane Maries Vej 24, Copenhagen 2100, Denmark

<sup>d</sup> Center for Integrated Molecular Brain Imaging (CIMBI), Juliane Maries Vej 24, Copenhagen 2100, Denmark

### ARTICLE INFO

#### Article history:

Received 9 July 2012

Revised 17 October 2012

Accepted 1 November 2012

Available online 10 November 2012

#### Keywords:

Cross-couplings

PET

Carbon-11

Methyl iodide

Palladium

### ABSTRACT

Cross-couplings are an alternative to conventional <sup>11</sup>C-methylations which are generally employed in PET tracer synthesis. Therefore, we set out to develop a general procedure for the synthesis of *para*-<sup>11</sup>CH<sub>3</sub> labeled aromatic amines from the corresponding *para*-aminoarylboronic esters in the presence of free amines. Aryl boronic esters containing primary, secondary, and tertiary amines were successfully converted into corresponding labeled methyl derivatives in sufficient radiochemical yield to apply this method for tracer development. This procedure was applied to the labeling of CIMBI-712, a promising candidate for the in vivo imaging of the 5-HT<sub>7</sub> receptor in the CNS.

© 2012 Elsevier Ltd. All rights reserved.

Positron emission tomography (PET) is widely used as a tool to image biological processes in the body. For example, it allows the imaging of neuroreceptors and transporters in vivo. Since its discovery in 1976, <sup>11</sup>C-methylation of amines and hydroxy-groups via [<sup>11</sup>C]CH<sub>3</sub>I has been the most commonly used strategy for obtaining <sup>11</sup>C-labeled PET tracers.<sup>1</sup> The disadvantage of this approach is twofold. Firstly, the presence of an *N*-methyl- or methoxy- group in the ligand is necessary for the synthesis of a viable precursor. Secondly, its applicability to various functional groups often makes time consuming protection/deprotection a necessity. Therefore, different <sup>11</sup>C-labeling strategies have been developed.<sup>1</sup> For example, cross-couplings via [<sup>11</sup>C]CH<sub>3</sub>I have been carried out to broaden scope, and in recent years, mainly the Stille reaction was applied in PET chemistry, even though examples where the Suzuki reaction has been used for <sup>11</sup>C-radiolabeling have appeared in the literature.<sup>2,3</sup>

Both the Stille and the Suzuki reactions have advantages and disadvantages. In general, the reactivity in a Stille reaction is higher and therefore gives faster reaction rates. However, in PET chemistry the very large excess of the precursor causes the concentration of this to remain constant during the labeling step, and the

reactions can be considered pseudo-first-order.<sup>4</sup> Therefore, the higher reactivity in a Stille reaction does not play a key role. Thus, a direct comparison of reactivities in preparative synthetic organic chemistry and radiochemistry can be misleading.

The Stille reaction is not dependent on the presence of a base. This is an advantage when working with compounds that are unstable under basic conditions. On the other hand, the Suzuki reaction uses less toxic reagents compared to the tin species applied in the Stille reaction. When a radiolabeled compound is to be used in vivo, non-toxic reagents and precursors are preferable. Therefore, we believe that the Suzuki reaction is the superior alternative for PET tracer production.

The use of the Suzuki reaction in PET chemistry has received limited attention. A review in 2011 described the various endeavors using the Suzuki reaction as a tool to insert <sup>11</sup>C-labeled

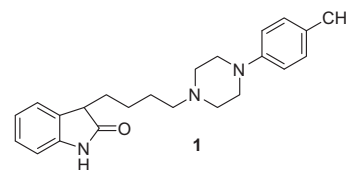
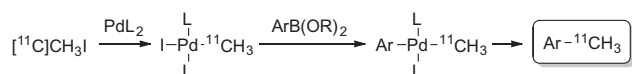


Figure 1. Structure of CIMBI-712.

\* Corresponding author.

E-mail address: [jekr@farma.ku.dk](mailto:jekr@farma.ku.dk) (J.L. Kristensen).

† Equally contributed.



**Figure 2.** Oxidative addition of  $[^{11}\text{C}]\text{MeI}$  followed by transmetalation and reductive elimination upon addition of the boronic substrate.

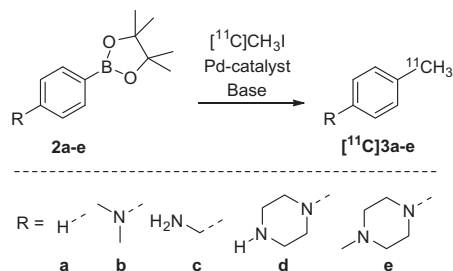


**Figure 3.** Model compounds portraying different amines encountered in PET tracers.

**Table 1**  
Effect of different Pd-systems on the RCY<sup>a</sup>

The reaction scheme shows the conversion of **2e** to **[ $^{11}\text{C}$ ]3e** using  $[^{11}\text{C}]\text{CH}_3\text{I}$ , a Pd catalyst,  $\text{K}_2\text{CO}_3$ , at  $60^\circ\text{C}$  in  $\text{DMF:H}_2\text{O}$  9:1.

Entry	Pd-catalyst	RCY (%)
1	$\text{Pd}(\text{PPh}_3)_4$	9
2	$\text{Pd}(\text{PPh}_3)_2\text{Cl}_2$	0
3	$\text{Pd}(\text{dppf})\text{Cl}_2$	0
4	$\text{Pd}_2(\text{dba})_3 + \text{P}(o\text{-tolyl})_3$	49

<sup>a</sup> Reaction was carried out with 40 equiv of boronic ester, 1 equiv of Pd-catalyst, 2 equiv of ligand, and 2 equiv of base.

**Table 2**  
Impact of the ester species on the RCY<sup>a</sup>

The reaction scheme shows the conversion of **2a-b** to **[ $^{11}\text{C}$ ]3a-b** using  $[^{11}\text{C}]\text{CH}_3\text{I}$ ,  $\text{K}_2\text{CO}_3$ ,  $\text{Pd}_2(\text{dba})_3$ ,  $\text{P}(o\text{-tolyl})_3$ , at  $100^\circ\text{C}$  in  $\text{DMF:H}_2\text{O}$  9:1. **2a-b** has  $\text{R}^2 = \text{pinacol}$ , and **4a-b** has  $\text{R}^2 = \text{neopentyl glycol}$ .

Entry	R <sup>1</sup>	R <sup>2</sup>	(RCY) (%)
1	H	pinacol	71
2	H	neopentyl glycol	72
3	$\text{N}(\text{CH}_3)_2$	pinacol	59
4	$\text{N}(\text{CH}_3)_2$	neopentyl glycol	58

<sup>a</sup> See Table 1 for the reaction conditions.

carbonyl groups or methyl groups.<sup>5</sup> Additionally, it remarks that the insertion of  $[^{11}\text{C}]\text{methyl}$  groups has received no further attention, and a literature search only revealed two separate investigations on this subject. The Suzuki reaction has been investigated by Hostetler et al.<sup>6</sup> and Doi et al.<sup>7</sup> using either microwave or conventional heating. Previously the Suzuki reaction has been used to label  $[\omega\text{-}^{11}\text{C}]\text{palmitic acid}$ <sup>2</sup> and  $[^{11}\text{C}]\text{dehydropravastatin}$ .<sup>3</sup> The applicability toward amine-containing compounds is still

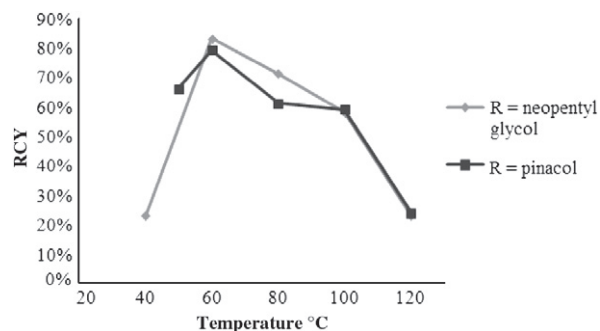
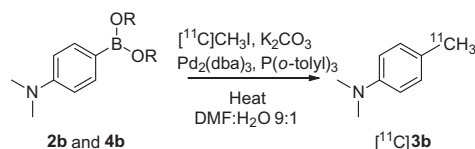


**Figure 4.** Impact of the reaction temperature on the RCY.

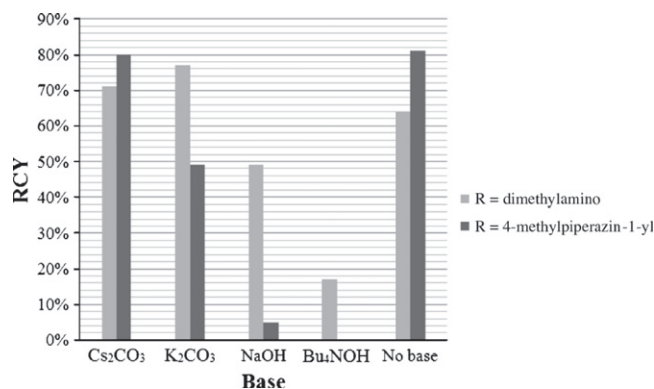
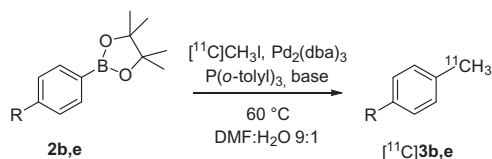


**Figure 5.** Impact of base on the RCY.

unknown and competing alkylation of the nitrogen could, in principle, be detrimental, as  $[^{11}\text{C}]\text{CH}_3\text{I}$  is known to react readily with amines. The possibility of applying the Suzuki reaction to these compounds is of great interest as many biologically active compounds contain amines.

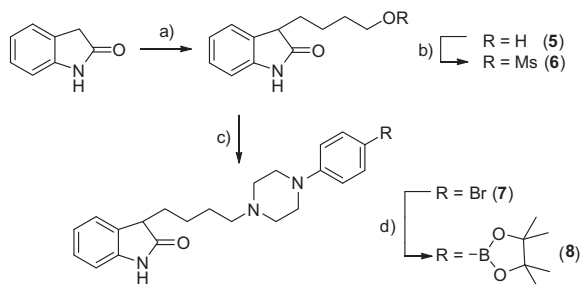
An example is the (phenylpiperazinyl-butyl)oxindoles developed by Volk et al. as selective 5-HT<sub>7</sub> antagonists.<sup>8</sup> Recently, we developed a promising compound within this chemical class, CIM-BI-712, see Figure 1.<sup>9</sup> Its selectivity profile makes it a prime candidate for PET applications, ideally setup to be labeled via the Suzuki reaction of the corresponding aryl boronic derivative.

As Hostetler et al.<sup>6</sup> and Doi et al.<sup>7</sup> reported, the reaction between an aryl boronic derivative and  $[^{11}\text{C}]\text{CH}_3\text{I}$  is a stepwise process, see Figure 2: first the oxidative addition, then the transmetalation, and finally reductive elimination. Thus, the palladium-carbon-11-complex can be formed quantitatively before the aryl boronic precursor is added. Thus,  $^{11}\text{C}$ -Suzuki reactions can be thought of as palladium-mediated rather than catalyzed as the Pd-catalyst is used in large excess compared to  $[^{11}\text{C}]\text{CH}_3\text{I}$ . This led us to hypothesize that  $N\text{-}^{11}\text{C}$ -methylation of amines should only be

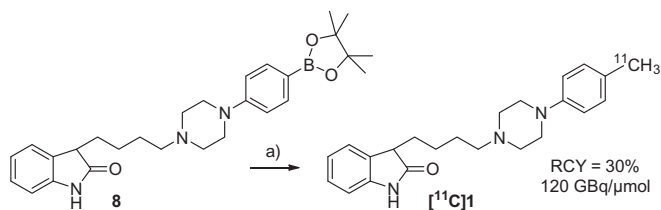
**Table 3**

Comparison of the impact of conventional heating and microwave irradiation on the RCY

Entry	Product	RCY (%) conventional heating	RCY (%) MW heating
1	 3b	77	54
2	 3c	82	5
3	 3d	64	77
4	 3e	49	86



**Scheme 1.** Reagents and conditions: (a) 1,4-butanediol, Raney-Nickel, 200 °C, 12 h, 70%; (b) MeSO<sub>2</sub>Cl, Et<sub>3</sub>N, THF, –78 °C to rt, 2 h; (c) 1-(4-bromophenyl)piperazine, Na<sub>2</sub>CO<sub>3</sub>, 130 °C, 55%; (d) bis(pinacolato)diboron, Pd(dppf)Cl<sub>2</sub>, KOAc, 1,4-dioxane, 100 °C, 12 h, 54%.



**Scheme 2.** Radiosynthesis of [<sup>11</sup>C]CIMBI-712. Reagents and conditions: (a) [<sup>11</sup>C]CH<sub>3</sub>I, K<sub>2</sub>CO<sub>3</sub>, Pd<sub>2</sub>(dba)<sub>3</sub>, P(*o*-tolyl)<sub>3</sub>, 60 °C, DMF:H<sub>2</sub>O (v:v 9:1).

observed to a minor degree. Therefore, the aim of this study was to develop a procedure in which compounds containing unprotected amines could be labeled via the Suzuki reaction, and eventually apply this procedure to the labeling of CIMBI-712.

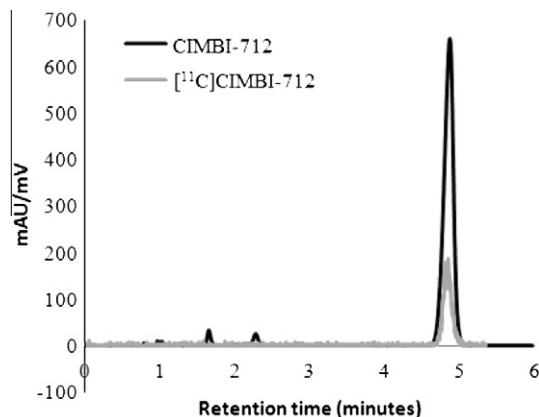


**Figure 6.** HPLC chromatograms of [<sup>11</sup>C]CIMBI-712 and CIMBI-712.

Primary, secondary, and tertiary amines are commonly observed moieties in various PET tracers. Therefore, the possibility to label model compounds bearing such motifs was investigated, see Figure 3. Reference compounds and precursors were either purchased or synthesized using standard procedures, see Supplementary data.

In general, the choice of the palladium-catalyst (Pd-ligand) affects the chemical yields quite dramatically.<sup>10</sup> Therefore, the impact on radiochemical yields (RCY) of four different Pd-ligand systems, was tested (Table 1). In accordance with the findings of Doi et al.,<sup>7</sup> Pd<sub>2</sub>(dba)<sub>3</sub> combined with P(*o*-tolyl)<sub>3</sub> was found to be the most efficient Pd-ligand system (Table 1).

The reactivity of the organoboron species of the precursors also influences the transmetalation in Suzuki couplings. Therefore, two different ester moieties were tested. The neopentyl and corresponding pinacol ester precursors displayed no impact on the RCY (Table 2).

Optimization of the reaction temperature was carried out using 4-(dimethylamino)phenylboronic esters. A range of temperatures was set from 40–120 °C for the neopentyl glycol based ester and 50–120 °C for the pinacol based ester (conditions shown in Table 1). The labeling of both compounds was highly affected by the reaction temperature. The RCY increased until 60 °C and decreased afterward for both compounds (Fig. 4). This is possibly due to the decomposition of PdL<sub>2</sub><sup>11</sup>CH<sub>3</sub>.

Furthermore, the Suzuki reaction is dependent on a base and therefore, the effect of the utilized base was investigated. Bu<sub>4</sub>NOH, NaOH, K<sub>2</sub>CO<sub>3</sub>, Cs<sub>2</sub>CO<sub>3</sub>, and the absence of a base were all tested (conditions shown in Table 1). The RCYs varied from 17–77%. Strong bases showed the lowest yields. Surprisingly, the radiosynthesis without an additional base resulted in rather high RCYs of 64% and 81%, respectively. This demonstrates that amine-containing compounds can provide suitably basic conditions for <sup>11</sup>C-Suzuki reactions. However, Cs<sub>2</sub>CO<sub>3</sub> and K<sub>2</sub>CO<sub>3</sub> provided the highest yields in our set-up and are thus preferable (Fig. 5).

To summarize, the standard conditions for <sup>11</sup>C-Suzuki cross-couplings are as follows: Pd<sub>2</sub>(dba)<sub>3</sub> and P(*o*-tolyl)<sub>3</sub> (1:2) in DMF is added to the trapped [<sup>11</sup>C]MeI and stirred at 60 °C for 2 minutes. The aryl boronic ester and base are then added and the mixture is heated at 60 °C for 5 minutes (see supporting information for full details). Using these conditions *p*-[<sup>11</sup>C]tolylmethanamine ([<sup>11</sup>C]3c), 1-(*p*-[<sup>11</sup>C]tolyl)piperazine ([<sup>11</sup>C]3d), and 1-methyl-4-(*p*-[<sup>11</sup>C]tolyl)piperazine ([<sup>11</sup>C]3e) were labeled starting from their respective precursors 2c–e with RCYs ranging from 49–82%.

Hostetler et al. demonstrated the use of microwave (MW) irradiation as a way of increasing the RCYs in <sup>11</sup>C-Suzuki reactions.<sup>6</sup>

Therefore, we applied MW conditions for labeling compounds **3b–e**. Instead of 5 minute conventional heating, 3 minutes of MW heating were applied. Changes in the RCY were variable. [ $^{11}\text{C}$ ]**3d** and [ $^{11}\text{C}$ ]**3e** showed moderately increased RCYs, whereas reduced RCYs for [ $^{11}\text{C}$ ]**3c** and [ $^{11}\text{C}$ ]**3b** were observed (Table 3).

CuI has previously been used to increase yields of Suzuki reactions.<sup>11</sup> As such [ $^{11}\text{C}$ ]**3c** and [ $^{11}\text{C}$ ]**3e** were obtained using CuI in 1:1 ratio with the respective boronic ester, but without improved RCYs.

We then utilized the protocol to prepare CIMBI-712, a potential 5-HT<sub>7</sub> PET tracer, see Figure 1.

The precursor was prepared via a four-step synthesis starting from oxindole (Scheme 1). 3-(4-Hydroxybutyl)-indolin-2-one (**5**) was formed by a Raney-Nickel catalyzed reaction between oxindole and 1,4-butanediol.<sup>8</sup> The resulting alcohol was then converted into the corresponding mesylate **6**<sup>8</sup> and reacted with 1-(4-bromophenyl)piperazine to give 3-{4-[4-(4-bromophenyl)piperazin-1-yl]butyl}indolin-2-one (**7**). Finally, the boronic ester **8** was formed via Miyaura borylation.

Labeling of **8** via the devised standard method (Scheme 2) followed by preparative HPLC purification (Fig. 6) yielded the labeled compound [ $^{11}\text{C}$ ]**1** with a radiochemical purity  $\geq 98\%$  in 30% RCY at the end of synthesis, with a typical specific activity of 120 GBq/ $\mu\text{mol}$ . Labeling using  $\text{Cs}_2\text{CO}_3$  was also attempted but was unsuccessful. We are currently evaluating CIMBI-712 as a PET tracer, and the results will be reported elsewhere.

In conclusion, a set of standard conditions for  $^{11}\text{C}$ -labeling via the Suzuki reaction has been identified. Using these conditions it was possible to label compounds containing primary, secondary,

and tertiary amines without competing alkylation at these amino groups. Finally, these conditions were used to label [ $^{11}\text{C}$ ]CIMBI-712, a potential new 5-HT<sub>7</sub> PET tracer.

### Supplementary data

Supplementary data associated with this article can be found, in the online version, at <http://dx.doi.org/10.1016/j.tetlet.2012.11.001>.

### References and notes

1. Allard, M.; Fouquet, E.; James, D.; Szlosek-Pinaud, M. *Curr. Med. Chem.* **2008**, *15*, 235–277.
2. Hostetler, E. D.; Fallis, S.; McCarthy, T. J.; Welch, M. J.; Katzenellenbogen, J. A. *J. Org. Chem.* **1998**, *63*, 1348–1351.
3. Ijuin, R.; Takashima, T.; Watanabe, Y.; Sugiyama, Y.; Suzuki, M. *Bioorg. Med. Chem.* **2012**, *20*, 3703–3709.
4. Chang, R. *Physical Chemistry for the Chemical and Biological Sciences*; University Science Books, 2000.
5. Pretze, M.; Grosse-Gehling, P.; Mamat, C. *Molecules* **2011**, *16*, 1129–1165.
6. Hostetler, E. D.; Terry, G. E.; Burns, H. D. *J. Labelled Compd. Radiopharm.* **2005**, *48*, 629–634.
7. Doi, H.; Ban, I.; Nonoyama, A.; Sumi, K.; Kuang, C.; Hosoya, T.; Tsukada, H.; Suzuki, M. *Chemistry* **2009**, *15*, 4165–4171.
8. Volk, B.; Barkoczy, J.; Hegedus, E.; Udvari, S.; Gacsalyi, I.; Mezei, T.; Pallagi, K.; Kompagne, H.; Levay, G.; Egyed, A.; Harsing, L. G.; Spedding, M.; Simig, G. *J. Med. Chem.* **2008**, *51*, 2522–2532.
9. Herth, M.; Volk, B.; Pallagi, K.; Bech, L.; Antoni, F.; Knudsen, G. M.; Kristensen, J. L. *ACS Chem. Neurosci.* **2012**. <http://dx.doi.org/10.1021/cn3001137>.
10. Nguyen, H. N.; Huang, X. H.; Buchwald, S. L. *J. Am. Chem. Soc.* **2003**, *125*, 11818–11819.
11. Deng, J. Z.; Paone, D. V.; Ginnetti, A. T.; Kurihara, H.; Dreher, S. D.; Weissman, S. A.; Stauffer, S. R.; Burgey, C. S. *Org. Lett.* **2009**, *11*, 345–347.

## **General information:**

Chemicals were purchased from Sigma or Merck. Unless otherwise stated, all chemicals were used without further purification. GC-MS analysis was performed on a Shimadzu. LC-MS analysis was performed on an Agilent 1100 system with a Hewlett Packard series 1100 MS detector. For Solid Phase Extraction (SPE), Sep-Pak®-C18-cartridges (Waters, USA) were used. Thin Layer Chromatography (TLC) was performed using plates from Merck (Silicagel 60 F254). <sup>1</sup>H-NMR spectra and <sup>13</sup>C-NMR spectra were recorded using a Bruker AC 300 spectrometer or a Bruker AC 400 spectrometer. Chemical shifts are quoted as  $\delta$ -values (ppm) downfield from tetramethylsilane (TMS). Preparative high performance liquid chromatography (HPLC) were performed on a Dionex system consisting of a pump P680A pump, a UVD 170U detector and a Scansys radiodetector. Analytical HPLC was performed on a Dionex system consisting of a pump P680A pump, a UVD 170U detector and a Scansys radiodetector, an ultimate3000 system with a Scansys radiodetector or a Waters system comprised of a 2795 separation unit, a 2996 diode array and a Scansys radiodetector. [<sup>11</sup>C]Methane was produced via the <sup>14</sup>N(p, $\alpha$ )<sup>11</sup>C reaction by bombardment of an [<sup>14</sup>N]N<sub>2</sub> containing 10% H<sub>2</sub> target with a 17 MeV proton beam in a Scanditronix MC32NI cyclotron. Microwave-assisted syntheses were carried out in a Scansys PET-SYN apparatus operating in single mode; the microwave cavity producing controlled irradiation at 2.45 GHz. The temperature was monitored by an IR sensor focused on a point on the reactor vial glass. The reactions were run in sealed vials (1 mL). Desired temperatures was obtained using variable power monitored by PID regulation.

## **Synthesis of 4-(4,4,5,5-tetramethyl-1,3,2-dioxaborolan-2-yl)-N,N-dimethylaniline (2b):**

4-(dimethylamino)phenylboronic acid (1 g, 6.06 mmol) was dissolved in 25 ml of CH<sub>2</sub>Cl<sub>2</sub> and added pinacol (718.7 mg, 6.08 mmol). This mixture was stirred for 15 h. The mixture was washed with 2x5 mL of brine and 3x5 mL of water. The organic phase was dried and concentrated *in vacuo*. Yield: 1.50 g (6.04 mmol, 99.7 %). <sup>1</sup>H-NMR (CDCl<sub>3</sub>, 300MHz)  $\delta$ : 7.67 (m, 2H), 6.68 (m, 2H), 2.9 (s, 6H), 1.32 (s, 12H). GC-MS: 247 m/z. Analytical data can be found in literature<sup>1</sup>

## **Synthesis of (4-(4,4,5,5-tetramethyl-1,3,2-dioxaborolan-2-yl)phenyl)methanamine (2c):**

*p*-bromobenzamine (1 g, 5.37 mmol) was dissolved in THF:Water 2:5. Boc<sub>2</sub>O (1.41 g, 6.45 mmol) and Na<sub>2</sub>CO<sub>3</sub> ( 1.67 g, 12.09 mmol) were then added and the mixture was refluxed for 12 h. Extraction was performed with 3x50 mL of EtOAc. The organic phase was dried with Na<sub>2</sub>SO<sub>4</sub> and

concentrated *in vacuo*. The residue was purified by flash chromatography using heptane : EtOAc 10:1. Yield: 1.36 g (89%, 4.79 mmol). <sup>1</sup>H-NMR (CDCl<sub>3</sub>, 400MHz) δ: 7.74 (dt, 2H), 7.18 (d, 2H), 4.28 (d, 2H), 1.48 (s, 9H). <sup>13</sup>C-NMR (CDCl<sub>3</sub>, 400MHz) δ: 156, 138, 132, 129, 121, 80, 44, 28. GC-MS: 285 m/z. Analytical data can be found in literature.<sup>2</sup> Tert-butyl-4-bromobenzylcarbamate (400 mg, 1.40 mmol) was dissolved in 10 mL of dry dioxane, potassium acetate (165 mg, 1.68 mmol), bis(pinacolato)diboron (426 mg, 1.68 mmol) and Pd(dppf)Cl<sub>2</sub> (10 mg, 0.01 mmol) were added and the reaction was stirred at 100 °C for 12 h. The mixture was stirred with 10 mL of sat. NaCl aqueous solution for 10 min. and extracted with 3x50 mL EtOAc. The combined organic phases were dried with Na<sub>2</sub>SO<sub>4</sub> and concentrated *in vacuo*. The resulting residue was purified by flash chromatography using heptane : EtOAc 10:1. The pure compound was treated with 2.0 M HCl in diethyl ether and the resulting deprotected HCl salt was filtered off. Yield: 276 mg (73%, 1.039 mmol). <sup>1</sup>H-NMR (CDCl<sub>3</sub> 400MHz) δ: 7.69 (d, 2H), 7.48 (d, 2H), 4.03 (s, 2H), 1.29 (s, 12H). Analytical data can be found in literature.<sup>3</sup>

#### **Synthesis of 1-(4-(4,4,5,5-tetramethyl-1,3,2-dioxaborolan-2-yl)phenyl)piperazine (2d):**

1-phenyl-piperazine (6.32 mL, 41.37 mmol) was dissolved in 75 mL of ethanol. This was slowly added 90 mL of a 1M Br<sub>2</sub> in EtOH solution (90 mmol). The reaction mixture was stirred at room temperature for 15 h. The mixture was added 140 mL of water and basified using 15% aqueous NaOH. 200 mL of EtOAc was added to achieve phase separation. Afterwards the water phase was extracted with 3x75 mL EtOAc and the combined organic phases were dried and concentrated *in vacuo* yielding 12.99 g of crude 1-(4-bromophenyl)piperazine. When necessary the product was purified by flash chromatography using CH<sub>2</sub>Cl<sub>2</sub>:MeOH:Et<sub>3</sub>N 10:1:0.01 and concentrated *in vacuo*. IR: 1493, 1236, 814 cm<sup>-1</sup>. <sup>1</sup>H-NMR (CDCl<sub>3</sub>, 300 MHz) δ: 7.32 (m, 2H), 6.77 (m, 2H), 3.11 (m, 4H), 3.03 (m, 4H). <sup>13</sup>C-NMR (CDCl<sub>3</sub>, 300MHz) δ: 150.9, 132.0, 117.8, 111.9, 50.3, 46.2. GC-MS: 240 m/z. Mp: 121-122°C. 1-(4-bromophenyl)piperazine (2 g, 8.29 mmol), Boc<sub>2</sub>O (1.9 g, 8.71 mmol), and sodium carbonate (1.97 g, 18.6 mmol) was dissolved in THF:Water 5:2 and refluxed for 12 h. Extraction was performed with 3x50 mL EtOAc. The combined organic phases were washed with 2x50 mL brine, dried and concentrated *in vacuo*. The resulting solid was purified by flash chromatography (EtOAc:Heptane 1:1) Yield: 2.04 g (72%, 5.98 mmol). <sup>1</sup>H-NMR (CDCl<sub>3</sub>, 300 MHz) δ: 7.33 (m, 2H), 6.78 (m, 2H), 3.56 (m, 4H), 3.09 (m, 4H), 1.48 (s). <sup>13</sup>C-NMR (CDCl<sub>3</sub>, 400 MHz) δ: 154.7, 150.2, 132.0, 118.2, 80.0, 49.3, 28.5. tert-butyl 4-(4-bromophenyl)piperazine-1-carboxylate (250 mg, 0.733 mmol), Potassium acetate (86 mg, 0.879 mmol) and Pd(dppf)Cl<sub>2</sub> (10

mg) was dissolved in 1,4-dioxane and heated to 100 °C with stirring. 4,4,4',4',5,5,5',5'-octamethyl-2,2'-bi(1,3,2-dioxaborolane) (223 mg, 0.879 mmol ) was then added and stirring was continued for 12 h. A crude sample was analyzed on GCMS, if the reaction was not finished a small amount of 4,4,4',4',5,5,5',5'-octamethyl-2,2'-bi(1,3,2-dioxaborolane) was added and stirring was continued for 2 hours. The reaction was then cooled to room temperature and stirred with 10 mL of brine for 10 min. The combined phases was extracted with 3x50 mL of EtOAc. The combined organic phases were dried and concentrated *in vacuo*. The crude product was purified by flash chromatography using EtOAc:Heptane 1:2. The pure compound was treated with 2.0 M HCl in diethyl ether and the resulting deprotected HCl salt was filtered off. Yield: 120.1 mg (50%, 0.370 mmol) <sup>1</sup>H-NMR (CDCl<sub>3</sub>, 400 MHz) δ: 7.72 (d, 2H), 6.90 (d, 2H), 3.23 (m, 4H), 3.03 (m, 4H), 1.33 (s, 12H).

**Synthesis of 1-methyl-4-(4-(4,4,5,5-tetramethyl-1,3,2-dioxaborolan-2-yl)phenyl)piperazine (2e):**

1.39 M t-BuLi (1.4 mL, 1.95 mmol) was dissolved in 10 mL dry THF at -78 °C. 1-(4-bromophenyl)-4-methylpiperazine (201.7 mg, 0.79 mmol) dissolved in 3 mL dry THF was added dropwise whilst the solution was stirred. The reaction was stirred for 15 min afterwards. B(Oi-Pr)<sub>3</sub> (0.36 mL, 2.35 mmol) was added dropwise and heated to room temperature. After reaching room temperature the reaction was stirred for one hour. Pinacol (141.2 mg, 1.19 mmol) was added and stirring was continued for two hours. The mixture was washed with 3x10 mL saturated aqueous NH<sub>4</sub>Cl:water 1:1, 2x10 mL saturated aqueous NaHCO<sub>3</sub> and 2x10 mL water. The organic phase was dried and evaporated *in vacuo*. The resulting residue was purified by flash chromatography using EtOAc:MeOH:Et<sub>3</sub>N (10:1:0.02). Yield: 107.5 mg (0.36 mmol, 45%). IR: 1361, 1237, 1140 cm<sup>-1</sup>. <sup>1</sup>H-NMR (CDCl<sub>3</sub>, 300 MHz) δ: 7.70 (m, 2H), 6.89 (m, 2H), 3.29 (t, 4H), 2.57 (t, 4H), 2.36 (s, 3H). <sup>13</sup>C-NMR (CDCl<sub>3</sub>, 300MHz) δ: 136.3, 114.5, 83.5, 55.1, 48.2, 46.3, 24. GC-MS: 302 m/z. Mp: 113-115 °C. Analytical data found in literature<sup>4</sup>

**Synthesis of 5,5-dimethyl-2-phenyl-1,3,2-dioxaborinane (4a):**

Phenylboronic acid (104.1 mg, 0.85 mmol) was dissolved in 25 mL of CH<sub>2</sub>Cl<sub>2</sub>, neopentyl glycol (93.2 mg, 0.89 mmol) was added and the reaction was stirred for 15 h. The organic phase was washed with 2x5 mL brine, 3x5 mL of water, dried and concentrated *in vacuo* yielding: 142.1 mg

(0.75 mmol, 88.2%). <sup>1</sup>H-NMR (CDCl<sub>3</sub>, 300MHz) δ: 7.78 (m, 2H), 7.40 (m, 1H), 7.35 (m, 2H) 3.77 (s, 4H), 1.03 (s, 6H). Analytical data found in literature<sup>5</sup>

#### **Synthesis of 4-(5,5-dimethyl-1,3,2-dioxaborinan-2-yl)-N,N-dimethylaniline (4b):**

4-(dimethylamino)phenylboronic acid (0.99 g, 6.00 mmol) was dissolved in 25 mL of CH<sub>2</sub>Cl<sub>2</sub> and added neopentyl glycol (635 mg, 6.10 mmol). This mixture was stirred for 15 h. The mixture was washed with 2x5 mL of brine and 3x5 mL of water. The organic phase was dried and concentrated *in vacuo*. Yield: 1.34 g (5.77 mmol, 96.2 %). <sup>1</sup>H-NMR (CDCl<sub>3</sub>, 300MHz) δ: 7.66 (m, 2H), 6.68 (m, 2H), 3.73 (s, 4H), 2.97 (s, 6H), 1.00 (s, 6H). GC-MS: 233 m/z. Analytical data found in literature<sup>1</sup>

#### **Synthesis of 3-(4-hydroxybutyl)indolin-2-one (5):**

Oxindole (5.32 g, 40 mmol), 1,4-butanediol (40 ml, 489 mmol) and 2 g of raney nickel in water slurry were heated to 200 °C in a pressurized container for 12 h. The resulting mixture was diluted using acetone and flushed through a pad of celite and concentrated *in vacuo*. Excess butane-1,4-diol was removed by kugelrohr distillation at 170 °C leaving a brown oil. The oil was purified by flash chromatography using EtOAc. Yield: 5.72 g (27.9 mmol, 69.8 %). <sup>13</sup>C-NMR (CDCl<sub>3</sub>, 400MHz) δ: 180.9, 141.8, 129.8, 128.1, 124.2, 122.4, 110.0, 62.6, 46.2, 32.7, 30.2, 22.2. Data corresponds to reported data in<sup>6</sup>

#### **Synthesis of 4-(2-oxoindolin-3-yl)butyl methanesulfonate (6):**

**5** (5.7205 g, 27.9 mmol) and Et<sub>3</sub>N ( 7.77 ml, 55.7 mmol) was dissolved in 50 ml of dry THF and cooled to -78°C. Mesyl chloride was added dropwise with stirring and the temperature was raised to rt. Upon reaching rt. the reaction was stirred for 1h. The crude was stored for further use.

#### **Synthesis of 3-(4-(4-(4-bromophenyl)piperazin-1-yl)butyl)indolin-2-one (7):**

1-(4-bromophenyl)piperazine (425 mg, 1.763 mmol) was melted at 130 °C, Na<sub>2</sub>CO<sub>3</sub> (187 mg, 1.763 mmol) and **6** (499 mg, 1.763 mmol) was and stirred until the mixture turned solid. The solid was dissolved in a mixture of EtOAc and water. The organic phase was concentrated *in vacuo* and purified using flash chromatography (EtOAc). Yield: 416.2 mg (55.1%, 0.972 mmol) IR: 1703, 1589, 1493, 815 cm<sup>-1</sup>. <sup>1</sup>H-NMR (CDCl<sub>3</sub>, 300MHz) δ: 7.77 (s, 1H), 7.31 (m, 2H), 7.20 (m, 2H), 7.02 (m, 1H), 6.86 (d, 1H, J = 7.3 Hz) 6.76 (m, 2H), 3.48 (t, 1H, J = 5.9 Hz) 3.17 (t, 4H, J = 4.7), 2.59 (m, 4H), 2.39 (t, 2H, J = 7.8 Hz), 2.00 (m, 2H), 1.57 (m, 2H), 1.41 (m, 2H). <sup>13</sup>C-NMR (CDCl<sub>3</sub>,



300MHz)  $\delta$ : 180.4, 150.3, 141.7, 131.9, 129.7, 128.0, 124.4, 122.4, 117.7, 111.9, 109.8, 58.3, 53.1, 48.9, 46.8, 30.4, 26.8, 23.8. LCMS: 429 m/z (M+1). Mp: 132-134°C.

**Synthesis of 3-(4-(4-(4-(4,4,5,5-tetramethyl-1,3,2-dioxaborolan-2-yl)phenyl)piperazin-1-yl)butyl)indolin-2-one (8):**

**7** (50 mg, 0.12 mmol), KOAc (22.9 mg, 0.23 mmol), Bis(pinacolato)diboron (35.6 mg, 0.14 mmol) and Pd(dddppf)Cl<sub>2</sub> (10 mg, 0.01 mmol) was dissolved in 10 mL of dry Dioxane, heated to 100 °C and stirred for 12 h. The reaction was then cooled to r.t, stirred with 10 mL of brine for 10 min and extracted with 3x50 mL EtOAc. The combined organic phases were dried, concentrated *in vacuo* and purified by flash chromatography (EtOAc). Yield: 30 mg (54 %, 0.06 mmol). <sup>1</sup>H-NMR (CDCl<sub>3</sub>, 300MHz)  $\delta$ : 8.62 (s b, 1H), 7.70 (d, 2H, J = 8.8 Hz) 7.22 (t, 2H, J = 7, 8.2 Hz ), 7.03 (m, 1H), 6.88 (m, 3H), 3.50 (t, 1H, J = 5.9 Hz) 3.31 (t, 4H, J = 5.3), 2.64 (t, 4H, J = 4.7 Hz), 2.42 (t, 2H, J = 7.9 Hz), 2.02 (m, 2H), 1.61 (m, 2H), 1.44 (m, 2H), 1.34 (s, 12H). <sup>13</sup>C-NMR (CDCl<sub>3</sub>, 400MHz)  $\delta$ : 189.8, 153.1, 141.4, 136.2, 129.6, 127.9, 124.2, 122.3, 114.5, 109.6, 83.4, 58.1, 52.8, 47.7, 45.8, 30.2, 26.2, 24.9, 23.6. High-res MS: 476.3094 (M+1)

**General labeling procedure for developing a standard procedure:**

Aryl boronic ester, palladium-catalyst and base were used in a ratio of 40:1:4. [<sup>11</sup>C]MeI was trapped in 300  $\mu$ L DMF. To the trapped [<sup>11</sup>C]MeI was added Pd-catalyst dissolved in 300  $\mu$ L of DMF:water 9:1 and heated to 60 °C. [<sup>11</sup>C]MeI was allowed to react for 2 min and the temperature was then adjusted to a predetermined temperature between 40 and 120 °C. Aryl boronic ester and the base of choice dissolved in 150  $\mu$ L of DMF:water 9:1 was added and allowed to react for 5 min. Results were analysed by HPLC using a Luna 5  $\mu$ m C18 100 Å coloumn (150 x 4.6 mm. 50:50 0.01 M Borax buffer : AcN).

**Standard labeling procedure:**

Aryl boronic ester, Pd<sub>2</sub>(dba)<sub>3</sub>, P(*o*-tolyl)<sub>3</sub> and base were used in a ratio of 40:1:2:4 with appropriate masses calculated from the use of 0.1 mg of P(*o*-tolyl)<sub>3</sub>. [<sup>11</sup>C]MeI was trapped in 300  $\mu$ L DMF. To the trapped [<sup>11</sup>C]MeI was added Pd-catalyst dissolved in 300  $\mu$ L of DMF:water 9:1 and heated to 60

°C. [<sup>11</sup>C]MeI was allowed to react for 2 min. Aryl boronic ester was added along with 0.5 M K<sub>2</sub>CO<sub>3</sub> dissolved in 150 μL of DMF:water 9:1 and allowed to react for 5 min. Results were analysed by HPLC using a Luna 5 μm C18 100 Å column (150 x 4.6 mm. 50:50 0.01 M Borax buffer : AcN).

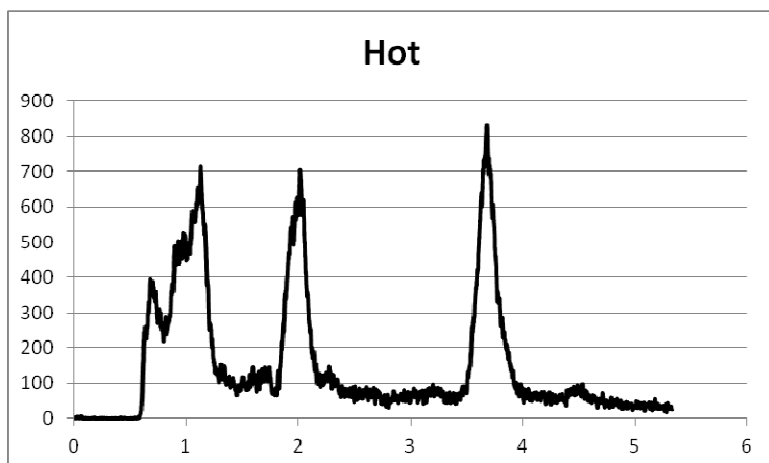
#### **Labeling procedure utilizing Microwave:**

Aryl boronic ester, Pd<sub>2</sub>(dba)<sub>3</sub>, P(*o*-tolyl)<sub>3</sub> and base were used in a ratio of 40:1:2:4 with appropriate masses calculated from the use of 0.1 mg of P(*o*-tolyl)<sub>3</sub>. [<sup>11</sup>C]MeI was trapped in 300 μL DMF. To the trapped [<sup>11</sup>C]MeI was added Pd-catalyst dissolved in 300 μL of DMF:water 9:1 and the reaction was then heated to 60 °C. [<sup>11</sup>C]MeI was allowed to react for 2 min. Aryl boronic ester was added along with 0.5 M K<sub>2</sub>CO<sub>3</sub> dissolved in 150 μL of DMF:water 9:1 and microwave irradiated for 3 min at 100 Mhz. Results were analysed by HPLC using a Luna 5 μm C18 100 Å column (150 x 4.6 mm. 50:50 0.01 M Borax buffer : AcN).

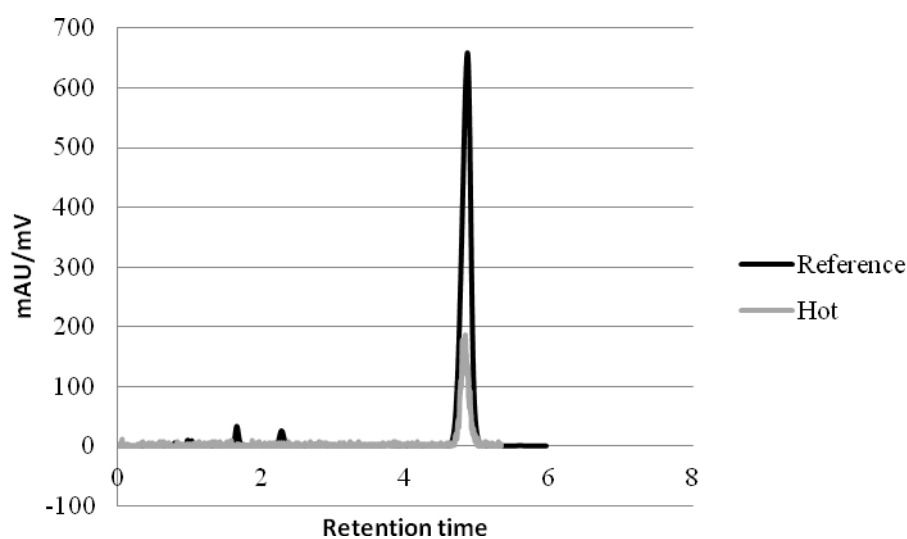
#### **Procedure for the labeling of [<sup>11</sup>C]CIMBI-712:**

**8**, Pd<sub>2</sub>(dba)<sub>3</sub>, P(*o*-tolyl)<sub>3</sub> and base were used in a ratio of 40:1:2:4 with appropriate masses calculated from the use of 0.1 mg of P(*o*-tolyl)<sub>3</sub>. [<sup>11</sup>C]MeI was trapped in 300 μL DMF. To the trapped [<sup>11</sup>C]MeI was added Pd-catalyst and base dissolved in 300 μL of DMF:water 9:1 and heated to 60 °C. [<sup>11</sup>C]MeI was allowed to react for 2 min. **8** was added along with 0.5 M K<sub>2</sub>CO<sub>3</sub> dissolved in 150 μL of DMF:water 9:1 and allowed to react for 5 min. Purification was performed by preparative HPLC using a Luna 5 μm C18(2) 100 Å column (Phenomenex Inc.) (250 x 10 mm, 50:50 0.01 M Borax buffer : AcN, flowrate: 9 mL/min). The collected fraction was trapped on a solid-phase C18 sep-pack extraction column and eluted with 3 ml EtOH. Results were analysed by HPLC using a Luna 5 μm C18 100 Å column (Phenomenex Inc.) (150 x 4.6 mm. 50:50 0.01 M Borax buffer : AcN, flowrate 2 mL/min).

Radio signal of a crude sample of CIMBI-712. Product peak at 3.677



Radio signal of purified CIMBI-712 and UV signal of reference compound



1. Kleeberg, C.; Dang, L.; Lin, Z. Y.; Marder, T. B. *Angewandte Chemie-International Edition* **2009**, *48*, 5350-5354.
2. Howell, S. J.; Spencer, N.; Philp, D. *Tetrahedron* **2001**, *57*, 4945-4954.
3. Ramalingam, K.; Nowotnik, D. P. *Organic Preparations and Procedures International* **1991**, *23*, 729-734.
4. Gerspacher, M. B., CH), Furet, Pascal (Basel, CH), Vangrevelinghe, Eric (Basel, CH), Pissot Sondermann, Carole (Basel, CH), Gaul, Christoph (Basel, CH), Holzer, Philipp (Basel, CH). Novartis AG (Basel, CH): United States, 2012.

5. Wilson, D. A.; Wilson, C. J.; Moldoveanu, C.; Resmerita, A. M.; Corcoran, P.; Hoang, L. M.; Rosen, B. M.; Percec, V. *J Am Chem Soc* **2010**, *132*, 1800-+.
6. Volk, B.; Mezei, T.; Simig, G. *Synthesis-Stuttgart* **2002**, 595-597.

## **Appendix 2**

### **Paper II**

Radiosynthesis and in Vivo Evaluation of Novel Radioligands for Pet Imaging of Cerebral 5-HT<sub>7</sub> Receptors

H. D. Hansen, M. M. Herth, A. Ettrup, **V. L. Andersen**, S. Lehel, A. Dyssegaard, J. L. Kristensen, and G. M. Knudsen

*Journal of Nuclear Medicine*, 55 (2014), 640-46.



# Radiosynthesis and In Vivo Evaluation of Novel Radioligands for PET Imaging of Cerebral 5-HT<sub>7</sub> Receptors

Hanne D. Hansen<sup>1,2</sup>, Matthias M. Herth<sup>1-4</sup>, Anders Ettrup<sup>1,2</sup>, Valdemar L. Andersen<sup>1-4</sup>, Szabolcs Lehel<sup>3</sup>, Agnete Dyssegaard<sup>1,2</sup>, Jesper L. Kristensen<sup>3</sup>, and Gitte M. Knudsen<sup>1,2</sup>

<sup>1</sup>Center for Integrated Molecular Brain Imaging, Copenhagen University Hospital Rigshospitalet, Copenhagen, Denmark;

<sup>2</sup>Neurobiology Research Unit, Rigshospitalet and University of Copenhagen, Copenhagen, Denmark; <sup>3</sup>Department of Drug Design and Pharmacology, Faculty of Health and Medical Sciences, University of Copenhagen, Copenhagen, Denmark; and <sup>4</sup>PET and Cyclotron Unit, Copenhagen University Hospital Rigshospitalet, Copenhagen, Denmark

The serotonin (5-hydroxytryptamine [5-HT])<sub>7</sub> receptor (5-HT<sub>7</sub>R) is the most recently discovered 5-HT receptor, and its physiologic and possible pathophysiologic roles are not fully elucidated. So far, no suitable 5-HT<sub>7</sub>R PET radioligand is available, thus limiting the investigation of this receptor in the living brain. Here, we present the radiosynthesis and in vivo evaluation of Cimbi-712 (3-{4-[4-(4-methylphenyl)piperazine-1-yl]butyl}p-1,3-dihydro-2H-indol-2-one) and Cimbi-717 (3-{4-[4-(3-methoxyphenyl)piperazine-1-yl]butyl}-1,3-dihydro-2H-indol-2-one) as selective 5-HT<sub>7</sub>R PET radioligands in the pig brain. The 5-HT<sub>7</sub>R distribution in the postmortem pig brain is also assessed. **Methods:** In vitro autoradiography with the 5-HT<sub>7</sub>R selective radioligand <sup>3</sup>H-labeled (R)-3-(2-(2-(4-methylpiperidin-1-yl)ethyl)pyrrolidine-1-sulfonyl)phenol (SB-269970) was performed on pig brain sections to establish the 5-HT<sub>7</sub>R binding distribution. Radio-labeling of 5-HT<sub>7</sub>R selective compounds was performed in an automated synthesis module in which we conducted either palladium-mediated cross coupling (<sup>11</sup>C-Cimbi-712) or conventional O-methylation (<sup>11</sup>C-Cimbi-717) using <sup>11</sup>C-Mel and <sup>11</sup>C-MeOTf, respectively. After intravenous injection of the radioligands in Danish Landrace pigs, the in vivo brain distribution of the ligands was studied. Specific binding of <sup>11</sup>C-Cimbi-712 and <sup>11</sup>C-Cimbi-717 to 5-HT<sub>7</sub>R was investigated by intravenous administration of SB-269970 before a second PET scan. **Results:** High 5-HT<sub>7</sub>R density was found in the thalamus and cortical regions of the pig brain by autoradiography. The radiosynthesis of both radioligands succeeded after optimization efforts (radiochemical yield, ~20%–30% at the end of synthesis). Time-activity curves of <sup>11</sup>C-Cimbi-712 and <sup>11</sup>C-Cimbi-717 showed high brain uptake and distribution according to 5-HT<sub>7</sub>R distribution, but the tracer kinetics of <sup>11</sup>C-Cimbi-717 were faster than <sup>11</sup>C-Cimbi-712. Both radioligands were specific for 5-HT<sub>7</sub>R, as binding could be blocked by pretreatment with SB-269970 for <sup>11</sup>C-Cimbi-717 in a dose-dependent fashion. For <sup>11</sup>C-Cimbi-717, nondisplaceable binding potentials of 6.4 ± 1.2 (*n* = 6) were calculated in the thalamus. **Conclusion:** Both <sup>11</sup>C-Cimbi-712 and <sup>11</sup>C-Cimbi-717 generated a specific binding in accordance with 5-HT<sub>7</sub>R distribution and are potential PET radioligands for 5-HT<sub>7</sub>R. <sup>11</sup>C-Cimbi-717 is the better candidate because of the more reversible tracer kinetics, and this radioligand showed a dose-dependent decline in cerebral binding after receptor blockade. Thus, <sup>11</sup>C-Cimbi-717 is currently the most

promising radioligand for investigation of 5-HT<sub>7</sub>R binding in the living human brain.

**Key Words:** <sup>11</sup>C-Cimbi-717; <sup>11</sup>C-Cimbi-712; 5-HT<sub>7</sub> receptor; PET; novel radioligand

**J Nucl Med 2014; 55:1–7**

DOI: 10.2967/jnumed.113.128983

**T**he serotonergic system plays a key modulatory role in the brain and is a target for many drug treatments for brain disorders either through reuptake blockade or interactions with one or more of the 14 subtypes of 5-hydroxytryptamine (5-HT) receptors. Our knowledge about the behavior of the 5-HT system in vivo is still scattered, and most of the understanding is derived from animal models. However, the use of imaging techniques such as positron emission tomography (PET) and the increasing number of radioligands for the 5-HT receptors enable in vivo investigation of the 5-HT system in the human brain.

The 5-HT<sub>7</sub> receptor (5-HT<sub>7</sub>R) is the most recently discovered 5-HT receptor, and its biologic functions are not fully elucidated. However, its implications in brain disorders such as depression and schizophrenia (*1*) make it an interesting target for both drug discovery and radioligand development. Both pharmacologic blockade of 5-HT<sub>7</sub>R and inactivation of the receptor gene led to an antidepressant-like behavioral profile in the forced swim test and in the tail suspension test (*2–5*). Pharmacologic blockade of 5-HT<sub>7</sub>R also presented anxiolytic effects in animal models of anxiety (*5,6*).

Currently, no well-validated radioligand is available for in vivo imaging of 5-HT<sub>7</sub>R. Interestingly, the 5-HT<sub>7</sub>R and the 5-HT<sub>1A</sub>R are the receptors for which 5-HT has the highest affinity. This is relevant for the aim of discovering a radioligand that is sensitive to changes in cerebral levels of endogenous 5-HT. If the competition model applies, the probability of measuring a signal change in response to a pharmacologic challenge that changes 5-HT levels will depend solely on the affinity of 5-HT to the target receptor (*7*).

Several potent and selective ligands for 5-HT<sub>7</sub>R have been discovered, but so far only a limited number of PET radioligands have been evaluated in vivo. <sup>11</sup>C-DR4446 had good blood–brain barrier permeability and was metabolically stable but showed only a minimal specific binding component (*8*). The 5-HT<sub>7</sub>R antagonist (R)-3-(2-(2-(4-methylpiperidin-1-yl)ethyl)pyrrolidine-1-sulfonyl)

Received Apr. 3, 2013; revision accepted Dec. 4, 2013.

For correspondence or reprints contact: Gitte M. Knudsen, Center for Integrated Molecular Brain Imaging, Copenhagen University Hospital, Rigshospitalet, Blegdamsvej 9, DK-2100 Copenhagen, Denmark.

E-mail: gmk@nru.dk

Published online: ■■■■■■■■■■

COPYRIGHT © 2014 by the Society of Nuclear Medicine and Molecular Imaging, Inc.

phenol (SB-269970) has been used as a lead structure for discovering  $^{18}\text{F}$ -labeled radioligands.  $^{18}\text{F}$ -1-[(2*S*)-1-(phenylsulfonyl)pyrrolidin-2-yl]ethyl]piperidin-4-yl 4-fluorobenzoate and 1-(2-[(2*R*)-1-[(2- $^{18}\text{F}$ -fluorophenyl)sulfonyl]pyrrolidin-2-yl]ethyl)-4-methylpiperidine ( $^{18}\text{F}$ -2FP3) were evaluated *ex vivo* in rats and *in vivo* in cats (9,10). However, no input function was obtained while evaluating  $^{18}\text{F}$ -2FP3. Furthermore, the 5-HT<sub>7</sub>R binding distribution was not evaluated in cats, thus making it difficult to verify if the binding of  $^{18}\text{F}$ -2FP3 was specific to 5-HT<sub>7</sub>R. We recently also reported the evaluation of a 5-HT<sub>7</sub>R PET radioligand,  $^{11}\text{C}$ -Cimbi-806, that displayed selectivity *in vitro*, but the lack of blocking effect by SB-269970 *in vivo* led us to conclude that this compound does not selectively image the 5-HT<sub>7</sub>R *in vivo* (11).

Further work with the oxindole compound class led to the synthesis of a group of compounds including Cimbi-712 (3-[4-[4-(4-methylphenyl)piperazine-1-yl]butyl]p-1,3-dihydro-2*H*-indol-2-one) and Cimbi-717 (3-[4-[4-(3-methoxyphenyl)piperazine-1-yl]butyl]-1,3-dihydro-2*H*-indol-2-one). The affinity of both Cimbi-712 and Cimbi-717 is in the lower nanomolar range for 5-HT<sub>7</sub>R, with an inhibition constant ( $K_i$ ) of 1.1 and 2.6 nM, respectively (12). Cimbi-712 is 2,191-fold selective for 5-HT<sub>7</sub>R over 5-HT<sub>1A</sub>R ( $K_i$  for the 5-HT<sub>1A</sub>R is 2,410 nM), whereas Cimbi-717 is 130-fold selective ( $K_i$  for the 5-HT<sub>1A</sub>R is 261 nM). From the outcome of the affinity testing on a range of receptors, Cimbi-712 displayed slightly higher selectivity for 5-HT<sub>7</sub>R than did Cimbi-717 (12).

Here, we report the  $^{11}\text{C}$ -labeling and *in vivo* evaluation, including receptor occupancy measurements, of two novel 5-HT<sub>7</sub>R selective PET radioligands in Danish Landrace pigs. For comparison between *in vivo* and postmortem receptor distribution, we also investigated the distribution of 5-HT<sub>7</sub>R in the pig brain.

## MATERIALS AND METHODS

### In Vitro Autoradiography

One brain hemisphere of a 30-kg Danish Landrace pig was sliced on a HM5000M cryostat (Microm International GmbH) in 20- $\mu\text{m}$  coronal sections except for the cerebellum, which was sliced in the sagittal plane. Sections were thaw-mounted on Superfrost Plus glass slides (Thermo Scientific) and stored at  $-80^\circ\text{C}$  until use. Autoradiography was performed at room temperature in 50 mM Tris-HCl buffer (pH 7.4) with 5 nM  $^3\text{H}$ -SB-269970 (1,476.3 MBq [39.9 mCi]/ $\mu\text{mol}$  at synthesis [January 2012]; PerkinElmer). Nonspecific binding was determined by adding 10  $\mu\text{M}$  SB-258719 (3-methyl-*N*-[(1*R*)-1-methyl-3-(4-methyl-1-piperidinyl)propyl]-*N*-methylbenzenesulfonamide hydrochloride; Tocris Bioscience). Sections were preincubated in buffer for approximately 30 min and then incubated with radioactive buffer for 2 h. Sections were then washed for  $1 \times 5$  min and for  $2 \times 10$  min in 50 mM Tris-HCl buffer, rinsed in distilled H<sub>2</sub>O for 20 s, and dried before exposure to tritium-sensitive plates (Fujifilm Europe GmbH) for 19 d.

Calibration, quantification, and data evaluation of all autoradiography images were done with ImageJ analysis software (<http://rsb.info.nih.gov/ij/>). Regions of interest were hand-drawn around anatomic landmarks—for example, borders of sections—for each brain region, and the mean pixel density was measured in each brain region as outcome. A third-degree exponential calibration function of decay-corrected  $^3\text{H}$ -microscales (GE Healthcare) was used to convert mean pixel density to receptor binding measured in kBq/mg tissue equivalents (TE). Finally, the decay-corrected specific activity of  $^3\text{H}$ -SB-269970 was used to convert kBq/mg TE to fmol/mg TE.

### Organic Synthesis

The precursors and reference compounds were synthesized as racemates as previously described (12,13).

### Radioligand Preparation

$^{11}\text{C}$ -Cimbi-717.  $^{11}\text{C}$ -methyl trifluoromethanesulfonate, produced using a fully automated system, was transferred in a stream of helium to a 1.1-mL vial containing the labeling precursor (0.3–0.4 mg, 0.8–1.0  $\mu\text{mol}$ ), 0.5 M K<sub>2</sub>CO<sub>3</sub> (14  $\mu\text{L}$ , 7  $\mu\text{mol}$ ), and MeCN (300  $\mu\text{L}$ ). The resulting sealed mixture was heated at  $60^\circ\text{C}$  for 5 min and then separated by high-performance liquid chromatography (HPLC) on a Luna 5- $\mu\text{m}$  C18(2) 100- $\text{\AA}$  column (Phenomenex Inc.) (250  $\times$  10 mm, 50:50 acetonitrile:0.01 M sodium borate buffer, at a flow rate of 6 mL/min). Retention times were 610 s for  $^{11}\text{C}$ -Cimbi-717 and 300 s for the precursor. The fraction corresponding to the labeled product was collected in sterile water (150 mL), and the resulting solution was passed through a solid-phase C18 Sep-Pak extraction column (Waters Corp.), which had been preconditioned with ethanol (10 mL), followed by isotonic sodium chloride solution (20 mL). The column was flushed with sterile water (3 mL). Then, the trapped radioactivity was eluted through a sterile filter with ethanol (3 mL), followed by isotonic sodium chloride solution (3 mL), into a 20-mL vial containing sodium phosphate-buffered saline (9 mL, 100 mM, pH 7), giving a 15-mL solution of racemic  $^{11}\text{C}$ -Cimbi-717 with a pH of approximately 7.

$^{11}\text{C}$ -Cimbi-712.  $^{11}\text{C}$ -Cimbi-712 was produced as described previously (13). The HPLC fraction corresponding to the labeled product was collected in sterile water (150 mL), and the resulting solution was passed through a solid-phase C18 Sep-Pak extraction column, which had been preconditioned with ethanol (10 mL), followed by water (20 mL). The trapped radioactivity was eluted through a sterile filter with ethanol (3 mL) into a 20-mL vial containing sodium phosphate-buffered saline (9 mL, 100 mM, pH  $\sim$ 7), giving a 12-mL solution of racemic  $^{11}\text{C}$ -Cimbi-712 with a pH of approximately 7.

### Determination of Radiochemical Purity and Specific Radioactivity

Chemical and radiochemical purities were assessed on the same sample by HPLC analysis. Specific activity of the radioligands was calculated from 3 consecutive HPLC analyses (average) and determined by comparing the area of the ultraviolet absorbance peak corresponding to the radiolabeled product on the HPLC chromatogram with a standard curve relating mass to ultraviolet absorbance ( $\lambda = 225$  nm).  $^{11}\text{C}$ -Cimbi-712 and  $^{11}\text{C}$ -Cimbi-717 were analyzed with HPLC using a Luna 5- $\mu\text{m}$  C18(2) 100- $\text{\AA}$  column (150  $\times$  4.6 mm, 50:50 MeCN:0.01 M borax buffer, at a flow rate of 2 mL/min). Retention times were 180 s for  $^{11}\text{C}$ -Cimbi-717 and 290 s for  $^{11}\text{C}$ -Cimbi-712.

### Animal Procedure

Eight female Danish Landrace pigs (mean weight  $\pm$  SD, 19  $\pm$  2.0 kg) were used for *in vivo* PET imaging. All animal procedures were approved by the Danish Council for Animal Ethics (journal no. 2012-15-2934-00156).

### PET Protocol

$^{11}\text{C}$ -Cimbi-712 was given as an intravenous bolus injection over 20 s, and the injected doses were 155 and 110 MBq for baseline scans ( $n = 2$ ) and 123 and 73 MBq for scans for which SB-269970 was preadministered ( $n = 2$ ).  $^{11}\text{C}$ -Cimbi-717 was also given as an intravenous bolus over 20 s, and the injected dose (mean  $\pm$  SD) was 236  $\pm$  117 MBq for baseline scans ( $n = 6$ ; range, 115–435 MBq) and 147  $\pm$  82.1 MBq for scans for which a preblocking agent was administered ( $n = 6$ ; range, 40–277 MBq). The pigs were subsequently scanned for 90 min in list mode with a high-resolution research tomograph (HRRT; Siemens AG), with scanning starting at the time of injection (0 min). Immediately after the baseline scan (90 min), SB-269970 (Tocris Bioscience), a selective 5-HT<sub>7</sub>R antagonist (14), was given intravenously as a bolus infusion (0.2, 1.0, or 4.2 mg/kg/h), and rescanning started after 30 min of pretreatment with SB-269970. In one pig, a 0.5 mg/kg dose of prazosin (Sigma Aldrich), an  $\alpha_1$  adren-



ergic receptor antagonist (15,16), was given as an intravenous infusion before injection of <sup>11</sup>C-Cimbi-717.

### Whole-Blood and Plasma Input Functions

During the first 30 min of the scans, radioactivity in arterial whole blood was continuously measured using an ABSS autosampler (Allogg Technology) counting coincidences in a lead-shielded detector. Concurrently, arterial whole blood was sampled manually at 2.5, 5, 10, 20, 30, 40, 50, 70, and 90 min after injection and radioactivity was measured in whole blood and plasma using a well counter (Cobra 5003; PerkinElmer). Cross calibration between the HRRT scanner, the autosampler, and the well counter allowed for the determination of plasma input functions.

### Metabolite Analysis

Radiolabeled parent compound and metabolites were measured in plasma using HPLC with online radioactivity detection. In short, <sup>11</sup>C-Cimbi-712 and <sup>11</sup>C-Cimbi-717 were separated from their respective radiolabeled metabolites by direct injection of plasma in a column-switching HPLC system. Whole-blood samples were centrifuged (3,500 rpm, 7 min), and the supernatant plasma fraction was collected and filtered through a 0.45- $\mu$ M syringe filter before analysis with online radioactive detection, as previously described (17,18).

### Determination of Free Fraction

The free fraction of <sup>11</sup>C-Cimbi-717 in pig plasma was measured using an equilibrium dialysis method as previously described (19) and calculated as the ratio between radioactivity in a buffer and plasma compartment after equilibrium between the chambers had been reached after 3 h.

### Quantification of PET Data

Ninety-minute list-mode PET data were reconstructed into 38 dynamic frames of increasing length (6  $\times$  10, 6  $\times$  20, 4  $\times$  30, 9  $\times$  60, 2  $\times$  180, 8  $\times$  300, and 3  $\times$  600 s). Images consisted of 207 planes of 256  $\times$  256 voxels of 1.22  $\times$  1.22  $\times$  1.22 mm. A summed picture of all counts in the 90-min scan was reconstructed for each pig and used for coregistration to a standardized MR imaging-based atlas of the Danish Landrace pig brain, similar to that previously published (18,19). The time-activity curves were calculated for the following volumes of interest: cerebellum, cortex, hippocampus, lateral and medial thalamus, caudate nucleus, and putamen. The activity in the striatum is defined as the mean radioactivity in the caudate nucleus and putamen. The activity in the thalamus is calculated as the mean radioactivity in the lateral and medial thalamus. Radioactivity in all volumes of interest was calculated as the average of radioactive concentration (Bq/mL) in the left and right sides. The outcome measure in the time-activity curves was calculated as radioactive concentration in the volume of interest (in kBq/mL) normalized to the injected dose corrected for animal weight (in kBq/kg), yielding standardized uptake values (g/mL).

Distribution volumes ( $V_T$ ) for the volumes of interest were calculated on the basis of 3 different models: the 1-tissue-compartment (1-TC), 2-tissue-compartment (2-TC), and Logan linearization models. A single parent fraction curve fitted to a biexponential function, obtained from the average across all scans in the study, was used to generate individual metabolite-corrected plasma concentration curves. The  $V_T$  of baseline and blocked conditions was used to determine the non-displaceable distribution volume ( $V_{ND}$ ) by use of the Lassen plot and thereby allow for calculation of the nondisplaceable binding potential  $BP_{ND}$  (20). All modeling was initiated with the same starting parameters, and SD coefficient variance was below 15% for macroparameters (the rate constant  $K_1$  and  $V_T$ ). Datasets that did not fulfill this criterion were not included in the results. Of the 176 fittings for <sup>11</sup>C-Cimbi-717, 2 failed for the 1-TC, 31 failed for the 2-TC, and 7 failed

for the Logan linearization model. Of the 40 attempts for <sup>11</sup>C-Cimbi-712, 2 failed for the 1-TC, 12 failed for the 2-TC, and 11 failed for the Logan linearization model.

## RESULTS

### 5-HT<sub>7</sub>R Distribution in the Pig Brain

The highest <sup>3</sup>H-SB-269970 binding was found in small subregions of the thalamus (62.2 fmol/mg TE), amygdala (48.3 fmol/mg TE), and cingulate cortex (44.9 fmol/mg TE) (Table 1; Fig. 1). Low binding was found in the striatum and especially in the cerebellum (13.4 fmol/mg TE). In the cortical regions, binding increased toward the posterior parts of the pig brain, with the highest cortical binding found in the cingulate lobe (Supplemental Fig. 1; supplemental materials are available at <http://jnm.snmjournals.org>).

### Radiochemistry

Radiolabeling of <sup>11</sup>C-Cimbi-712 has previously been described (13). In brief, <sup>11</sup>C-Cimbi-712 was labeled with a radiochemical yield (RCY) of 0.3–0.5 GBq and with a specific activity of 106  $\pm$  68 GBq/ $\mu$ mol ( $n = 4$ ) in a total synthesis time of 40–50 min.

Radiolabeling of <sup>11</sup>C-Cimbi-717 underwent extensive optimization (Supplemental Table 1) as compared with <sup>11</sup>C-Cimbi-712 (13), now using 0.3 mg of precursor, 14  $\mu$ L of 0.5 M K<sub>2</sub>CO<sub>3</sub> (1 equivalent), and <sup>11</sup>C-CH<sub>3</sub>OTf on a fully automated system (decay-corrected RCY,  $\sim$ 20%) (Fig. 2). Two major radioactive peaks were detected. The minor peak corresponded to <sup>11</sup>C-Cimbi-717 ( $\sim$ 600 s) (further information is in the supplemental materials). The precursor eluted approximately 300 s before the radiolabeled product as indicated by the ultraviolet-absorption chromatogram (Supplemental Fig. 2). The radiosynthesis, including HPLC purification and formulation, generated an injectable solution of <sup>11</sup>C-Cimbi-717 (radiochemical purity > 97%, chemical purity > 98%) within 40–50 min. Typically, 0.2–0.4 GBq of <sup>11</sup>C-Cimbi-717 were

**TABLE 1**  
5-HT<sub>7</sub>R Distribution in Different Brain Regions Determined by <sup>3</sup>H-SB-269970 Autoradiography

Region	Specific binding (fmol/mg TE)	Number of sections in region
<b>Cortical regions</b>		
Prefrontal	32.7 $\pm$ 1.60	2
Frontal	38.3 $\pm$ 2.68	5
Temporal	41.0 $\pm$ 3.03	7
Cingulate	44.9 $\pm$ 2.60	16
Occipital	33.2 $\pm$ 2.40	4
<b>Striatum</b>		
Putamen	21.6 $\pm$ 1.64	5
Caudate	24.4 $\pm$ 2.81	5
Thalamus	45.6 $\pm$ 0.19	3
Thalamus (high-binding subregion)	62.0 $\pm$ 5.53	2
Hypothalamus	43.0 $\pm$ 6.03	3
Hippocampus	37.5 $\pm$ 3.35	6
Amygdala	48.3 $\pm$ 5.01	4
Cerebellum	13.4 $\pm$ 2.22	2

5-HT<sub>7</sub>R distribution is determined as specific binding of 5 nM <sup>3</sup>H-SB-269970 in fmol/mg TE. Values are given as mean  $\pm$  SD. Mean is for 3 independent experiments.

RGB

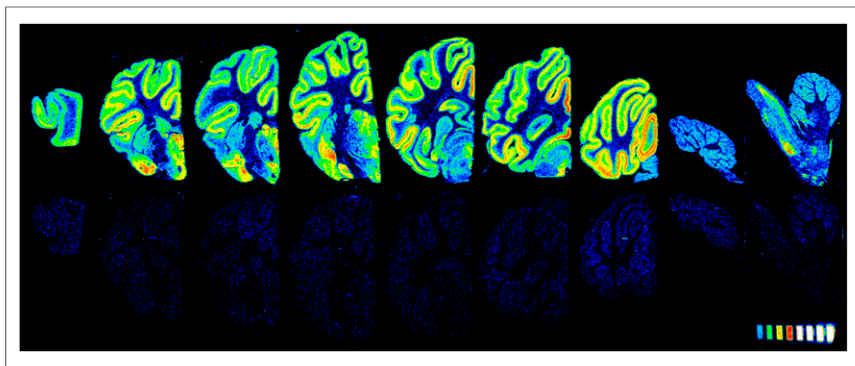


**FIGURE 1.** Representative sections of 5-HT<sub>7</sub>R autoradiography. Sections were incubated with 5 nM <sup>3</sup>H-SB-269970 to determine total binding (upper row) and with 10 μM SB-258719 to determine nonspecific binding (lower row).

isolated, with a specific activity of  $69.7 \pm 41.0$  GBq/μmol ( $n = 12$ ) at the end of synthesis. No precursor could be detected in the final formulation.

### In Vivo Distribution

With <sup>11</sup>C-Cimbi-712, the highest brain uptake was observed in the thalamus and the lowest uptake in the cerebellum. Time-activity curves displayed slow kinetics, with peak uptake after approximately 50 min (Fig. 3A). Pretreatment of the animals with 1.0 mg/kg/h SB-269970 decreased binding by approximately 50% in all regions. Like <sup>11</sup>C-Cimbi-712, <sup>11</sup>C-Cimbi-717 showed the highest brain uptake in the thalamus and the lowest uptake in the cerebellum (Fig. 3D). The <sup>11</sup>C-Cimbi-717 time-activity curves indicated reversible binding in the pig brain, with fast brain uptake and a more pronounced decline in tissue time-activity curves than was found for <sup>11</sup>C-Cimbi-712 (Fig. 3B). Pretreatment of the animal with SB-269970 (1.0 mg/kg/h and 4.2 mg/kg/h) decreased <sup>11</sup>C-Cimbi-717 uptake and increased the rate of washout in all brain regions.

Because no significant changes were observed between the baseline and blocking experiments in the composition of parent compound and other metabolites over the time course of the scan (data not shown), a single parent fraction obtained from the average over all scans with <sup>11</sup>C-Cimbi-717 was computed and used to generate arterial plasma input time-activity curves. No

significant changes in arterial input function were observed between the baseline and blocking experiments. Receptor binding of <sup>11</sup>C-Cimbi-717 quantified with the 1-TC model showed the  $V_T$  to be highest in the thalamus ( $16 \pm 2.5$  mL/cm<sup>3</sup>) and lowest in the cerebellum ( $6.6 \pm 1.2$  mL/cm<sup>3</sup>), indicating good regional separation, as also confirmed by the time-activity curves (Fig. 3B).  $V_T$  was also calculated for all doses of SB-269970 and prazosin (Fig. 4C). A dose-dependent reduction in  $V_T$  was observed with SB-269970, with significant reductions with the doses 1.0 mg/kg/h ( $P < 0.01$ ) and 4.2 mg/kg/h ( $P < 0.001$ ) in all regions except the cerebellum. The slope of the occupancy curve for prazosin was not significantly different from 0, supporting the likelihood that prazosin does not alter the binding of <sup>11</sup>C-Cimbi-717 in vivo.

Receptor binding of <sup>11</sup>C-Cimbi-712 was quantified with the 1-TC model.  $V_{TS}$  were—as with <sup>11</sup>C-Cimbi-717—highest in the thalamus (87.5 and 54.9 mL/cm<sup>3</sup>) and lowest in the cerebellum (35.2 and 32.1 mL/cm<sup>3</sup>). The  $V_{TS}$  of the pretreated scans revealed a decrease in binding, although the decrease could not be reliably statistically assessed (Fig. 4A). The occupancy slopes were, however, significantly different from 0, verifying that SB-269970 did block the binding of <sup>11</sup>C-Cimbi-712.

Based on occupancy plots of <sup>11</sup>C-Cimbi-717 (Fig. 4D), the  $V_{ND}$  and occupancy were extracted from the linear regression. The <sup>11</sup>C-Cimbi-717  $V_{ND}$  was on average  $2.1 \pm 0.8$  mL/cm<sup>3</sup> (mean  $\pm$  SD,  $n = 5$ ), and intravenous pretreatment with 0.2 mg/kg/h SB-269970 resulted in 25.4% occupancy, whereas pretreatment with the higher doses of 1.0 and 4.2 mg/kg/h resulted in 59.9% and 75.4% occupancy, respectively. Consequently, the  $BP_{ND}$  of <sup>11</sup>C-Cimbi-717 at baseline in the thalamus and cerebellum were calculated to be  $6.4 \pm 1.2$  and  $2.1 \pm 0.6$  ( $n = 6$ ), respectively.

Treatment with 1.0 mg/kg/h SB-269970 before <sup>11</sup>C-Cimbi-712 injection resulted in an occupancy of 75.3% and a  $V_{ND}$  of 8.57 mL/cm<sup>3</sup> (Fig. 4B). Consequently, the  $BP_{ND}$  of <sup>11</sup>C-Cimbi-712 in the thalamus is 7.3 based on average  $V_{TS}$  and  $V_{ND}$ s.

Comparison of the in vitro and in vivo binding data revealed significant positive correlations between <sup>3</sup>H-SB-269970 binding in vitro and <sup>11</sup>C-Cimbi-712 ( $P = 0.016$ ) and <sup>11</sup>C-Cimbi-717 ( $P < 0.001$ ) binding in vivo (Fig. 5). The free fraction of <sup>11</sup>C-Cimbi-717 in plasma was on average 6.7% at equilibrium.

### Metabolism

Radio-HPLC analysis of pig plasma revealed that after intravenous injection, <sup>11</sup>C-Cimbi-717 was relatively slowly metabolized (50% remaining after 30 min), and two radiometabolites were observed (Fig. 6). The polar metabolite fraction increased during the 90-min scanning time. The other more lipophilic metabolite was detected in relatively low amounts (~15%). However, this metabolite was less lipophilic than <sup>11</sup>C-Cimbi-717.

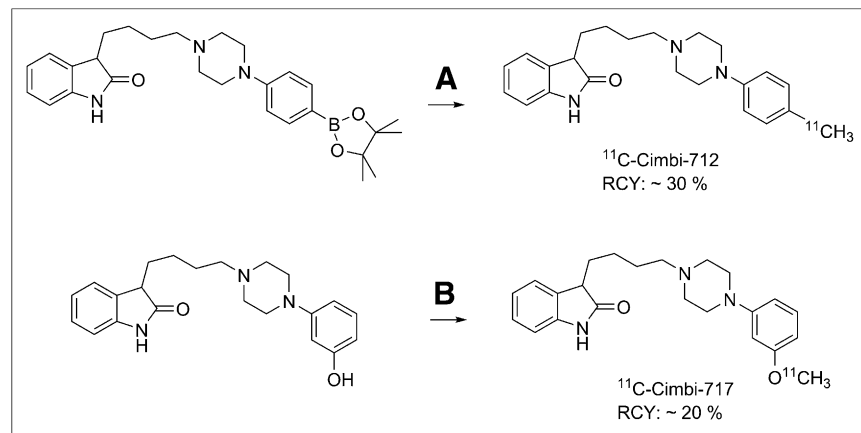


**FIGURE 2.** Radiosyntheses of <sup>11</sup>C-Cimbi-712 and <sup>11</sup>C-Cimbi-717. Reagents and conditions: <sup>11</sup>C-CH<sub>3</sub>I, K<sub>2</sub>CO<sub>3</sub>, Pd<sub>2</sub>(dba)<sub>3</sub>, P(o-tolyl)<sub>3</sub>, 60°C, DMF:H<sub>2</sub>O (v:v 9:1) (A) and <sup>11</sup>C-CH<sub>3</sub>OTf, 0.3 mg precursor, MeCN, K<sub>2</sub>CO<sub>3</sub> (1 equivalent), 60°C, 5 min (B).

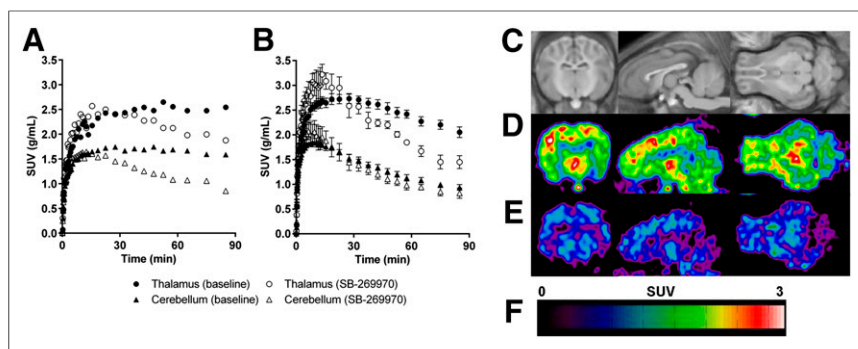


**FIGURE 3.** (A) Time–activity curves for <sup>11</sup>C-Cimbi-712 at baseline (● and ▲, *n* = 2) and after blocking with 1.0 mg/kg/h SB-269970 (○ and △, *n* = 2). (B) Time–activity curves for <sup>11</sup>C-Cimbi-717 at baseline (● and ▲, *n* = 6) and after blocking with 1.0 mg/kg/h SB-269970 (○ and △, *n* = 3). (C) MR-based atlas of pig brain. (D) <sup>11</sup>C-Cimbi-717 baseline summed PET images from 0 to 90 min. (E) SB-269970–pretreated <sup>11</sup>C-Cimbi-717 summed PET images from 0 to 90 min. (F) Color bar of standardized uptake value (SUV) (g/mL). Error bars = SEM.

## DISCUSSION

Here we have presented the radiosyntheses and in vivo evaluation of two novel 5-HT<sub>7</sub>R radioligands, <sup>11</sup>C-Cimbi-712 and <sup>11</sup>C-Cimbi-717. To enable comparisons between in vitro and in vivo data, we have also assessed for the first time the cerebral 5-HT<sub>7</sub>R distribution in the pig brain.

Consistent with observations in the human brain (21,22) and brain membrane binding assays in different species (23), in vitro data with <sup>3</sup>H-SB-269970 showed that 5-HT<sub>7</sub>R distribution in the

pig brain was fairly homogeneous in the neocortex but differed more across the remaining brain regions. Our data also showed that the hypothalamus, thalamus, and amygdala are areas with high 5-HT<sub>7</sub>R density, as is in line with the involvement of 5-HT<sub>7</sub>R in circadian rhythm controlled by the suprachiasmatic nucleus (24,25). As described for human brain tissue, <sup>3</sup>H-SB-269970 binding in the pig striatum was low. We found low 5-HT<sub>7</sub>R binding in the pig cerebellum, corresponding to a study showing low amounts of 5-HT<sub>7</sub>R messenger RNA in cerebellum in pigs (26). We found a general high binding in the cerebral cortex of the pig brain as reported earlier for membrane binding assays (23). Although the cortical binding pattern did not resemble that of 5-HT<sub>2A</sub>R or 5-HT<sub>1A</sub>R (27), we confirmed the specificity of <sup>3</sup>H-SB-269970 through autoradiographic blocking experiments with the specific 5-HT<sub>1A</sub>R and 5-HT<sub>2A</sub>R antagonists WAY-100635 and MDL-100907 (data not shown). No displacement was found with WAY-100635, but in accordance with the affinity of MDL-100907 (*K*<sub>i</sub> ~ 50 nM) toward 5-HT<sub>7</sub>R (28), a 40% displacement was observed.

Although <sup>11</sup>C-Cimbi-717 was successfully labeled in sufficient RCY for the PET experiments, we did not succeed in further

optimizing the RCY. We speculate that the major radioactive side product is due to methylation of the oxindole moiety, and if so, the introduction of a protecting group at the N-1 position of the oxindole may reduce the formation of the observed side product. Although the racemic material could be separated on chiral HPLC, the stereogenic center epimerizes rapidly. Thus, all compounds in this study have been investigated as the racemate. The quantification is therefore an average of binding of two enantiomers, and it is possible that one of the enantiomers is superior to the other.

In vivo evaluation of <sup>11</sup>C-Cimbi-717 demonstrated a high brain uptake and a binding distribution similar to that of 5-HT<sub>7</sub>R found in vitro; thalamus has the highest and cerebellum the lowest *V*<sub>T</sub>, consistent with the <sup>3</sup>H-SB-269970 autoradiography. <sup>11</sup>C-Cimbi-717 binding in the striatum was not quite in line with the correlation between in vivo binding in other regions and in vitro autoradiography binding. Further analysis of these differences revealed that this discrepancy between 5-HT<sub>7</sub>R binding in vivo and in vitro was larger for the putamen than for the caudate nucleus; thus, the discrepancy could be due to binding to an unknown target, for which either of the enantiomers of <sup>11</sup>C-Cimbi-717 has affinity. However, the occupancy plot did not reveal lower displacement in the striatal regions. We suspect

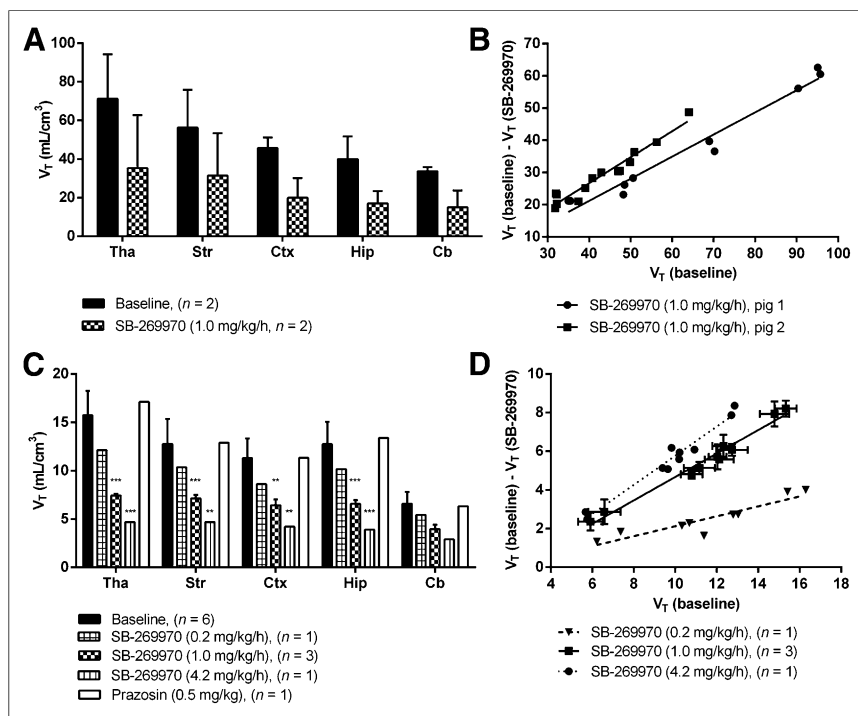


**FIGURE 4.** (A) *V*<sub>T</sub>s for <sup>11</sup>C-Cimbi-712 quantified by 1-TC modeling. (B) Occupancy plots for <sup>11</sup>C-Cimbi-712, where *V*<sub>T</sub>s for individual pigs are shown. (C) *V*<sub>T</sub>s for <sup>11</sup>C-Cimbi-717 quantified by 1-TC modeling. (D) Occupancy plots for <sup>11</sup>C-Cimbi-717 with 3 different doses of SB-269970. In A and C, bars represent mean ± SD; in B and D, bars represent mean ± SEM. \*\**P* < 0.01 and \*\*\**P* < 0.001 in comparison to baseline data within each volume of interest on statistical analysis with 2-way ANOVA and Bonferroni posttest. Tha = thalamus; Str = striatum; Ctx = cortex; Hip = hippocampus; Cb = cerebellum.

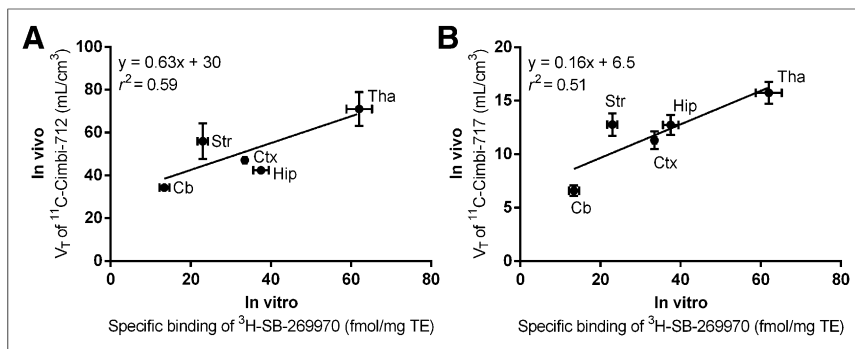


**FIGURE 5.** Comparison of 5-HT<sub>7</sub>R brain distribution determined by <sup>3</sup>H-SB-269970 autoradiography and by in vivo PET experiments using baseline  $V_T$ s of <sup>11</sup>C-Cimbi-712 ( $n = 2$ ) (A) and <sup>11</sup>C-Cimbi-717 ( $n = 6$ ) (B). Cb = cerebellum; Ctx = cortex; Hip = hippocampus; Str = striatum; Tha = thalamus. Error bars represent mean  $\pm$  SEM.

that the difference observed between the in vitro and in vivo results are due to inhomogeneity in the autoradiography experiments. With autoradiography, only a few cross sections were evaluated, whereas in PET, binding in the whole region is evaluated. The putamen is near the amygdala in the pig brain, and partial-volume effects may affect the signal from this high-binding region, leading to an overestimation of the <sup>11</sup>C-Cimbi-712 and <sup>11</sup>C-Cimbi-717 binding in the putamen. The correlation between in vitro and in vivo binding was not as strong for <sup>11</sup>C-Cimbi-712 as for <sup>11</sup>C-Cimbi-717. Along with the difference in binding in the striatum, <sup>11</sup>C-Cimbi-712 also displayed equal uptake in the hippocampus and cerebellum, a finding that is not in line with what we see with <sup>3</sup>H-SB-269970 autoradiography. This discrepancy in binding between <sup>11</sup>C-Cimbi-712 and <sup>11</sup>C-Cimbi-717 in the hippocampus could be due to off-target binding. Highest binding is, however, still observed in the thalamus, consistent with the autoradiography results.

Pretreatment with SB-269970 resulted in a dose-dependent decrease in <sup>11</sup>C-Cimbi-717 binding in the pig brain supporting 5-HT<sub>7</sub>R selectivity in vivo for <sup>11</sup>C-Cimbi-717.  $V_T$  decreased in all regions examined, including the cerebellum. Although this decrease in

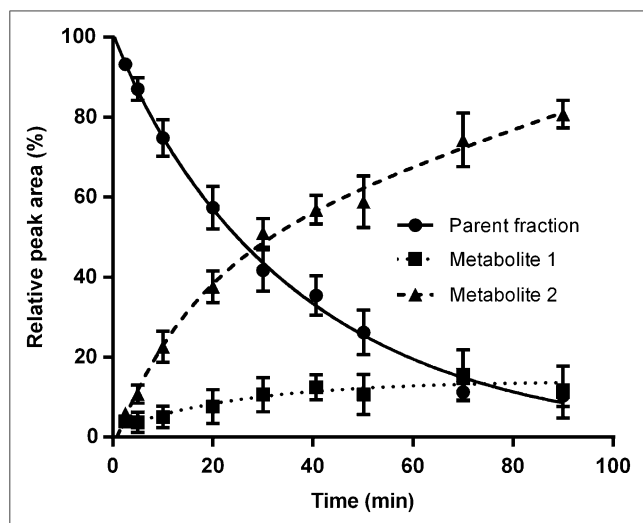


**FIGURE 6.** Metabolism of <sup>11</sup>C-Cimbi-717. Three radioactive compounds could be detected with radio-HPLC: <sup>11</sup>C-Cimbi-717 (parent compound) and two radiolabeled metabolites, both of which had lower retention time than parent compound. Data are presented as mean  $\pm$  SEM.

binding in the cerebellum was not statistically significant, it confirms the in vitro autoradiography data and the literature data that have found 5-HT<sub>7</sub>R to be present in the cerebellum (26). This decrease in binding in the cerebellum also invalidates the cerebellum as a reference region for a reference tissue model analysis of the PET data. In the absence of a reference region, we determined the nondisplaceable binding using the occupancy plot. Because of the affinity of Cimbi-717 for the  $\alpha_1$  adrenergic receptor ( $K_i = 47$  nM) (12), we ensured that pretreatment with prazosin, an  $\alpha_1$  adrenergic receptor antagonist, did not result in any significant decrease in <sup>11</sup>C-Cimbi-717  $V_T$ . <sup>11</sup>C-Cimbi-712 binding was blocked with

SB-269970, supporting the possibility that this radioligand also labels 5-HT<sub>7</sub>R specifically. The slow kinetics of <sup>11</sup>C-Cimbi-712, however, complicate modeling of the binding, resulting in large variations in the outcome measures ( $V_T$ ) and consequently also larger uncertainties in the calculated occupancy and  $V_{ND}$ .

The average nonspecific binding in the pig brain,  $V_{ND}$ , of <sup>11</sup>C-Cimbi-717 as determined by the occupancy plot was 2.1 mL/cm<sup>3</sup> and thus comprised about 15% of the  $V_T$  in the high-binding regions. This ratio of specific-to-nonspecific binding is larger than what is obtained by other PET ligands evaluated in the same species, for example, approximately 50% for <sup>11</sup>C-NS14492 and approximately 35% for <sup>11</sup>C-SB2047145 (19,29).

Modeling of the <sup>11</sup>C-Cimbi-717 data was done with the 1-TC model first because of the simplicity of the model, second because more regions converged with this model compared with 2-TC, and finally because the Akaike information criterion was generally lower for the 1-TC than for the 2-TC (Supplemental Table 2). The Logan linearization model underestimated the  $V_T$  values by 10%–15% compared with both the 1-TC and the 2-TC.

The systemic metabolism of <sup>11</sup>C-Cimbi-717 was relatively slow compared with other radioligands evaluated in pigs (11,18,19), with approximately 60% of the total plasma activity arising from the parent compound left after 20 min. Metabolism was nonsignificantly faster after blockade with SB-269970, as could be explained by an increased availability in the blood and thus an increased availability to enzymatic degradation. No effects on metabolism were observed with prazosin.

## CONCLUSION

<sup>11</sup>C-Cimbi-712 and <sup>11</sup>C-Cimbi-717 were both successfully radiolabeled in sufficient RCYs for in vivo evaluation in the pig. Of the two novel radioligands for brain imaging of 5-HT<sub>7</sub>R, <sup>11</sup>C-Cimbi-717 generated the highest brain uptake and showed more reversible tracer kinetics than <sup>11</sup>C-Cimbi-712—benefits that are important for quantification. Both <sup>11</sup>C-Cimbi-712 and <sup>11</sup>C-Cimbi-717 had a regional distribution pattern compatible with 5-HT<sub>7</sub>R distribution in the pig brain, as assessed independently by autoradiography. Finally, <sup>11</sup>C-Cimbi-717 showed a dose-dependent decrease in binding after pretreatment with the 5-HT<sub>7</sub>R-specific antagonist SB-269970. We conclude, on the basis of these pre-clinical data, that <sup>11</sup>C-Cimbi-717 may be a useful radioligand for in vivo imaging of 5-HT<sub>7</sub>R binding sites in the human brain.

## DISCLOSURE

The costs of publication of this article were defrayed in part by the payment of page charges. Therefore, and solely to indicate this fact, this article is hereby marked "advertisement" in accordance with 18 USC section 1734. Financial support by the Intra European Fellowship (MC-IEF-275329), the Faculty of Health at the University of Copenhagen, and particularly the Lundbeck Foundation is gratefully acknowledged. The John and Birthe Meyer Foundation and the Toyota Foundation are acknowledged for financial support for the HRRT scanner and HPLC system, respectively. No other potential conflict of interest relevant to this article was reported.

## ACKNOWLEDGMENTS

We thank the staff at the PET and Cyclotron Units for expert technical assistance. We also thank Mette Værum Olesen for excellent technical assistance with animal preparation.

## REFERENCES

1. Matthys A, Haegeman G, Van Craenenbroeck K, Vanhoenacker P. Role of the 5-HT<sub>7</sub> receptor in the central nervous system: from current status to future perspectives. *Mol Neurobiol.* 2011;43:228–253.
2. Bonaventure P, Kelly L, Aluisio L, et al. Selective blockade of 5-hydroxytryptamine (5-HT)<sub>7</sub> receptors enhances 5-HT transmission, antidepressant-like behavior, and rapid eye movement sleep suppression induced by citalopram in rodents. *J Pharmacol Exp Ther.* 2007;321:690–698.
3. Guscott M, Bristow LJ, Hadingham K, et al. Genetic knockout and pharmacological blockade studies of the 5-HT<sub>7</sub> receptor suggest therapeutic potential in depression. *Neuropharmacology.* 2005;48:492–502.
4. Hedlund PB, Huitron-Resendiz S, Henriksen SJ, Sutcliffe JG. 5-HT<sub>7</sub> receptor inhibition and inactivation induce antidepressantlike behavior and sleep pattern. *Biol Psychiatry.* 2005;58:831–837.
5. Wesolowska A, Nikiforuk A, Stachowicz K, Tatarczynska E. Effect of the selective 5-HT<sub>7</sub> receptor antagonist SB 269970 in animal models of anxiety and depression. *Neuropharmacology.* 2006;51:578–586.
6. Volk B, Barkoczy J, Hegedus E, et al. (Phenylpiperazinyl-butyl)oxindoles as selective 5-HT<sub>7</sub> receptor antagonists. *J Med Chem.* 2008;51:2522–2532.
7. Paterson LM, Tyacke RJ, Nutt DJ, Knudsen GM. Measuring endogenous 5-HT release by emission tomography: promises and pitfalls. *J Cereb Blood Flow Metab.* 2010;30:1682–1706.
8. Zhang M-R, Haradahira T, Maeda J, et al. Synthesis and preliminary PET study of the 5-HT<sub>7</sub> receptor antagonist [<sup>11</sup>C]DR4446. *J Labelled Comp Radiopharm.* 2002;45:857–866.
9. Andriès J, Lemoine L, Mouchel-Blaisot A, et al. Looking for a 5-HT<sub>7</sub> radiotracer for positron emission tomography. *Bioorg Med Chem Lett.* 2010;20:3730–3733.
10. Lemoine L, Andries J, Le Bars D, Billard T, Zimmer L. Comparison of 4 radiolabeled antagonists for serotonin 5-HT<sub>7</sub> receptor neuroimaging: toward the first PET radiotracer. *J Nucl Med.* 2011;52:1811–1818.
11. Herth MM, Hansen HD, Ettrup A, et al. Synthesis and evaluation of [<sup>11</sup>C]Cimbi-806 as a potential PET ligand for 5-HT(7) receptor imaging. *Bioorg Med Chem.* 2012;20:4574–4581.
12. Herth MM, Volk B, Pallagi K, et al. Synthesis and in vitro evaluation of oxindole derivatives as potential radioligands for 5-HT(7) receptor imaging with PET. *ACS Chem Neurosci.* 2012;3:1002–1007.
13. Andersen VL, Herth MM, Lehel S, Knudsen GM, Kristensen JL. Palladium-mediated conversion of para-aminoarylboronic esters into para-aminoaryl-<sup>11</sup>C-methanes. *Tetrahedron Lett.* 2013;54:213–216.
14. Lovell PJ, Bromidge SM, Dabbs S, et al. A novel, potent, and selective 5-HT(7) antagonist: (R)-3-(2-(2-(4-methylpiperidin-1-yl)ethyl)pyrrolidine-1-sulfonyl) phenol (SB-269970). *J Med Chem.* 2000;43:342–345.
15. Cavero I, Roach AG. The pharmacology of prazosin, a novel antihypertensive agent. *Life Sci.* 1980;27:1525–1540.
16. Schwinn DA, Johnston GI, Page SO, et al. Cloning and pharmacological characterization of human alpha-1 adrenergic receptors: sequence corrections and direct comparison with other species homologues. *J Pharmacol Exp Ther.* 1995;272:134–142.
17. Gillings N. A restricted access material for rapid analysis of [<sup>11</sup>C]-labeled radiopharmaceuticals and their metabolites in plasma. *Nucl Med Biol.* 2009;36:961–965.
18. Ettrup A, Palmer M, Gillings N, et al. Radiosynthesis and evaluation of <sup>11</sup>C-CIMBI-5 as a 5-HT<sub>2A</sub> receptor agonist radioligand for PET. *J Nucl Med.* 2010;51:1763–1770.
19. Kornum BR, Lind NM, Gillings N, Marnier L, Andersen F, Knudsen GM. Evaluation of the novel 5-HT<sub>4</sub> receptor PET ligand [<sup>11</sup>C]SB207145 in the Gottingen minipig. *J Cereb Blood Flow Metab.* 2009;29:186–196.
20. Cunningham VJ, Rabiner EA, Slifstein M, Laruelle M, Gunn RN. Measuring drug occupancy in the absence of a reference region: the Lassen plot re-visited. *J Cereb Blood Flow Metab.* 2010;30:46–50.
21. Hagan JJ, Price GW, Jeffrey P, et al. Characterization of SB-269970-A, a selective 5-HT(7) receptor antagonist. *Br J Pharmacol.* 2000;130:539–548.
22. Varnäs K, Thomas DR, Tupala E, Tiihonen J, Hall H. Distribution of 5-HT<sub>7</sub> receptors in the human brain: a preliminary autoradiographic study using [<sup>3</sup>H] SB-269970. *Neurosci Lett.* 2004;367:313–316.
23. Thomas DR, Atkinson PJ, Hastie PG, Roberts JC, Middlemiss DN, Price GW. [<sup>3</sup>H]-SB-269970 radiolabels 5-HT<sub>7</sub> receptors in rodent, pig and primate brain tissues. *Neuropharmacology.* 2002;42:74–81.
24. Lovenberg TW, Baron BM, de Lecea L, et al. A novel adenylyl cyclase-activating serotonin receptor (5-HT<sub>7</sub>) implicated in the regulation of mammalian circadian rhythms. *Neuron.* 1993;11:449–458.
25. Sprouse J, Li X, Stock J, McNeish J, Reynolds L. Circadian rhythm phenotype of 5-HT<sub>7</sub> receptor knockout mice: 5-HT and 8-OH-DPAT-induced phase advances of SCN neuronal firing. *J Biol Rhythms.* 2005;20:122–131.
26. Bhalla P, Saxena PR, Sharma HS. Molecular cloning and tissue distribution of mRNA encoding porcine 5-HT<sub>7</sub> receptor and its comparison with the structure of other species. *Mol Cell Biochem.* 2002;238:81–88.
27. Ettrup A, Kornum BR, Weikop P, Knudsen GM. An approach for serotonin depletion in pigs: effects on serotonin receptor binding. *Synapse.* 2011;65:136–145.
28. Roth BL, Craig SC, Choudhary MS, et al. Binding of typical and atypical antipsychotic agents to 5-hydroxytryptamine-6 and 5-hydroxytryptamine-7 receptors. *J Pharmacol Exp Ther.* 1994;268:1403–1410.
29. Ettrup A, Mikkelsen JD, Lehel S, et al. <sup>11</sup>C-NS14492 as a novel PET radioligand for imaging cerebral alpha7 nicotinic acetylcholine receptors: in vivo evaluation and drug occupancy measurements. *J Nucl Med.* 2011;52:1449–1456.



## Appendix 3

### Paper III

<sup>11</sup>C-Labeling and Preliminary Evaluation of Vortioxetine as a Pet Radioligand

**V. L. Andersen**, H. D. Hansen, M. M. Herth, G. M. Knudsen, and J. L. Kristensen

*Bioorganic & Medicinal Chemistry Letters*, 24 (2014), 2408-11.







## <sup>11</sup>C-labeling and preliminary evaluation of vortioxetine as a PET radioligand



Valdemar L. Andersen<sup>a,b</sup>, Hanne D. Hansen<sup>a</sup>, Matthias M. Herth<sup>a</sup>, Gitte M. Knudsen<sup>a</sup>, Jesper L. Kristensen<sup>a,b,\*</sup>

<sup>a</sup> Center for Integrated Molecular Brain Imaging (CIMBI), Rigshospitalet and University of Copenhagen, Blegdamsvej 9, 2100 Copenhagen, Denmark

<sup>b</sup> Department of Drug Design and Pharmacology, Faculty of Health and Medical Sciences, University of Copenhagen, Universitetsparken 2, 2100 Copenhagen, Denmark

### ARTICLE INFO

#### Article history:

Received 13 March 2014

Revised 9 April 2014

Accepted 10 April 2014

Available online 19 April 2014

#### Keywords:

Cross-coupling

Vortioxetine

PET

Carbon-11

Palladium

### ABSTRACT

Vortioxetine is a new multi-modal drug against major depressive disorder with high affinity for a range of different serotonergic targets in the CNS. We report the <sup>11</sup>C-labeling of vortioxetine with [<sup>11</sup>C]MeI using a Suzuki-protocol that allows for the presence of an unprotected amine. Preliminary evaluation of [<sup>11</sup>C]vortioxetine in a Danish Landrace pig showed rapid brain uptake and brain distribution in accordance with the pharmacological profile, all though an unexpected high binding in cerebellum was also observed. [<sup>11</sup>C]vortioxetine displayed slow tracer kinetics with peak uptake after 60 min and with limited wash-out from the brain. Further studies are needed but this radioligand may prove to be a valuable tool in unraveling the clinical effects of vortioxetine.

© 2014 Elsevier Ltd. All rights reserved.

Major depressive disorder (MDD) is a prevalent disease that is considered by the WHO to be one of the leading causes of disability worldwide.<sup>1</sup> MDD has traditionally been treated with tricyclic anti-depressants (TCAs) monoamine oxidase inhibitors (MAOIs), selective serotonin reuptake inhibitors (SSRIs) and serotonin–nor-epinephrine reuptake inhibitors (SNRI's).<sup>2</sup>

Recently, a new drug for the treatment of MDD made its way to the market. Vortioxetine (**1**) is a multi-modal acting drug with high affinity for a range of serotonergic targets, see [Figure 1](#).<sup>3</sup> The anti-depressant effects of **1** are thought to be mediated through three serotonergic targets: (1) inhibition of the 5-HTT which leads to an increase in extracellular 5-HT levels in the brain (in analogy to previous antidepressants); (2) agonism of 5-HT<sub>1A</sub>R, which is believed to shorten the time to onset of clinical effects,<sup>4</sup> and (3) antagonism of 5-HT<sub>3</sub>R. Preclinical studies indicate that antagonism of 5-HT<sub>3</sub>R (among many other effects) could have positive effects on mood and cognitive dysfunction in patients with depression.<sup>5</sup>

The recommended starting dose of **1** is 10 mg per day, and PET studies in humans have shown that the occupancy at the 5-HTT is ~50% at 5 mg whereas the 5-HT<sub>1A</sub>R occupancy as measured in a small sample was not measurable.<sup>6</sup> The occupancy at other 5-HTRs is currently unknown and the exact mode of action of **1** remains to be fully elucidated. Here, we set out to develop a <sup>11</sup>C-labeled

version of **1** for PET studies. Access to such a radiotracer would open the possibility for conducting studies in different patient groups who respond differently to treatment, in analogy to previous studies with [<sup>11</sup>C]Clozapine.<sup>12</sup> Based on the in vitro receptor affinities reported for **1** one would expect to see binding in thalamus,<sup>7,8</sup> cortex,<sup>9</sup> hippocampus<sup>9,10</sup> and striatum.<sup>8,11</sup>

The commonly employed <sup>11</sup>C-labeling strategy of O-, N- or S-methylation is not an option for labeling vortioxetine, whereas the aromatic methyl-groups are possible sites for labeling via a Suzuki-coupling with a suitable boronic acid derivative.<sup>13</sup> In theory, two different labeling sites are possible: the *ortho*- and the *para*-position. We chose to focus on the 2-position, as the required precursor would be readily available.

As **1** contains a secondary amine, one could envisage two labeling strategies, see [Scheme 1](#): in route A, a precursor with a suitable protecting group (Pg) on the secondary amine is first <sup>11</sup>C-labeled and the Pg is subsequently removed. This would appear to be the safe option as labeling of the precursor using route B (in which the two steps are reversed) in principle could lead to labeling at the secondary nitrogen instead. The disadvantage with route A is that it requires a subsequent deprotection step after the <sup>11</sup>C-labeling, with concurrent loss of radiochemical yield, whereas Route B gives [<sup>11</sup>C]**1** directly. We have previously developed procedures for the Pd-mediated <sup>11</sup>C-labeling of aryl boronic derivatives containing unprotected amines<sup>14</sup> and decided to try and developed a radio synthesis based on route B.

\* Corresponding author. Tel.: +45 35336487; fax: +45 35306040.

E-mail address: [jesper.kristensen@sund.ku.dk](mailto:jesper.kristensen@sund.ku.dk) (J.L. Kristensen).

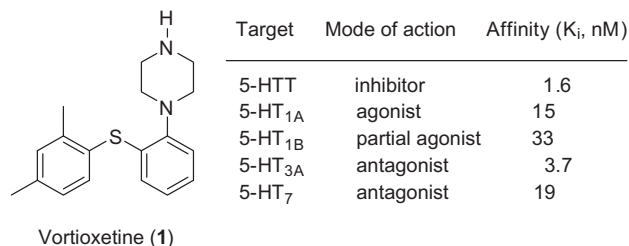
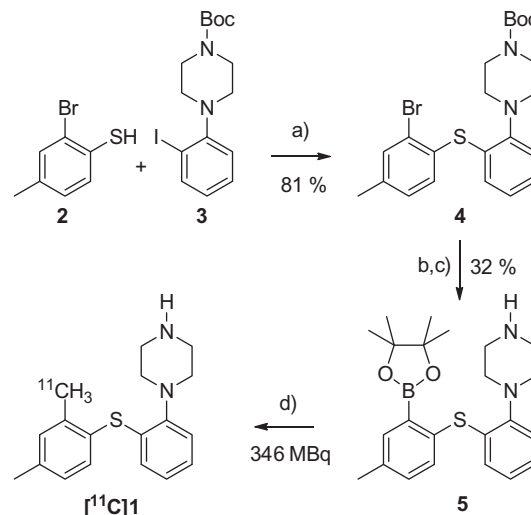


**Figure 1.** Structure and selected pharmacological profile of vortioxetine (1) at various human 5-HT receptors.<sup>3</sup>

The required precursor was synthesized as outlined in Scheme 2. Starting from 2-bromo-4-methylbenzenethiol (2) and *tert*-butyl 4-(2-iodophenyl)piperazine-1-carboxylate (3) the synthesis of the required precursor was carried out in a three step sequence starting with a Palladium catalysed thioether formation via coupling of 2 and 3 to give 4 in 81% isolated yield.<sup>15</sup> The use of dry, degassed toluene and microwave irradiation at 100 °C proved essential for an efficient coupling; otherwise debrominated 4 was the main product. Installment of a boronic ester moiety via a Pd-catalyzed coupling with bis(pinacolato)diboron and Pd(dppf)Cl<sub>2</sub> followed by liberation of the secondary amine via Boc-deprotection provided the desired precursor 5 in 32% yield.<sup>16</sup>

We previously showed that by trapping [<sup>11</sup>C]CH<sub>3</sub>I as a [<sup>11</sup>C]CH<sub>3</sub>-PdL<sub>n</sub>-I complex, it is possible to subsequently label aryl boronic derivatives that contain free amines.<sup>14</sup> Using this method 5 was converted to [<sup>11</sup>C]1 in 40% radiochemical yield. Following preparative HPLC-purification it was possible to isolate 346 MBq [<sup>11</sup>C]1 in >98% radiochemical purity and a specific activity of 478 GBq/μmol.<sup>17</sup> Yields were found to be extremely dependent on the quality of the palladium/ligand catalyst, as N-methylation rather than cross-coupling occurred in several instances, see Figure 2. Thus, a freshly prepared catalyst mixture was found to be essential for successful synthesis of [<sup>11</sup>C]1.

[<sup>11</sup>C]1 was injected into a Danish Landrace pig (Fig. 3).<sup>18</sup> A swift brain uptake was observed and, as expected from the pharmacological profile, with high binding in cortex, thalamus, hippocampus, striatum. High binding in cerebellum was also observed which is unexpected as none of the identified targets are reported as having high densities in this part of the brain. Target densities have been determined in the pig brain with autoradiography for the 5-HTT ([<sup>3</sup>H]escitalopram),<sup>19</sup> the 5-HT<sub>1A</sub>R ([<sup>3</sup>H]WAY-100635),<sup>19</sup> the 5-HT<sub>7</sub>R ([<sup>3</sup>H]SB-269970),<sup>14b</sup> and for the 5-HT<sub>3</sub>R

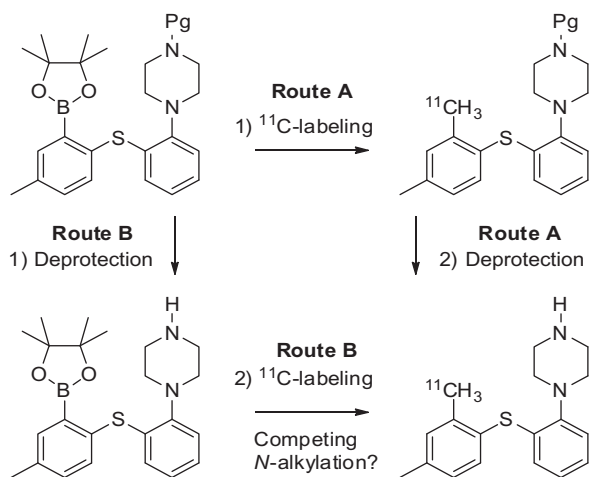


**Scheme 2.** Synthesis of precursor and <sup>11</sup>C-labeling of vortioxetine (1). Reagents and conditions: (a) Pd<sub>2</sub>dba<sub>3</sub>, DPEphos, *t*-BuOK, toluene, 100 °C (MW), 30 min; (b) bis(pinacolato)diboron, Pd(dppf)Cl<sub>2</sub>, KOAc, 1,4-dioxane, 100 °C, 12 h; (c) TFA, CH<sub>2</sub>Cl<sub>2</sub>; (d) [<sup>11</sup>C]CH<sub>3</sub>I, Pd<sub>2</sub>dba<sub>3</sub>, P(*o*-tolyl)<sub>3</sub>, K<sub>2</sub>CO<sub>3</sub>, 60 °C DMF/H<sub>2</sub>O 9:1, 5 min.

([<sup>3</sup>H]-(*S*)-Zacopride).<sup>20</sup> Areas with high density of 5-HT<sub>1A</sub>R include the cortex and the hippocampus. 5-HT<sub>7</sub>R density is high in the thalamus and in the cortex, but based on the affinity of 1 for these two targets it is most likely that the uptake of [<sup>11</sup>C]1 in the cortex arises from [<sup>11</sup>C]1 binding to the 5-HT<sub>1A</sub>R.<sup>21</sup>

The high uptake in the striatum is likely due to the high density of 5-HTT and possibly also due to binding to the 5-HT<sub>1B</sub>R. The area with the largest 5-HT<sub>3</sub>R density in the pig brain is the spinal cord (substantia gelatinosa), however this region is too small to be identified on the PET image and the region is not available in the pig atlas. It is therefore difficult to analyze whether binding to the 5-HT<sub>3</sub>R contributes to the PET signal.

The uniform uptake of [<sup>11</sup>C]1 could also indicate that the compound is very lipophilic and therefore has a large fraction of non-specific binding in the brain. The radio ligand displayed slow tracer kinetics with peak uptake after 60 min and with limited wash-out from the brain within the data acquisition time. This complicates the use of compartment models when performing kinetic modeling for quantification of binding, however in humans it may be possible to use reference tissue models although this needs to be validated.



**Scheme 1.** Possible radiolabeling approaches to <sup>11</sup>C-labeling of vortioxetine.

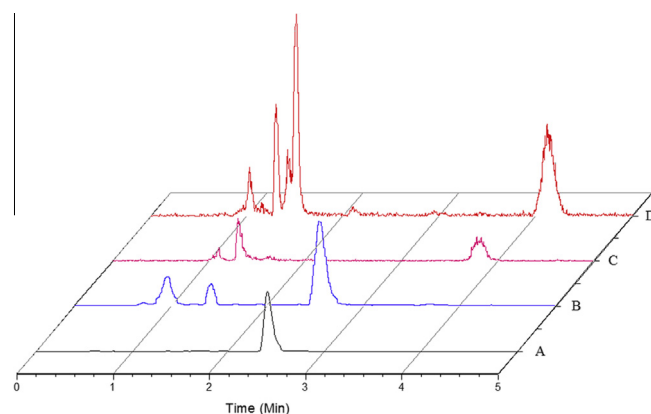


**Figure 2.** Effect of the state of the palladium–ligand combination on the amount of N-methylation. (A) Reference spectrum of 1 (with UV-detection). (B) Successful <sup>11</sup>C-labeling of 1. (C) Unsuccessful <sup>11</sup>C-labeling of 1—product with retention time ~4 min presumably the N-methylated precursor. (D) No Pd catalyst added—product with retention time ~4 min presumably the N-methylated precursor.

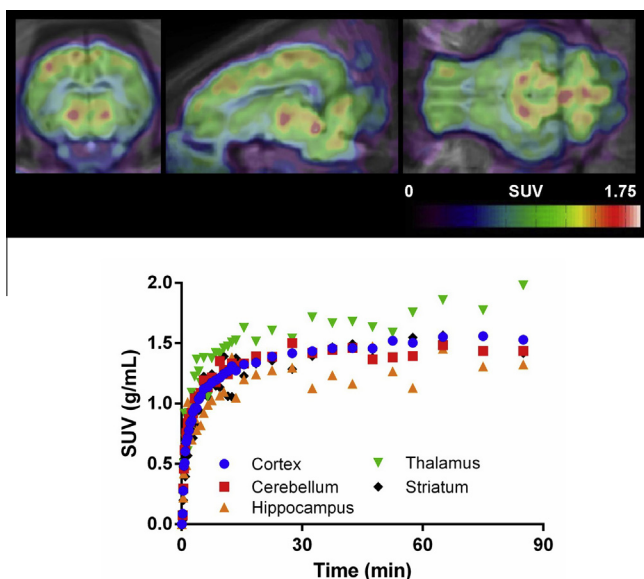


**Figure 3.** Top: Coronal, sagittal and transverse (left to right) summed PET images (0–90 min, 3 mm Gaussian filtering) of [<sup>11</sup>C]1 in the pig brain. Bottom: Time-activity curves showing absolute radioligand uptake for the indicated brain regions. SUV: standardized uptake value.

The protein binding of [<sup>11</sup>C]1 in pig plasma was determined to 98% measured after 2.5 h dialysis.<sup>22</sup> This level of protein binding is similar to that found in humans.<sup>3</sup>

In conclusion, vortioxetine was <sup>11</sup>C-labeled using the Suzuki reaction and its kinetics was evaluated in the pig brain. The tracer crossed the blood-brain barrier readily and binding to multiple sites within the brain was observed. Further investigations are necessary, but [<sup>11</sup>C]vortioxetine could prove to be an important tool making it is possible to follow the pharmacokinetics of an antidepressant with a new mechanism of action and thus aid uncovering of the underlying mechanism for 1's effect on MDD.

## Acknowledgments

The Lundbeck Foundation and the University of Copenhagen is gratefully acknowledged for financial support.

## References and notes

- Murray, C. J. L.; Lopez, A. D. *Science* **1996**, *274*, 740.
- (a) Bauer, M.; Monz, B. U.; Montejo, A. L.; Quail, D.; Dantchev, N.; Demyttenaere, K.; Garcia-Cebrian, A.; Grassi, L.; Perahia, D. G. S.; Reed, C.; Tylee, A. *Eur. Psychiatry* **2008**, *23*, 66; (b) Artigas, F. *ACS Chem. Neurosci.* **2013**, *4*, 5.
- Bang-Andersen, B.; Ruhland, T.; Jørgensen, M.; Smith, G.; Frederiksen, K.; Jensen, K. G.; Zhong, H.; Nielsen, S. M.; Hogg, S.; Mørk, A.; Stensbøl, T. B. *J. Med. Chem.* **2011**, *54*, 3206.
- Blier, P.; Ward, N. M. *Biol. Psychiatry* **2003**, *53*, 193.
- Ye, J. H.; Ponnudurai, R.; Schaefer, R. *CNS Drug Rev.* **2001**, *7*, 199.
- Areberg, J.; Luntang-Jensen, M.; Sogaard, B.; Nilausen, D. O. *Basic Clin. Pharmacol. Toxicol.* **2012**, *110*, 401.
- Hedlund, P. B.; Sutcliffe, J. G. *Trends Pharmacol. Sci.* **2004**, *25*, 481.
- Houle, S.; Ginovart, N.; Hussey, D.; Meyer, J. H.; Wilson, A. A. *Eur. J. Nucl. Med.* **2000**, *27*, 1719.
- Ito, H.; Halldin, C.; Farde, L. *J. Nucl. Med.* **1999**, *40*, 102.
- Besret, L.; Dauphin, F.; Guillouet, S.; Dhilly, M.; Gourand, F.; Blaizot, X.; Young, A. R.; Petit-Taboué, M. C.; Mickala, P.; Barbelivien, A.; Rault, S.; Barre, L.; Baron, J. C. *Life Sci.* **1997**, *62*, 115.
- Varnas, K.; Hurd, Y. L.; Hall, H. *Synapse* **2005**, *56*, 21.
- Lundberg, T.; Lindstrom, L. H.; Hartvig, P.; Eckernas, S. A.; Ekblom, B.; Lundqvist, H.; Fasth, K. J.; Gullberg, P.; Langstrom, B. *Psychopharmacology* **1989**, *99*, 8.
- (a) Hostetler, E. D.; Terry, G. G.; Burns, H. D. *J. Label. Compd. Radiopharm.* **2005**, *48*, 629; (b) Doi, H.; Ban, I.; Nonoyama, A.; Sumi, K.; Kuang, C.; Hosoya, T.; Tsukada, H.; Suzuki, M. *Chem. Eur. J.* **2009**, *15*, 4165; Review: (c) Pretze, M.; Große-Gehling, P.; Mamat, C. *Molecules* **2011**, *16*, 1129.

- (a) Andersen, V. L.; Herth, M. M.; Lehel, S.; Knudsen, G. M.; Kristensen, J. L. *Tetrahedron Lett.* **2013**, *54*, 213; (b) Hansen, H. D.; Herth, M. M.; Ettrup, A.; Andersen, V. L.; Lehel, S.; Dyssegaard, A.; Kristensen, J. L.; Knudsen, G. M. *J. Nucl. Med.* **2014**, *55*, 640.
- Experimental section—synthesis of precursor: *tert*-butyl 4-(2-((2-bromo-4-methylphenyl)thio)phenyl)piperazine-1-carboxylate (**4**): *tert*-BuOK (311 mg, 2.78 mmol), Pd<sub>2</sub>dba<sub>3</sub> (57.8 mg, 0.063 mmol), DPEphos (136 mg, 0.252 mmol), 2-bromo-4-methylbenzenethiol (512 mg, 2.52 mmol) and *tert*-butyl 4-(2-iodophenyl)piperazine-1-carboxylate (980 mg, 2.52 mmol) was dissolved in dry toluene (4 mL), kept under nitrogen and degassed using a stream of nitrogen for 10 min. The mixture was then heated to 100 °C (MW). The resulting crude was purified by dry column vacuum chromatography using heptane to heptane/EtOAc 10:1 (rf = 0.48 heptane/EtOAc 3:1) yielding 950 mg of **4** as a slightly yellow oil (81%). <sup>1</sup>H NMR (CDCl<sub>3</sub>, 400 MHz) δ: 1.49 (s, 9H) 2.35 (s, 3H) 2.97–3.03 (m, 4H) 3.50–3.55 (m, 4H) 6.85 (dd, *J* = 7.78, 1.51 Hz, 1H) 6.95–6.99 (m, 1H) 7.04–7.08 (m, 2H) 7.17–7.23 (m, 2H) 7.51 (d, *J* = 1.00 Hz, 1H). <sup>13</sup>C NMR (CDCl<sub>3</sub>, 400 MHz) δ: 20.8, 28.5, 51.6, 79.7, 120.4, 124.6, 127.3, 127.7, 129.0, 129.6, 131.7, 132.1, 134.0, 134.2, 139.6, 150.4, 154.9. LC–MS (*m*+1): 464 *m/z*.
- 1-(2-((4-Methyl-2-(4,4,5,5-tetramethyl-1,3,2-dioxaborolan-2-yl)phenyl)thio)phenyl)piperazine (**5**): Pd(dppf)Cl<sub>2</sub> (13.3 mg, 0.018 mmol), bis(pinacolato)diboron (169 mg, 0.665 mmol), KOAc (178 mg, 1.81 mmol) and **4** (280 mg, 0.604 mmol) was dissolved in dry 1,4-dioxane (10 mL), degassed with nitrogen for 10 min and heated to 100 °C for 18 h. The resulting crude was purified by dry column vacuum chromatography using heptane to heptane/EtOAc 10:1 (rf = 0.55 heptane/EtOAc 3:1). Yielding 124 mg of Boc-protected **5** as a slightly yellow oil (40%). <sup>1</sup>H NMR (CDCl<sub>3</sub>, 400 MHz) δ: 1.15 (s, 12H) 1.50 (s, 9H) 2.38 (s, 3H) 3.05 (br s, 4H) 3.58 (br s, 4H) 6.74 (d, *J* = 7.83 Hz, 1H) 6.88 (t, *J* = 7.46 Hz, 1H) 7.00 (m, 1H) 7.06 (m, 1H) 7.22 (d, *J* = 7.82 Hz, 1H) 7.35 (d, *J* = 7.83 Hz, 1H) 7.63 (s, 1H). <sup>13</sup>C NMR (CDCl<sub>3</sub>, 400 MHz) δ: 21.1, 24.6, 28.5, 51.4, 79.6, 83.8, 119.5, 124.5, 125.6, 127.2, 132.3, 134.6, 134.8, 136.4, 137.1, 137.4, 155.0. LC–MS (*m*+1): 511 *m/z*. This material was Boc-deprotected in the following way: (90 mg, 0.176 mmol) was dissolved in CH<sub>2</sub>Cl<sub>2</sub> (10 mL) and TFA (0.5 mL) was added and the mixture was stirred for 30 min. The resulting mixture was then washed with saturated aqueous NaHCO<sub>3</sub> (3 × 10 mL) and the organic phase was evaporated to dryness yielding 57 mg of **5** as a slightly yellow oil, 0.14 mmol, 79%. <sup>1</sup>H NMR (CDCl<sub>3</sub>, 400 MHz) δ: 1.13 (s, 10H) 2.38 (s, 3H) 3.37 (d, *J* = 12.23 Hz, 8H) 6.77 (d, *J* = 7.58 Hz, 1H) 6.93 (s, 1H) 7.02–7.05 (m, 1H) 7.09 (d, *J* = 7.09 Hz, 1H) 7.23 (d, *J* = 6.36 Hz, 1H) 7.34 (d, *J* = 7.82 Hz, 1H) 7.66 (s, 1H). <sup>13</sup>C NMR (CDCl<sub>3</sub>, 400 MHz) δ: 21.0, 24.5, 44.2, 48.3, 83.9, 119.8, 125.5, 125.9, 127.4, 132.5, 134.1, 134.7, 136.5, 137.6, 147.2. LC–MS (*m*+1): 411 *m/z*.
- <sup>11</sup>C-labeling of **1**: **5**, Pd<sub>2</sub>(dba)<sub>3</sub>, P(*o*-tolyl)<sub>3</sub> and base were used in a ratio of 40:1:2:4 with appropriate masses calculated from the use of 0.1 mg of P(*o*-tolyl)<sub>3</sub>. [<sup>11</sup>C]MeI was trapped in 300 μL DMF. To the trapped [<sup>11</sup>C]MeI was added Pd-catalyst and K<sub>2</sub>CO<sub>3</sub> dissolved in 300 μL of DMF/water 9:1 and heated to 60 °C. [<sup>11</sup>C]MeI was allowed to react for 2 min. **5** was added dissolved in 150 μL of DMF/water 9:1 and allowed to react for 5 min. Purification was performed by preparative HPLC using a Luna 5 μm C18(2) 100 Å column (Phenomenex Inc.) (250 × 10 mm, 50:50 citrate buffer pH 4.62; AcN, flowrate: 9 mL/min). The collected fraction was trapped on a solid-phase C18 sep-pack extraction column and eluted with 3 mL EtOH. Results were analyzed by HPLC using a Luna 5 μm C18 100 Å column (Phenomenex Inc.) (150 × 4.6 mm, 50:50 citrate buffer pH 4.62; AcN, flowrate 2 mL/min). Starting activities around 100 GBq EOB as [<sup>11</sup>C]CH<sub>4</sub>. Yields as determined by HPLC: 40%. Isolated yields: 161.4–346 MBq. Specific activities: 8–478 GBq/μmol. Total synthesis time: 55 min.
- PET data acquisition*: A female Danish Landrace pig (18 kg) was tranquilized by intramuscular (im) injection of 0.5 mg/kg midazolam. Anaesthesia was induced by im injection of a Zoletil veterinary mixture (1.25 mg/kg tiletamin, 1.25 mg/kg zolazepam, and 0.5 mg/kg midazolam; Virbac Animal Health, France). Following induction, anaesthesia was maintained by intravenous (iv) infusion of 15 mg/kg/h propofol (B. Braun Melsungen AG). During anaesthesia the pig was endotracheally intubated and ventilated (volume 200 mL, frequency 16 per min). Venous access was granted through two catheters in the peripheral milk veins. The Danish Council for Animal Ethics approved the animal procedures (journal no. 2012-15-2934-00156). [<sup>11</sup>C]1 was given as an intravenously (iv) bolus injection and the injected dose was 124 MBq (*n* = 1). The pig was subsequently scanned for 90 min in list-mode with a high resolution research tomography (HRRT) scanner (Siemens AG, Munich, Germany), where scanning started at the time of injection (0 min). Image reconstruction and analysis: ninety-minute list-mode PET data were reconstructed into 38 dynamic frames of increasing length (6 × 10, 6 × 20, 4 × 30, 9 × 60, 2 × 180, 8 × 300, and 3 × 600 s). Images consisted of 207 planes of 256 × 256 voxels of 1.22 × 1.22 × 1.22 mm. A summed picture of all counts in the 90-min scan was reconstructed and used for co-registration to a standardized MRI-based atlas of the Danish Landrace pig brain. The time-activity curve was calculated for the following volumes of interest (VOIs): cerebellum, cortex, hippocampus, lateral and medial thalamus, caudate nucleus, and putamen. Striatum is defined as the mean radioactivity in caudate nucleus and putamen. The radioactivity in thalamus is calculated as the mean radioactivity in the lateral and medial thalamus. Radioactivity in all VOIs was calculated as the average of radioactive concentration (Bq/mL) in the left and right sides. Outcome measure in the time-activity curves (TACs) was calculated as radioactive concentration in VOI (in kBq/mL) normalized to the injected dose corrected for animal weight (in kBq/kg), yielding standardized uptake values (g/mL).

19. Ettrup, A.; Kornum, B. R.; Weikop, P.; Knudsen, G. M. *Synapse* **2011**, *65*, 136.
20. Fletcher, S.; Barnes, N. M. *Neurosci. Lett.* **1999**, *269*, 91.
21. Herth, M. M.; Volk, B.; Pallagi, K.; Bech, L. K.; Antoni, F. A.; Knudsen, G. M.; Kristensen, J. L. *ACS Chem. Neurosci.* **2012**, *1002*, 3.
22. Plasma protein binding assay: The free fraction of [<sup>11</sup>C]1 in plasma,  $f_p$ , was estimated using an equilibrium dialysis chamber method. The dialysis was conducted in chambers (Harvard Biosciences) separated by cellulose membrane with a protein cut-off of 10,000 Da. Small amounts of [<sup>11</sup>C]1 (~5 MBq) were added to 5 mL plasma sample from the pig. Plasma (500  $\mu$ L) was then dialysed at 37 °C against an equal volume of buffer (135 mM NaCl, 3.0 mM KCl, 1.2 mM CaCl<sub>2</sub>, 1.0 mM MgCl<sub>2</sub>, and 2.0 mM KH<sub>2</sub>PO<sub>4</sub>, pH 7.4). Counts per minute in 400  $\mu$ L of plasma and buffer were determined in a well counter after various dialysis times (0.5, 1, 2, and 2.5 h), and  $f_p$  of [<sup>11</sup>C]1 was calculated as the ratio of radioactivity in buffer and plasma. Equilibrium in  $f_p$  was reached after 1 h of dialysis.

# Appendix 4

## Paper IV

Evaluation of 3-Ethyl-3-(phenylpiperazinylbutyl)oxindoles as PET ligands for the 5-HT<sub>7</sub> Receptor –  
Synthesis, pharmacology, radiolabeling and in vivo Brain Imaging

M. M. Herth, **V. L. Andersen**, H. D. Hansen, N. Stroth, B. Volk, A. Ettrup, S. Lehel, P.  
Svenningsson, G. M. Knudsen and J. L. Kristensen

*Journal of Medicinal Chemistry* (To be submitted).



# Evaluation of 3-Ethyl-3-(phenylpiperazinylbutyl)oxindoles as PET ligands for the 5-HT<sub>7</sub> receptor – synthesis, pharmacology, radiolabeling and in vivo brain imaging in pigs

Matthias M. Herth,<sup>§,†</sup> Valdemar L. Andersen,<sup>§,†</sup> Hanne D. Hansen,<sup>§</sup> Nikolas Stroth,<sup>‡</sup> Balázs Volk,<sup>‡</sup> Szabolcs Lehel,<sup>#</sup> Per Svenningsson,<sup>‡</sup> Gitte M. Knudsen,<sup>§</sup> Jesper L. Kristensen.<sup>§,†,\*</sup>

<sup>§</sup>Center for Integrated Molecular Brain Imaging, Rigshospitalet and University of Copenhagen, Blegdamsvej 9, DK-2100 Copenhagen, Denmark. <sup>†</sup>Department of Drug Design and Pharmacology, Faculty of Health and Medical Sciences, University of Copenhagen, Universitetsparken 2, DK-2100 Copenhagen, Denmark. <sup>#</sup>PET and Cyclotron Unit, Rigshospitalet, Blegdamsvej 9, DK-2100 Copenhagen, Denmark. <sup>‡</sup>Egis Pharmaceuticals Plc., P.O. Box 100, H-1475 Budapest, Hungary. <sup>‡</sup>Center for Molecular Medicine, Department of Neurology and Clinical Neuroscience, Karolinska Institute and Karolinska University Hospital, 17176 Stockholm, Sweden

**KEYWORDS:** Serotonin, 5-HT<sub>7</sub>, Selectivity, <sup>11</sup>C-labeling, PET

**ABSTRACT:** The 5-HT<sub>7</sub> G protein-coupled receptor is an important target for drug development. It is involved in various central nervous system (CNS) functions and disorders. Recently, we have described the successful synthesis and evaluation of two potential racemic oxindole-based 5-HT<sub>7</sub> PET tracers. In this work, we show that both tracers cannot be resolved into their enantiomers. In order to address this epimerization process, we blocked the chiral center of these parent compounds with an alkyl group. The newly developed compounds could be chirally separated and showed a similar pharmacological profile. Two ligands were selected for <sup>11</sup>C-labeling and evaluated in vivo. The tracers showed high brain uptake in 5-HT<sub>7</sub>-enriched brain regions. Surprisingly, both ligands could not be displaced by a 5-HT<sub>7</sub>-selective inverse agonist, SB-269970. Instead, a slight increase in brain uptake was observed.

The 5-HT<sub>7</sub> G protein-coupled receptor is the latest addition to the serotonin receptor subfamily.<sup>1,2</sup> Although the functional significance of this receptor is largely unknown, several reports have associated the human 5-HT<sub>7</sub> receptor with a variety of central nervous system (CNS) functions and disorders.<sup>3</sup> For example, the antidepressant effect of the atypical antipsychotic drugs amisulpride and lurasidone could be explained by 5-HT<sub>7</sub> receptor antagonism.<sup>4-7</sup> The availability of an appropriate 5-HT<sub>7</sub> receptor positron emission tomography (PET) radioligand would provide a significant advance in the understanding of the neurobiology and eventual dysfunctions of the 5-HT<sub>7</sub> receptor, because PET molecular imaging enables quantification of neuroreceptor binding in vivo. We have investigated a number of ligands from different compound classes for that purpose.<sup>8-14</sup> Cimbi-712 (**1**) and Cimbi-717 (**2**) displayed the most promising profile for selective 5-HT<sub>7</sub> receptor PET imaging in thalamic regions (Figure 1, Table 1). Subsequently, <sup>11</sup>C-labeling of both compounds was carried out and the in vivo PET behavior of both radioligands evaluated in pigs. High brain uptake and specific labeling of 5-HT<sub>7</sub> receptors could be detected.<sup>14,15</sup> These results encouraged us to further evaluate the potential of this compound class as PET ligands for the 5-HT<sub>7</sub> receptor. **1** and **2** were evaluated in their racemic form. The use of racemic mixtures in PET can complicate the data analysis as the two enantiomers may very well have different pharmacological profiles and kinetics (on/off-rates etc.).

Thus, we set out to evaluate the enantiopharmacology of **1** and **2**. Unfortunately, rapid racemization was observed after

separation on chiral HPLC at room temperature for both compounds (see supporting information for further data). The observed epimerisation is due to the acidic nature of the chiral center at the 3-position of the oxindole moiety, so we decided to investigate the influence of blocking the 3-position. This blockade will enable the separation of the compounds into their corresponding enantiomers.

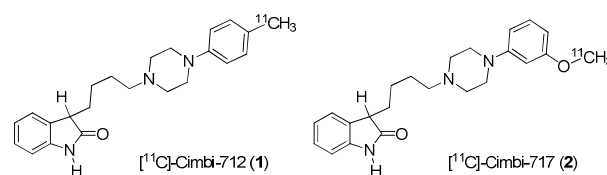


**Figure 1.** Structure of oxindole-ligands previously investigated as PET ligands for the 5-HT<sub>7</sub> receptor.<sup>14</sup>

Volk et al. have previously reported that 3-Et-oxindoles have a similar pharmacological profile to non-substituted oxindoles.<sup>16</sup> We could also show that other alkyl chains at the 3-position (-Me, -Et, -EtF and -Pr) did not alter the affinity towards the 5-HT<sub>7</sub> receptor significantly (see supporting information). Thus, we decided to target the two compounds in which the H is replaced by an ethyl-group (**3** and **4** compared to **1** and **2**) for further studies (Figure 2). The compounds were synthesized using similar procedures as previously described (see supporting information for details).<sup>16,17</sup>

All four compounds (**1-4**) were tested for efficacy in a heterologous cell line overexpressing human 5-HT<sub>7(a)</sub>. Initial experiments indicated inverse agonism, in that cellular cAMP concentrations were reduced below the level found in untreated control cells (Figure 3A). Subsequent concentration-response studies showed complete antagonism of 1 μM 5-HT-induced cAMP accumulation (Figure 3B) and curve fitting of the data (Figure 3C) yielded inhibitory potencies in the low nanomolar range (IC<sub>50</sub> values: 1.9, 5.6, 15.3 and 6.8 nM for compounds **1-4**).

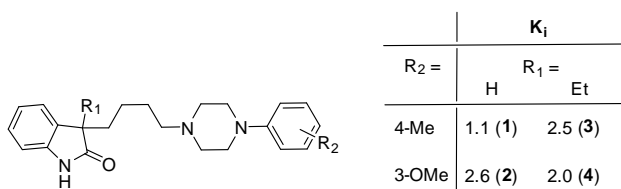


**Figure 2:** Affinity (K<sub>i</sub> values, in nM) of **1**, **2**, **3** and **4** for the 5-HT<sub>7</sub> receptor. Data represent n = 6 from three independent experiments, each carried out in duplicate.

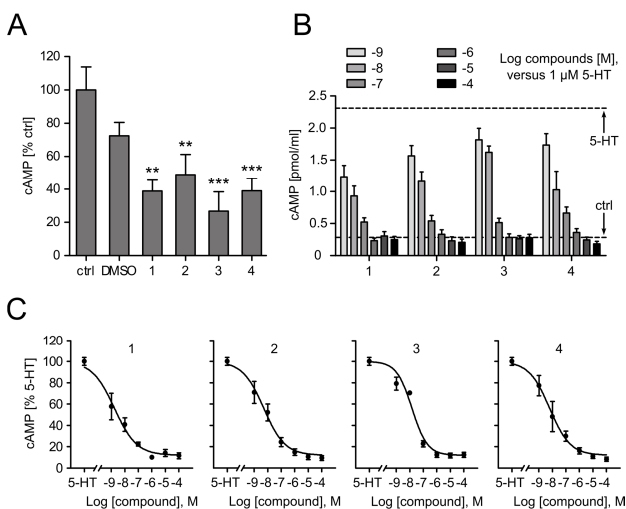


**Figure 3:** Pharmacological characterization of compound efficacy in HeLa cells stably expressing human 5-HT<sub>7(a)</sub>. Cells were exposed to test compounds in the absence or presence of 1 μM 5-HT and cellular cAMP was measured after 15 minutes of treatment. In the absence of 5-HT, all four compounds (at 10 μM) exhibit inverse agonist activity (A). In the presence of 5-HT, all compounds are potent and efficacious antagonists (B, C). All data are displayed as means ± SEM. Data in A were analyzed by one-way ANOVA with Dunnett's multiple comparison test, and asterisks indicate significant differences from untreated controls (\*\*p<0.01, \*\*\*p<0.001; n = 6-11 from four independent experiments). Concentration-response curves in C were derived from data in B via nonlinear regression (n = 6 from three independent experiments, each carried out in duplicate).

Chiral resolution of **3** and **4** on HPLC (see experimental section for details) provided both enantiomers. Subsequently, the racemic mixture as well as the pure enantiomers were

screened against a broad selection of targets at the PDSP screening facilities to fully evaluate the potential of these compounds as PET ligands.

(+)-**3** and (+)-**4** showed at least a 5 fold higher affinity towards the 5-HT<sub>7</sub> receptor compared to (-)-**3** and (-)-**4**. The racemic compounds, **3** and **4** had affinities comparable to (+)-**3** and (+)-**4**, respectively, and also comparable to the 3-unsubstituted oxindole derivatives **1** and **2**. However, α<sub>1</sub> – affinities were decreased. Table 1 displays selected affinities towards targets where cross affinity could become an issue. Other targets showed affinity > 10 μM. Compounds **1**, **2**, **3**, (+)-**3**, **4** and (+)-**4** were at least 2.5-fold selective over sigma receptors and at least 5-fold more selective for the 5-HT<sub>2A</sub> receptors. At other targets tested, a selectivity of more than one order of magnitude was detected. Only (+)-**4** showed lower selectivity over H1 receptors (~4 fold).

In general, it appears that C-3 alkylation does not improve the affinity towards the 5-HT<sub>7</sub> receptor, but improves the selectivity towards other receptors.

A PET radioligand has to fulfill several requirements to selectively image only one target. For example, high affinity towards the target-in-question must be accompanied by an acceptable level of selectivity towards other targets in the regions of interest. The receptor density (B<sub>max</sub>) is a measure of how many receptors are present in a given region of interest. A seeming lack of selectivity of a compound towards a certain receptor may be compensated by a high B<sub>max</sub> in a particular region.<sup>18</sup>

**Table 1:** Selectivity profile of promising structures. Affinities [K<sub>i</sub>-values] were determined by PDSP (n=3) and displayed in nM.

	K <sub>i</sub> [nM]							
	<b>1</b>	<b>3</b>	(+)- <b>3</b>	(-)- <b>3</b>	<b>2</b>	<b>4</b>	(+)- <b>4</b>	(-)- <b>4</b>
5-HT <sub>7</sub>	4.1	6.5	5.6	82	7.5	7.8	11	56
5-HT <sub>1A</sub>	491	469	787	633	130	83	192	151
5-HT <sub>2A</sub>	35	39	94	110	239	98	352	66
5-HTT	112	295	271	827	253	250	376	1439
H <sub>1</sub>	323	529	135	61	164	502	42	2405
α <sub>1</sub>	103	431	951	487	167	434	>10k	794
σ <sub>1</sub>	45	37	33	390	59	42	46	249
σ <sub>2</sub>	24	40	347	61	49	22	152	16

Therefore, the observed PET images are a function of the relative affinity of the ligands towards a target and the B<sub>max</sub> value of that target in a specific region. In general, a 10–100-fold higher binding to the target compared to other targets in a particular region is acceptable.<sup>18</sup> Based on these guidelines, **3**, (+)-**3**, **4** and (+)-**4** displayed very promising profiles for selective 5-HT<sub>7</sub> receptor imaging in the thalamus (Table 2; see supporting information for further explanations), whereas the previously evaluated compounds **1** and **2** displayed a questionable profile against α<sub>1</sub> – receptors in the thalamus. However, selective 5-HT<sub>7</sub> receptor imaging with **3**, (+)-**3**, **4**, or (+)-**4** could be problematic in other brain regions (see supporting information for details). In general, introduction of an alkyl



group to the oxindole moiety increased the selectivity/ $B_{\max}$  ratio for the critical  $\alpha_1$  – receptor. This could be further improved by enantioselective resolution of the ethylated derivatives. Unfortunately, selectivity/ $B_{\max}$  ratios for the sigma receptors could not be calculated due to a lack of human  $B_{\max}$  values. Future studies have to determine if these receptors have to be considered off-targets.

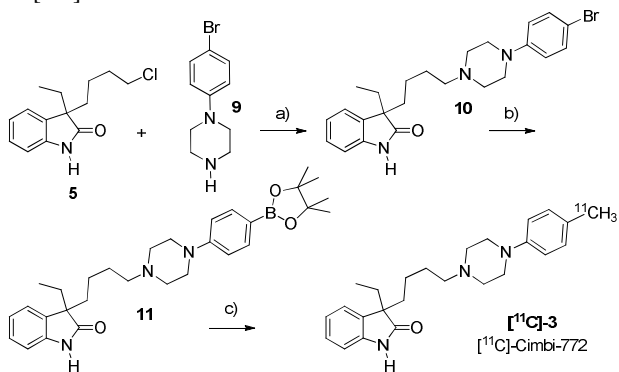
**Table 2:** Selectivity/ $B_{\max}$  ratio of the different compounds for the 5-HT<sub>7</sub> receptor relative to other cross-affinity targets in the thalamus. Data is based on values reported in Table 1 and Table S2. (PDSP determined  $K_i$  values and human  $B_{\max}$  values)

	Selectivity over $B_{\max}$ ratio							
	1	3	(+)-3	(-)-3	2	4	(+)-4	(-)-4
5-HT <sub>1A</sub>	359	216	421	23	52	31	52	8
5-HT <sub>2A</sub>	17	12	34	3	63	25	64	2
5-HTT	32	54	58	12	40	38	41	30
H <sub>1</sub>	236	244	72	2	65	193	11	128
$\alpha_1$	4	9	23	1	3	8	123	2
$\sigma_1$	n.c.	n.c.	n.c.	n.c.	n.c.	n.c.	n.c.	n.c.
$\sigma_2$	n.c.	n.c.	n.c.	n.c.	n.c.	n.c.	n.c.	n.c.

n.c.: not calculated, Human  $B_{\max}$  values of  $\sigma_1$  and  $\sigma_2$  could not be found in the literature

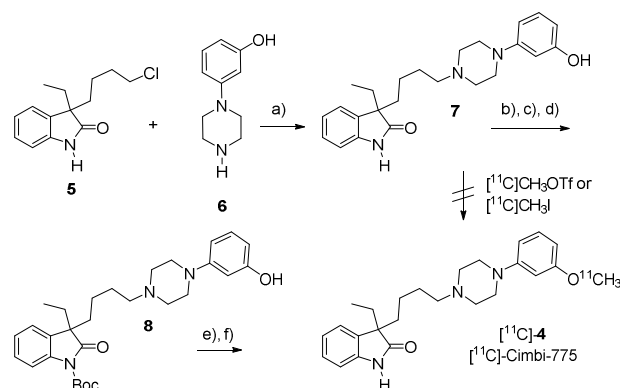
For practical reasons, we decided to start with <sup>11</sup>C-labelling of both racemic compounds to allow us to optimize the labeling procedure. In addition, use of the racemic compounds (**3**, **4**) would enable a direct in vivo PET imaging comparison between these and the unsubstituted oxindoles (**1**, **2**).

The radiosynthesis of [<sup>11</sup>C]-**3** ([<sup>11</sup>C]Cimbi-772) was carried out similar to a recently published procedure for <sup>11</sup>C-suzuki cross couplings.<sup>15</sup> It is noteworthy that the formation of the [<sup>11</sup>C]Me-Pd-I complex prior to the addition of the precursor is essential for a successful cross-coupling. The average specific activity was 343 GBq/ $\mu$ mol (range 183-542GBq/ $\mu$ mol), with radiochemical purity being above 97%. Thus, typically an amount of 122–230 MBq could be isolated from a 40 min beam. Scheme 1 summarizes the precursor and radiosynthesis of [<sup>11</sup>C]Cimbi-772.



**Scheme 1:** Synthesis of the precursor and [<sup>11</sup>C]Cimbi-772: a) Na<sub>2</sub>CO<sub>3</sub>, 180 °C, 1h; b) KOAc, Bis(pinacolato)diboron, Pd(dppf)Cl<sub>2</sub>, 1,4-dioxane, 100 °C, 12h ; c) Pd<sub>2</sub>(dba)<sub>3</sub>, P(*o*-tolyl)<sub>3</sub>, K<sub>2</sub>CO<sub>3</sub>, [<sup>11</sup>C]CH<sub>3</sub>I, DMF:water 9:1, 60 °C, 5 min

Initially, we tried to <sup>11</sup>C-label **4** ([<sup>11</sup>C]Cimbi-775) using the same conditions as reported for the synthesis of the structurally related compound **2** via direct alkylation at the phenolic position.<sup>14</sup> All attempts to produce the desired PET ligand using this approach were unsuccessful, and a single undesired byproduct was observed. We speculate that C-3 alkylation of the oxindole influences the reactivity of the oxindole core leading to competing labeling at this position. Therefore, a new labeling strategy was developed in which the phenolic hydroxyl-group was transiently TBDPS-protected, facilitating selective Boc-protection of the oxindole. Subsequent desilylation provided a suitable precursor, which was O-alkylated with [<sup>11</sup>C]CH<sub>3</sub>OTf followed by Boc-deprotection yielding the desired tracer [<sup>11</sup>C]-**2**. Average specific activities were around 234GBq/ $\mu$ mol (range 78-331 GBq/ $\mu$ mol) with a radiochemical purity above 97%. Typically, an amount of 152-211 MBq could be isolated using a 40 min beam (Scheme 2).



**Scheme 2:** Synthesis of the precursor and [<sup>11</sup>C]Cimbi-775: a) Na<sub>2</sub>CO<sub>3</sub>, 180 °C, 1h; b) TBDPSCl, NaH, DMF, 110 °C, 12h c) Boc<sub>2</sub>O, NaHDMS, THF, -5 °C, 30 min d) NH<sub>4</sub>F, MeOH, 70 °C, 30 min e) [<sup>11</sup>C]CH<sub>3</sub>I, 2M NaOH, DMF, 140 °C, 5 min f) TFA/CH<sub>2</sub>Cl<sub>2</sub> (1:1), 80 °C, 5 min

[<sup>11</sup>C]Cimbi-772 and [<sup>11</sup>C]Cimbi-775 were evaluated in Danish Landrace pigs using a high resolution research tomography (HRRT) PET scanner. Summed PET images (Figure 4a and 4b) show that both radioligands readily enter the pig brain and distribute to known regions with 5-HT<sub>7</sub> receptor distribution.<sup>14</sup> Following i.v. injection of either [<sup>11</sup>C]Cimbi-772 or [<sup>11</sup>C]Cimbi-775, the peak uptake reached 2.5 SUV in the thalamus. The tracer kinetics of both radioligands were fairly slow, in that the peak uptake was not reached until ~30 min for [<sup>11</sup>C]Cimbi-772 and ~10 min for [<sup>11</sup>C]Cimbi-775. Consequently, a limited wash-out of radioligand was seen within the PET acquisition time of 90 min.

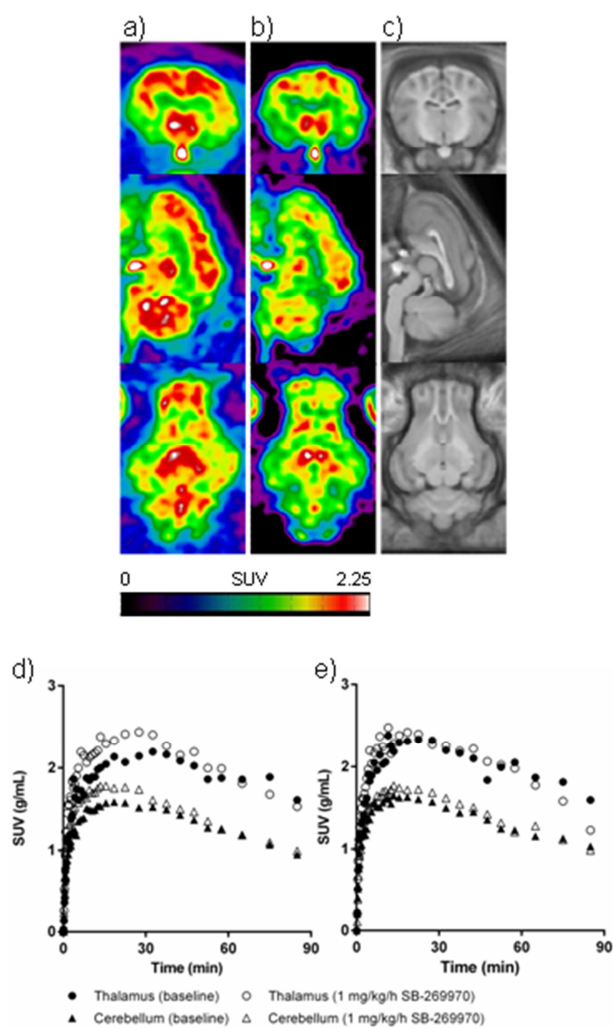


**Figure 4:** Summed PET images (0-90 min) of [ $^{11}\text{C}$ ]Cimbi-772 (a) and [ $^{11}\text{C}$ ]Cimbi-775 (b). MRI-based atlas of the pig brain (c). Time activity curves at baseline (solid symbols) and after pretreatment with SB-269970 (open symbols) for [ $^{11}\text{C}$ ]Cimbi-772 ( $n=2$ ) (d) and [ $^{11}\text{C}$ ]Cimbi-775 ( $n=1$ ) (e). Baseline and pretreatment

To investigate the specificity of binding of the radioligands, we administered 1.0 mg/kg/h of SB-269970, a selective 5-HT<sub>7</sub> receptor inverse agonist,<sup>19,20</sup> 30 min prior to the second injection of radioligand. No significant blocking effects could be detected for either of the radioligands, on the contrary it appeared that the uptake of especially [ $^{11}\text{C}$ ]Cimbi-772 was increased (Figure 4d and 4e).

This lack of displacement could be due to the increased lipophilicity of [ $^{11}\text{C}$ ]Cimbi-772 and [ $^{11}\text{C}$ ]Cimbi-775 compared to Cimbi-712 and Cimbi-717, which should increase the non-specific binding (NSB) in the brain (supporting information for details, Table S1). However, assuming that NSB is uniform throughout the brain, the observed binding cannot be solely attributed to NSB since the radioligands distribute in a pattern similar to the 5-HT<sub>7</sub> receptor distribution determined in vitro. Cross-affinities of the aforementioned targets could explain

this behavior, but [ $^{11}\text{C}$ ]Cimbi-772 and [ $^{11}\text{C}$ ]Cimbi-775 displayed a slightly improved in vitro selectivity profile compared to that of the successfully applied 5-HT<sub>7</sub> receptor PET ligands, [ $^{11}\text{C}$ ]Cimbi-712 (**1**) and [ $^{11}\text{C}$ ]Cimbi-717 (**2**). However we cannot rule out cross-affinities to other targets. Finally, the dose of the blocking agent could be too low. However, the used dose of SB-269970 has previously resulted in 60 % occupancy with [ $^{11}\text{C}$ ]Cimbi-717<sup>14</sup> and consequently, we find this dose appropriate for testing the specificity of our novel 5-HT<sub>7</sub> receptor radioligands.

Interestingly, these results are very similar to those obtained with the 5-HT<sub>7</sub> selective tracer, [ $^{11}\text{C}$ ]Cimbi-806 [18]. Cimbi-806 could displace [ $^3\text{H}$ ]SB-269970 in vitro, but SB-269970 could not displace [ $^{11}\text{C}$ ]Cimbi-806 in vivo. One explanation of this behavior could simply be that [ $^{11}\text{C}$ ]Cimbi-772, [ $^{11}\text{C}$ ]Cimbi-775 and [ $^{11}\text{C}$ ]Cimbi-806 are not selective for the 5-HT<sub>7</sub> receptor in vivo. However, the observed in vivo accumulation fits with receptor distribution as determined by in vitro autoradiography.<sup>14</sup> In the original study by Volk et al., all oxindole structures are reported as antagonists.<sup>16</sup> However, Volk et al. did observe a difference in the antagonistic efficacy between the C-3 alkylated and unsubstituted oxindole derivatives. Recently, some studies have shown differences in binding after competition or blocking with inverse agonists, antagonists and agonists.<sup>21, 22</sup> Furthermore, the compounds could bind to different receptor binding sites or cause different degrees of receptor internalization, what may influence the possibility to perform blocking or competition studies. However, more studies are warranted in order to investigate the importance of functional differences of compounds for PET radioligand binding.

## Conclusion

A set of potential 5-HT<sub>7</sub> receptor 3-Ethyl-3-(phenylpiperazinyl-butyl)oxindoles PET radioligands was successfully synthesized and evaluated. **3**, (+)-**3**, **4** and (+)-**4** displayed a promising in vitro profile for PET imaging of the 5-HT<sub>7</sub> receptor in thalamus. In comparison to the non-alkylated derivatives, **1** and **2**, it appears that alkylation of the 3-oxindole position improves the overall selectivity profile, but does not improve the affinity towards the 5-HT<sub>7</sub> receptor. Radiolabeling of **3** and **4** succeeded after optimization efforts and allowed us to evaluate both racemates in vivo. Both racemates entered the brain and accumulated in brain regions reflecting the expected distribution of 5-HT<sub>7</sub> receptors. No significant blocking of radioligand binding was observed after administration of the 5-HT<sub>7</sub> receptor specific inverse agonist, SB-269970, which calls into question the selectivity of both radioligands in vivo. Further studies have to be conducted to clarify if a functional difference between alkylated and non-alkylated oxindole PET ligands could lead to the observed effect.

## Experimental Section

**General.** The labeling procedure of selected compounds and the PET scanning protocol are described below. The general chemistry, experimental information, spectral data of all new compounds and determination of lipophilicities and  $K_i$  values are supplied in the Supporting information. Purity of all final

compounds was determined by HPLC or GC analysis and is >96%.

#### Labelling procedures

**[<sup>11</sup>C]Cimbi-772.** [<sup>11</sup>C]methyl iodide ([<sup>11</sup>C]MeI) produced using a fully automated system was transferred in a stream of helium to a 1.1-mL vial containing DMF (300 µL). To this vial was added Pd<sub>2</sub>(dba)<sub>3</sub> (0.3 mg), P(*o*-tolyl)<sub>3</sub>, and 2.6 µL of a 0.5M K<sub>2</sub>CO<sub>3</sub> solution dissolved in DMF:H<sub>2</sub>O 9:1 (150 µL). The resulting mixture was heated at 60 °C for 2 min. Afterwards, precursor dissolved in DMF:H<sub>2</sub>O 9:1 (150 µL) was added and the mixture was heated at 60 °C for another 5 min. Purification of the crude product was accomplished using HPLC (Luna 5µ C<sub>18</sub>(2) 100 Å, 250 x 10.00 mm 5 micron; 0.01M Borax buffer: MeCN (30:70, flow rate: 9 mL/min, RT: 475 sec ([<sup>11</sup>C]Cimbi-772). The fraction corresponding to the labeled product was collected in sterile water (150 mL), and the resulting solution was passed through a solid-phase C18 Sep-Pak extraction column (Waters Corp.), which had been preconditioned with ethanol (10 mL), followed by isotonic sodium chloride solution (20 mL). The column was flushed with sterile water (3 mL). Then, the trapped radioactivity was eluted with ethanol (3 mL) into a 20-mL vial containing phosphate buffer (9 mL, 100 mM, pH 7), giving a 12 mL solution of [<sup>11</sup>C]Cimbi-772. In a total synthesis time of 45–50 min, 0.1–0.2 GBq of [<sup>11</sup>C]Cimbi-772 was produced.

**[<sup>11</sup>C]Cimbi-775.** [<sup>11</sup>C]methyl iodide ([<sup>11</sup>C]MeI) produced using a fully automated system was transferred in a stream of helium to a 1.1-mL vial containing the labeling precursor 21 (0.3–0.4 mg), DMF (300 µL) and 4 µL of a 2N NaOH solution. The resulting mixture was heated at 140 °C for 5 min. Afterwards, the solution was subsequently cooled to 80 °C by nitrogen cooling before 500 µL of a TFA:CH<sub>2</sub>Cl<sub>2</sub> solution (1:1) was added. The solution was stirred for further 5 min at this temperature and then quenched with 3.5 mL of HPLC eluent. Purification of the crude product was accomplished using HPLC (Luna 5µ C<sub>18</sub>(2) 100 Å, 250 x 10.00 mm 5 micron; EtOH/0.1 H<sub>3</sub>PO<sub>4</sub> (20:80, flow rate: 6 mL/min, RT: 650 sec ([<sup>11</sup>C]Cimbi-775). The fraction corresponding to the labeled product was collected in sterile water (150 mL), and the resulting solution was passed through a solid-phase C18 Sep-Pak extraction column (Waters Corp.), which had been preconditioned with ethanol (10 mL), followed by isotonic sodium chloride solution (20 mL). The column was flushed with sterile water (3 mL). Then, the trapped radioactivity was eluted with ethanol (3 mL), followed by isotonic sodium chloride solution (3 mL) into a 20-mL vial containing phosphate buffer (9 mL, 100 mM, pH 7), giving a 15 mL solution of [<sup>11</sup>C]Cimbi-775 with a pH of approximately 7. In a total synthesis time of 45–50 min, 0.4–0.5 GBq of [<sup>11</sup>C]Cimbi-775 was produced.

#### PET scanning protocol

[<sup>11</sup>C]Cimbi-772 was given as an intravenous (i.v.) bolus injection and the injected dose was 61 and 153 MBq for baseline scans (n=2) and 153 and 194 MBq for scans where SB-269970 was pre-administered (n=2). [<sup>11</sup>C]Cimbi-775 was also given as an i.v. bolus injection and the injected dose was 286 and 129

MBq for baseline scans (n=2) and 155 MBq for the scan where SB-269970 was administered (n=1). The pigs were subsequently scanned for 90 min in list-mode with a high resolution research tomography (HRRT) scanner (Siemens AG, Munich, Germany), where scanning started at the time of injection (0 min). Immediately after the baseline scan (90 min), SB-269970 (Tocris Bioscience, Bristol, United Kingdom) was given i.v. as bolus infusion (1.0 mg/kg/h) and rescanning started after 30 min of pre-treatment with SB-269970.

#### ASSOCIATED CONTENT

Full experimental details on the synthesis of compounds, the conditions for the chiral resolution, in vitro characterization, lipophilicity measurements, animal procedures and quantification of PET data. This material is available free of charge via the Internet at <http://pubs.acs.org>.

#### AUTHOR INFORMATION

##### Corresponding Author

\* jesper.kristensen@sund.ku.dk.

#### ACKNOWLEDGMENT

This work was supported by the Intra European Fellowship (MC-IEF-275329). The Faculty of Health and Medical Sciences, University of Copenhagen, and the Lundbeck Foundation (Cimbi) is gratefully acknowledged. The authors wish to thank the staff at the PET and Cyclotron unit for expert technical assistance and Mette Værum Olesen for animal assistance. K<sub>i</sub> determinations at neuroreceptors were generously provided by the National Institute of Mental Health's Psychoactive Drug Screening Program, Contract no. HHSN-271-2008-00025-C (NIMH PDSP). The NIMH PDSP is directed by Bryan L. Roth, MD PhD, at the University of North Carolina at Chapel Hill, and Project Officer Jamie Driscoll at NIMH, Bethesda MD, USA. The John & Birthe Meyer Foundation and the Toyota foundation are acknowledged for granting the HRRT scanner and the HPLC system, respectively.

#### REFERENCES

1. Glennon, R. A. Higher-end serotonin receptors: 5-HT<sub>5</sub>, 5-HT<sub>6</sub>, and 5-HT<sub>7</sub>. *Journal of Medicinal Chemistry* 2003, 46, 2795-2812.
2. Hoyer, D.; Hannon, J. P.; Martin, G. R. Molecular, pharmacological and functional diversity of 5-HT receptors. *Pharmacology Biochemistry and Behavior* 2002, 71, 533-554.
3. Matthys, A.; Haegeman, G.; Van Craenenbroeck, K.; Vanhoenacker, P. Role of the 5-HT<sub>7</sub> Receptor in the Central Nervous System: from Current Status to Future Perspectives. *Molecular Neurobiology* 2011, 43, 228-253.
4. Cassano, G. B.; Jori, M. C.; Investigators, A. Efficacy and safety of amisulpride 50 mg versus paroxetine 20 mg in major depression: a randomized, double-blind, parallel group study. *International Clinical Psychopharmacology* 2002, 17, 27-32.

5. Lecrubier, Y.; Boyer, P.; Turjanski, S.; Rein, W. Amisulpride versus imipramine and placebo in dysthymia and major depression. *Journal of Affective Disorders* 1997, 43, 95-103.
6. Abbas, A. I.; Hedlund, P. B.; Huang, X. P.; Tran, T. B.; Meltzer, H. Y.; Roth, B. L. Amisulpride is a potent 5-HT7 antagonist: relevance for antidepressant actions in vivo. *Psychopharmacology* 2009, 205, 119-128.
7. Cates, L. N.; Roberts, A. J.; Huitron-Resendiz, S.; Hedlund, P. B. Effects of lurasidone in behavioral models of depression. Role of the 5-HT7 receptor subtype. *Neuropharmacology* 2013, 70, 211-217.
8. Zhang, M. R.; Haradahira, T.; Maeda, J.; Okauchi, T.; Kida, T.; Obayashi, S.; Suzuki, K.; Suhara, T. Synthesis and preliminary PET study of the 5-HT7 receptor antagonist [C-11]DR4446. *Journal of Labelled Compounds & Radiopharmaceuticals* 2002, 45, 857-866.
9. Andries, J.; Lemoine, L.; Mouchel-Blaisot, A.; Tang, S.; Verdurand, M.; Le Bars, D.; Zimmer, L.; Billard, T. Looking for a 5-HT7 radiotracer for positron emission tomography. *Bioorganic & Medicinal Chemistry Letters* 2010, 20, 3730-3733.
10. Herth, M. M.; Hansen, H. D.; Ettrup, A.; Dyssegaard, A.; Lehel, S.; Kristensen, J.; Knudsen, G. M. Synthesis and evaluation of [C-11]Cimbi-806 as a potential PET ligand for 5-HT7 receptor imaging. *Bioorganic & Medicinal Chemistry* 2012, 20, 4574-4581.
11. Herth, M. M.; Volk, B.; Pallagi, K.; Bech, L. K.; Antoni, F. A.; Knudsen, G. M.; Kristensen, J. L. Synthesis and In Vitro Evaluation of Oxindole Derivatives as Potential Radioligands for 5-HT7 Receptor Imaging with PET. *ACS Chemical Neuroscience* 2012, 3, 1002-1007.
12. Zimmer, L.; Billard, T. Molecular imaging of the serotonin 5-HT7 receptors: from autoradiography to positron emission tomography. *Reviews in the Neurosciences* 2014, 25, 357-365.
13. Lacivita, E.; Niso, M.; Hansen, H. D.; Di Pilato, P.; Herth, M. M.; Lehel, S.; Ettrup, A.; Montenegro, L.; Perrone, R.; Berardi, F.; Colabufo, N. A.; Leopoldo, M.; Knudsen, G. M. Design, synthesis, radiolabeling and in vivo evaluation of potential positron emission tomography (PET) radioligands for brain imaging of the 5-HT7 receptor. *Bioorganic & Medicinal Chemistry* 2014, 22, 1736-1750.
14. Hansen, H. D.; Herth, M. M.; Ettrup, A.; Andersen, V. L.; Lehel, S.; Dyssegaard, A.; Kristensen, J. L.; Knudsen, G. M. Radiosynthesis and In Vivo Evaluation of Novel Radioligands for PET Imaging of Cerebral 5-HT7 Receptors. *Journal of Nuclear Medicine* 2014, 55, 640-646.
15. Andersen, V. L.; Herth, M. M.; Lehel, S.; Knudsen, G. M.; Kristensen, J. L. Palladium-mediated conversion of para-aminoarylboronic esters into para-aminoaryl-C-11-methanes. *Tetrahedron Letters* 2013, 54, 213-216.
16. Volk, B.; Barkoczy, J.; Hegedus, E.; Udvari, S.; Gacsalyi, I.; Mezei, T.; Pallagi, K.; Kompagne, H.; Levay, G.; Egyed, A.; Harsing, L. G.; Spedding, M.; Simig, G. (Phenylpiperazinyl-butyl)oxindoles as selective 5-HT(7) receptor antagonists. *Journal of Medicinal Chemistry* 2008, 51, 2522-2532.
17. Volk, B.; Gacsalyi, I.; Pallagi, K.; Poszavacz, L.; Gyonos, I.; Szabo, E.; Bako, T.; Spedding, M.; Simig, G.; Szenasi, G. Optimization of (Arylpiperazinylbutyl)oxindoles Exhibiting Selective 5-HT7 Receptor Antagonist Activity. *Journal of Medicinal Chemistry* 2011, 54, 6657-6669.
18. Paterson, L. M.; Kornum, B. R.; Nutt, D. J.; Pike, V. W.; Knudsen, G. M. 5-HT radioligands for human brain imaging with PET and SPECT. *Medicinal Research Reviews* 2013, 33, 54-111.
19. Mahe, C.; Loetscher, E.; Feuerbach, D.; Muller, W.; Seiler, M. P.; Schoeffter, P. Differential inverse agonist efficacies of SB-258719, SB-258741 and SB-269970 at human recombinant serotonin 5-HT7 receptors. *European Journal of Pharmacology* 2004, 495, 97-102.
20. Romero, G.; Pujol, M.; Pauwels, P. J. Reanalysis of constitutively active rat and human 5-HT7(a) receptors in HEK-293F cells demonstrates lack of silent properties for reported neutral antagonists. *Naunyn-Schmiedeberg's Archives of Pharmacology* 2006, 374, 31-39.
21. Suter, T. M.; Chesterfield, A. K.; Bao, C.; Schaus, J. M.; Krushinski, J. H.; Statnick, M. A.; Felder, C. C. Pharmacological characterization of the cannabinoid CB1 receptor PET ligand ortholog, [H-3]MePPEP. *European Journal of Pharmacology* 2010, 649, 44-50.
22. Terry, G.; Liow, J. S.; Chernet, E.; Zoghbi, S. S.; Phebus, L.; Felder, C. C.; Tauscher, J.; Schaus, J. M.; Pike, V. W.; Halldin, C.; Innis, R. B. Positron emission tomography imaging using an inverse agonist radioligand to assess cannabinoid CB(1) receptors in rodents. *Neuroimage* 2008, 41, 690-698.

# Evaluation of 3-Ethyl-3-(phenylpiperazinylbutyl)oxindoles as PET ligands for the 5-HT<sub>7</sub> Receptor – Synthesis, pharmacology, radiolabeling and in vivo Brain Imaging

Matthias M. Herth,<sup>§,†</sup> Valdemar L. Andersen,<sup>§,†</sup> Hanne D. Hansen,<sup>§</sup> Nikolas Stroth,<sup>‡</sup> Balázs Volk,<sup>‡</sup> Anders Ettrup,<sup>§</sup> Szabolcs Lehel,<sup>#</sup> Per Svenningsson,<sup>‡</sup> Gitte M. Knudsen,<sup>§</sup> Jesper L. Kristensen.<sup>§,†</sup>

<sup>§</sup>Center for Integrated Molecular Brain Imaging, Rigshospitalet and the University of Copenhagen, Blegdamsvej 9, DK-2100 Copenhagen, Denmark.

<sup>†</sup>Department of Drug Design and Pharmacology, Faculty of Health and Medical Sciences, University of Copenhagen, Universitetsparken 2, DK-2100 Copenhagen, Denmark.

<sup>#</sup>PET and Cyclotron Unit, Rigshospitalet, Blegdamsvej 9, DK-2100 Copenhagen, Denmark.

<sup>‡</sup>Egis Pharmaceuticals Plc., P.O. Box 100, H-1475 Budapest, Hungary.

<sup>‡</sup> Center for Molecular Medicine, Department of Neurology and Clinical Neuroscience, Karolinska Institute and Karolinska University Hospital, 17176 Stockholm, Sweden

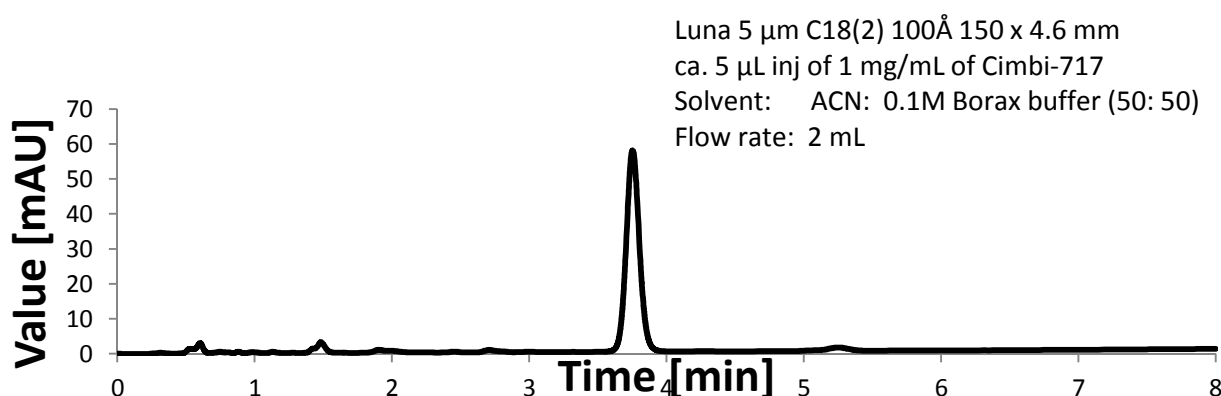
## Table of contents

1. Chiral resolution of 3-unsubstituted phenylpiperazinyl-butylloxindoles
2. General
3. Structure Activity Studies of 3-Alkyl-3-(phenylpiperazinylbutyl)oxindoles
4. Organic syntheses
5. Chiral resolution and stability test of Cimbi-772 and Cimbi-775
6. PDSP Screening
7. Receptor distribution of colocalized targets
8. Selectivity/B<sub>max</sub> ratio for 5-HT<sub>7</sub>
9. In vitro characterization
10. Determination of lipophilicities
11. Preparative radio-HPLC chromatogram of [<sup>11</sup>C]Cimbi-775
12. Preparative radio-HPLC chromatogram of [<sup>11</sup>C]Cimbi-772
13. Analytical HPLC chromatogram of [<sup>11</sup>C]Cimbi-772 and [<sup>11</sup>C]Cimbi-775
14. Determination of radiochemical purity and specific radioactivity
15. Animal procedures
16. Quantification of PET data
17. References
18. Selected analytical data

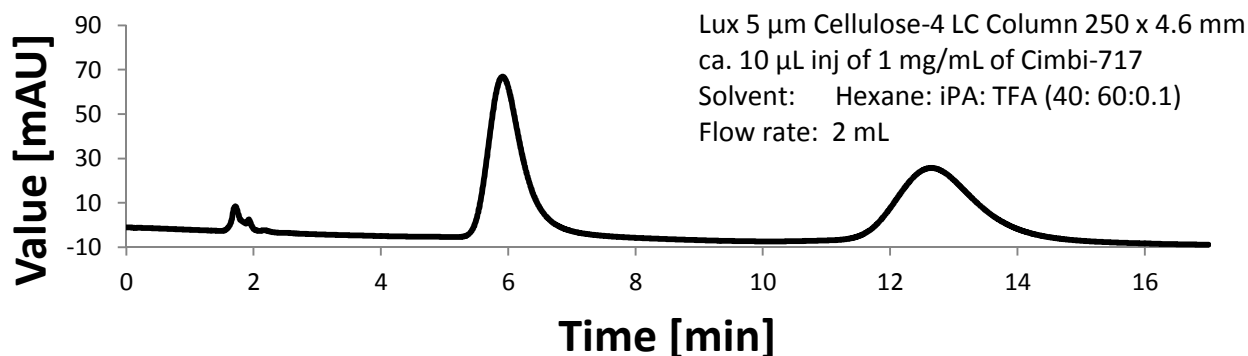
## 1. Chiral resolution of 3-unsubstitued phenylpiperazinyl-butyloxindoles

Cimbi-717 and Cimbi-712 were separated using chiral HPLC. A) shows the purity of Cimbi-717, whereas B) the chiral resolution. C) displays the chiral resolution of Cimbi-712. Unfortunately, reinjection of both separated fractions showed epimerisation after 5 minutes. Complete conversion was observed within 30 minutes.

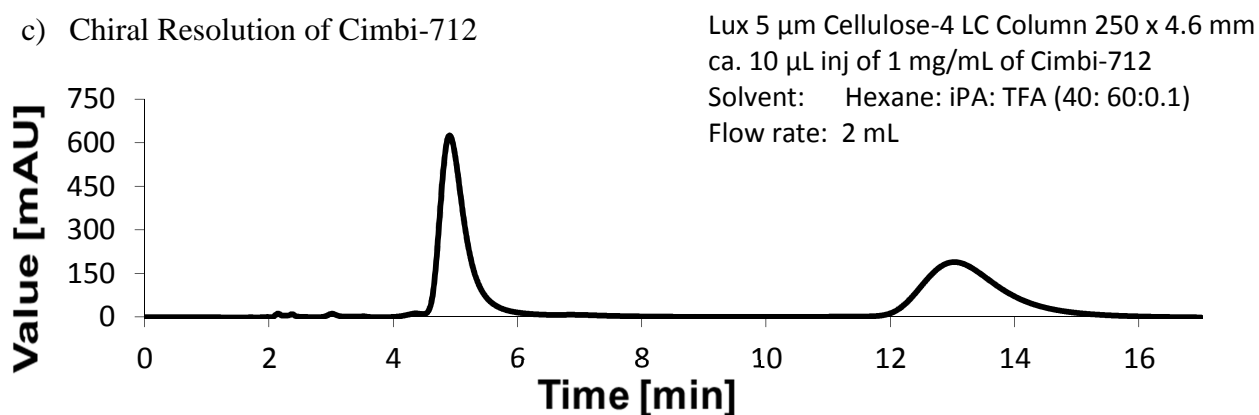
a) RP-HPLC of Cimbi-717



b) Chiral Resolution of Cimbi-717



c) Chiral Resolution of Cimbi-712

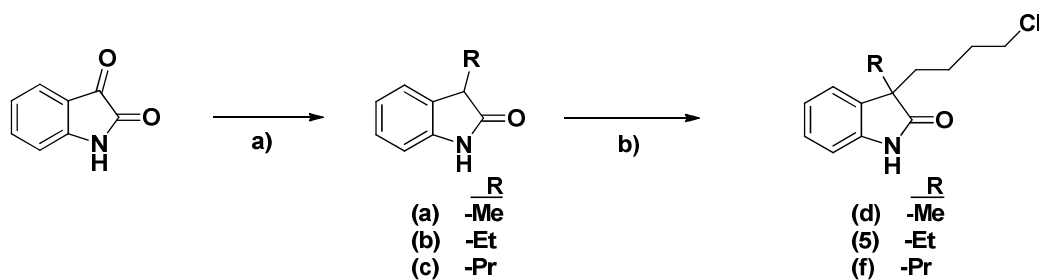


## 2. General

Chemicals were purchased from Acros, Fluka, Sigma, Tocris, ABX or Merck. Unless otherwise stated, all chemicals were used without further purification. Flash chromatography was performed on silica gel 60 (35-70  $\mu\text{m}$ ). Thin layer chromatography (TLC) was performed using plates from Merck (silica gel 60 F254 and aluminium oxide 60 F254).  $^1\text{H}$ -NMR and  $^{13}\text{C}$ -NMR spectra were recorded using a Bruker AC 300 spectrometer or a Bruker AC 400 spectrometer. Chemical shifts are quoted as  $\delta$  values (ppm) downfield from tetramethylsilane (TMS) internal standard. Infrared spectroscopy was performed on a Perkin Elmer FT-IR Spektrometer (Spectrum One). Melting points were determined on a Stanford Research Systems Optimelt system. For Solid Phase Extraction (SPE), Sep-Pak®-C18-cartridges (Waters, USA) were used. GC-MS measurements were performed on a Shimadzu apparatus (GCMS-QP 5050). LC-MS tests were performed on 6410 Triple Quad LC/MS instrument. Field desorption mass spectra (FD-MS) were recorded using a Finnigan MAT90 spectrometer and electrospray ionization mass spectrometry (ESI-MS) were performed on a ThermoQuest Navigator-Instrument. High resolution mass spectra (HRMS) were recorded on a Q-TOF Premier (Waters, USA) and Maxis Impact (BrukerDaltonics, Germany) spectrometer. Analytical and preparative high performance liquid chromatography (HPLC) were performed on a Dionex system consisting of a pump P680A pump, a UVD 170U detector and a Scansys radiodetector. Lipophilicities were determined using a Dionex Ultimate 3000 HPLC equipped with a degasser, an autosampler, a column-oven and a UV-detector. Chiral Resolution was performed on a Lux 5  $\mu\text{m}$  Cellulose-4 LC Column 250 x 4.6 mm. PET scanning was performed with a high-resolution research tomography scanner (HRRT, Siemens AG). [ $^{11}\text{C}$ ]Methane was produced via the  $^{14}\text{N}(\text{p},\alpha)^{11}\text{C}$  reaction by bombardment of an [ $^{14}\text{N}$ ]N $_2$  containing 10% H $_2$  target with a 17 MeV proton beam in a Scanditronix MC32NI cyclotron. Full spectral data of previously published compounds can be found in the indicated references.

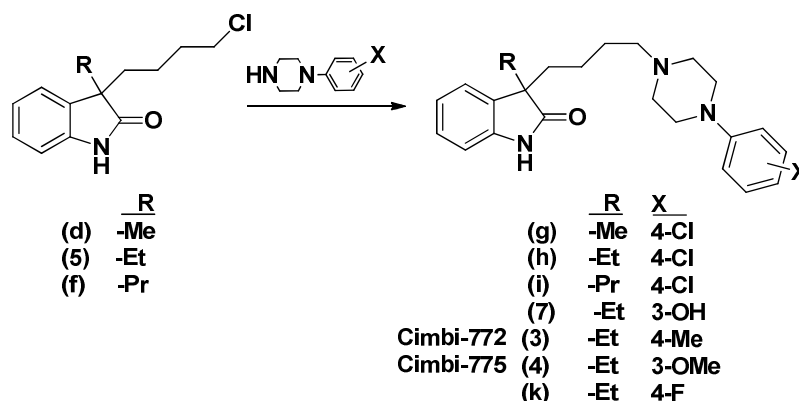
## 3. Structure Activity Studies of 3-Alkyl-3-(phenylpiperazinybutyl)oxindoles

A convenient organic synthesis route to 3-alkyl-3-( $\omega$ -chloroalkyl)-oxindoles has been described by Volk et al. [1]. Briefly, isatins were reductively alkylated with alcohols in the presence of Raney nickel under hydrogen pressure. The resulting 3-alkyloxindoles were further C-3 alkylated using 2 equivalents n-BuLi and 1,4-bromochlorobutane (Scheme 1). The resulted intermediates were finally linked to 1-(4-chlorophenyl)piperazine by applying neat reaction conditions (Scheme 2).



Scheme S1: General procedure for the preparation of 3-alkyl-3-( $\omega$ -chloroalkyl)-oxindoles: a) ROH, Ra-Ni, 15 bar H<sub>2</sub>, 180 °C, 3-4 h, 85 – 95% b) n-BuLi, Br-(CH<sub>2</sub>)<sub>4</sub>-Cl, THF, from -78 °C to RT, 4h, > 80%

In general, fewer products were observed using these chloro-intermediates compared to previously applied mesylates, even at higher reaction temperature [2]. Furthermore, in contrast to the mesylated derivative, the halogenated compound did not decompose at room temperature.

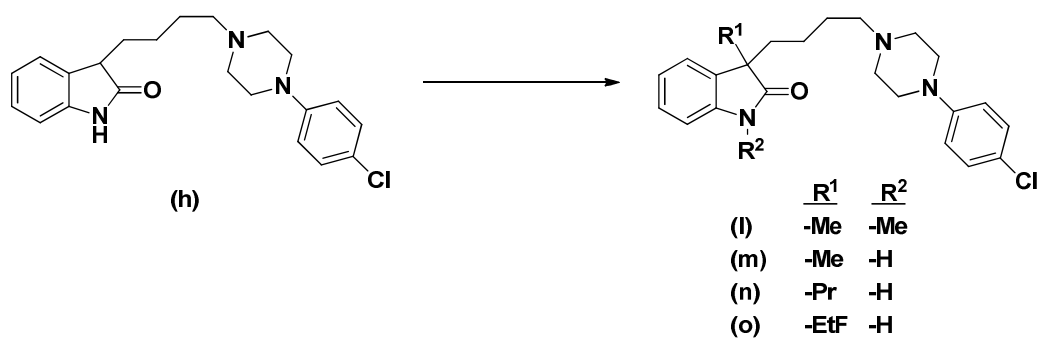


Scheme S2: Synthesis of 3-alkyl-oxindol derivatives: Na<sub>2</sub>CO<sub>3</sub>, 180 °C, 1h, 73-85%

The second approach aiming at a C-3 alkylation at a later stage, only resulted in limited success (Scheme 3). Methyl iodide lead to bis-methylation (In addition to the C-3-position also the N-1-position was alkylated), whereas the alkylation with propyl iodide completely failed. Alkylation with 1,2-bromofluoroethane resulted in the desired product, however only in 24%. Therefore, alkylation earlier in the synthesis sequence is preferable.

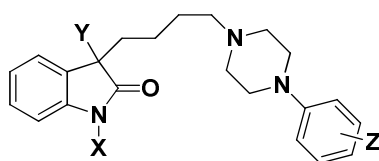
In a next evaluation step, we determined the affinity towards the 5-HT<sub>7</sub> receptor binding site. Alkylation at the C-3 position of the oxindole did not alter the affinity towards the 5-HT<sub>7</sub> receptor in any significant. Low nanomolar K<sub>i</sub>-values below 10 nM were detected for all reference compounds and consequent labeling should thus enable 5-HT<sub>7</sub> PET imaging (Table S1). Only one exception could be detected. Bisalkylation leading to compound 15 reduced the affinity by a factor of 5-8. This is in line with previously reported data [1].





Scheme S3: C-3 Alkylation of oxindole derivatives by alkylhalides: n-BuLi, RX, THF, from -78 °C to RT, 12h, 0-55%

Table S1: Human recombinant 5-HT<sub>7</sub> affinity: The influence of the C-3 position of the oxindole



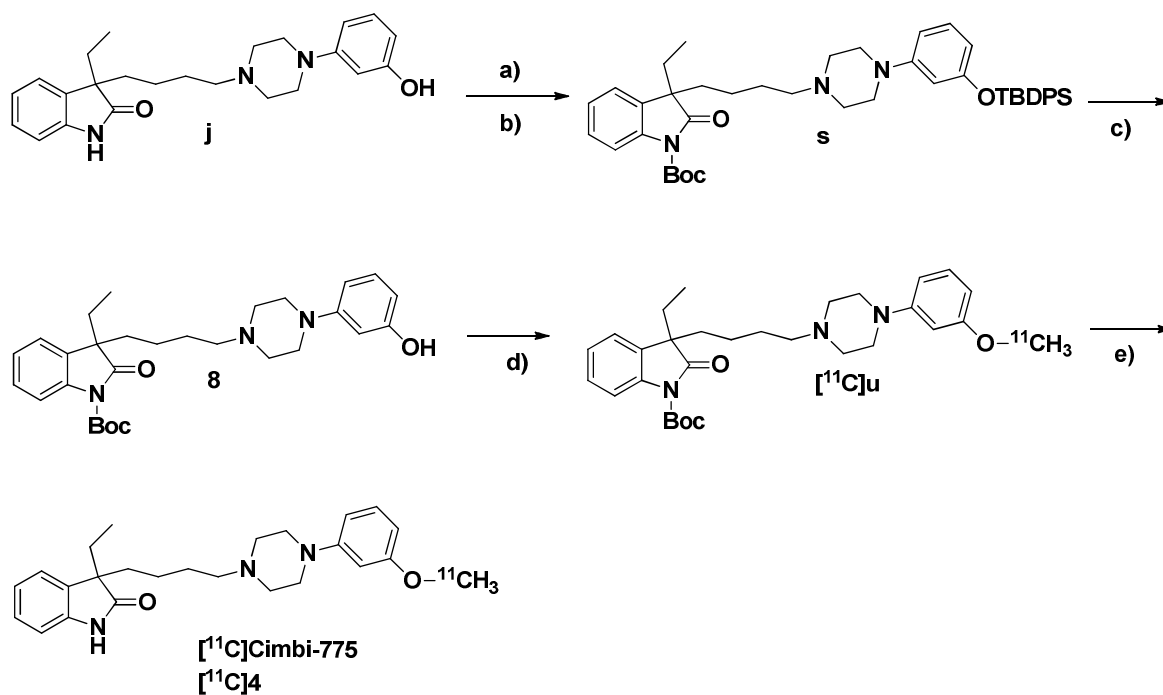
compound	Z	X	Y	5-HT <sub>7</sub> <sup>a</sup> K <sub>i</sub> (nM)	LogD <sub>7.4</sub>
p	4-Cl	-H	-H	7.0	4.56
g/m	4-Cl	-H	-Me	1.2	4.98
n	4-Cl	-H	-Et	0.7	5.76
o	4-Cl	-H	-EtF	1.4	5.72
i/n	4-Cl	-H	-Pr	3.5	5.92
l	4-Cl	-Me	-Me	16	> 7
<b>Cimbi-717 (2)</b>	3-OMe	-H	-H	2.6; 7.5 <sup>b</sup>	4.73
<b>Cimbi-775 (4)</b>	3-OMe	-H	-Et	2.0; 7.8 <sup>b</sup>	5.75
(+)-4	3-OMe	-H	-Et	11 <sup>b</sup>	5.75
(-)-4	3-OMe	-H	-Et	56 <sup>b</sup>	5.75
q	4-F	-H	-H	1.1	4.65
k	4-F	-H	-Et	0.5	5.72
r	3-OH	-H	-H	27.5	3.40
7, j	3-OH	-H	-Et	8.9	4.40
<b>Cimbi-712 (1)</b>	4-Me	H	-H	1.1; 4.1 <sup>b</sup>	5.19
<b>Cimbi-772 (3)</b>	4-Me	H	-Et	2.5; 6.5 <sup>b</sup>	6.17
(+)-3	4-Me	H	-Et	5.6 <sup>b</sup>	6.17
(-)-3	4-Me	H	-Et	82 <sup>b</sup>	6.17

Affinities were determined by PDSP

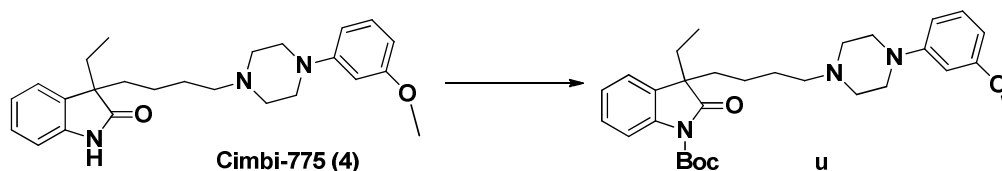
#### 4. Organic Syntheses

Compounds a, b, c, 5, h, k, p, q, r, 9, Cimbi-712 (1), Cimbi-717 (2), Cimbi-775 (4) were synthesized as previously published [1-4].

#### General Synthesis Strategies:



Scheme S4: Synthesis of the precursor and  $[^{11}\text{C}]$ Cimbi-775: a) TBDPSCl, NaH, DMF, 110 °C, 12h b) Boc<sub>2</sub>O, NaHDMs, THF, -5 °C, 30 min c) NH<sub>4</sub>F, MeOH, 70 °C, 30 min d)  $[^{11}\text{C}]\text{CH}_3\text{I}$ , 2M NaOH, DMF, 140 °C, 5 min e) TFA/CH<sub>2</sub>Cl<sub>2</sub> (1:1), 80 °C, 5 min



Scheme S5: Synthesis of **u**: Boc<sub>2</sub>O, NaHDMs, THF, -5 °C, 30 min

### General Procedure for the Preparation of 3-Alkyl-3-( $\omega$ -chloroalkyl)-oxindoles.

To a mixture of n-BuLi in hexane (2.5 M, 20 mL, 0.05 mol) and THF (20 mL), the solution of the appropriate 3-alkyloxindole (0.02 mol) in THF (25 mL) was added dropwise at  $-78\text{ }^{\circ}\text{C}$ , under argon atmosphere. Then the 1-bromo-4-chlorobutane (3.38 g, 0.02 mol) was added dropwise, and the reaction mixture was allowed to warm to room temperature. The stirring was continued for 3 additional hours, the mixture was quenched with ethanol (20 mL), and the solvents were evaporated. The residue was dissolved in ethyl acetate and extracted with water. The organic layer was dried over  $\text{Na}_2\text{SO}_4$  and evaporated. The oily residue crystallized upon trituration with hexane (20 mL). The white solid was filtered, washed with hexane, and dried. The products were used without further purification.

### 3-methyl-3-( $\omega$ -chlorobutyl)oxindole (d)

n-BuLi in hexane (2.5 M, 20 mL, 0.05 mol), 3-methyloxindole (2.95 g, 0.02 mol) and 1-bromo-4-chlorobutane (3.38 g, 0.02 mol), yielded in (d) (3.88 g, 16.4 mmol, 82%) as a white solid. Mp 94-95  $^{\circ}\text{C}$ ;  $^1\text{H-NMR}$  ( $\text{CDCl}_3$ , 300 MHz):  $\delta$  8.74 (1H, bs), 7.24-7.13 (2H, m), 7.06-7.01 (1H, m), 6.92 (1H, d,  $J = 7.5$  Hz), 3.40 (2H, t,  $J = 6$  Hz), 1.98-1.88 (1H, m), 1.82-1.61 (3H, m), 1.39 (3H, s), 1.30 - 1.17 (1H, m), 1.14-0.99 (1H, m);  $^{13}\text{C-NMR}$  ( $\text{CDCl}_3$ , 75 MHz):  $\delta$  183.3, 140.5, 134.37, 127.9, 122.9, 122.7, 110.0, 49.0, 44.67, 37.7, 32.7, 24.0, 22.1; LCMS (ESI) RT: 3.68 min,  $m/z$ : 238.1  $[\text{M}+\text{H}]^+$  at 210 and 254 nm;  $R_f$ : 0.46 (EtOAc/Heptane 1:1)

### 3-propyl-3-( $\omega$ -chlorobutyl)oxindole (f)

n-BuLi in hexane (2.5 M, 20 mL, 0.05 mol), 3-Propyloxindole (3.5 g, 0.02 mol) and 1-bromo-4-chlorobutane (3.38 g, 0.02 mol) yielded in (f) (3.92 g, 14.8 mmol, 74 %) as a white solid. Mp 97-98  $^{\circ}\text{C}$ ;  $^1\text{H-NMR}$  ( $\text{CDCl}_3$ , 300 MHz):  $\delta$  8.69 (1H, bs), 7.25-7.16 (1H, m), 7.12-7.10 (1H, m), 7.06-7.01 (1H, m), 6.91 (1H, d,  $J = 7.5$  Hz), 3.38 (2H, t,  $J = 6$  Hz), 1.95-1.57 (6H, m), 1.28-1.00 (3H, m), 0.94-0.83 (1H, m), 0.78 (3H, t,  $J = 9$  Hz);  $^{13}\text{C-NMR}$  ( $\text{CDCl}_3$ , 75 MHz):  $\delta$  182.8, 141.2, 132.8, 127.8, 123.1, 122.6, 109.8, 53.7, 44.6, 40.4, 37.3, 32.8, 21.8, 17.6, 14.3; LCMS (ESI) RT: 4.17 min,  $m/z$ : 266.1  $[\text{M}+\text{H}]^+$  at 210 and 254 nm;  $R_f$ : 0.62 (EtOAc/Heptane 1:1)

### General Procedure to couple 3-(4-chlorobutyl)-3-alkylindolin-2-one with 4-piperazines

The secondary amine (12 mmol) was heated to 180  $^{\circ}\text{C}$  under slow stirring. Then 3-(4-chlorobutyl)-3-alkylindolin-2-one (12 mmol) and sodium carbonate (1.36 g, 12 mmol) were added. After 1 h

reaction time, the brown melt was cooled to ambient temperature. Ethyl acetate and water were added and the layers were separated. The organic layer was dried over MgSO<sub>4</sub> and evaporated. The residual oil or solid was purified by column chromatography with the indicated eluent.

**3-{4-[4-(4-Chlorophenyl)piperazine-1-yl]-butyl}-3-methyl-1,3-dihydro-2H-indol-2-one (g)**

1-(4-chlorophenyl)-piperazine (0.486 g, 2.48 mmol), sodium carbonate (0.26 g, 2.48 mmol) and 3-methyl-3-( $\omega$ -chlorobutyl)oxindole (0.26 g, 2.48 mmol) yielded in (g) (0.71 g, 1.8 mmol, 73 %) as a white solid. (g) was purified using EtOAc. Mp 182–183 °C; <sup>1</sup>H-NMR (CDCl<sub>3</sub>, 300 MHz):  $\delta$  8.41 (1H, bs), 7.21–7.12 (4H, m), 7.05–7.00 (1H, m), 6.89 (1H, d, J = 7.5 Hz), 6.78 (2H, d, J = 9 Hz), 3.09 (4H, t, J = 6 Hz), 2.49 (4H, t, J = 6 Hz), 2.24 (2H, t, J = 9 Hz), 1.99–1.89 (1H, m), 1.82–1.72 (1H, m), 1.51–1.36 (2H, m), 1.38 (3H, s), 1.20–1.05 (1H, m), 0.99–0.84 (1H, m); <sup>13</sup>C-NMR (CDCl<sub>3</sub>, 75 MHz):  $\delta$  183.28, 150.03, 140.56, 134.63, 129.06, 127.82, 124.58, 123.03, 122.62, 117.31, 109.86, 58.34, 53.15, 49.20, 49.09, 38.44, 27.01, 24.13, 22.67; LCMS (ESI) RT: 2.41 min, m/z: 398.1 [M+H]<sup>+</sup> at 210 and 254 nm; R<sub>f</sub>: 0.2 (EtOAc); HRMS (ESI) [MH<sup>+</sup>] cald. for C<sub>23</sub>H<sub>29</sub>ClN<sub>3</sub>O 398.1999, found 398.2000

**3-{4-[4-(4-Chlorophenyl)piperazine-1-yl]-butyl}-3-propyl-1,3-dihydro-2H-indol-2-one (i)**

1-(4-chlorophenyl)-piperazine (0.37 g, 1.89 mmol), sodium carbonate (0.2 g, 1.9 mmol) and 3-propyl-3-( $\omega$ -chlorobutyl)oxindole (0.5 g, 1.89 mmol) yielded in (i) (0.68 g, 1.60 mmol, 85 %) as a white solid. (i) was purified using EtOAc/Heptane 3:1. Mp 129–130 °C; <sup>1</sup>H-NMR (CDCl<sub>3</sub>, 300 MHz):  $\delta$  8.41 (1H, bs), 7.20–7.09 (4H, m), 7.05–7.00 (1H, m), 6.87 (1H, d, J = 7.5 Hz), 6.78 (2H, d, J = 9 Hz), 3.09 (4H, t, J = 6 Hz), 2.49 (4H, t, J = 6 Hz), 2.23 (2H, t, J = 9 Hz), 1.97–1.67 (4H, m), 1.47–1.32 (2H, m), 1.16–1.05 (2H, m), 0.96–0.85 (2H, m), 0.78 (3H, t, J = 6 Hz); <sup>13</sup>C-NMR (CDCl<sub>3</sub>, 75 MHz):  $\delta$  183.0, 149.99, 141.41, 133.11, 129.05, 127.73, 124.59, 123.15, 122.51, 117.32, 109.78, 58.31, 53.93, 53.10, 49.15, 40.56, 38.04, 27.01, 22.31, 17.69, 14.43; LCMS (ESI) RT: 2.29 min, m/z: 426.1 [M+H]<sup>+</sup> at 210 and 254 nm; R<sub>f</sub>: 0.3 (EtOAc/Heptane 3:1); HRMS (ESI) [MH<sup>+</sup>] cald. for C<sub>25</sub>H<sub>33</sub>ClN<sub>3</sub>O 426.2313, found 426.2320

**3-{4-[4-(3-Hydroxyphenyl)piperazine-1-yl]-butyl}-3-ethyl-1,3-dihydro-2H-indol-2-one (7) (j)**

1-(3-Hydroxyphenyl)-piperazine (0.33 g, 1.88 mmol), sodium carbonate (0.2 g, 1.88 mmol) and 3-ethyl-3-( $\omega$ -chlorobutyl)oxindole (0.5 g, 1.88 mmol) yielded in (j) (0.49 g, 1.26 mmol, 67 %) as a white solid. (j) was purified using EtOAc. Mp 224–225 °C; <sup>1</sup>H-NMR (DMSO-d<sub>6</sub>, 400

MHz):  $\delta$  10.99 (1H, bs), 10.41 (1H, s), 7.23–7.16 (2H, m), 7.04–6.98 (2H, m), 6.86 (1H, d,  $J = 8$  Hz), 6.43–6.30 (3H, m), 6.67 (2H, d,  $J = 12$  Hz), 3.43 (2H, d,  $J = 8$  Hz), 3.10 (2H, t,  $J = 8$  Hz), 3.04–2.93 (4H, m), 1.82–1.66 (4H, m), 1.67–1.58 (2H, m), 1.04–0.91 (1H, m), 0.89–0.73 (1H, m), 0.51 (3H, t,  $J = 8$  Hz);  $^{13}\text{C}$ -NMR (DMSO- $d_6$ , 75 MHz):  $\delta$  180.57, 158.25, 150.74, 142.47, 131.93, 129.72, 127.58, 123.00, 121.49, 109.16, 107.49, 107.01, 103.16, 54.86, 52.97, 50.32, 45.38, 36.39, 30.13, 23.06, 21.24, 8.37; LCMS (ESI) RT: 4.98 min,  $m/z$ : 394.2  $[\text{M}+\text{H}]^+$  at 210 and 254 nm;  $R_f$ : 0.1 (EtOAc); HRMS (ESI)  $[\text{MH}]$  cald. for  $\text{C}_{24}\text{H}_{31}\text{N}_3\text{O}_2$  393.2654, found 393.2652

**3-{4-[4-(4-Methylphenyl)piperazine-1-yl]-butyl}-3-ethyl-1,3-dihydro-2H-indol-2-one (3)**  
**(Cimbi-772)**

1-(4-Methylphenyl)-piperazine (210 mg, 1.192 mmol), sodium carbonate (126 mg, 1.192 mmol) and 3-ethyl-3-( $\omega$ -chlorobutyl)oxindole (300 mg, 1.192 mmol) yielded in (3) (312 mg, 0.797 mmol, 66.9%) as a white solid. (3) was purified using EtOAc. Mp 127.8–128.3 °C;  $^1\text{H}$ -NMR ( $\text{CDCl}_3$ , 400 MHz):  $\delta$  9.28 (1H, s), 7.19 (1H, m), 7.12 (1H, m), 7.05 (3H, m), 6.91 (1H, d,  $J = 7.8$  Hz), 6.82 (2H, m), 3.10 (4H, m), 2.52 (4H, m), 2.26 (5H, m), 1.94 (2H, m), 1.80 (2H, m), 1.43 (2H, m), 1.13 (1H, m), 0.93 (1H, m), 0.64 (3H, t,  $J = 7.4$  Hz);  $^{13}\text{C}$ -NMR ( $\text{CDCl}_3$ , 75 MHz):  $\delta$  182.8, 149.1, 141.5, 132.5, 129.5, 129.0, 127.5, 122.9, 122.2, 116.2, 109.5, 58.2, 54.2, 53.1, 49.5, 37.5, 30.9, 26.8, 22.2, 20.3, 8.0; LCMS (ESI) RT: 5.36 min,  $m/z$  392.1  $[\text{M}+\text{H}]^+$  at 210 and 254 nm;  $R_f$ : 0.12 (EtOAc); HRMS (ESI)  $[\text{MH}^+]$  cald. for  $\text{C}_{25}\text{H}_{34}\text{N}_3\text{O}$  392.269, found 392.2710

**3-{4-[4-(4-Chlorophenyl)piperazine-1-yl]-butyl}-1,3-dimethyl-1,3-dihydro-2H-indol-2-one (1)**

To a mixture of  $n\text{-BuLi}$  in hexane (2.5 M, 0.732 mL, 1.83 mmol) and dry THF (10 mL), a solution of the appropriate 3-alkyloxindole (352 mg, 0.92 mmol) in dry THF (10 mL) was added dropwise at  $-78$  °C, under argon atmosphere. Then MeI (0.014 g, 0.1 mmol) was added dropwise, and the reaction mixture was allowed to warm to room temperature. The stirring was continued for 12 additional hours, the mixture was quenched with ethanol (20 mL), and the solvents were evaporated. The residue was dissolved in ethyl acetate and extracted with water. The organic layer was dried over  $\text{Na}_2\text{SO}_4$  and evaporated. The oily residue was columned with EtOAc/ $\text{Et}_3\text{N}$  (300:3) to yield 125 mg (0.3, 53%) as a white solid.  $^1\text{H}$ -NMR ( $\text{CDCl}_3$ , 300 MHz):  $\delta$  7.25 (1H, t,  $J = 6$  Hz), 7.18–7.15 (3H, m), 7.05 (1H, t,  $J = 6$  Hz), 6.81 (3H, t,  $J = 9$  Hz), 3.20 (3H, s), 3.10 (4H, t,  $J = 6$  Hz), 2.49 (4H, t,  $J = 6$  Hz), 2.24 (2H, t,  $J = 9$  Hz), 1.98–1.88 (1H, m), 1.80–1.70 (1H, m), 1.46–1.33 (2H, m), 1.35 (3H, s), 1.04–0.83 (2H, m);  $R_f = 0.28$  (EtOAc/ $\text{Et}_3\text{N}$  250:3)

**3-{4-[4-(4-Chlorophenyl)-piperazine-1-yl]-butyl}-3--(2-fluoroethyl)-1,3-dihydro-2H-indol-2-one (o)**

To a mixture of n-BuLi in hexane (2.5 M, 0.52 mL, 1.3 mmol) and dry THF (5 mL), the solution of the appropriate 3-alkyloxindole (200 mg, 0.52 mmol) in dry THF (10 mL) was added dropwise at –78 °C, under argon atmosphere. Then 1,2-bromofluoroethane (0.164 g, 1.3 mol) was added dropwise, and the reaction mixture was allowed to warm to room temperature. The stirring was continued for 12 additional hours, the mixture was quenched with ethanol (20 mL), and the solvents were evaporated. The residue was dissolved in ethyl acetate and extracted with water. The organic layer was dried over Na<sub>2</sub>SO<sub>4</sub> and evaporated. The oily residue was columned with EtOAc/Et<sub>3</sub>N (300:3) to yield 50 mg (0.12 mmol, 24%) as a white solid. Mp 123–124 °C; <sup>1</sup>H-NMR (CDCl<sub>3</sub>, 300 MHz): δ 9.14 (1H, s), 7.24-7.11 (4H, m), 7.03 (1H, m), 6.89 (1H, d, J = 6 Hz), 6.76 (2H, d, J = 9 Hz), 4.31 (1H, m), 4.16 (1H, m), 3.08 (4H, t, J = 6 Hz), 2.48 (4H, t, J = 6 Hz), 2.44 – 2.33 (1H, m), 2.23 (2H, t, J = 6 Hz), 2.17-2.00 (1H, m), 1.97-1.91 (1H, m), 1.86-1.76 (1H, m), 1.52-1.30 (2H, m), 1.19-1.05 (1H, m), 0.97-0.86 (1H, m); <sup>13</sup>C-NMR (CDCl<sub>3</sub>, 75 MHz): δ 182.20, 149.98, 141.39, 131.49, 129.04, 128.30, 124.58, 123.38, 122.65, 117.31, 110.18, 80.77 (d, J = 140 Hz), 58.22, 53.09, 51.25, 49.14, 38.16, 37.89, 26.88, 21.94; LCMS (ESI) RT: 2.66 min, m/z: 430.29 [M+H]<sup>+</sup> at 210 and 254 nm; R<sub>f</sub> = 0.25 (EtOAc/Et<sub>3</sub>N 250:3); HRMS (ESI) [MH<sup>+</sup>] calcd. for C<sub>24</sub>H<sub>30</sub>ClFN<sub>3</sub>O 430.2055, found 430.2069

**tert-butyl 3-ethyl-3-{4-[4-(3-hydroxyphenyl)piperazin-1-yl]butyl}-2-oxoindoline-1-carboxylate (8)**

To a solution of (7) (0.520, 1.323 mmol) in dry DMF (10 mL) was added, NaH (36 mg 1.523 mmol) and TBDPSCl (0.971 g, 1.323 mmol). The resulting mixture was stirred over night at 110 °C and then poured into water, and extracted with ethyl acetate. The combined organic layers were washed 3 x with water, then with brine, dried over MgSO<sub>4</sub>, and concentrated in vacuo to afford (Sa). The crude mixture was used without further purification. LC-MS (ESI) m/z: 632.5; RT: 6.75 min; R<sub>f</sub>: 0.7 (EtOAc/MeOH 10:0.3)

Afterwards, (Sa) (1.323 mmol) was dissolved in dry THF, cooled to -5 °C, added 1M NaHMDS (1.323 mL, 1.323 mmol) and stirred for ½ h. Boc<sub>2</sub>O (275 mg, 1.323 mmol) was added and stirred for 1 h. Excess NaHMDS was quenched with 6 mL AcOH:THF 1:4 and then 40 mL water. Extraction was made with 3x10 mL EtOAc. The combined organic phases were washed with 2x10

mL brine, dried, concentrated *in vacuo* to yield in crude 8, which was used without further purification. LC-MS (ESI) m/z: 732.6; RT: 7.12 min; R<sub>f</sub>: 0.7 (EtOAc/MeOH 10:0.3)

Finally, 20 (1.323 mmol) and NH<sub>4</sub>F (0.23 g, 3.3 mmol) was dissolved in dry 10 mL MeOH and heated at 70 °C for 30 min. Afterwards, the solvent was removed, the residue dissolved in NH<sub>4</sub>OH and extracted 3 times with CHCl<sub>3</sub>. The combined organic layers were dried (Na<sub>2</sub>SO<sub>4</sub>) and evaporated. The crude oil was columned with EtOAc/heptane (1:1) to yield 21 (0.83 g, 1.68 mmol, 51%) as a white solid. Mp 68–69 °C; <sup>1</sup>H-NMR (CDCl<sub>3</sub>, 300 MHz): δ 7.81 (1H, d, J = 5 Hz), 7.34–7.27 (1H, m), 7.18 – 7.04 (3H, m), 6.45 – 6.42 (1H, m), 6.34 – 6.31 (2H, m), 3.18 (4H, t, J = 6 Hz), 2.65 (4H, t, J = 6 Hz), 2.37 (2H, t, J = 6 Hz), 1.97–1.89 (2H, m), 1.82–1.71 (2H, m), 1.66 (9H, s), 1.55–1.39 (2H, m), 1.13–0.79 (2H, m), 0.62 (3H, t, J = 6 Hz); <sup>13</sup>C-NMR (CDCl<sub>3</sub>, 75 MHz): δ 179.16, 171.60, 157.66, 152.17, 149.17, 139.95, 130.80, 127.97, 124.60, 122.66, 114.81, 108.01, 107.57, 103.66, 84.41, 68.63, 57.74, 53.97, 52.52, 48.20, 38.10, 33.42, 32.08, 28.15, 25.78, 22.19, 8.60; LCMS (ESI) RT: 5.60 min, m/z: 494.4 [M+H]<sup>+</sup> at 210 and 254 nm; R<sub>f</sub> = 0.25 (EtOAc/heptane 1:1); HRMS (ESI) [MH<sup>+</sup>] calcd. for C<sub>29</sub>H<sub>40</sub>N<sub>3</sub>O<sub>4</sub> 494.3013, found 494.3031

Remark: Unfortunately, a direct protection approach with Boc<sub>2</sub>O and Na<sub>2</sub>CO<sub>3</sub> did not lead to any success. This is in contrast to a reported procedure for unsubstituted oxindoles [4].

### **tert-butyl-3-ethyl-3-(4-(4-(3-methoxyphenyl)piperazin-1-yl)butyl)-2-oxindoline-1-carboxylate (u)**

Cimbi-775 (20 mg, 0.049 mmol) was dissolved in dry THF, cooled to -5 °C, added 1M NaHMDS (0.049 mL, 0.049 mmol) and stirred for ½ h. Boc<sub>2</sub>O (10.24 mg, 0.049 mmol) was added and stirred for 1 h. Excess NaHMDS was quenched with 6 mL AcOH:THF 1:4 and then 40 mL water. Extraction was made with 3x10 mL EtOAc. The combined organic phases were washed with 2x10 mL brine, dried, concentrated *in vacuo* to yield in crude (u). LCMS (ESI) RT: 6.07 min, m/z: 508.4 [M+H]<sup>+</sup> at 210 and 254 nm

### **3-(4-(4-(4-bromophenyl)piperazin-1-yl)butyl)-3-ethylindolin-2-one (10)**

1-(4-bromophenyl)piperazine (479 mg, 1.986 mmol), 3-(4-chlorobutyl)-3-ethylindolin-2-one (500 mg, 1.98 mmol), and Na<sub>2</sub>CO<sub>3</sub> (211 mg, 1.986 mmol) was heated to 180 °C and stirred for 3 h. After cooling to rt. the resulting solid was dissolved in a mixture of EtOAc and water. The organic phase was concentrated *in vacuo* and purified using flash chromatography (EtOAc). Yield: 557.2 mg

(61.5%). 145-145.5 °C; <sup>1</sup>H-NMR (CDCl<sub>3</sub>, 400 MHz): δ 7.73 (1H, s), 7.33 (2H, m), 7.21 (1H, td, J = 7.59, 1.38 Hz), 7.12 (1H, m), 7.06 (1H, m), 6.88 (1H, d, J = 7.78 Hz), 6.76 (2H, m), 3.16 (4H, m), 2.56 (4H, brs), 2.31 (2H, t, J = 7.65 Hz), 1.93 (2H, m), 1.79 (2H, m), 1.45 (2H, m), 1.12 (1H, m), 0.93 (1H, m), 0.64 (3H, t, J = 7.40 Hz); <sup>13</sup>C-NMR (CDCl<sub>3</sub>, 75 MHz): δ 181.8, 150.2, 141.1, 132.5, 131.8, 127.6, 123.2, 122.5, 117.6, 109.3, 58.1, 54.10, 52.8, 48.7, 37.5, 31.1, 26.9, 22.2, 8.5; LCMS (ESI): RT: 5.97 min, m/z: 457.2 [M+H]<sup>+</sup> at 210 and 254 nm; R<sub>f</sub> = 0.18 (EtOAc); HRMS (ESI) [MH] cald. for C<sub>24</sub>H<sub>31</sub>BrN<sub>3</sub>O 456.1645, found 456.1657

### **3-ethyl-3-(4-(4-(4-(4,4,5,5-tetramethyl-1,3,2-dioxaborolan-2-yl)phenyl)piperazin-1-yl)butyl)indolin-2-one (11)**

10 (77 mg, 0.169 mmol), KOAc (19.8 mg, 0.202 mmol), Bis(pinacolato)diboron (86 mg, 0.337 mmol) and Pd(dddppf)Cl<sub>2</sub> (10 mg, 0.01 mmol) was dissolved in 10 mL of dry Dioxane, heated to 100 °C and stirred for 12 h. The reaction was then cooled to r.t, stirred with 10 mL of brine for 10 min and extracted with 3x50 mL EtOAc. The combined organic phases were dried, concentrated *in vacuo* and purified by column chromatography using pure heptane to pure ethyl acetate yielding 43 mg (50.6%) as a dark yellow oil. <sup>1</sup>H-NMR (CDCl<sub>3</sub>, 400 MHz): δ 7.70 (2H, d, J = 8.78 Hz), 7.59 (1H, s), 7.20 (1H, td, J = 7.65, 1.38 Hz), 7.13 (1H, m), 7.07 (1H, td, J = 7.40, 0.88 Hz), 6.87 (3H, m), 3.24 (4H, t, J = 4.77 Hz), 2.52 (4H, brs), 2.27 (2H, t, J = 7.53 Hz), 1.93 (2H, m), 1.79 (2H, m), 1.44 (2H, m), 1.33 (12H, s), 1.12 (1H, m), 0.92 (1H, m), 0.64 (3H, t, J = 7.40 Hz); <sup>13</sup>C-NMR (CDCl<sub>3</sub>, 75 MHz): δ 182.3, 153.23, 141.2, 136.1, 132.6, 127.6, 123.1, 122.5, 114.3, 109.4, 83.4, 58.1, 54.2, 52.8, 47.8, 37.5, 31.1, 24.8, 24.6, 22.3, 8.5; LC-MS (ESI): RT: 7.00 min, m/z: 504.3 [M+H]<sup>+</sup> at 210 and 254 nm; R<sub>f</sub> = 0.73 (EtOAc); HRMS (ESI) [MH<sup>+</sup>] cald. for C<sub>30</sub>H<sub>43</sub>BN<sub>3</sub>O<sub>3</sub> 504.3397, found 504.3420

### **5. Chiral resolution of Cimbi-772 (3) and Cimbi-775 (4)**

Analytic resolution: 5 µL of the desired racemate (1 mg/1 mL MeCN) were injected on a Lux 5 µm Cellulose-4 LC Column 250 x 4.6 mm. The sample was eluted with 20mM AmmBi: MeCN:DEA (40:60:0.1) with a flowrate of 1 mL/min. 1) Retention time (RT) of the separated enantiomers of Cimbi.772: a) 12.45 min b) 16.81 min 2) RT of the enantiomers of Cimbi-775: a) 11.956 mi b) 14.13 min;

Chiral separation was carried out using a Jasco PU 880 pump, a spectraseries UV100 detector connected to a Merck Hitachi D-2000 chromato-integrator and a DiacelChiralpak IF (5 µm 10 mm x



250 mm) column. Cimbi-772 was separated using heptane:IPA:DEA 90:10:0.1 at 4.5 ml/min and Cimbi-775 was separated using heptane:IPA:DEA 80:20:0.1 at 4.5 ml/min.

### a) Optical Rotation

Optical rotation was measured on a Bellingham + stanley ADP410 polarimeter at 689 nm.

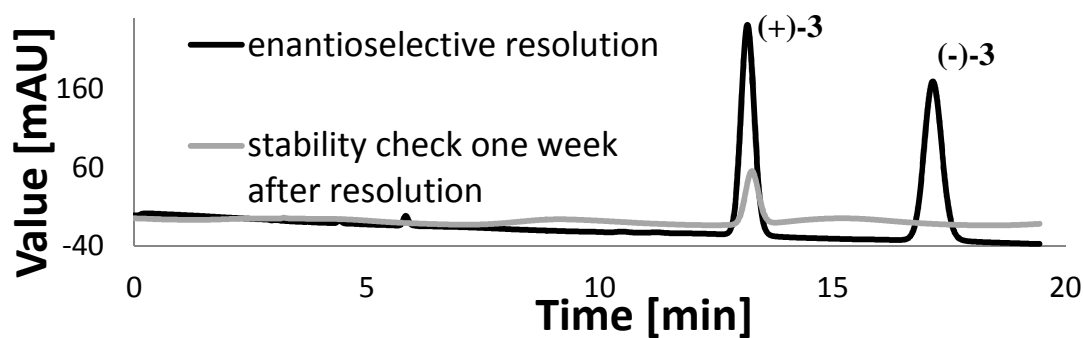
(-)-3:  $[\alpha]_D^{20} = -16$  (c = 0.5, CHCl<sub>3</sub>)

(+)-3:  $[\alpha]_D^{20} = +16$  (c = 0.5, CHCl<sub>3</sub>)

(-)-4:  $[\alpha]_D^{20} = -16$  (c = 0.5, CHCl<sub>3</sub>)

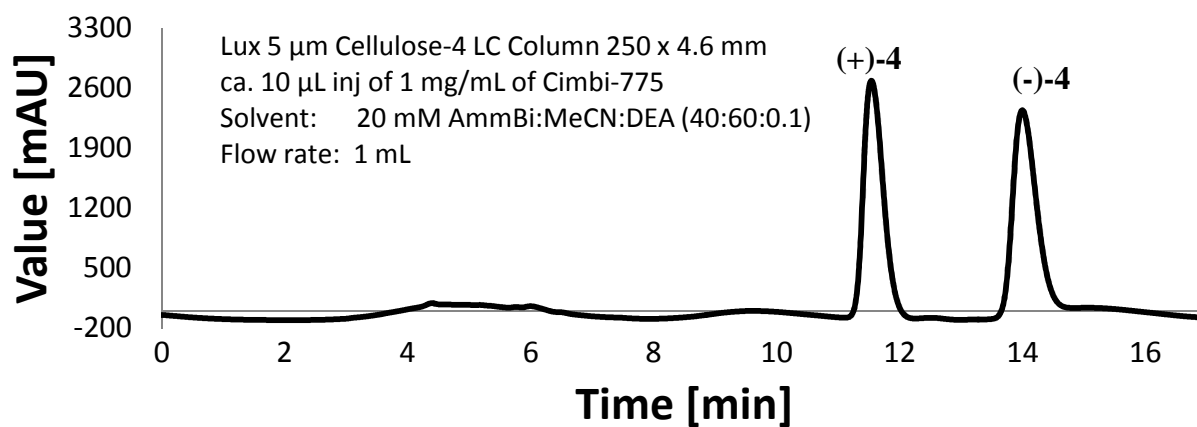
(+)-4:  $[\alpha]_D^{20} = +16$  (c = 0.5, CHCl<sub>3</sub>)

### b) Chiral resolution of Cimbi-772 (3) and stability test

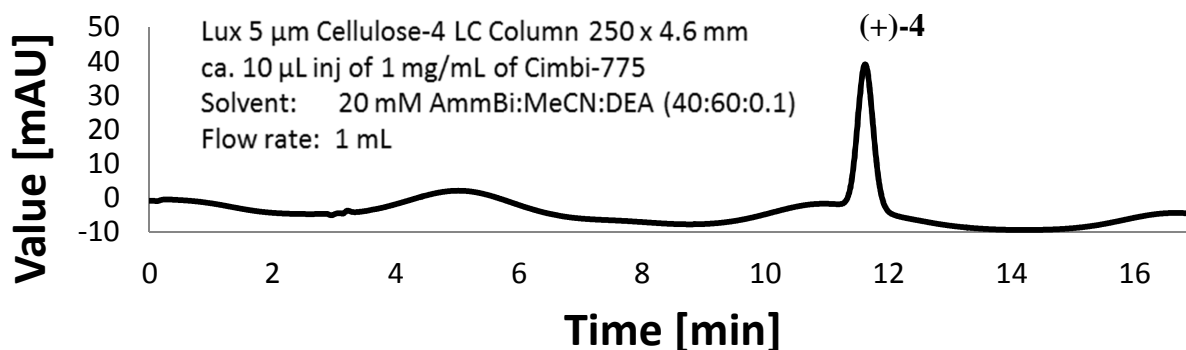


Chiral resolution and stability test of one enantiomer of Cimbi-772, the same HPLC conditions as above were used

### c) Chiral resolution of Cimbi-775 (4)



#### d) Stability test of (+)-4



### 6. PDSP Screening

In vitro radioligand binding assays were performed by the NIMH Psychoactive Drug Screening Program at the Department of Biochemistry, Case Western Reserve University, Cleveland, Ohio, USA (Bryan Roth, Director). Compounds Cimbi-712, Cimbi-717, Cimbi-772, Cimbi-772-1, Cimbi-775 and Cimbi-775-1 were assayed for their affinities for a broad spectrum of receptors and transporters in competitive binding experiments in vitro using cloned human receptors. Reported values of the inhibition coefficient ( $K_i$ ) are mean  $\pm$  SD of four separate determinations.

### 7. Receptor distribution of colocalized targets

Table S2 shows the receptor Distribution of colocalized Targets. Bmax values are reported in fmol/mg wet tissue or in fmol/mg protein.

Table S2: Receptor distribution of colocalized targets

	5-HT <sub>7</sub> <sup>[5]</sup>	5-HT <sub>1A</sub> <sup>[6, 7]</sup>	5-HT <sub>2A</sub> <sup>[8]</sup>	$\alpha_1$	H <sub>1</sub> <sup>[9]</sup>	sigma <sup>[10]</sup>	SERT <sup>[8]</sup>
<b>cortex</b>	2.3	73	56	283 <sup>[11]</sup>	14	101	4.3
<b>Hippocampus</b>	5.7	82	24	234 <sup>[12]</sup>	6.4	73	2.6
<b>thalamus</b>	12	4	6	88 <sup>[12]</sup>	4	58	10

## 8. Selectivity/ $B_{\max}$ ratio for 5-HT<sub>7</sub>

Table S3: Selectivity/ $B_{\max}$  ratio for 5-HT<sub>7</sub> of the compounds relative to other relevant targets in different brain regions. Data are based on values reported in Table 1 and Table S2. Human  $B_{\max}$  values were used.

$$\text{Selectivity}/B_{\max} \text{ ratio} = \left( \frac{K_{d,\text{off-target}}}{K_{d,\text{target}}} \right) \left( \frac{B_{\text{avail},\text{target}}}{B_{\text{avail},\text{off-target}}} \right)$$

		versus 5-HT <sub>1A</sub>	versus 5-HT <sub>2A</sub>	versus $\alpha_1$	versus H1	versus sigma	versus SERT
<b>Cimbi-775 (4)</b>	cortex	0.3	0.5	0.5	17.8	0.15	17
	hippocampus	0.7	2.9	1.4	-	0.42	70
	thalamus	32	25	7.6	193	1.11	38
<b>(+)-4</b>	cortex	0.5	1.3	7.5	1.05	0.09	18
	hippocampus	1.2	7.6	22	-	0.32	74
	thalamus	52	64	123	11	0.86	41
<b>Cimbi-717 (2)</b>	cortex	0.5	1.3	0.2	6.0	0.2	18
	hippocampus	1.2	7.5	0.5	-	0.61	73
	thalamus	52	63	3.0	67	1.6	40
<b>Cimbi-772 (3)</b>	cortex	2.3	0.2	0.5	22	0.12	24
	hippocampus	5	1.4	1.6	-	0.4	99
	thalamus	216	12	9.0	244	1.1	54
<b>(+)-3</b>	cortex	4.4	0.6	1.3	6.6	0.1	25
	hippocampus	9.7	3.9	4.1	-	0.5	106
	thalamus	421	34	23	72	1.2	58
<b>Cimbi-712 (1)</b>	cortex	3.7	0.4	0.2	21.8	0.24	14
	hippocampus	8.3	2.0	0.6	-	0.85	59
	thalamus	359	17.1	3.4	236	2.2	32

Remark: Exemplarily, we would like to calculate one selectivity/ $B_{\max}$  ratio for Cimbi-712 in thalamus for the target (5-HT<sub>7</sub>) and for the off-target (5-HT<sub>1A</sub>): The affinity of Cimbi-712 for the 5-HT<sub>7</sub> receptor is 4.1 nM and for the 5-HT<sub>1A</sub> receptor, it is 491 nM (Table 1 and Table S3).  $B_{\text{avail}}/B_{\max}$  in thalamus is 12 fmol/mg original wet tissue for the 5-HT<sub>7</sub> receptor and 4 fmol/mg original wet tissue for the 5-HT<sub>1A</sub> receptor.

$$\text{selectivity}/B_{\max} \text{ ratio}_{5\text{-HT}_7/5\text{-HT}_{1A}} = S \times D = \left( \frac{491 \text{ nM}}{4.1 \text{ nM}} \right) \left( \frac{12 \frac{\text{fmol}}{\text{mg wet tissue}} \text{ 5-HT}_7 \text{ receptor}}{4 \frac{\text{fmol}}{\text{mg wet tissue}} \text{ 5-HT}_{1A} \text{ receptor}} \right) = 359.26 \frac{5\text{-HT}_7}{5\text{-HT}_{1A}}$$

Thus, the selectivity/ $B_{\max}$  ratio of Cimbi-712 for 5-HT<sub>7</sub> in thalamus is 359-fold relative to the 5-HT<sub>1A</sub> receptor. Of course, one should critically review the selectivity/ $B_{\max}$  ratio. The original in

in vitro data can vary considerably due to different determination methods. In addition, it is important to remember that in vitro binding characteristics may not always predict in vivo binding characteristics. That is, because radioligands which are suitable for in vitro quantification may not necessarily be ideal for in vivo PET imaging. PET tracers have to enter the brain through the blood–brain barrier (BBB). The tracer can be a substrate of efflux pumps. Metabolism or pharmacokinetics could further limit its use [13]. Nonetheless, when taken these pre-considerations into account, the selectivity/ $B_{\max}$  ratio is a good estimate of the in vivo binding of a given compound.

## **9. In vitro characterization**

### Cell culture and cAMP accumulation assay

HeLa cells stably expressing the human 5-HT<sub>7(a)</sub> receptor [HeLa h5-HT<sub>7(a)</sub>; kindly provided by Dr. Mark Hamblin] were used to determine activity of the test compounds in vitro. We have previously described the pharmacological profile of HeLa h5-HT<sub>7(a)</sub> and recently used these cells to characterize novel ligands of 5-HT<sub>7</sub> [14, 15]. Cells were cultured in a standard incubator at 37°C and 5% CO<sub>2</sub>/95% air. Growth medium consisted of DMEM supplemented with 10% fetal bovine serum, 2 mM L-glutamine and 250 µg/ml Geneticin (G418). Cells were seeded into 96-well plates (Sarstedt, Helsingborg, Sweden) at a density of 20,000 cells per well 24 hours before experiments. About 18 hours prior to treatment, cells were switched to serum-free medium (DMEM supplemented with 2 mM L-glutamine). All drug solutions were freshly prepared on the day of a given experiment, either from powder (5-HT, pargyline, theophylline) or from 10 mM stocks in DMSO (test compounds). Serial dilutions of the test compounds were prepared in ddH<sub>2</sub>O. The final concentration of DMSO was 1% (v/v) at the highest concentration of test compounds, and 1% DMSO was used as a vehicle control in all experiments. To test for agonist activity, cells were treated with 10 µM of test compounds for 15 minutes. To test for antagonist activity, cells were treated with 1 µM 5-HT for 15 minutes in the absence or presence of increasing concentrations of test compounds. Untreated cells were used to establish baseline concentrations of cAMP in all experiments. To prevent degradation of 5-HT and cAMP, all wells contained a final concentration of 5 µM pargyline and 2.5 mM theophylline. After 15 minutes of treatment, cells from each well were harvested and lysed in 100 µl of 0.1 M HCl containing 1% (v/v) Triton X-100. Intracellular concentrations of cAMP were measured using a kit (cyclic AMP Complete ELISA; Abnova, Taipei City, Taiwan) according to the manufacturer's instructions for acetylated samples.

### Determination of antagonist potencies

Results from individual cAMP accumulation assays were normalized (cAMP concentration after treatment with 1  $\mu$ M 5-HT = 100%) and then pooled to construct concentration-response curves for the test compounds. Nonlinear regression and curve fitting were carried out in GraphPad Prism 5 (GraphPad, La Jolla, USA) using a four-parameter equation, with the top plateau fixed at 100%. Based on the observation of complete antagonism (5-HT-induced cAMP suppressed to baseline) for all four test compounds, the bottom plateau was fixed at the average value of normalized cAMP observed at the highest test compound concentration (100  $\mu$ M). Inhibitory potencies (IC<sub>50</sub> values) were derived from nonlinear regression and best-fit curves were plotted.

### Additional notes

All cell culture reagents (DMEM, FBS, L-glutamine, Geneticin) were from Life Technologies. DMSO, 5-HT, pargyline and theophylline were from Sigma-Aldrich.

## **10. Lipophilicity[16]**

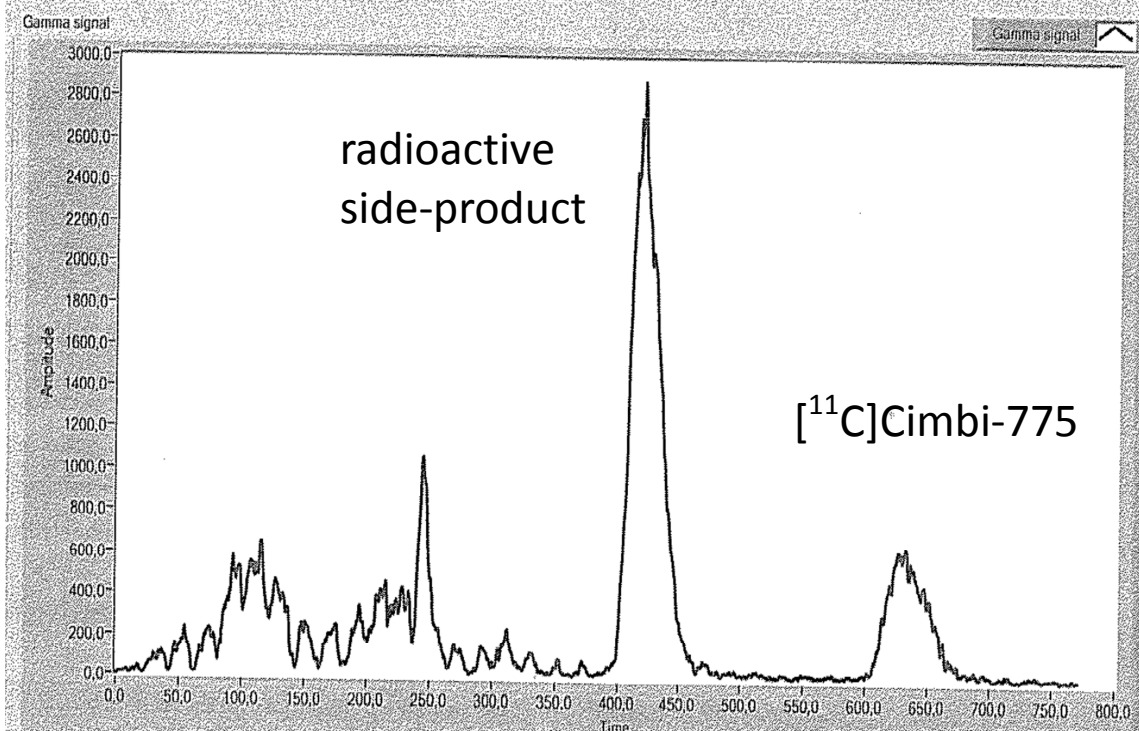
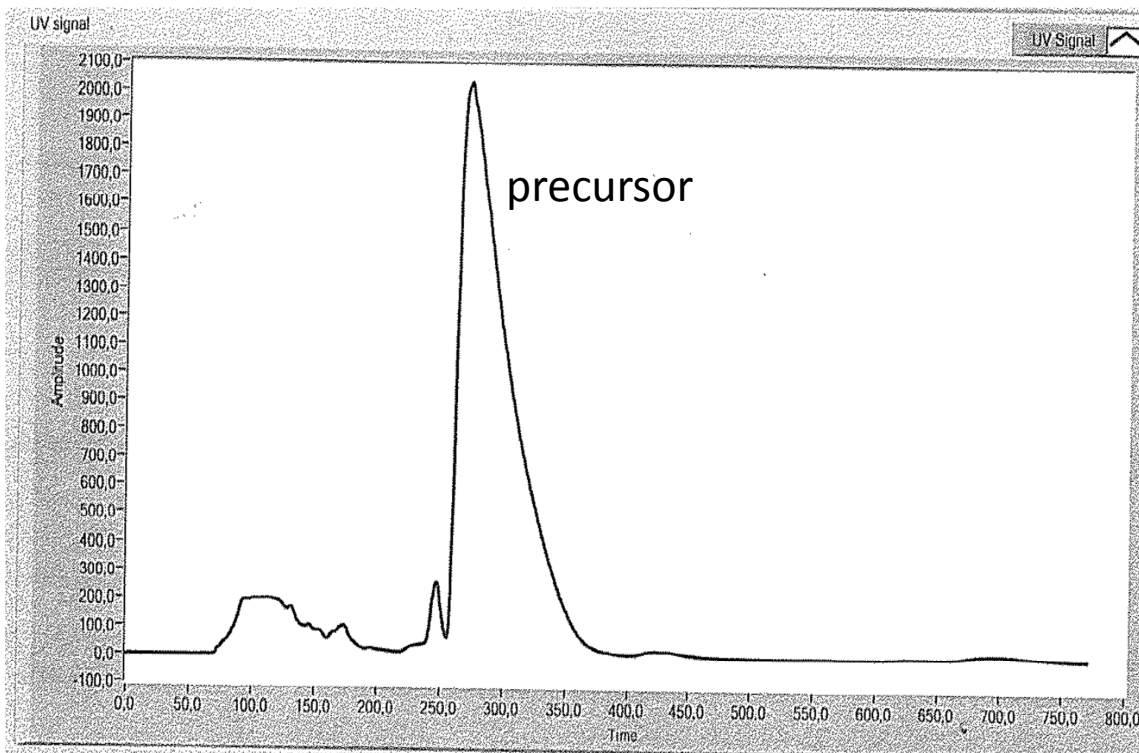
Lipophilicities were determined using a Dionex Ultimate 3000 UHPLC equipped with degasser, autosampler, column-oven and UV-detector. The eluent was 50:50 (v/v) 20 mM sodium phosphate-buffer (pH = 7.4) and MeOH. Injected volumes were 100  $\mu$ L with a flow rate of 1 mL/min. The determination was carried out on a Luna C18(2) 5 $\mu$ m 100 $\text{\AA}$  (150 mm  $\times$  4.6 mm, 5  $\mu$ m) and UV detection was conducted at 254 nm. The logarithm of retention factor of reference compounds (phenol, acetophenone, *p*-cresol, benzene, toluene, chlorobenzene, benzophenone, naphthalene, diphenyl and phenanthrene) and tested compounds was calculated, and a plot of the reference values against their known logD values was used to interpolate logD values for tested compounds. Lipophilicity data are displayed in Table S1.

Lipophilicity discussion: The development of a successful *in vivo* PET probe for neuroreceptor imaging requires high selectivity for the target, blood-brain-barrier (BBB) passage and a low non-specific binding of the ligand. Especially, the lipophilicity of the compound influences the last two parameters (ideal log D<sub>7,4</sub> = 2-3 [17]). Therefore, we decided to determine the lipophilicity of our final ligands and to compare them to previously published oxindoles which bear no alkyl moiety at the 3-position [2]. Calculated logD<sub>7,4</sub> values are displayed in Table 1.

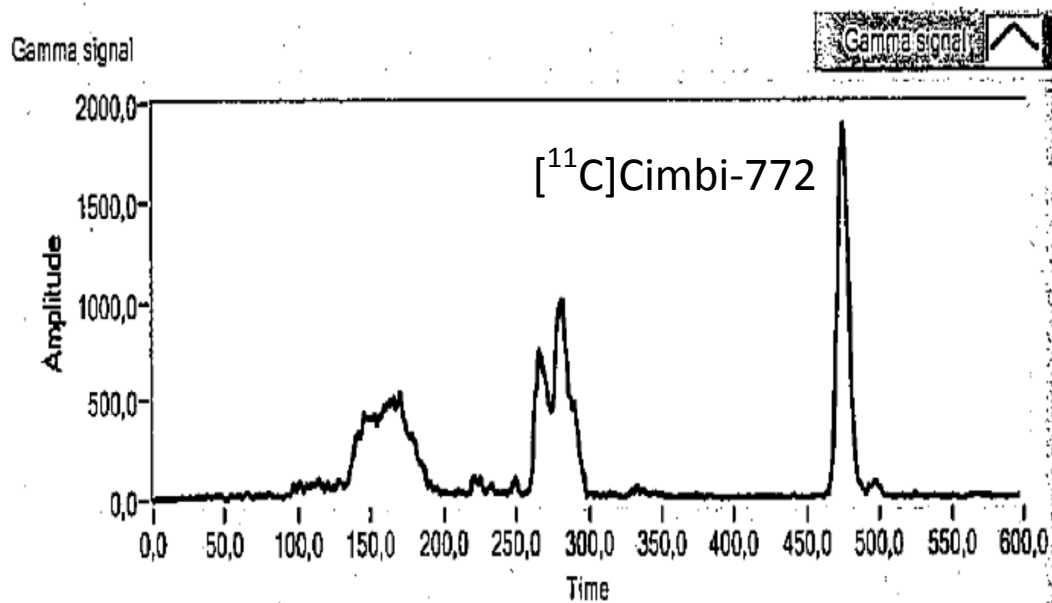
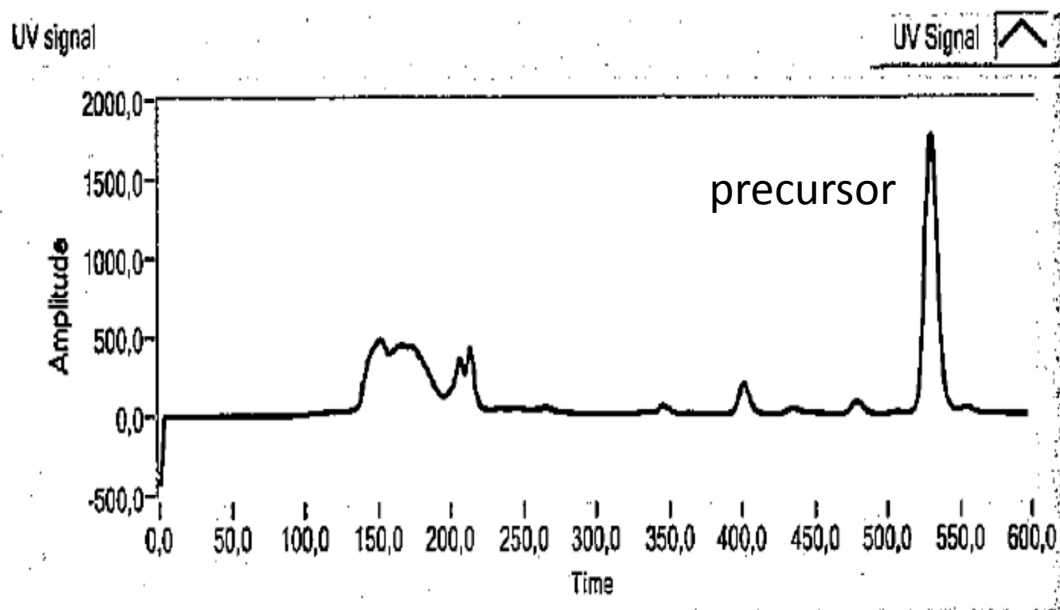
C-3 alkylation increased the  $\log D_{7.4}$  value about a factor of  $\sim 0.5$  per additional carbon atom. Respectively, different BBB passage and non-specific binding of these alkylated oxindole ligands could be expected and possibly change imaging properties in regards to PET. However, the determined values were still in a reasonable range to continue with their evaluation process. Further, fluorination of the ethyl moiety reduced the lipophilicity slightly and as expected, hydroxyl derivatives decreased the lipophilicity by a factor of one compared C-3 ethylated compounds. Finally, N-alkylation increased the lipophilicity dramatically and exclude further use of such compounds for PET.

At this stage, it is worthwhile to comment on the relatively high determined  $\log D_{7.4}$  values in this study, keeping in mind that the ideal interval for small molecules to penetrate the BBB was reported to be 2-3 [17]. However, in our set-up other known CNS-PET ligands (e.g. MDL 100907, altanserin or WAY 100635) show similarly high values. Therefore, we believe that these compounds may have similarly good properties for molecular imaging.

# 11. Preparative radio-HPLC chromatogram of [<sup>11</sup>C]Cimbi-775

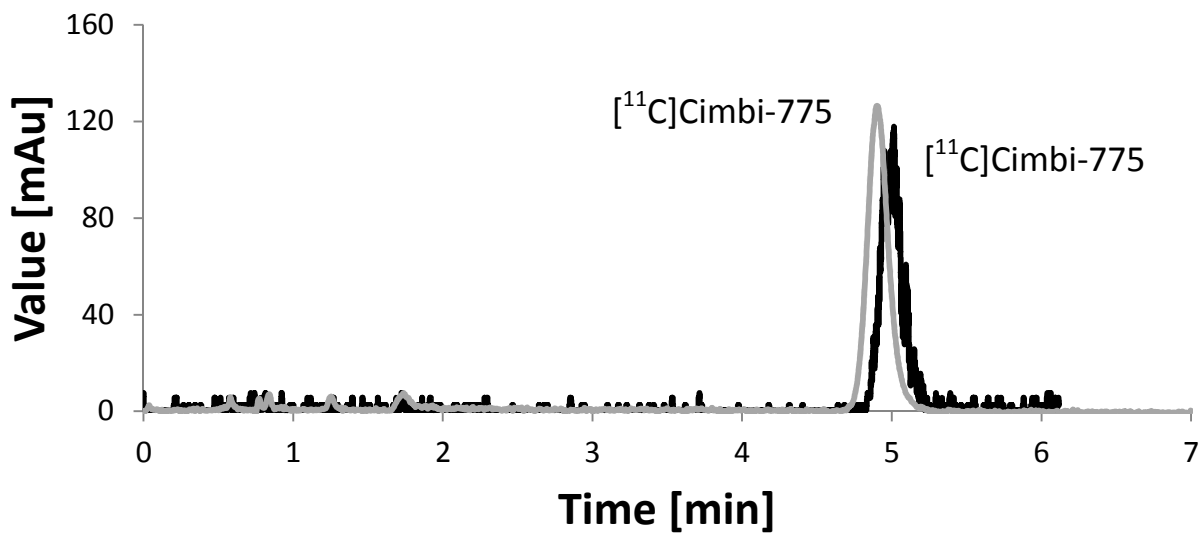
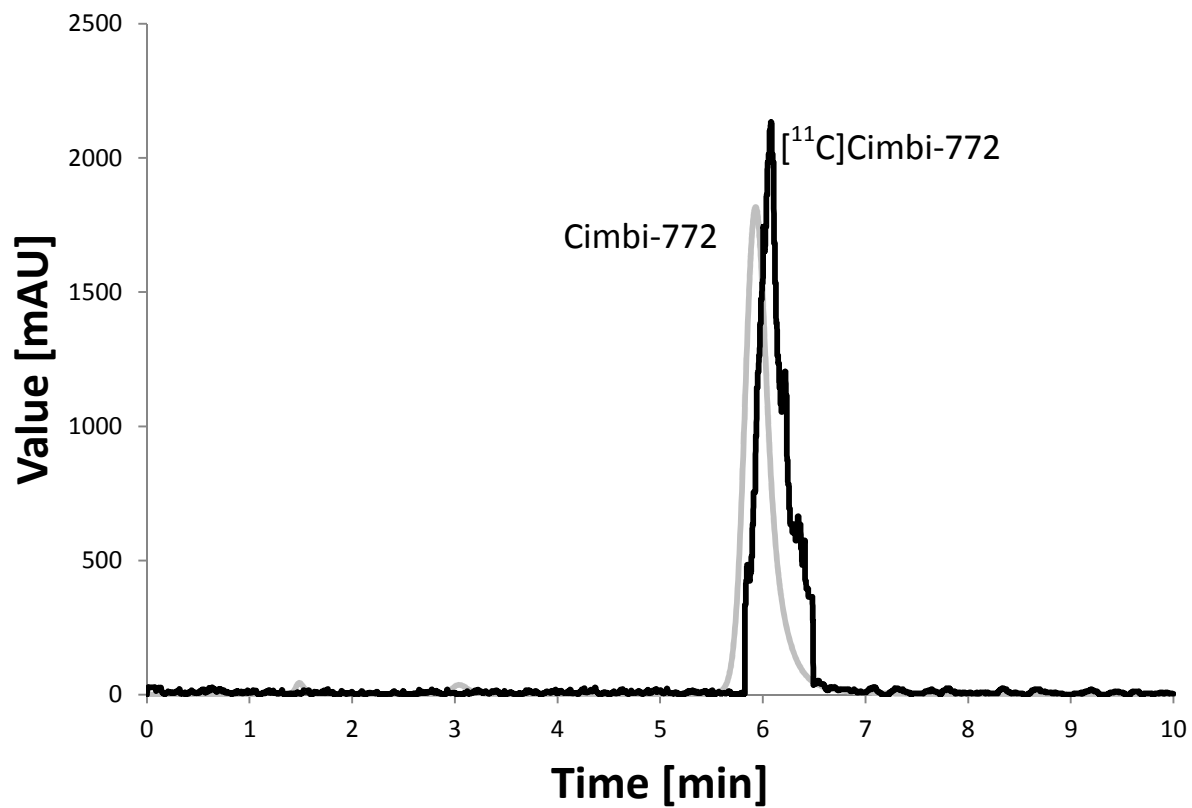


## 12. Preparative radio-HPLC chromatogram of [ $^{11}\text{C}$ ]Cimbi-772





13. Analytical HPLC chromatogram of [ $^{11}\text{C}$ ]Cimbi-772 and [ $^{11}\text{C}$ ]Cimbi-775



#### **14. Determination of radiochemical purity and specific radioactivity**

The radiotracer preparation was visually inspected for clarity, and absence of colour and particles. Chemical and radiochemical purities were assessed on the same aliquot by HPLC analysis. Specific activity ( $A_s$ ) of the radiotracers were calculated from three consecutive HPLC analyses (average) and determined by the area of the UV absorbance peak corresponding to the radiolabeled product on the HPLC chromatogram and compared to a standard curve relating mass to UV absorbance ( $\lambda = 225 \text{ nm}$ ). Column used for [ $^{11}\text{C}$ ]Cimbi-775: Luna 5  $\mu\text{m}$  C18(2) 100 $\text{\AA}$  column (Phenomenex Inc.) (150 x 4.6 mm (50:50 acetonitrile: 0.01% borax buffer; flow rate: 2 mL/min. retention times: [ $^{11}\text{C}$ ]Cimbi-775 = 4.580 min). Column used for [ $^{11}\text{C}$ ]Cimbi-772: Luna 5  $\mu\text{m}$  C18(2) 100 $\text{\AA}$  column (Phenomenex Inc.) (150 x 4.6 mm (50:50 acetonitrile: 0.01% borax buffer; flow rate: 2 mL/min. retention times: [ $^{11}\text{C}$ ]Cimbi-772 = 6.007 min).

#### **15. Animal procedures**

Four female Danish Landrace pigs (mean weight  $\pm$  S.D.,  $18 \pm 2.3 \text{ kg}$ ) were used for in vivo PET imaging. Tranquillization, anaesthesia, monitoring and euthanasia of animals were performed as previously described (ref). All animal procedures were approved by the Danish Council for Animal Ethics (journal no. 2012-15-2934-00156).

#### **16. Quantification of PET data**

Ninety-minute list-mode PET data were reconstructed into 38 dynamic frames of increasing length (6x10, 6x20, 4x30, 9x60, 2x180, 8x300, and 3x600 seconds). Images consisted of 207 planes of 256 x 256 voxels of 1.22 x 1.22 x 1.22 mm. A summed picture of all counts in the 90-min scan was reconstructed for each pig and used for co-registration to a standardized MRI-based atlas of the Danish Landrace pig brain, similar to that previously published[18, 19]. The time activity curves (TACs) were calculated for the following volumes of interest (VOIs): cerebellum, cortex, hippocampus, lateral and medial thalamus, caudate nucleus, and putamen. Striatum is defined as the mean radioactivity in caudate nucleus and putamen. The activity in thalamus is calculated as the mean radioactivity in the lateral and medial thalamus. Radioactivity in all VOIs was calculated as the average of radioactive concentration (Bq/mL) in the left and right sides. Outcome measure in the time-activity curves (TACs) was calculated as radioactive concentration in VOI (in kBq/mL) normalized to the injected dose corrected for animal weight (in kBq/kg), yielding standardized uptake values (g/mL).

## 17. References

1. Volk, B., et al., *(Phenylpiperazinyl-butyl)oxindoles as selective 5-HT(7) receptor antagonists*. Journal of Medicinal Chemistry, 2008. 51(8): p. 2522-2532.
2. Herth, M.M., et al., *Synthesis and In Vitro Evaluation of Oxindole Derivatives as Potential Radioligands for 5-HT7 Receptor Imaging with PET*. ACS Chemical Neuroscience, 2012. 3(12): p. 1002-1007.
3. Andersen, V.L., et al., *Palladium-mediated conversion of para-aminoarylboronic esters into para-aminoaryl-C-11-methanes*. Tetrahedron Letters, 2013. 54(3): p. 213-216.
4. Rajeswaran, W.G. and L.A. Cohen, *Studies on protection of oxindoles*. Tetrahedron, 1998. 54(38): p. 11375-11380.
5. Varnas, K., et al., *Distribution of 5-HT7 receptors in the human brain: a preliminary autoradiographic study using [H-3]SB-269970*. Neuroscience Letters, 2004. 367(3): p. 313-316.
6. Hall, H., et al., *Autoradiographic localization of 5-HT1A receptors in the post-mortem human brain using [H-3]WAY-100635 and [C-11]WAY-100635*. Brain Research, 1997. 745(1-2): p. 96-108.
7. Hall, H., et al., *Whole hemisphere autoradiography of the postmortem human brain*. Nuclear Medicine and Biology, 1998. 25(8): p. 715-719.
8. Varnas, K., C. Halldin, and H. Hall, *Autoradiographic distribution of serotonin transporters and receptor subtypes in human brain*. Human Brain Mapping, 2004. 22(3): p. 246-260.
9. Kanba, S. and E. Richelson, *Histamine H-1-Receptors in Human-Brain Labeled with [Doxepin-H-3*. Brain Research, 1984. 304(1): p. 1-7.
10. Weissman, A.D., et al., *Sigma-Receptors in Post-Mortem Human Brains*. Journal of Pharmacology and Experimental Therapeutics, 1988. 247(1): p. 29-33.
11. Grossisseroff, R., et al., *Autoradiographic Analysis of Alpha-1-Noradrenergic Receptors in the Human Brain Postmortem - Effect of Suicide*. Archives of General Psychiatry, 1990. 47(11): p. 1049-1053.
12. DePaermentier, F., et al., *Brain alpha-adrenoceptors in depressed suicides*. Brain Research, 1997. 757(1): p. 60-68.
13. Paterson, L.M., et al., *5-HT radioligands for human brain imaging with PET and SPECT*. Medicinal Research Reviews, 2013. 33(1): p. 54-111.
14. Sjogren, B., M.W. Hamblin, and P. Svenningsson, *Cholesterol depletion reduces serotonin binding and signaling via human 5-HT7(a) receptors*. European Journal of Pharmacology, 2006. 552(1-3): p. 1-10.
15. Lacivita, E., et al., *Investigations on the 1-(2-Biphenyl)piperazine Motif: Identification of New Potent and Selective Ligands for the Serotonin(7) (5-HT7) Receptor with Agonist or Antagonist Action in Vitro or ex Vivo*. Journal of Medicinal Chemistry, 2012. 55(14): p. 6375-6380.
16. OECD Guideline for Testing of Chemicals, adopted 30.03.89.
17. Rowley, M., et al., *Effect of plasma protein binding on in vivo activity and brain penetration of glycine/NMDA receptor antagonists*. Journal of Medicinal Chemistry, 1997. 40(25): p. 4053-4068.
18. Kornum, B.R., et al., *Evaluation of the novel 5-HT4 receptor PET ligand [11C]SB207145 in the Gottingen minipig*. J Cereb Blood Flow Metab, 2009. 29(1): p. 186-196.

19. Ettrup, A., et al., *Radiosynthesis and Evaluation of 11C-CIMBI-5 as a 5-HT<sub>2A</sub> Receptor Agonist Radioligand for PET*. *J Nucl Med*, 2010. 51(11): p. 1763-1770.

## Appendix 5

Development of a C-11-Labeled Tetrazine for Rapid Tetrazine-Trans-Cyclooctene Ligation

M. M. Herth, **V. L. Andersen**, S. Lehel, J. Madsen, G. M. Knudsen, and J. L. Kristensen

*Chemical Communications*, 49 (2013), 3805-07.



Development of a  $^{11}\text{C}$ -labeled tetrazine for rapid tetrazine–*trans*-cyclooctene ligation†Matthias M. Herth,<sup>\*abc</sup> Valdemar L. Andersen,<sup>abc</sup> Szabolcs Lehel,<sup>c</sup> Jacob Madsen,<sup>c</sup> Gitte M. Knudsen<sup>a</sup> and Jesper L. Kristensen<sup>b</sup>Cite this: *Chem. Commun.*, 2013, **49**, 3805Received 6th February 2013,  
Accepted 18th March 2013

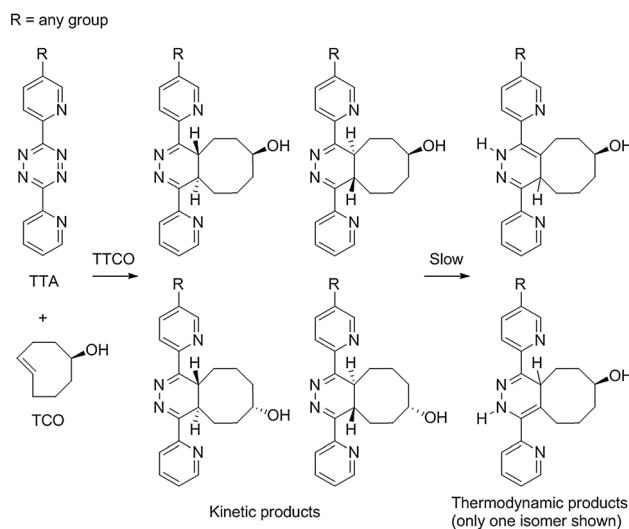
DOI: 10.1039/c3cc41027g

www.rsc.org/chemcomm

Tetrazine–*trans*-cyclooctene ligations are remarkably fast and selective reactions even at low micro-molar concentrations. In bioorthogonal radiochemistry, tools that enable conjugation of radioactive probes to pre-targeted vectors are of great interest. Herein, we describe the successful development of the first  $^{11}\text{C}$ -labelled tetrazine and its reaction with *trans*-cyclooctenol.

Bioorthogonal chemical reactions between two exogenous moieties, without interfering with native biochemical processes in living beings, may serve as powerful diagnostic applications in molecular imaging.<sup>1</sup> Potentially, these ligations could permit *in vivo* long-term positron emission tomography (PET imaging) using short-lived isotopes such as fluorine-18 ( $t_{1/2} \sim 110$  min) or carbon-11 ( $t_{1/2} \sim 20.4$  min), which are routinely applied in non-invasive clinical PET imaging. The basic principle relies on a pre-targeting approach enabling repeatable PET imaging of applied pre-targeting vectors (the *in vivo* click approach).<sup>1</sup> Snapshots at multiple time-points provide long-term imaging information without applying long-lived nuclides. This strategy results in a superior image contrast compared to conventional long-term imaging techniques and the ability to administer higher radioactive doses.<sup>2</sup>

Bioorthogonal conjugations, like the Staudinger ligation or the strain-promoted azide–alkyne cycloaddition,<sup>3</sup> have found widespread applications within *in vivo* click chemistry.<sup>4</sup> However, the slow reaction kinetics ( $k_2 \leq 40 \text{ M}^{-1} \text{ s}^{-1}$ ) necessitated a high dose and a large excess of secondary reagent to achieve detectable ligation<sup>1</sup> (see ESI† for further details).



**Scheme 1** Tetrazine–*trans*-cyclooctene (TTCO) ligation between two asymmetric synthons.

Recently, Blackman introduced a rapid inverse-electron-demand Diels–Alder reaction between electron-deficient tetrazines (TTA) and strained *trans*-cyclooctene (TCO) derivatives often referred to as tetrazine–*trans*-cyclooctene (TTCO) ligation (Scheme 1).

The fast reaction kinetics ( $k_2 = 2000$  to  $22\,000 \text{ M}^{-1} \text{ s}^{-1}$ ) and selectivity of this catalyst-free coupling make it an ideal candidate for effective applications at low concentrations.<sup>1,5</sup> In addition, this ligation can be performed in water and its conjugates are stable towards biological nucleophiles.<sup>6</sup> Therefore, the TTCO could be applied to quantitative and repetitive *in vivo* click PET or single photon emission computed tomography (SPECT) imaging. Compared to other imaging methods, PET and SPECT bear the advantage of high sensitivity (the level of detection approaches  $10^{-12} \text{ M}$  of the tracer) and isotropism (*i.e.* ability to detect organ accumulation accurately regardless of tissue depth).<sup>7</sup>

Rossin *et al.* proved for the first time the potential of the tetrazine ligation approach on a pre-targeted antibody for SPECT molecular imaging.<sup>1</sup> PET is beneficial over SPECT,

<sup>a</sup> Center for Integrated Molecular Brain Imaging, Rigshospitalet and University of Copenhagen, Blegdamsvej 9, DK-2100 Copenhagen, Denmark.

E-mail: matthias.herth@nru.dk; Fax: +45 3545 6713; Tel: +45 3545 6711

<sup>b</sup> Department of Drug Design and Pharmacology, Faculty of Health and Medical Sciences, University of Copenhagen, Universitetsparken 2, DK-2100 Copenhagen, Denmark. Fax: +45 3533 6041; Tel: +45 3533 6487

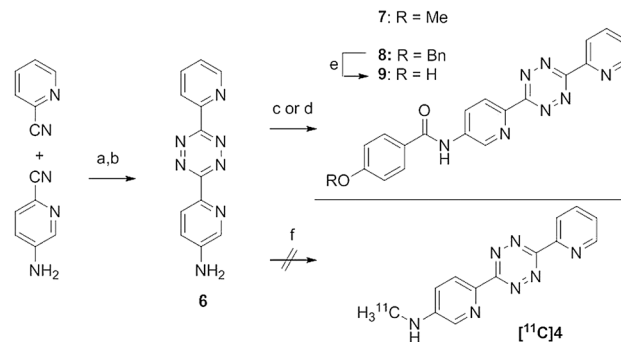
<sup>c</sup> PET and Cyclotron Unit, Rigshospitalet, Blegdamsvej 9, DK-2100 Copenhagen, Denmark. Fax: +45 3545 3545; Tel: +45 3545 8621

† Electronic supplementary information (ESI) available: Comparison of bio-orthogonal reaction kinetics, experimental procedures, HPLC conditions and spectroscopic data of selected compounds. See DOI: 10.1039/c3cc41027g

because PET results in higher spatial and temporal resolution and better quantification.<sup>7</sup> Therefore, Devaraj *et al.* extended this TTCO approach to PET by *in vivo* clicking an <sup>18</sup>F-labeled polymer to a TCO modified antibody.<sup>8</sup> However, this strategy is disadvantaged by violating the tracer principle, *i.e.*, that radioactive compounds' kinetics reflect physiological processes without interfering with the physiology itself. This requirement is typically met at concentrations in the nanomolar range. In the aforementioned approach, pharmacological doses ( $\mu\text{M}$ ) of the labeled polymer are used because the precursor cannot be separated from the final labeled product. As a result, toxicology and approval concerns might arise. Labeling of a small, well defined molecule reduces these concerns substantially since the precursor and the labeled product are easily separated at nanomolar concentrations. In 2010, Li *et al.* described the first synthesis of a small molecule (an <sup>18</sup>F-labeled *trans*-cyclooctene derivative) for the TTCO.<sup>6</sup> However, this approach has one drawback as the <sup>18</sup>F-label was attached to the TCO instead of the TTA.<sup>6</sup> This requires that the TTA be attached to the pre-targeting vector. Although several advances have been made recently, TTA chemistry is still in its infancy.<sup>9</sup> Furthermore, asymmetric TTAs with suitable chemical handles for conjugation with biomolecules are challenging to create.<sup>9</sup> However, the biggest drawback of attaching the TTA-unit to a vector is the very poor solubility and possible low long-term *in vivo* stability of the highly nitrogen rich TTAs. In addition, TTAs are explosive,<sup>10</sup> a cause for concern when handled in micromolar quantities. In contrast, the strategy to conjugate easy, commercially available and stable *trans*-cyclooctene derivatives to the pre-targeting vector and subsequently to image them *via* a labeled TTA is very promising and the labeled TTA can then be applied in nanomolar quantities.

Besides the aforementioned possibility to conduct *in vivo* click chemistry using the TTCO, this fast and selective ligation could also enable traditional labeling of complex molecules such as proteins, antibodies or nanoparticles. Even small molecules such as peptides could benefit from an effective and prompt labeling approach. A broader set of secondary labeling synthons is still required to address the chemical diversity of targeting vectors. Today, the largest and most promising potential to develop novel PET molecular imaging tracers is innovative radiochemistry.<sup>6,11</sup> The use of the TTCO for labelling small molecules is challenging as several isomers are formed in the reaction, which complicates subsequent characterisation (Scheme 1). Initially, a mixture of kinetic products is formed, which then isomerises over time to the thermodynamically more stable ones.<sup>6</sup> Thus, complete characterisation of the product mixture is very difficult, if not impossible. Nevertheless, Selvaraj *et al.* used this tetrazine ligation approach to label and evaluate successfully a small cyclic RGD peptide without separating the isomers.<sup>12</sup> Likewise, Li *et al.* did not separate all possible isomers when analyzing their <sup>18</sup>F-labeled TTCO adduct.<sup>6</sup>

Herein, we report the development of a rapid TTCO between a <sup>11</sup>C-labeled TTA and a *trans*-cyclooctenol (TCO). This development based carbon-11 was prioritized as it displays some advantages over fluorine-18 during development research, *e.g.* the possibility



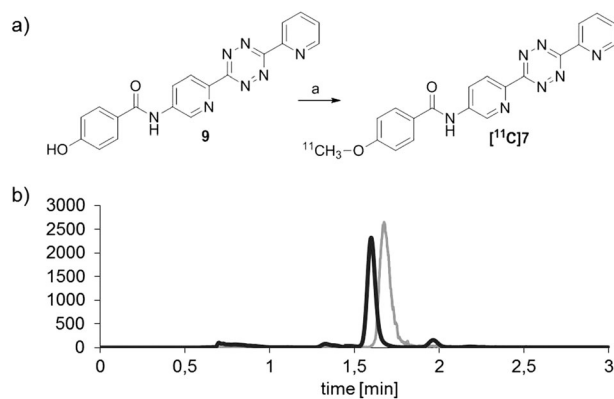
**Scheme 2** Synthesis and functionalization of the tetrazine matrix: (a) hydrazine (98%),  $\text{H}_2\text{O}$ ,  $90^\circ\text{C}$ , 12 h, 31%; (b) DDQ, toluene, 12 h, 50%; (c) *p*-anisoyl chloride, pyridine,  $130^\circ\text{C}$ , MW, 5 min, 98%; (d) *p*-(benzyloxy)benzoyl chloride, pyridine,  $130^\circ\text{C}$ , MW, 5 min, 92%; (e) Pd/C, ammonium formate, isopropanol,  $70^\circ\text{C}$ , MW, 20 min, 90%,<sup>‡</sup> (f) various conditions (see ESI<sup>†</sup> for details)

to conduct repeat PET studies in the same subject within hours or usually under simpler insertion conditions.

Initially, we focused on the introduction of carbon-11 on aniline **6** and later—since phenols are more easily labeled than anilines<sup>13</sup>—we used a novel developed phenol derivative **9**. The necessary tetrazine matrix was synthesized according to Blackman (Scheme 2).<sup>6</sup> Purification processes were optimized and **6** was isolated. In contrast to the reported procedures,<sup>5,6</sup> the amino moiety of **6** could not be easily functionalized as the amido, alkyl or amidosulfonyl derivatives (see ESI<sup>†</sup> for details), and all attempts to introduce a <sup>11</sup>C-labeled methyl group directly on the aniline failed (Scheme 2).

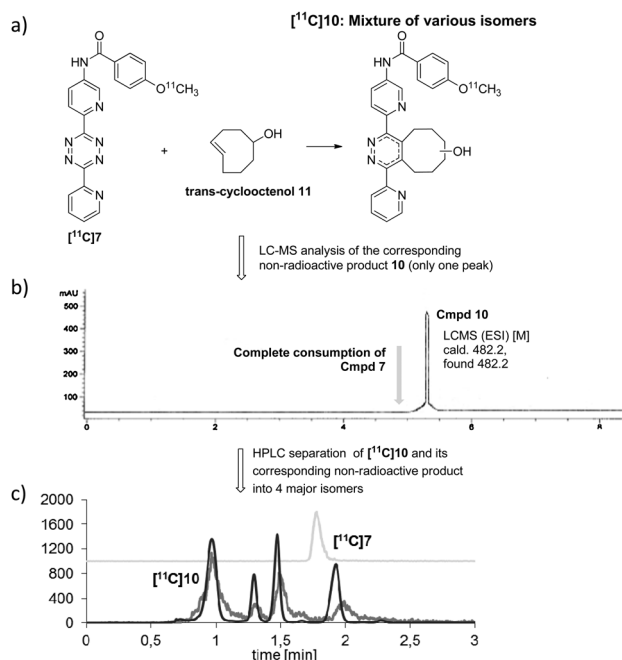
Afterwards, phenol **9** and its corresponding reference **7** were synthesised. The synthesis of the amide derivatives succeeded with microwave heating, whereas conventional heating of the corresponding acid chloride with **6** failed (Scheme 2).

With the precursor **9** and its reference **7** in hand, we optimized the radiolabeling conditions for [<sup>11</sup>C]**7** ( $\log D_{7,4} = 3.37$ ) (see ESI<sup>†</sup> for details). The highest RCY ( $33 \pm 5\%$ ,  $n = 5$ , EOS) was obtained using 0.3 mg precursor (0.8  $\mu\text{mol}$ ) dissolved in 0.3 mL DMF, 0.8  $\mu\text{L}$  2 N NaOH (2 equiv.) and [<sup>11</sup>C]MeI at  $80^\circ\text{C}$  for 2 min. [<sup>11</sup>C]**7** could be synthesized, separated *via* semi-preparative HPLC and formulated in a radiochemical purity of >98% (Scheme 3) in a synthesis



**Scheme 3** <sup>11</sup>C-radiolabeling of TTA derivative: (a) radiosynthesis of [<sup>11</sup>C]**7** succeeded in 33% RCY: [<sup>11</sup>C]CH<sub>3</sub>I, NaOH (2 equiv.), DMF,  $80^\circ\text{C}$ ; (b) analytical HPLC chromatogram of [<sup>11</sup>C]**7** and its standard **7** (UV at 254 nm; black; radio: grey).





**Scheme 4** (a) Tetrazine ligation of  $[^{11}\text{C}]7$  (radio: light grey) and *trans*-cyclooctenol resulting in the Diels-Alder conjugates  $[^{11}\text{C}]10$ ; (b) LC-MS trace of **10**; (c) radio and UV-HPLC diagram of  $[^{11}\text{C}]10$ , **10** and  $[^{11}\text{C}]7$  (UV at 254 nm; black; radio: dark grey).

time of 50–60 min (EOB to EOS) with an average specific activity of 60 GBq  $\mu\text{mol}^{-1}$  (range 40–80 GBq  $\mu\text{mol}^{-1}$ ). Thereby, 0.4–0.8 GBq was typically produced.

Initially, we tested the non-radioactive TCO of **7** and *trans*-cyclooctenol **11** (Scheme 4a). As indicated by an instant colour change from pink to yellow, the conjugation proceeded immediately in DMSO, DMF,  $\text{H}_2\text{O}$  and phosphate buffer. Only one UV peak was observed by LC-MS with the expected mass with no traces of **7** remaining in the mixture (Scheme 4b). The identity of the product was also confirmed by HRMS. In addition, NMR showed that the double bond of **11** disappeared suggesting complete consumption of **11**. However, the complex aliphatic part of the NMR spectrum hints the formation of several isomers, as outlined in Scheme 1. Therefore, an analytical method was pursued to try and separate the possible isomers. Four major isomers could be identified (Luna 5  $\mu\text{m}$  C18(2) 100 Å column (Phenomenex Inc.), 150  $\times$  4.6 mm, 50:50 acetonitrile:IP-buffer (5 mM Na-decanesulfonate, 25 mM phosphate buffer); pH = 2.6 adjusted with  $\text{H}_3\text{PO}_4$ , flow rate: 2 mL  $\text{min}^{-1}$ ) (Scheme 4c). These isomers served as HPLC standards for determination of the radiolabeled product  $[^{11}\text{C}]10$  and were stable in DMSO and  $\text{H}_2\text{O}$  for at least 7 days.

Next we turned our attention to the TCO with  $[^{11}\text{C}]7$  (Scheme 4a). To our delight,  $[^{11}\text{C}]7$  proceeded with 50–500  $\mu\text{M}$  of **11** to  $[^{11}\text{C}]10$  at a conversion rate of >98% in EtOH,

0.1% phosphate buffer or in the HPLC eluent (MeCN: 0.1% phosphate buffer 1 : 1). Analysis of the final  $^{11}\text{C}$ -TTCO conjugate was started within 20 s, and again 4 major peaks were observed (as judged from the radioactive trace). They corresponded to the UV-trace (Scheme 4c). In addition, the HPLC chromatogram showed complete consumption of  $[^{11}\text{C}]7$ .

In conclusion, we describe here the development of a  $^{11}\text{C}$ -labeled tetrazine for rapid tetrazine–*trans*-cyclooctene ligation. Labeling of  $[^{11}\text{C}]7$  succeeded in a 33% RCY and the final click ligation proceeded very rapidly to produce various isomers of  $[^{11}\text{C}]10$  within 20 s. The secondary  $^{11}\text{C}$ -labeling synthon  $[^{11}\text{C}]7$  is the first described  $^{11}\text{C}$ -labeled TTA which could be used as a click agent for conventional or bioorthogonal labeling of nanoparticles such as polymers or antibodies.

The authors wish to thank the staff at the PET and Cyclotron unit for expert technical assistance, Peter Brøsen and François Crestey for helping with HRMS measurements. Financial support from the Intra European Fellowship (MC-IEF-275329), the Faculty of Health and Medical Sciences at the University of Copenhagen and the Lundbeck Foundation is gratefully acknowledged.

## Notes and references

† **7** and **9** were isolated as salts, only **9** was stable under basic conditions and could be isolated as its free base.

- R. Rossin, P. R. Verkerk, S. M. van den Bosch, R. C. M. Vulders, I. Verel, J. Lub and M. S. Robillard, *Angew. Chem., Int. Ed.*, 2010, **49**, 3375–3378.
- D. M. Goldenberg, R. M. Sharkey, G. Paganelli, J. Barbet and J. F. Chatal, *J. Clin. Oncol.*, 2006, **24**, 823–834; D. M. Goldenberg, E. A. Rossi, R. M. Sharkey, W. J. McBride and C. H. Chang, *J. Nucl. Med.*, 2008, **49**, 158–163.
- W. R. Algar, D. E. Prasuhn, M. H. Stewart, T. L. Jennings, J. B. Blanco-Canosa, P. E. Dawson and I. L. Medintz, *Bioconjugate Chem.*, 2011, **22**, 825–858; R. D. Carpenter, S. H. Hausner and J. L. Sutcliffe, *ACS Med. Chem. Lett.*, 2011, **2**, 885–889.
- S. T. Laughlin, J. M. Baskin, S. L. Amacher and C. R. Bertozzi, *Science*, 2008, **320**, 664–667.
- M. L. Blackman, M. Royzen and J. M. Fox, *J. Am. Chem. Soc.*, 2008, **130**, 13518–13519.
- Z. Li, H. Cai, M. Hassink, M. L. Blackman, R. C. D. Brown, P. S. Conti and J. M. Fox, *Chem. Commun.*, 2010, **46**, 8043–8045.
- G. L. Wolf, *CRC Press: Boca Raton*, 1995, vol. 3; M. M. Herth, M. Barz, D. Moderegger, M. Allmeroth, M. Jahn, O. Thews, R. Zentel and F. Rösch, *Biomacromolecules*, 2009, **10**, 1697–1703.
- N. K. Devaraj, G. M. Thurber, E. J. Keliher, B. Marinelli and R. Weissleder, *Proc. Natl. Acad. Sci. U. S. A.*, 2012, **109**, 4762–4767.
- J. Yang, M. R. Karver, W. Li, S. Sahu and N. K. Devaraj, *Angew. Chem., Int. Ed.*, 2012, **51**, 5222–5225; G. Clavier and P. Audebert, *Chem. Rev.*, 2010, **110**, 3299–3314; N. K. Devaraj, *SYNFACTS*, 2012, 2147–2152.
- T. Wei, W. H. Zhu, X. W. Zhang, Y. F. Li and H. M. Xiao, *J. Phys. Chem.*, 2009, **113**, 9404–9412; D. E. Chavez, M. A. Hiskey and R. D. Gilardi, *Angew. Chem., Int. Ed.*, 2000, **112**, 1861–1863.
- P. H. Elsinga, *Methods*, 2002, **27**, 208–217.
- R. Selvaraj, S. Liu, M. Hassink, C. Huang, L. Yap, R. Park, J. M. Fox, Z. Li and P. S. Conti, *Bioorg. Med. Chem. Lett.*, 2011, **21**, 5011–5014.
- A. Bauman, M. Piel, R. Schirrmacher and F. Rösch, *Tetrahedron Lett.*, 2003, **44**, 9165–9167.